



uOttawa

L'Université canadienne  
Canada's university

**FACULTÉ DES ÉTUDES SUPÉRIEURES  
ET POSTDOCTORALES**



**uOttawa**

L'Université canadienne  
Canada's university

**FACULTY OF GRADUATE AND  
POSTDOCTORAL STUDIES**

**David R. Stuart**

-----  
AUTEUR DE LA THÈSE / AUTHOR OF THESIS

**Ph.D. (Chemistry)**

-----  
GRADE / DEGREE

**Department of Chemistry**

-----  
FACULTÉ, ÉCOLE, DÉPARTEMENT / FACULTY, SCHOOL, DEPARTMENT

**Transition Metal Catalyzed Oxidative Functionalization and Preparation of Aromatic Heterocycles**

-----  
TITRE DE LA THÈSE / TITLE OF THESIS

**Keith Fagnou**

-----  
DIRECTEUR (DIRECTRICE) DE LA THÈSE / THESIS SUPERVISOR

-----  
CO-DIRECTEUR (CO-DIRECTRICE) DE LA THÈSE / THESIS CO-SUPERVISOR

**André Beauchemin**

**Robert Ben**

**Jeffrey Manthorpe**

**Laurel Shafer (University of British  
Columbia)**

**Gary W. Slater**

-----  
Le Doyen de la Faculté des études supérieures et postdoctorales / Dean of the Faculty of Graduate and Postdoctoral Studies

# **Transition Metal Catalyzed Oxidative Functionalization and Preparation of Aromatic Heterocycles**

By

**David R. Stuart**

B. Sc., University of Victoria, 2005

A thesis submitted to the Faculty of Graduate and Postdoctoral Studies  
In partial fulfillment of the requirements for the  
Philosophiae Doctor (Ph.D.) degree in chemistry

Candidate

Supervisor

David R. Stuart

Prof. Keith Fagnou

Ottawa-Carleton Chemistry Institute  
Faculty of Science  
University of Ottawa



Library and Archives  
Canada

Published Heritage  
Branch

395 Wellington Street  
Ottawa ON K1A 0N4  
Canada

Bibliothèque et  
Archives Canada

Direction du  
Patrimoine de l'édition

395, rue Wellington  
Ottawa ON K1A 0N4  
Canada

*Your file* *Votre référence*  
ISBN: 978-0-494-65574-0  
*Our file* *Notre référence*  
ISBN: 978-0-494-65574-0

**NOTICE:**

The author has granted a non-exclusive license allowing Library and Archives Canada to reproduce, publish, archive, preserve, conserve, communicate to the public by telecommunication or on the Internet, loan, distribute and sell theses worldwide, for commercial or non-commercial purposes, in microform, paper, electronic and/or any other formats.

The author retains copyright ownership and moral rights in this thesis. Neither the thesis nor substantial extracts from it may be printed or otherwise reproduced without the author's permission.

---

In compliance with the Canadian Privacy Act some supporting forms may have been removed from this thesis.

While these forms may be included in the document page count, their removal does not represent any loss of content from the thesis.

**AVIS:**

L'auteur a accordé une licence non exclusive permettant à la Bibliothèque et Archives Canada de reproduire, publier, archiver, sauvegarder, conserver, transmettre au public par télécommunication ou par l'Internet, prêter, distribuer et vendre des thèses partout dans le monde, à des fins commerciales ou autres, sur support microforme, papier, électronique et/ou autres formats.

L'auteur conserve la propriété du droit d'auteur et des droits moraux qui protègent cette thèse. Ni la thèse ni des extraits substantiels de celle-ci ne doivent être imprimés ou autrement reproduits sans son autorisation.

---

Conformément à la loi canadienne sur la protection de la vie privée, quelques formulaires secondaires ont été enlevés de cette thèse.

Bien que ces formulaires aient inclus dans la pagination, il n'y aura aucun contenu manquant.

  
**Canada**

Dedicated to Prof. Keith Fagnou:  
My mentor and good friend.

# Abstract

Aromatic heterocycles, particularly those containing nitrogen, have been identified as important motifs in a wide variety of pharmaceuticals, agrochemicals, fine chemicals, and materials of technological interest. Thus, the development of efficient methods for both the functionalization and preparation of these compounds has received much attention from the synthetic community. Traditional transition metal catalysis has featured prominently in both of these veins; however, there has been a recent surge of interest in the development of catalytic methodologies aimed at the conversion of C-H bonds to more highly oxidized functionality. This body of work describes both the functionalization and preparation of aromatic *N*-heterocycles in this context.

Described in this thesis is the development of methods for both the functionalization and preparation of nitrogen containing aromatic heterocycles from readily available precursors devoid of pre-activation. First, the advancement of palladium(0)-catalyzed direct arylation of quinoline and isoquinoline *N*-oxides with aryl bromides as a viable solution to the “2-azine organometallic problem” is presented (Chapter 2). This project serves in the formation of the pharmaceutically relevant 2-arylquinolines and 1-arylisoquinolines. These studies also assisted in the identification of a catalyst system (Pd(OAc)<sub>2</sub> (5 mol%), PMe<sup>t</sup>Bu<sub>2</sub>•HBF<sub>4</sub> (10 mol%)) enabling high regioselectivity in the direct arylation of unsymmetrical azine *N*-oxides, such as isoquinoline *N*-oxide and 3-substituted pyridine *N*-oxides. The experimental observations were validated computationally with a concerted metallation deprotonation transition state model.

In a subsequent section, the development and mechanistic investigation of the palladium(II)-catalyzed oxidative cross-coupling of two unactivated arenes is presented (Chapter 3). The physical parameters of this century-old problem are addressed and observations which may provide solutions to both regio- and chemoselectivity are described for the oxidative arylation of indoles. Protocols for the C2- and C3-oxidative arylation of *N*-pivaloyl and *N*-acetylindole, respectively, are offered. Additionally, the mechanism is discussed, including the observation that both the oxidant (AgOAc or Cu(OAc)<sub>2</sub>) and nitrogen protecting group (pivaloyl or acetyl) appear to have a significant effect on regioselectivity.

Finally, the rhodium(III)-catalyzed oxidative coupling of acetanilides or enamides with alkynes to form highly decorated indoles or pyrroles, respectively, is described (Chapter 4). This methodology was applied to the synthesis of Paullone, a pharmaceutical agent. An in-depth mechanistic evaluation of this oxidative indole-forming annulation process based on kinetic studies and free energy correlations is also reported.

# Acknowledgments

I would first like to acknowledge and thank all the people that were beside me day-after-day in the lab and at the bench; the camaraderie and support have made these some of the most memorable and fulfilling years of my life. To the senior members of the lab who showed me the ropes as a rookie – thank you! I will always be grateful to Louis-Charles (LC) Campeau, in particular, whose enthusiasm, guidance, and determination in tackling challenging problems taught me a lot about successful approaches to synthetic organic chemistry. His continued interest in my scientific growth is very much appreciated.

The group has grown and evolved tremendously since the time I joined in 2005 and I have had the pleasure of working with an incredibly dynamic and talented collection of people. To all the undergraduates that I supervised: thank you for all of your hard work and tenacity, the completeness of this thesis would not be at the stage that it is without your contributions. Ben, Derek, and David: I know the innovations that we made to foosball will revolutionize the game forever, thank you for all the laughs and intense matches. To all the people who had a hand in reading and editing this thesis (Ben, Sophie, Ho-Yan, LC, Keith, and Catherine) I greatly appreciate your criticism and comments and will be forever grateful for your attention to detail. To all the people who have made doing chemistry that much easier at the University of Ottawa: Glenn Facey and Cheryl McDowall (NMR), Clem Kazakoff (mass spectrometry), and all the people at Science Stores, thank you for all of your help over the years. A particular thank you to Betty Yakimenko for her administrative expertise and general concern for our well being. I would also like to extend a special thank you to my family for all their encouragement and support over the years; it has really kept me motivated.

Keith – I don't know if I can accurately convey the debt of gratitude I owe you. The last four years have been amazing, both scientifically and personally, and I thank you for that. Your mentorship and support has been a constant source of inspiration for me. Thank you for all the guidance that you have given me, particularly in the last 6 months, your continued support has made this challenging time in my life that much easier and less stressful. I will measure my own career a success if I am half the supervisor to future students that you have been to me. Thank you.

Most importantly, I would like to acknowledge my beautiful wife, Catherine. Your enduring love and support is what has driven me to be the best that I can, and I only hope that I can one day repay you. These last four year have been an adventure and you have been the best companion I could ask for. I look forward to the adventures ahead of us and know that with you by my side we can accomplish anything. Thank you, with all my heart.

# Table of Contents

ABSTRACT .....	III
ACKNOWLEDGMENTS .....	V
TABLE OF CONTENTS .....	VII
LIST OF FIGURES .....	IX
LIST OF SCHEMES .....	X
LIST OF TABLES .....	XII
GLOSSARY OF ABBREVIATIONS .....	XIII
<b>1 .....</b>	<b>1</b>
INTRODUCTION .....	1
1.1. Construction and Functionalization of Heterocycles .....	1
1.2. Description of the Mechanistic Possibilities for Transition Metal Catalyzed C-H Bond Cleavage .....	3
1.3. Evolution of the Concerted Metallation Deprotonation (CMD) Transition State .....	5
<b>2 .....</b>	<b>13</b>
PALLADIUM(0) CATALYZED DIRECT ARYLATION OF AZINE N-OXIDES .....	13
2.1. Introduction .....	13
2.1.1. Direct Arylation of $\pi$ -Rich Heterocycles .....	17
2.1.2. Direct Arylation of $\pi$ -Deficient Heterocycles .....	21
2.1.3. Mechanistic Consideration in Direct Arylation of Azine N-Oxides .....	27
2.2. Results and Discussion .....	29
2.2.1. Reaction Development and Investigation of Aryl Halide Compatibility in the Direct Arylation of Quinoline and Isoquinoline N-Oxide .....	29
2.2.2. Correlation to a CMD Pathway .....	35
2.3. Outlook and Perspectives .....	36
<b>3 .....</b>	<b>37</b>
PALLADIUM(II) CATALYZED OXIDATIVE CROSS-COUPLING OF UNACTIVATED ARENES .....	37
3.1. Introduction .....	37
3.1.1. Oxidative Homo-coupling of Type I or Type III Arenes .....	40
3.1.2. Oxidative Homo-coupling of Type II Arenes .....	42
3.1.3. Oxidative Cross-coupling between Type I and Type III Arenes .....	43
3.1.4. Oxidative Cross-coupling between Type II and Type III Arenes .....	45
3.1.5. Oxidative Cross-Coupling between Type III Arenes .....	47
3.2. Results and Discussion .....	48
3.2.1. Reaction Development and Investigation of Functional Group Compatibility .....	48
3.2.2. Kinetics and Mechanistic Evaluation for the Oxidative Cross-Coupling of N-Acetyl and N-Pivaloylindole with Unactivated Arenes .....	58
3.3. Outlook and Perspectives .....	78
<b>4 .....</b>	<b>79</b>
RHODIUM(III) CATALYZED OXIDATIVE PREPARATION OF INDOLES AND PYRROLES .....	79
4.1. Introduction .....	79
4.1.1. Transition Metal-Catalyzed Oxidative Approaches in Indole Synthesis .....	83
4.1.2. Rhodium(III) as an Oxidant in Organic Synthesis .....	86
4.2. Results and Discussion .....	91
4.2.1. Rhodium(III)-Catalyzed Annulation of Acetanilides with Internal Alkynes: Reaction Development and Scope .....	91
4.2.2. Rhodium(III)-Catalyzed Annulation of Enamides with Internal Alkynes: Reaction Development and Scope .....	102
4.2.3. Synthesis of Paullone .....	107

4.2.4. Kinetic and Mechanistic Analysis of the Rhodium(III)-Catalyzed Annulation of Acetanilides with Internal Alkynes.....	112
4.2.5. Optimization of an Alkyne Hydroarylation Protocol.....	134
4.3. <i>Outlook and Perspectives</i> .....	137
<b>5 .....</b>	<b>138</b>
SUPPORTING INFORMATION .....	138
5.1. <i>General Methods</i> .....	138
5.2. <i>Quinoline and Isoquinoline N-Oxides</i> .....	139
5.2.1. Oxidation Methods and Characterization of Oxidation Products.....	139
5.2.2. Methods and Characterization for 2-Arylquinoline <i>N</i> -Oxide Products.....	141
5.2.3. Reduction Methods and Characterization of 2-Arylquinoline Products.....	150
5.2.4. Methods and Characterization of 1-Arylisoquinoline Products.....	152
5.3. <i>Oxidative Arylation of Indoles</i> .....	157
5.3.1. Intramolecular Oxidative Ring Closure of <i>N</i> -Benzoylindole.....	157
5.3.2. Acetylation of Indoles and Characterization Data.....	158
5.3.3. Oxidative C3-Arylation of <i>N</i> -Acetylindoles and Characterization Data.....	162
5.3.4. Pivaloylation of Indoles and Characterization Data.....	169
5.3.5. Oxidative C2-Arylation of <i>N</i> -Pivaloylindoles.....	173
5.3.6. Preparation of Materials for Mechanistic Investigation and Kinetic Experiments .....	178
5.4. <i>Oxidative Annulation of Acetanilide and Enamides with Internal Alkynes</i> .....	183
5.4.1. Preparation and Characterization of Acetanilides.....	183
5.4.2. Preparation and Characterization of Internal Alkynes.....	188
5.4.3. Oxidative Annulation of Acetanilides and Characterization Data.....	196
5.4.4. Deacetylation of <i>N</i> -Acetylindoles.....	213
5.4.5. Preparation and Characterization of Enamides.....	214
5.4.6. Oxidative Annulations of Enamides and Characterization Data.....	215
5.4.7. Synthesis and Characterization of Intermediates <i>en route</i> to Paullone.....	223
5.4.8. Description of Kinetic Experiments and Mechanistic Investigation.....	227
5.4.9. Procedure for the Hydroarylation of Internal Alkynes.....	237
<b>6 .....</b>	<b>238</b>
APPENDIX .....	238
<i>Claims to Original Research</i> .....	238
<i>Publications from This Work</i> .....	239
<i>Presentations from This Work</i> .....	239

# List of Figures

FIGURE 1.1. REPRESENTATIVE EXAMPLES OF NITROGEN CONTAINING HETEROCYCLES OF HIGH UTILITY. ....	2
FIGURE 1.2. FAGNOU'S PROPOSAL FOR THE MECHANISM OF C-H BOND CLEAVAGE IN INTRAMOLECULAR DIRECT ARYLATION.....	8
FIGURE 1.3. CMD TRANSITION STATE FOR THE DIRECT ARYLATION OF PENTAFLUOROBENZENE. <sup>A</sup> .....	9
FIGURE 1.4. CONTRIBUTION OF EACH CARBON ATOM TO THE HOMO OF THIAZOLE AND THIAZOLE <i>N</i> -OXIDE. <sup>B</sup> .....	9
FIGURE 1.5. ACTIVATION-STRAIN ANALYSIS APPLIED TO THE CMD PATHWAY.....	11
FIGURE 2.1. BIARYL NATURAL PRODUCTS AND PHARMACEUTICALS.....	14
FIGURE 2.2. LOWEST ENERGY TRANSITION STATE CALCULATED FOR PYRIDINE <i>N</i> -OXIDE DIRECT ARYLATION.....	28
FIGURE 2.3. EXPERIMENTAL AND COMPUTATIONAL RESULTS FOR COMPETITION EXPERIMENTS BETWEEN ELECTRONICALLY DIFFERENT PYRIDINE <i>N</i> -OXIDES (COMPUTATIONAL RESULT SHOWN ABOVE THE ARROW, EXPERIMENTAL RESULT SHOWN BELOW THE ARROW).....	29
FIGURE 2.4. EXPERIMENTAL AND COMPUTATIONAL RESULTS FOR REGIOSELECTIVITIES IN THE DIRECT ARYLATION OF 3-SUBSTITUTED PYRIDINE <i>N</i> -OXIDES.....	29
FIGURE 3.1. CLASSIFICATION OF ARENES IN OXIDATIVE HOMO-COUPLING AND CROSS-COUPLING OF SIMPLE ARENES.....	39
FIGURE 3.2. INITIAL RATE VS. INITIAL CONCENTRATION OF Pd(TFA) <sub>2</sub> .....	59
FIGURE 3.3. INITIAL RATE VS. INITIAL CONCENTRATION OF BENZENE.....	60
FIGURE 3.4. INITIAL RATE VS. INITIAL CONCENTRATION OF <i>N</i> -PIVALOYLINDOLE.....	60
FIGURE 3.5. INITIAL RATE VS. INITIAL CONCENTRATION OF SILVER ACETATE.....	61
FIGURE 3.6. INITIAL RATE VS. INITIAL CONCENTRATION OF PIVALIC ACID.....	62
FIGURE 3.7. PRODUCT FORMATION VS TIME (DKIE).....	63
FIGURE 3.8. ARRHENIUS PLOT FOR THE C2 ARYLATION OF <i>N</i> -PIVALOYLINDOLE.....	66
FIGURE 3.9. DEUTERIUM LOSS AS A FUNCTION OF TIME.....	71
FIGURE 3.10. INFLUENCE OF C6-SUBSTITUTION ON C3,C2-PALLADIUM MIGRATION.....	73
FIGURE 3.11. HAMMETT CORRELATION FOR 6-X- <i>N</i> -PIVALOYLINDOLES.....	73
FIGURE 3.12. RELATIVE ENERGIES OF SELECTED AMIDE CONFORMATIONS OF <i>N</i> -ACETYLINDOLE.....	76
FIGURE 3.13. RELATIVE ENERGIES OF SELECTED AMIDE CONFORMATIONS OF <i>N</i> -PIVALOYLINDOLE.....	77
FIGURE 3.14. DIFFERENCES IN AMIDE CONFORMATION FOR <i>N</i> -ACETYL AND <i>N</i> -PIVALOYLINDOLE AS IT RELATES TO REGIOSELECTIVITY.....	77
FIGURE 4.1. REPRESENTATIVE INDOLES AND PYRROLES IN NATURE AND MEDICINAL CHEMISTRY.....	80
FIGURE 4.2. PROPOSED TRANSITION STATE FOR JONES CYCLORHODATION OF <i>N</i> -PHENYL IMINES.....	90
FIGURE 4.3. STRUCTURE OF FLAVOPIRIDOL AND THE PAULLONE CORE.....	108
FIGURE 4.4. POTENTIAL ALKYNES FOR THE SYNTHESIS OF PAULLONE.....	111
FIGURE 4.5. INITIAL RATE VERSUS INITIAL CONCENTRATION OF RHODIUM.....	114
FIGURE 4.6. INITIAL RATE VERSUS INITIAL CONCENTRATION OF ACETANILIDE.....	115
FIGURE 4.7. LINEWEAVER-BURKE PLOT ACETANILIDE CONCENTRATION.....	116
FIGURE 4.8. INITIAL RATE VERSUS INITIAL CONCENTRATION OF ALKYNE.....	117
FIGURE 4.9. INITIAL RATE VERSUS INITIAL CONCENTRATION OF COPPER(II) ACETATE.....	119
FIGURE 4.10. COSY CORRELATIONS OF COMPOUND 4.30.....	124
FIGURE 4.11. NOESY CORRELATIONS OF COMPOUND 4.30.....	125
FIGURE 4.12. INITIAL RATE VERSUS INITIAL CONCENTRATION OF ACETIC ACID.....	128
FIGURE 4.13. EXPERIMENTAL AND SIMULATED DATA FOR THE PROPOSED CATALYTIC CYCLE.....	129
FIGURE 4.14. HAMMETT CORRELATION FOR <i>PARA</i> -SUBSTITUTED ACETANILIDES.....	131
FIGURE 4.15. ARRHENIUS PLOT FOR THE RHODIUM CATALYZED ANNULATION OF ACETANILIDES WITH INTERNAL ALKYNES.....	133
FIGURE 4.16. EFFECT OF CONCENTRATION AND TEMPERATURE ON HYDROARYLATION.....	136

# List of Schemes

SCHEME 1.1. OVERVIEW OF WORK DESCRIBED HEREIN. ....	3
SCHEME 1.2. POTENTIAL ROUTES FOR C-H BOND CLEAVAGE. ....	5
SCHEME 1.3. PROPOSALS TAKEN FROM THE ORIGINAL REPORTS BY KRESGE AND BROWN <sup>E</sup> AND RYABOV. ....	7
SCHEME 2.1. CATALYTIC CYCLE FOR TRADITIONAL PALLADIUM-CATALYZED CROSS-COUPLING. ....	15
SCHEME 2.2. GENERAL CATALYTIC CYCLE FOR DIRECT ARYLATION WITH AN ARYL HALIDE AND A SIMPLE ARENE. ....	17
SCHEME 2.3. OHTA'S REGIOSELECTIVE DIRECT ARYLATION OF INDOLES. ....	18
SCHEME 2.4. SAMES' C2-SELECTIVE DIRECT ARYLATION OF INDOLE CATALYZED BY PALLADIUM AND RHODIUM. ....	19
SCHEME 2.5. SANFORDS'S DIRECT ARYLATION OF INDOLES VIA Pd(II)/Pd(IV) MANIFOLD. ....	19
SCHEME 2.6. GAUNT'S COPPER-CATALYZED DIRECT ARYLATION OF INDOLES. ....	19
SCHEME 2.7. MIURA'S DIRECT ARYLATION OF IMIDAZOLE AND THIAZOLE. ....	20
SCHEME 2.8. OHTA'S DIRECT ARYLATION OF FURAN AND THIOPHENE. ....	20
SCHEME 2.9. GENERAL CONDITIONS FOR THE DIRECT ARYLATION OF HETEROCYCLES. ....	21
SCHEME 2.10. GENERAL STRATEGY FOR <i>N</i> -OXIDE UTILITY IN PYRIDINE ARYLATION AND FUNCTIONALIZATION. ....	23
SCHEME 2.11. DIRECT ARYLATION OF PYRIDINE CATALYZED BY Pd/C. ....	23
SCHEME 2.12. DIRECT ALKYLATION/ARYLATION OF PYRIDINES AND QUINOLINE VIA Rh(I)-CATALYSIS. ....	24
SCHEME 2.13. DIRECT ARYLATION OF PYRIDINE VIA 1,2-ADDITION/OXIDATION PROTOCOL. ....	25
SCHEME 2.14. DIRECT ARYLATION OF <i>N</i> -IMINOPYRIDINIUM YLIDES. ....	25
SCHEME 2.15. DIRECT ARYLATION OF AZINE <i>N</i> -OXIDES. ....	26
SCHEME 2.16. DIRECT ARYLATION OF AZOLE <i>N</i> -OXIDES. ....	26
SCHEME 2.17. EXPERIMENTAL AND CALCULATED RESULTS FOR REGIOSELECTIVITY. ....	36
SCHEME 3.1. GENERAL CATALYTIC CYCLE OF THE OXIDATIVE CROSS-COUPLING OF TWO SIMPLE ARENES. ....	38
SCHEME 3.2. HOMO-COUPLING OF PYRROLES (TYPE I ARENE). ....	40
SCHEME 3.3. HOMO-COUPLING OF BENZENE (TYPE III ARENE) BY CATALYTIC PALLADIUM. ....	41
SCHEME 3.4. HOMO-COUPLING OF THIOPHENES (TYPE I ARENE) BY CATALYTIC PALLADIUM. ....	42
SCHEME 3.5. CYCLOPHANE FORMATION VIA INTRAMOLECULAR OXIDATIVE HOMO-COUPLING OF INDOLAZINES (TYPE I ARENE). ....	42
SCHEME 3.6. PROPOSED CATALYTIC CYCLE FOR THE HOMO-COUPLING OF 2-ARYLPYRIDINES (TYPE II ARENES). ....	43
SCHEME 3.7. INTRA- AND INTERMOLECULAR OXIDATIVE CROSS-COUPLING BETWEEN TYPE I AND III ARENES MEDIATED BY STOICHIOMETRIC PALLADIUM. ....	44
SCHEME 3.8. OXIDATIVE CROSS-COUPLING OF BENZOFURAN (TYPE I ARENE) AND BENZENE (TYPE III ARENE). ....	44
SCHEME 3.9. OXIDATIVE CROSS-COUPLING BETWEEN BENZO[H]QUINOLINE (TYPE II ARENE) AND BENZENE (TYPE III ARENE). ....	45
SCHEME 3.10. OXIDATIVE CROSS-COUPLING BETWEEN OTHER TYPE II ARENES AND BENZENE (TYPE III ARENE). ....	47
SCHEME 3.11. OXIDATIVE CROSS-COUPLING BETWEEN PYRIDINE <i>N</i> -OXIDE (TYPE II ARENE) AND BENZENE (TYPE III ARENE). ....	48
SCHEME 3.12. INDOLE ANNULATION VIA OXIDATIVE HECK REACTION. ....	48
SCHEME 3.13. APPLICATION OF OPTIMIZED REACTION CONDITIONS. ....	51
SCHEME 3.14. COMPETITION EXPERIMENTS FOR ELECTRONICALLY DISSIMILAR ARENES. ....	64
SCHEME 3.15. COMPETITION EXPERIMENTS FOR THE XYLENE SERIES. ....	65
SCHEME 3.16. DEUTERIUM INCORPORATION EXPERIMENTS ON <i>N</i> -ACETYLLINDOLE. ....	67
SCHEME 3.17. DEUTERIUM INCORPORATION EXPERIMENTS ON <i>N</i> -PIVALOYLINDOLE. ....	68
SCHEME 3.18. PREPARATION OF DEUTERIUM LABELED 5-METHOXY- <i>N</i> -PIVALOYLINDOLES. ....	69
SCHEME 3.19. COMPETITION EXPERIMENTS BETWEEN 3.41 AND 3.39-2-D. ....	69
SCHEME 3.20. COMPETITION EXPERIMENTS BETWEEN 3.41 AND 3.39-3-D. ....	69
SCHEME 3.21. PLAUSIBLE MECHANISM FOR THE C2 ARYLATION OF <i>N</i> -PIVALOYLINDOLE. ....	72
SCHEME 3.22. GAUNT'S PROPOSED INTERMEDIATE FOR ACETATE ASSISTED C2-ARYLATION. ....	76
SCHEME 4.1. LAROCK INDOLE SYNTHESIS. ....	81
SCHEME 4.2. PROPOSED MECHANISM OF LAROCK INDOLE SYNTHESIS. ....	82
SCHEME 4.3. PALLADIUM CATALYZED FORMATION OF PYRROLES FROM IODOACRYLATES. ....	83
SCHEME 4.4. OBSERVED PRODUCTS FROM MULTIPLE ALKYNE INSERTION. ....	84
SCHEME 4.5. OXIDATIVE INTRAMOLECULAR CYCLIZATION OF <i>N</i> -ARYLENAMINES. ....	84
SCHEME 4.6. JIAO'S INTERMOLECULAR COUPLING OF ANILINES WITH ACETYLENEDICARBOXYLATE ESTERS. ....	85

SCHEME 4.7. OXIDATIVE CARBOAMINATION OF 1,3-DIENES. ....	86
SCHEME 4.8. RHODIUM(III)-CATALYZED FORMATION OF LACTAMS FROM AROMATIC AMINO-ALCOHOLS.....	87
SCHEME 4.9. GENERAL REACTION AND MECHANISM FOR ANNULATION OF BENZOIC ACID BY INTERNAL ALKYNES. ....	88
SCHEME 4.10. FORMATION OF POLYAROMATIC COMPOUNDS VIA RHODIUM(III)-CATALYSIS.....	89
SCHEME 4.11. EVIDENCE FOR C-N BOND REDUCTIVE ELIMINATION FROM A RHODIUM(III) CENTER.....	89
SCHEME 4.12. JONES' ONE-POT PROCEDURE FOR THE PREPARATION OF ISOQUINOLINE SALTS.....	89
SCHEME 4.13. GRUSHIN'S RH(III)-CATALYZED OXIDATIVE CARBOXYLATION OF TOLUENE. ....	91
SCHEME 4.14. COMPATIBILITY OF PROTECTED ALKYNES IN THE ANNULATION OF ACETANILIDES. ....	100
SCHEME 4.15. REGIOSELECTIVITY FOR ANNULATION OF ACETANILIDES WITH ENYNE SUBSTRATES. ....	102
SCHEME 4.16. FORMATION OF A TETRASUBSTITUTED PYRROLE WITH (E)-4.13.....	103
SCHEME 4.17. USE OF (Z)-4.13 IN THE FORMATION OF TETRASUBSTITUTED PYRROLES. ....	103
SCHEME 4.18. EVALUATION OF ENAMIDE ISOMERIZATION BY <sup>1</sup> H NMR SPECTROSCOPY.....	104
SCHEME 4.19. RETROSYNTHETIC AVENUES FOR THE CONSTRUCTION OF THE PAULLONE CORE. ....	109
SCHEME 4.20. OUR RETROSYNTHETIC ANALYSIS OF THE PAULLONE CORE. ....	110
SCHEME 4.21. FINAL SYNTHETIC ROUTE TO PAULLONE. ....	112
SCHEME 4.22. BASIC MECHANISM FOR THE ANNULATION OF ACETANILIDES WITH INTERNAL ALKYNES.....	113
SCHEME 4.23. INVESTIGATING THE REVERSIBILITY OF ACETANILIDE CYCLORHODATION. ....	116
SCHEME 4.24. LITERATURE PRECEDENT AND RATIONALE FOR THE KINETIC BEHAVIOR OBSERVED FOR ALKYNES. ....	118
SCHEME 4.25. INVESTIGATION OF AN OXIDATIVELY INDUCED REDUCTIVE ELIMINATION.....	118
SCHEME 4.26. MECHANISTIC RATIONALE FOR ALKYNE INFLUENCE OVER ACETANILIDE REGIOSELECTIVITY. ....	122
SCHEME 4.27. COMPETITION EXPERIMENT BETWEEN ELECTRONICALLY DIFFERENT ALKYNES. ....	122
SCHEME 4.28. POTENTIAL STRUCTURES OF THE OBSERVED SIDE PRODUCT. ....	124
SCHEME 4.29. TESTING THE HYPOTHESIS THAT 4.30 IS AN INTERMEDIATE IN THE CATALYTIC CYCLE.....	126
SCHEME 4.30. PROPOSED FORMATION OF 4.30 VIA PROTO-DERHODATION.....	126
SCHEME 4.31. PROPOSED CATALYTIC CYCLE BASED ON EXPERIMENTAL EVIDENCE. ....	127
SCHEME 4.32. DETERMINATION OF A DEUTERIUM KINETIC ISOTOPE EFFECT. ....	130
SCHEME 4.33. COMPETITION EXPERIMENTS OF 3,5-DISUBSTITUTED ACETANILIDES.....	132
SCHEME 4.34. FORMATION OF HYDROARYLATION PRODUCT OVER STARTING MATERIALS. ....	135
SCHEME 4.35. INTERMOLECULAR HYDROARYLATION OF ALKYNES. ....	137

# List of Tables

TABLE 2.1. REACTION DEVELOPMENT FOR THE DIRECT ARYLATION OF QUINOLINE <i>N</i> -OXIDE. <sup>A</sup> .....	30
TABLE 2.2. COMPATIBLE ARYL HALIDES IN THE DIRECT ARYLATION OF QUINOLINE <i>N</i> -OXIDE. <sup>A</sup> .....	31
TABLE 2.3. SELECTED EXAMPLES IN THE REDUCTION OF 2-ARYLQUINOLINE <i>N</i> -OXIDES. <sup>A</sup> .....	33
TABLE 2.4. LIGAND EFFECTS ON THE REGIOSELECTIVITY OF THE DIRECT ARYLATION OF ISOQUINOLINE <i>N</i> -OXIDE. <sup>A</sup> .....	34
TABLE 2.5. REGIOSELECTIVITY AND SCOPE IN THE DIRECT ARYLATION OF ISOQUINOLINE <i>N</i> -OXIDE. <sup>A</sup> .....	35
TABLE 3.1. OPTIMIZATION FOR THE INTRAMOLECULAR OXIDATIVE RING CLOSURE OF <i>N</i> -BENZOYLINDOLE, 3.13. <sup>A</sup> .....	50
TABLE 3.2. OPTIMIZATION FOR THE C3 OXIDATIVE ARYLATION OF <i>N</i> -ACETYLINDOLES. <sup>A</sup> .....	52
TABLE 3.3. SCOPE OF COMPATIBLE FUNCTIONALITY ON INDOLE IN THE C3 OXIDATIVE ARYLATION OF <i>N</i> -ACETYLINDOLES. <sup>A</sup> .....	53
TABLE 3.4. SCOPE OF COMPATIBLE ARENES IN THE C3 OXIDATIVE ARYLATION OF <i>N</i> -ACETYLINDOLE. <sup>A</sup> .....	53
TABLE 3.5. OPTIMIZATION FOR THE THERMAL C3 OXIDATIVE ARYLATION OF <i>N</i> -ACETYLINDOLES AND REPRESENTATIVE EXAMPLES. <sup>A</sup> .....	55
TABLE 3.6. OPTIMIZATION FOR THE C2 OXIDATIVE ARYLATION OF <i>N</i> -PIVALOYLINDOLES. <sup>A</sup> .....	56
TABLE 3.7. SCOPE OF COMPATIBLE FUNCTIONALITY ON INDOLE IN THE C2 OXIDATIVE ARYLATION OF <i>N</i> -PIVALOYLINDOLES. <sup>A</sup> .....	57
TABLE 3.8. SCOPE OF COMPATIBLE ARENES IN THE C2 OXIDATIVE ARYLATION OF <i>N</i> -PIVALOYLINDOLE. <sup>A</sup> .....	58
TABLE 3.9. ACETATE ASSISTED REGIOSELECTIVITY OF <i>N</i> -ACETYL AND <i>N</i> -PIVALOYLINDOLES. <sup>A</sup> .....	75
TABLE 4.1 REACTION DEVELOPMENT IN THE RHODIUM(III)-CATALYZED SYNTHESIS OF INDOLES. <sup>A</sup> .....	93
TABLE 4.2. RE-OPTIMIZATION OF THE REACTION CONDITIONS FOR THE ANNULATION OF ACETANILIDES WITH INTERNAL ALKYNES. <sup>A</sup> .....	94
TABLE 4.3. ACETANILIDE APPLICABILITY UNDER BOTH FIRST AND SECOND GENERATION CONDITIONS. <sup>A</sup> .....	96
TABLE 4.4. ALKYNE APPLICABILITY UNDER BOTH FIRST AND SECOND GENERATION CONDITIONS. <sup>A</sup> .....	98
<b>TABLE 4.5.</b> DETERMINATION OF OPTIMAL PROTECTING GROUPS FOR PROPARGYL ALCOHOLS. <sup>A</sup> .....	99
TABLE 4.6. REMOVAL OF ACETYL GROUP. <sup>A</sup> .....	99
TABLE 4.7. REACTION DEVELOPMENT IN THE RHODIUM(III)-CATALYZED SYNTHESIS OF PYRROLES. <sup>A</sup> .....	105
TABLE 4.8. REACTION SCOPE UNDER OPTIMIZED CONDITIONS. <sup>A</sup> .....	107
TABLE 4.9. EFFECT OF TEMPERATURE ON ACETANILIDE REGIOSELECTIVITY. <sup>A</sup> .....	120
TABLE 4.10. EFFECT OF ALKYNE IDENTITY ON ACETANILIDE REGIOSELECTIVITY. ....	121
TABLE 4.11. INFLUENCE OF ALKYNE EQUIVALENTS ON ACETANILIDE REGIOSELECTIVITY. ....	123
TABLE 4.12. DEPENDENCE OF ACID STRENGTH ON YIELD OF ALKYNE HYDROARYLATION PRODUCT. <sup>A</sup> .....	135

# Glossary of Abbreviations

Ac – acetyl	HPA/HPMV – heteropoly acid
acac – acetylacetonate	HRMS – high resolution mass spectrometry
AcO – acetate	L – generic ligand
AcOH – acetic acid	M – generic metal
<i>t</i> -AmOH – <i>tert</i> -amylalcohol	Me – methyl
Ar – generic aryl group	MOM – methoxymethyl
BHT – 2,6-di- <i>tert</i> -butyl-4-methylphenol	NMR – nuclear magnetic resonance
Bn – benzyl	NOESY – nuclear overhauser effect spectroscopy
Boc – <i>t</i> -butoxycarbonyl	[O] – generic oxidant
dtbpy – 2,6-di- <i>tert</i> -butylpyridine	Ph – phenyl group
<i>n</i> -Bu – <i>n</i> -butyl	Piv – pivaloyl
<i>t</i> -Bu – <i>t</i> -butyl	PivOH – pivalic acid
Bz – benzoyl	<i>n</i> -Pr – <i>n</i> -propyl
CDCl <sub>3</sub> – chloroform- <i>d</i> <sub>3</sub>	py – pyridine
CDK – cyclin dependant kinase	R – generic carbon containing group
CMD – concerted metallation-deprotonation	S <sub>E</sub> Ar – electrophilic aromatic substitution
COD – 1,5-cyclooctadiene	TBAF – <i>tetra</i> -butylammonium fluoride
COE – cyclooctene	TBS – <i>tert</i> -butyl-di-methylsilyl
COSY – correlation spectroscopy	Tf – trifluoromethanesulfonyl
Cp* – 1,2,3,4,5-pentamethylcyclopentadienyl	TFA – trifluoroacetic acid or trifluoroacetate
Cy – cyclohexyl	THF – tetrahydrofuran
DBU – 1,8-diazabicyclo[5.4.0]undec-7-ene	TIPS – <i>tri</i> -isopropylsilyl
DCE – 1,2-dichloroethane	TMB – trimethoxybenzene
DCM – dichloromethane	TMS – trimethylsilyl or tetramethylsilyl
DKIE – deuterium kinetic isotope effect	TON – turn over number
DMA – <i>N,N</i> -dimethylacetamide	Ts – <i>p</i> -toluenesulfonyl
DMAD – dimethylacetylenedicarboxylate	X – generic halide
DMF – <i>N,N</i> -dimethylformamide	°C – degrees Celsius
$E_{dist}$ – energy of distortion	
$E_{int}$ – energy of interaction	
$\Delta E^\ddagger/E_a$ – energy of activation	
Et – ethyl	
FG – generic functional group	
FTIR – Fourier transform infrared	
GCMS – gas chromatography mass spectrometry	
GSK – glycogen synthase kinase	
Het – generic aromatic heterocycle	
<i>n</i> -Hex – <i>n</i> -hexyl	
HMDS – hexamethyldisilazide	

# Introduction

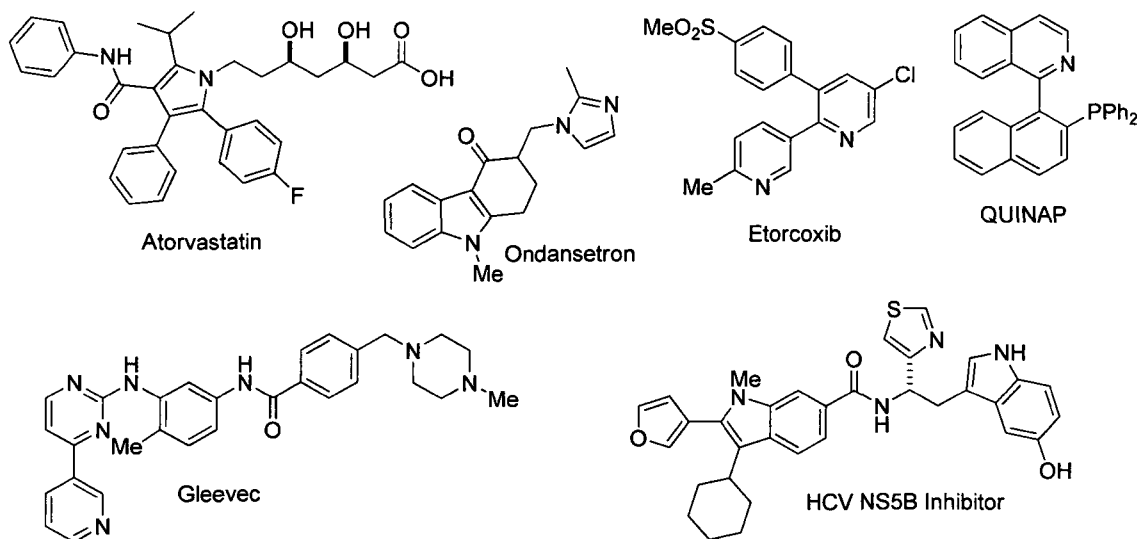
## 1.1. Construction and Functionalization of Heterocycles.

A recent survey of three leading pharmaceutical companies (GlaxoSmithKline, AstraZeneca, and Pfizer) containing a data set of 128 drug candidate molecules found that 88% of these contained aromatic heterocycles.<sup>1</sup> Of the drug candidates that accommodated aromatic heterocycles 95% of these heterocycles were nitrogen containing. Finally, approximately half of the heterocycles were purchased preformed and therein functionalized, where as the other half were synthesized as part of the synthetic route to the candidate molecule. Representative examples of important nitrogen containing heterocycles from the pharmaceutical and fine chemical sectors are shown in Figure 1.1. Thus, aromatic nitrogen containing heterocycles occupy a privileged position and the development of methods for both the efficient functionalization and preparation of these compounds from readily accessible, unfunctionalized starting materials is warranted.

---

<sup>1</sup> Carey, J. S.; Laffan, D.; Thomson, C.; Williams, M. T. *Org. Biomol. Chem.* **2006**, *4*, 2337.

**Figure 1.1.** Representative examples of nitrogen containing heterocycles of high utility.

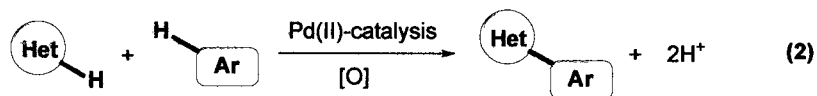
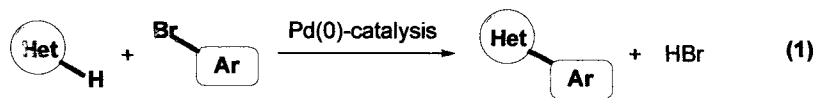


Transition metal catalysis has featured prominently in both of these veins, however, there has been a recent surge of interest in the development of catalytic methodologies aimed at conversion of C-H bonds to more highly oxidized functionality.<sup>2</sup> This body of work describes both the functionalization and preparation of aromatic *N*-heterocycles in this context (Scheme 1.1). First described is the advancement of palladium(0)-catalyzed direct arylation of quinoline and isoquinoline *N*-oxides (**Het**) with aryl bromides as a viable solution to the “2-azine organometallic problem” (Chapter 2, equation 1 of Scheme 1.1). This project serves in the formation of the pharmaceutically relevant 2-arylquinolines and 1-arylisquinolines. Following this is the development and mechanistic investigation of the palladium(II)-catalyzed oxidative cross-coupling of two unactivated arenes (Chapter 3, equation 2 of Scheme 1.1). Issues of regioselectivity are addressed and protocols for oxidative C2- and C3-arylation of *N*-pivaloyl and *N*-acetylindoles (**Het**), respectively, are described. Finally, the rhodium(III)-catalyzed oxidative coupling of acetanilides or enamides (**FG**) with alkynes (**FG'**) to form highly decorated indoles or pyrroles (**Het**), respectively, is described (Chapter 4, equation 3 of Scheme 1.1). An in-depth mechanistic evaluation of this oxidative indole-forming annulation process is also reported.

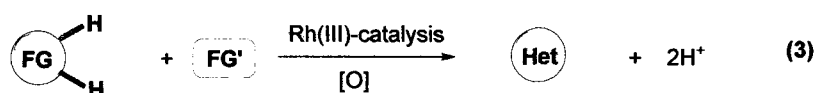
<sup>2</sup> For a review on transition metal catalyzed functionalization of heteroaromatics, see: (a) Seregin, I. V.; Gevorgyan, V. *Chem. Soc. Rev.* **2007**, *36*, 1173. (b) Lewis, J. C.; Bergman, R. G.; Ellman, J. A. *Acc. Chem. Res.* **2008**, *41*, 1013. For a general discussion of the utility of C-H bonds in organic synthesis, see: *Handbook of C-H Transformations: Applications in Organic Synthesis*, Dyker, G. ed. Wiley-VCH: Weinheim, **2005**.

**Scheme 1.1.** Overview of work described herein.

**Functionalization of Heterocycles:**



**Preparation of Heterocycles:**



## 1.2. Description of the Mechanistic Possibilities for Transition Metal Catalyzed C-H Bond Cleavage.

A common element to all of the reactions developed and described within this dissertation is the cleavage of a C( $sp^2$ )-H bond by a transition metal catalyst and so a general discussion of the possible mechanisms for this process is pertinent. Additionally, this discussion will be in the context of C-H bond cleavage at an aromatic substrate *via* palladium catalyzed direct arylation, although other processes involving C-H bond cleavage are described in Chapter 4. Direct arylation represents a convenient platform for the discussion of the mechanism of C-H bond cleavage simply due to the large number of mechanistic proposals that have been put forward to describe the manner in which this process takes place. The various possibilities are illustrated in Scheme 1.2 (A – D) and each pathway will be discussed in turn.

Electrophilic, nucleophilic, and electron-neutral metal species have been implicated in the mechanism of arene metallation to interact with aromatic substrates of varying electronic dispositions. In the field of direct arylation, historically, the hypothesis most

commonly suggested is electrophilic metallation.<sup>3</sup> This is often a leading proposal for processes involving electron-rich aromatics, though these proposals are rarely accompanied or validated by mechanistic work. An electrophilic metallation or electrophilic aromatic substitution ( $S_{EAr}$ ) type process (Scheme 1.2, path **A**) would involve nucleophilic attack by an arene on an electrophilic palladium(II) species to generate a Wheland intermediate. This would be followed by a fast deprotonation and reductive elimination of the biaryl product. A C-H activation (oxidative insertion) process (Scheme 1.2, path **C**), a much less common proposal, would involve oxidative addition of a palladium(II) species to a palladium(IV) species by insertion into a C-H bond of an aromatic substrate. While this process has been observed for low-valent late transition metals, such as rhodium(I),<sup>4</sup> it has only been proposed, with no substantial evidence for Pd(II).<sup>5</sup> The carbo-palladation, or Heck-type pathway, (Scheme 1.2, path **D**) first proposed for the direct arylation of 5-membered electron-rich heteroaromatics, is characterized by *syn*-addition of a palladium-carbon bond across a unit of unsaturation of an aromatic coupling partner. While *anti*- $\beta$ -hydride elimination is a high energy process, the formation of a  $\pi$ -allyl species that can stereochemically isomerize and accomplish a *syn*- $\beta$ -hydride elimination is suggested.<sup>6</sup> More recently, a concerted metallation-deprotonation (CMD) pathway (Scheme 1.2, path **B**) has received much attention in the literature.<sup>7</sup> This mechanism was originally proposed for the direct arylation of simple and electron-deficient arenes<sup>8</sup> where it was thought an  $S_{EAr}$  mechanism not possible. However, recently the CMD mechanism has been used to accurately describe experimental outcomes for a wide range of arenes including electron-rich

---

<sup>3</sup> This was originally proposed for the arylation of electron-rich heteroaromatics and has since been referenced approximately 100 times for other direct arylation reactions. Pivsa-Art, S.; Satoh, T.; Kawamura, Y.; Miura, M.; Nomura, M. *Bull. Chem. Soc. Jpn.*, **1998**, *71*, 467.

<sup>4</sup> Colby, D. A.; Bergman, R. G.; Ellman, J. A. *Chem. Rev.* **2009**, DOI: 10.1021/cr900005n.

<sup>5</sup> This mechanism has been proposed, but not experimentally confirmed, for Pd(II), see: Campo, M. A.; Huang, Q.; Yao, T.; Tian, Q.; Larock, R. C. *J. Am. Chem. Soc.* **2003**, *125*, 11506.

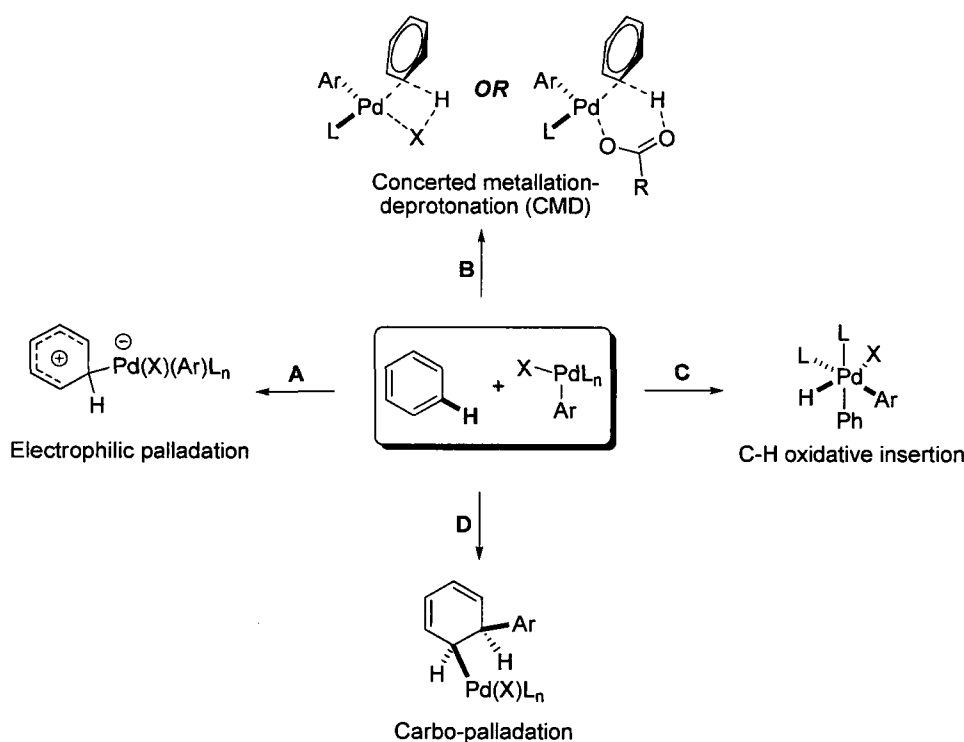
<sup>6</sup> This mechanism has been proposed as a mechanistic possibility, see: (a) Toyota, M.; Ilangovan, A.; Okamoto, R.; Masaki, T.; Arakawa, M.; Ihara, M. *Org. Lett.* **2002**, *4*, 4293. This mechanism has also been proposed but dismissed, see: (b) Hennessy, E. J.; Buchwald, S. L. *J. Am. Chem. Soc.* **2003**, *125*, 12084.

<sup>7</sup> A CMD pathway may be characterized by a 4 or 6-membered transition state. A 4-membered transition state may be more specifically termed a  $\sigma$ -bond metathesis, where as a 6-membered transition state does not fall into this classification.

<sup>8</sup> This mechanism has been proposed for simple and electron deficient arenes, see: (a) Lafrance, M.; Rowley, C. N.; Woo, T. K.; Fagnou, K.; *J. Am. Chem. Soc.* **2006**, *128*, 8754; (b) Lafrance, M.; Fagnou, K.; *J. Am. Chem. Soc.* **2006**, *128*, 16496 (c) Garcia-Cuadrado, D.; Braga, A. A. C.; Maseras, F.; Echavarren, A. M.; *J. Am. Chem. Soc.* **2006**, *128*, 1066; (d) Garcia-Cuadrado, D.; de Mendoza, P.; Braga, A. A. C.; Maseras, F.; Echavarren, A. M.; *J. Am. Chem. Soc.* **2007**, *129*, 6880.

aromatics originally believed to react with palladium *via*  $S_EAr$ .<sup>9</sup> In a CMD pathway palladium-carbon bond formation takes place concurrent with cleavage of the C-H bond of the arene and loss of HX. While this concerted mechanism may appear as an intercepted Wheland intermediate, the defining difference between a CMD pathway and an  $S_EAr$  pathway is the absence of any carbocation character or loss of aromaticity on the simple arene. The evolution of the CMD transition state will be elaborated on to provide context for the mechanistic discussions that follow in Chapters 2 – 4.

**Scheme 1.2.** Potential routes for C-H bond cleavage.



### 1.3. Evolution of the Concerted Metallation Deprotonation (CMD) Transition State.

The concerted metallation-deprotonation (CMD) transition state has a much more rich history than palladium catalyzed direct arylation and dates back to mechanistic

<sup>9</sup> Gorelsky, S. I.; Lapointe, D.; Fagnou, K. *J. Am. Chem. Soc.* **2008**, *130*, 10848.

proposals for the stoichiometric mercuration of arenes in the 1950's and '60's.<sup>10</sup> However, the recent interest in direct arylation as a viable synthetic tool has resulted in considerable mechanistic scrutiny of this reaction, and the CMD pathway, as well as S<sub>E</sub>Ar, have emerged as the most likely mechanistic scenarios. For this reason, and the intensified use of computational methods in mechanistic investigations, the nature of the CMD transition state has evolved dramatically.

In Kresge and Brown's investigation of the stoichiometric mercuration of arenes, an in-depth mechanistic analysis, including kinetic studies, lead to an intramolecular 6-membered transition state which "presents an attractive route for ejection of the acetate".<sup>10d</sup> The transition state depicted by Kresge and Brown (Scheme 1.3) provides little structural information regarding the arene, however, their detailed kinetic studies revealed a preference for reaction of electron-rich aromatics over those that are electron-deficient. Additionally, the C-H bond cleavage was associated with a large primary deuterium kinetic isotope effect (DKIE) of ~ 6, a value of significant magnitude and typically not associated with an S<sub>E</sub>Ar mechanism.<sup>11</sup> Thus, they concluded their investigation with a proposal for a concerted transition state which has newly garnered the name concerted metallation-deprotonation (CMD). In the 1980's, after a detailed mechanistic study of the cyclopalladation of *N,N*-dimethylbenzylamine, Ryabov arrived at essentially the same mechanistic conclusion as Kresge and Brown, and stated "... a tight highly ordered transition state in which the leaving hydrogen is abstracted by acetate..." is operative (Scheme 1.3).<sup>12</sup> Similar to Kresge and Brown, Ryabov observed a preponderance of electron-rich benzylamines to react over electron-deficient ones ( $\rho = -1.6$  when  $\sigma_{meta}$  used) and a modest DKIE of 2.2 was obtained.

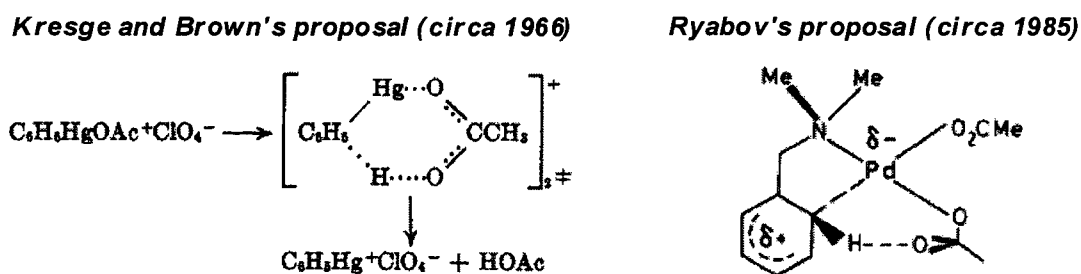
---

<sup>10</sup> (a) Brown, H. C.; McGary, Jr., C. W. *J. Am. Chem. Soc.* **1955**, *77*, 2306. (b) Winstein, S.; Traylor, T. G. *J. Am. Chem. Soc.* **1955**, *77*, 3747. (c) de la Mare, P. B. D.; Hilton, I. C.; Varma, S. *J. Chem. Soc.* **1960**, 4044. (d) Kresge, A. J.; Dubeck, M.; Brown, H. C. *J. Org. Chem.* **1966**, *32*, 745. (e) Kresge, A. J.; Brennan, J. F. *J. Org. Chem.* **1966**, *32*, 752.

<sup>11</sup> Though DKIE's are not typically associated with S<sub>E</sub>Ar it has been observed in some cases, such as the sulfonation of nitrobenzene (DKIE of ~1.6) see: Brand, J. C. D.; Jarvie, A. W. P.; Horning, W. C. *J. Chem. Soc.* **1959**, 3844.

<sup>12</sup> Ryabov, A. D.; Sakodinskaya, I. K.; Yatsimirsky, A. K. *J. Chem. Soc., Dalton Trans.* **1985**, 2629.

**Scheme 1.3.** Proposals taken from the original reports by Kresge and Brown<sup>10e</sup> and Ryabov.<sup>12</sup>



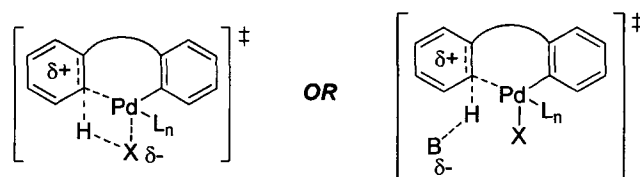
While Kresge and Brown's proposal is relatively uninformative with respect to the arene, Ryabov portrays a partial positive charge (early Wheland intermediate) on the arene. Twenty years after Ryabov's work on this system, Davies and Macgregor computationally investigated the validity of his proposal.<sup>13</sup> They quantitatively confirmed, *via* computations, the experimentally observed Hammett correlation and the modest DKIE obtained by Ryabov. However, their theoretical findings on the mechanism and structure of the transition state were characterized by a rate determining agostic interaction of an aromatic C-H bond with palladium, followed by a concerted proton transfer from the arene to coordinated acetate. Furthermore, at no point did they find any significant evidence for contribution from a Wheland intermediate. One year later, Davies and Macgregor investigated the mechanism of C-H bond cleavage for the same aromatic system, *N,N*-dimethylbenzylamine, with the  $[\text{Cp}^*\text{Ir}(\text{OAc})]^+$  fragment.<sup>14</sup> Once more, there was no evidence for contribution from a Wheland intermediate and they arrived at the same concerted transition state in which proton transfer from the arene to acetate takes place. However, in this case they observed very little evidence for an agostic interaction of the C-H bond with iridium. Thus, with the assistance of computational chemistry, the CMD pathway has evolved from an intercepted Wheland intermediate to the concerted transition state which characterizes it today. Moreover, these studies demonstrate that consideration of the CMD reaction coordinates must include the aromatic substrate, metal center, and ligand environment of the metal.

<sup>13</sup> Davies, D. L.; Donald, S. M. A.; Macgregor, S. A. *J. Am. Chem. Soc.* **2005**, *127*, 13754.

<sup>14</sup> Davies, D. L.; Donald, S. M. A.; Al-Duaij, O.; Macgregor, S. A.; Pölleth, M. *J. Am. Chem. Soc.* **2006**, *128*, 4210.

At about the same time, Fagnou and co-workers, along with a host of other researchers, proposed a similar concerted transition state to account for a lack of strong electronic bias in the intramolecular direct arylation of simple arenes (Figure 1.2).<sup>15</sup> This group has gone on to develop intermolecular direct arylation protocols for aromatic substrates previously believed to lack the electronic requirements for intermolecular reactivity, such as simple and electron-deficient arenes.<sup>16</sup> Within these reports, Fagnou and his collaborators have closely examined the structural and electronic requirements for the CMD transition state.<sup>8a,b,9</sup> The direct arylation of pentafluorobenzene, an extremely electron deficient arene, was found computationally to have a low-energy CMD transition state (Figure 1.3) and all correlations to available experimental data (DKIE and competition experiments) validated this proposal. Central to this proposal was the observation that relative rates of reactivity paralleled C-H bond acidity and that more electron-deficient arenes reacted preferentially, thus further distancing the CMD mechanism from an S<sub>E</sub>Ar mechanism.

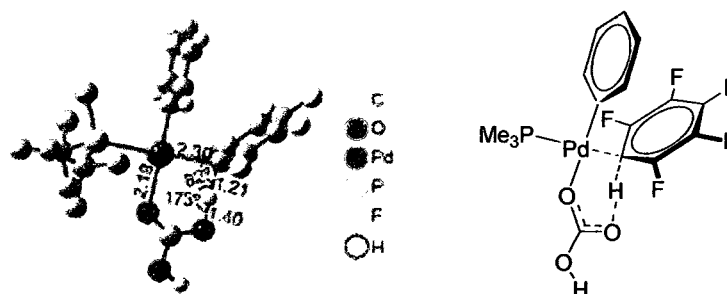
**Figure 1.2.** Fagnou's proposal for the mechanism of C-H bond cleavage in intramolecular direct arylation.



<sup>15</sup> (a) Gonzalez, J. J.; Garcia, N.; Gomez-Lor, B.; Echavarren, A. M. *J. Org. Chem.* **1997**, *62*, 1286. (b) Martin-Matute, B.; Matea, C.; Cardenas, D. J.; Echavarren, A. M. *Chem. Eur. J.* **2001**, *7*, 234. (c) Campeau, L. C.; Parisien, M.; Leblanc, M.; Fagnou, K. *J. Am. Chem. Soc.* **2004**, *126*, 9186. (d) Mota, A. J.; Dedieu, A.; Bour, C.; Suffert, J. *J. Am. Chem. Soc.* **2005**, *127*, 7171. (e) Campeau, L. C.; Parisien, M.; Jean, A.; Fagnou, K. *J. Am. Chem. Soc.* **2006**, *128*, 581. (f) Özdemir, I.; Demir, S.; Çetinkaya, B.; Gourlaouen, C.; Maseras, F.; Bruneau, C.; Dixneuf, P. H. *J. Am. Chem. Soc.* **2008**, *130*, 1156.

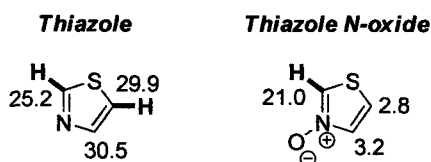
<sup>16</sup> (a) Campeau, L. C.; Rousseaux, S.; Fagnou, K. *J. Am. Chem. Soc.* **2005**, *127*, 18020. (b) Leclerc, J. P.; Fagnou, K. *Angew. Chem. Int. Ed.* **2006**, *45*, 7781. (c) Campeau, L. C.; Bertrand-Laperle, M.; Leclerc, J.-P.; Villemure, E.; Gorelsky, S.; Fagnou, K. *J. Am. Chem. Soc.* **2008**, *130*, 3276. (d) Caron, L.; Campeau, L. C.; Fagnou, K. *Org. Lett.* **2008**, *10*, 4533. (e) Campeau, L.-C.; Stuart, D. R.; Leclerc, J.-P.; Bertrand-Laperle, M.; Villemure, E.; Sun, H.-Y.; Lasserre, S.; Guimond, N.; Lecavallier, M.; Fagnou, K. *J. Am. Chem. Soc.* **2009**, *131*, 3291. Also, see ref 8a,b.

**Figure 1.3.** CMD transition state for the direct arylation of pentafluorobenzene.<sup>8a</sup>



Perhaps one of the most impressive features, thus far, of the CMD mechanism is its ability to accurately predict the regioselective outcome in reactions complicated by poor regioselectivity. The direct arylation of azole substrates was previously believed to be governed by azole  $\pi$ -nucleophilicity resulting in C5-arylation and C-H acidity resulting C2-arylation; and while C5-arylation is generally preferred, C5/C2-diarylation side products are often observed.<sup>17</sup> As part of a program that employs *N*-oxide activation of azine heterocycles, the Fagnou group has detailed the development of sequential C2, C5, C4-direct arylation of thiazole *N*-oxide and the CMD transition state accurately predicts this relative reactivity profile.<sup>16c</sup> In addition to this, an interesting relationship between the relative regioselectivity and relative contribution of each carbon atom to the HOMO of the heterocycle was revealed by molecular orbital analysis (Figure 1.4). Therefore, *this study suggests that both the relative electron density and C-H acidity may be operative in the CMD transition state.*

**Figure 1.4.** Contribution of each carbon atom to the HOMO of thiazole and thiazole *N*-oxide.<sup>16b</sup>



<sup>17</sup> See ref. 15b and references therein.

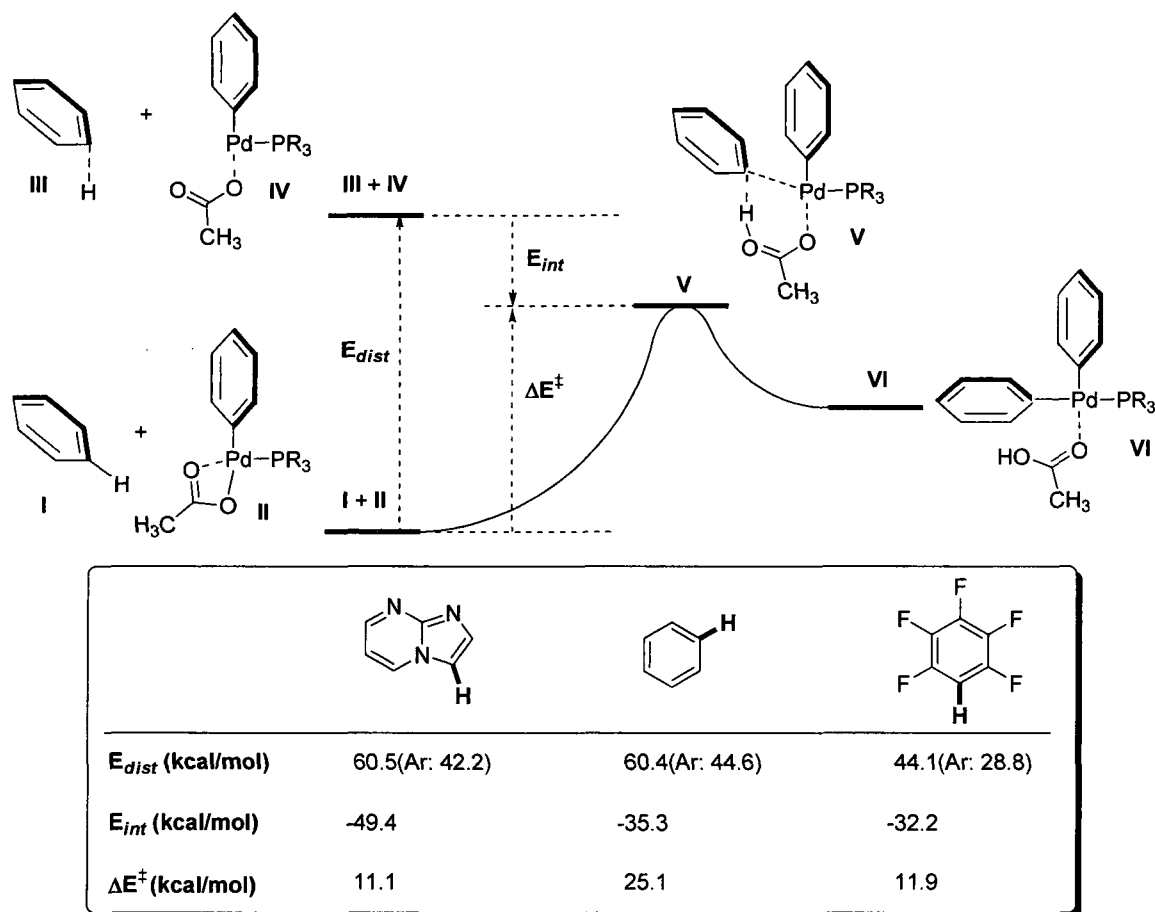
Recognizing that multiple arene properties may influence the nature/structure of the CMD transition state, an activation-strain analysis<sup>18</sup> was applied to this mechanism in order to cast light on its applicability to a broad range of electronically dissimilar arenes.<sup>9</sup> In this form of analysis the individual energy of distortion ( $E_{dist}$ ) of each component is the loss in energy incurred due to the distortion from the ground-state structure to the conformation necessary for the transition state (**I**  $\rightarrow$  **III** and **II**  $\rightarrow$  **IV**; Figure 1.5). Additionally, the energy of interaction ( $E_{int}$ ) is a result of bringing the two distorted structures together (**III** + **IV**  $\rightarrow$  **V**; Figure 1.5). The energy loss ( $E_{dist}$ ) and gain ( $E_{int}$ ) together provide the overall activation energy of the transition state ( $\Delta E^\ddagger$ ) and therefore allows for an evaluation of the contribution of each component individually. While  $E_{int}$  appears to be directly related to the available electron-density, and therefore nucleophilicity, of the arene,  $E_{dist}$  seems to parallel C-H bond acidity in many cases but is not necessarily governed by it. The representative examples, shown below the energy diagram, illustrate that the electron-rich triazole has a relatively large energy of distortion (42.2 kcal/mol), but, also a large energy gain from a strong energy of interaction ( $E_{int} = -49.4$  kcal/mol) and this directly reflects the available electron-density of the arene. Additionally, the electron-deficient pentafluorobenzene has a very low  $E_{dist}$  of 28.8 kcal/mol (for the arene), but this is not well compensated by a relatively low  $E_{int}$  of -32.2 kcal/mol; thus confirming the lack of electron density of this arene, but its ready ability to distort. Therefore, the overall energy of the transition state for the triazole and pentafluorobenzene are very similar at 11.1 and 11.9 kcal/mol, respectively. In one case this is due to a large stabilizing  $E_{int}$  of the nucleophilic arene and in the other case due to a low  $E_{dist}$  of the electron-deficient arene. Benzene is characterized by an unfavorably high energy of distortion and a poor energy of interaction in both cases and these energy values together, therefore, result in the highest activation energy of the arenes investigated by Fagnou and Gorelsky.<sup>9</sup> Finally, considering the CMD mechanism in this way sheds some light on the experimental results of Kresge and Brown<sup>10e</sup> and Ryabov.<sup>12</sup> The modest negative  $\rho$ -value obtained from Hammett correlations, in each of their studies, need not necessarily point

---

<sup>18</sup> For a recent example of this method of analysis applied to palladium-catalyzed cross-coupling reactions, see: Legault, C. Y.; Garcia, Y.; Merlic, C. A.; Houk, K. N. *J. Am. Chem. Soc.* **2007**, *129*, 12664, and references therein.

toward a Wheland intermediate,<sup>19</sup> but rather a large stabilizing  $E_{int}$  (arene nucleophilicity) in the CMD pathway. As well, the presence of a DKIE is indicative of the concerted nature of the CMD transition state, and the relative magnitude is a function of the geometry (linearity) of that transition state.

**Figure 1.5.** Activation-strain analysis applied to the CMD pathway.



The pioneering experimental work by Kresge and Brown and Ryabov, as well as, the improvements made by Davies and Macgregor and Fagnou and Gorelsky, as well as many other researchers, to this mechanistic proposal has demonstrated the applicability of the CMD transition state over an electronically diverse set of arenes. Moreover, the pertinent

<sup>19</sup> Hammett plots for reactions known to proceed *via* an electrophilic aromatic substitution pathway are: bromination ( $\rho = -12.1$ ), chlorination ( $\rho = -8.1$ ), and Friedel-Crafts ethylation ( $\rho = -2.4$ ), see: Fujiwara, Y.; Asano, R.; Moritani, I.; Teranishi, S. *J. Org. Chem.* **1976**, *41*, 1681, and references therein.

literature described in this chapter should provide a solid platform for the presentation and discussion of mechanistic evaluations put forth in Chapters 3 and 4.

# Palladium(0) Catalyzed Direct Arylation of Azine *N*-Oxides

## 2.1. Introduction

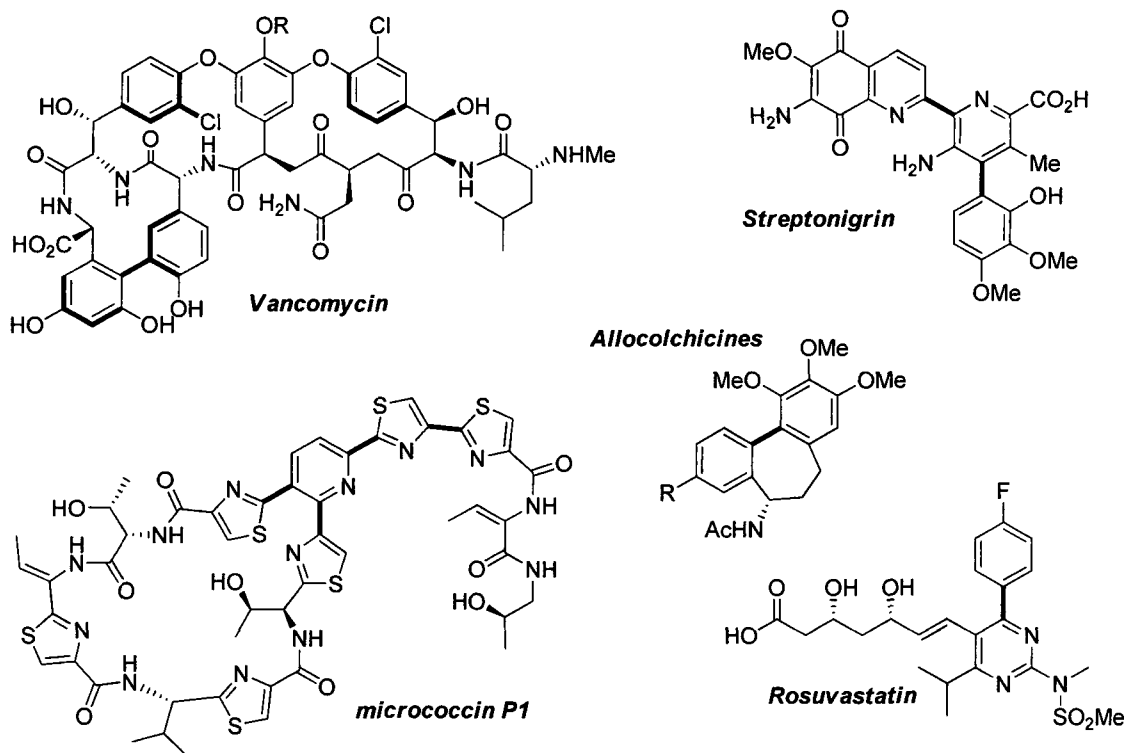
The preparation of biaryl molecules is merited by their pervasiveness in biologically active natural products and pharmaceuticals<sup>20</sup> (Figure 2.1) and efforts towards this end have been ongoing for over a century. For the past half century palladium(0) catalysis has dominated the field largely due to the high yields, exclusive chemoselectivity, and, more recently, very mild conditions under which reactions may be conducted. This branch of palladium-catalysis has been extensively documented and reviewed in the literature<sup>21</sup> and as a result only a brief discussion of its underlying concepts will be given in order to provide context for the advancement of direct arylation.

---

<sup>20</sup> (a) Horton, D. A.; Bourne, G. T.; Smythe, M. L. *Chem. Rev.* **2003**, *103*, 893. (b) Bringmann, G.; Mortimer, A. J. P.; Keller, P. A.; Gresser, M. J.; Breuning, M. *Angew. Chem. Int. Ed.* **2005**, *44*, 5384.

<sup>21</sup> (a) Hassan, J.; Svignon, M.; Gozzi, C.; Schultz, E.; Lemaire, M. *Chem. Rev.* **2002**, *102*, 1359. (b) *Metal-Catalyzed Cross-Coupling Reactions*; Diederich, F.; Stang, P. J., Eds.; Wiley-VCH: New York, **2004**.

**Figure 2.1.** Biaryl natural products and pharmaceuticals.



Traditional palladium-catalyzed cross-coupling employs two pre-activated arenes in the form of an aryl halide (or pseudo-halide) and an aryl organometallic, such as a boronic acid (or ester),<sup>22</sup> stannane,<sup>23</sup> Grignard,<sup>24</sup> or organo-zinc reagent.<sup>25</sup> This pre-activation enables the catalyst to afford the biaryl product as an exclusive regioisomer. However, this approach is not devoid of the challenges associated with regioselectivity as they are encountered at the installation of the pre-activating groups. Pre-activated arenes are typically prepared from simple arenes and the installation of these functional groups leads to additional steps, time, and cost of a synthetic sequence, if the substrate is not commercially available. Furthermore, the stability of the organometallic component under certain reaction conditions represents a significant drawback to these types of cross-couplings in addition to

<sup>22</sup> (a) Miyaura, N.; Yamada, K.; Suzuki, A. *Tetrahedron Lett.* **1979**, *20*, 3737. (b) Miyaura, N.; Suzuki, A. *Chem. Rev.* **1995**, *95*, 2457.

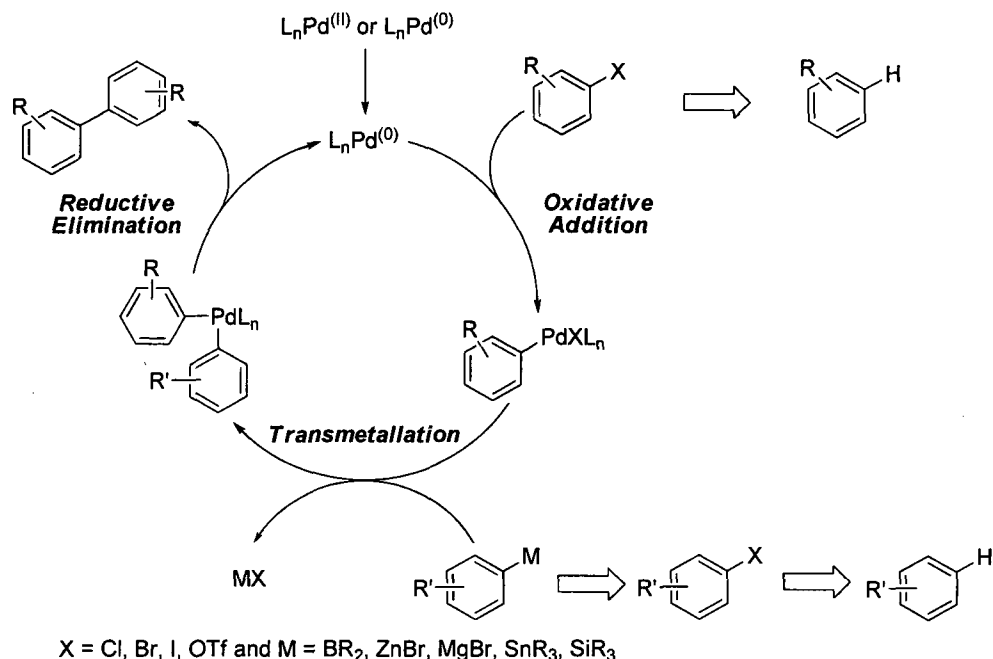
<sup>23</sup> Milstein, D.; Stille, J. K. *J. Am. Chem. Soc.* **1978**, *100*, 3636.

<sup>24</sup> Tamao, K.; Kiso, Y.; Sumitani, K.; Kumada, M. *J. Am. Chem. Soc.* **1972**, *94*, 9268.

<sup>25</sup> Baba, S.; Negishi, E. *J. Am. Chem. Soc.* **1976**, *98*, 6729.

the stoichiometric amount of, in some cases toxic, metal waste that is produced (Scheme 2.1).

**Scheme 2.1.** Catalytic cycle for traditional palladium-catalyzed cross-coupling.



Over the past three decades chemists have focused on the replacement of one of the two coupling partners with a simple arene in order to increase efficiency and reduce waste in the formation of biaryls. As previously described, this innovation in palladium catalysis has been termed direct arylation and has been extensively reviewed in the literature.<sup>26</sup> While methods exist in which one of the two coupling partners are replaced with a simple arene the most common variation is the replacement of the aryl organometallic with a simple arene (Scheme 2.2). This serves three purposes: 1) aryl halides are more commercially abundant, where as aryl organometallics are more difficult to prepare, or potentially unstable under the reaction conditions; 2) the only waste produced is a haloacid, HX; and 3) an oxidant is not

<sup>26</sup> For general reviews on direct arylation, please see: (a) Alberico, D.; Scott, M. E.; Lautens, M. *Chem. Rev.* **2007**, *107*, 174. (b) Campeau, L.-C.; Stuart, D. R.; Fagnou, K. *Aldrichmica Acta* **2007**, *40*, 35. For a review on direct arylation/functionalization of heteroaromatics, see: ref. 2a. For reviews on direct arylation/functionalization of heterocycles with rhodium(I), see: ref. 4

required for catalyst turn-over.<sup>27</sup> However, while this innovation introduces enhanced efficiency to the reaction it also introduces the issue of C-H bond regioselectivity. Since the advent of direct arylation, chemists have been devising methods to secure products from these reactions as single regioisomers. The two major avenues that have emerged to this end are the use of Lewis basic directing groups and the use of arenes that have a pre-disposition to regioselective palladation as a result of the electronic properties of the arene. The ability of pendant Lewis basic directing groups to induce a regioselective cyclometallation<sup>28</sup> has been exploited in the direct arylation of benzene derivatives, and will not be discussed in this introduction.<sup>29,30,31,32,33</sup> The subject of this thesis is the functionalization and preparation of heterocycles and therefore this introduction will focus on the direct arylation of both  $\pi$ -rich and  $\pi$ -deficient heterocycles, and in particular,  $\pi$ -deficient azine heterocycles.

---

<sup>27</sup> Palladium-catalyzed direct arylation between a simple arene and an aryl organometallic, under a Pd(II)/Pd(0) manifold, requires an oxidant for catalyst turn-over.

<sup>28</sup> For a review on cyclometallation please see: Ryabov, A. D. *Chem. Rev.* **1990**, *90*, 403.

<sup>29</sup> For representative reports using phenols/alcohols, see: (a) Satoh, T.; Kawamura, Y.; Miura, M.; Nomura, M. *Angew. Chem. Int. Ed.* **1997**, *36*, 1740. (b) Satoh, T.; Inoh, J.-I.; Kawamura, Y.; Miura, M.; Nomura, M. *Bull. Chem. Soc. Jpn.* **1998**, *71*, 2239. (c) Kawamura, Y.; Satoh, T.; Miura, M.; Nomura, M. *Chem. Lett.* **1999**, 961. (d) Kawamura, Y.; Satoh, T.; Miura, M.; Nomura, M. *Chem. Lett.* **1998**, 931. (e) Bedford, R. B.; Coles, S. J.; Hursthouse, M. B.; Limmert, M. E. *Angew. Chem., Int. Ed.* **2003**, *42*, 112. (f) Bedford, R. B.; Limmert, M. E. *J. Org. Chem.* **2003**, *68*, 8669. (g) Oi, S.; Watanabe, S.-I.; Fukita, S.; Inoue, Y. *Tetrahedron Lett.* **2003**, *44*, 8665. (h) Terao, Y.; Wakui, H.; Satoh, T.; Miura, M.; Nomura, M. *J. Am. Chem. Soc.* **2001**, *123*, 10407. (i) Terao, Y.; Wakui, H.; Nomoto, M.; Satoh, T.; Miura, M.; Nomura, M. *J. Org. Chem.* **2003**, *68*, 5236.

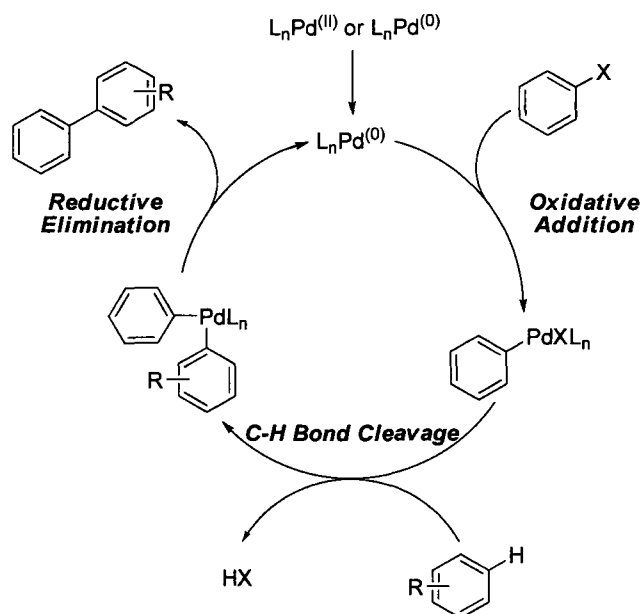
<sup>30</sup> For representative reports using ketones, see (a) Satoh, T.; Kametani, Y.; Terao, Y.; Miura, M.; Nomura, M. *Tetrahedron Lett.* **1999**, *40*, 5345. (b) Satoh, T.; Miura, M.; Nomura, M. *J. Organomet. Chem.* **2002**, *653*, 151. (c) Terao, Y.; Kametani, Y.; Wakui, H.; Satoh, T.; Miura, M.; Nomura, M. *Tetrahedron* **2001**, *57*, 5967. (d) Kakiuchi, F.; Kan, S.; Igi, K.; Chatani, N.; Murai, S. *J. Am. Chem. Soc.* **2003**, *125*, 1698. (e) Kakiuchi, F.; Matsuura, Y.; Kan, S.; Chatani, N. *J. Am. Chem. Soc.* **2005**, *127*, 5936.

<sup>31</sup> For representative reports using amides/anilides, see : (a) Kametani, Y.; Satoh, T.; Miura, M.; Nomura, M. *Tetrahedron Lett.* **2000**, *41*, 2655. (b) Kalyani, D.; Deprez, N. R.; Desai, L. V.; Sanford, M. S. *J. Am. Chem. Soc.* **2005**, *127*, 7330.

<sup>32</sup> For representative reports using imines, see: (a) Oi, S.; Ogino, Y.; Fukita, S.; Inoue, Y. *Org. Lett.* **2002**, *4*, 1783. (b) Ackermann, L. *Org. Lett.* **2005**, *7*, 3123. (c) Ueura, K.; Satoh, T.; Miura, M. *Org. Lett.* **2005**, *7*, 2229.

<sup>33</sup> For representative reports using pyridines, quinolines and other heterocycles, see: (a) ref. 13b. (b) Shabashov, D.; Daugulis, O. *Org. Lett.* **2005**, *7*, 3657. (c) Zaitsev, V. G.; Shabashov, D.; Daugulis, O. *J. Am. Chem. Soc.* **2005**, *127*, 13154. (d) Oi, S.; Fukita, S.; Hirata, N.; Watanuki, N.; Miyano, S.; Inoue, Y. *Org. Lett.* **2001**, *3*, 2579. (e) Ackermann, L.; Althammer, A.; Born, R. *Angew. Chem., Int. Ed.* **2006**, *45*, 2619.

**Scheme 2.2.** General catalytic cycle for direct arylation with an aryl halide and a simple arene.



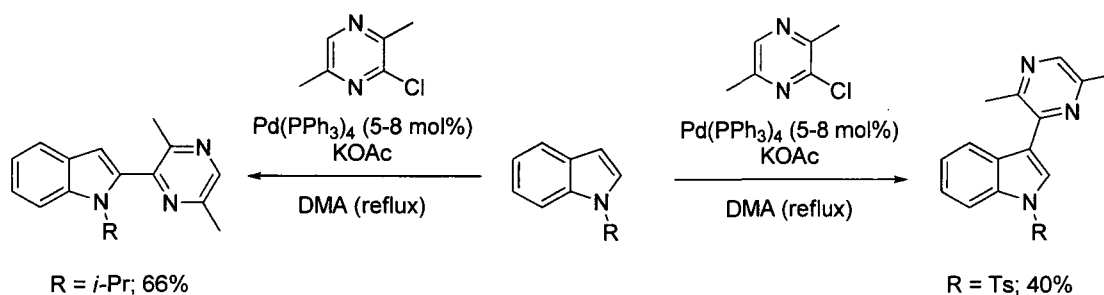
### 2.1.1. Direct Arylation of $\pi$ -Rich Heterocycles.

The direct arylation of  $\pi$ -rich heterocycles has a rich history and has received considerable attention from the direct arylation community since its origins.<sup>26</sup> This is perhaps a consequence of the typically good regioselectivity observed for these compounds in direct arylation reactions, which was originally proposed to be a result of the inherent nucleophilicity of the individual heterocycles.<sup>3</sup> As previously described in Chapter 1 (*vide supra*), the inherent nucleophilicity is only one physical parameter that contributes to the ability to perform direct arylation on  $\pi$ -rich heterocycles. Additionally, invoking a CMD transition state in the direct arylation of  $\pi$ -rich heterocycles accurately predicts experimentally observed regioselectivity.<sup>9</sup> A number of these heterocycles have been found to undergo efficient direct arylation and these include: indoles and indolazines, pyrroles, oxazoles and benzoxazoles, imidazoles and benzimidazoles, thiazoles and benzothiazoles, thiophenes and benzothiophenes, and furans and benzofurans.<sup>26</sup> Palladium is primarily used as the catalyst in these processes, though other metals have been featured in this capacity. Although palladium is typically the catalyst of choice, reaction conditions vary widely from heterocycle to heterocycle; and, even within the same class of heterocycle family, conditions

vary depending on the desired regioselectivity. Representative examples will be presented from the literature to convey the breadth of heterocycles used in direct arylation and to demonstrate the variation in reaction conditions.

**Indoles and pyrroles in direct arylation.** Indoles are one of the most prevalent heterocycles explored in direct arylation reactions, likely due to the vast number of biologically active compounds that contain this motif. One of the most sought after goals in indole direct arylation is the ability to dictate C3 or C2-arylation. Ohta reported the first example of an intermolecular direct arylation of indoles with chloropyrazines.<sup>34</sup> The authors found that when the indole nitrogen was left unprotected or alkyl-protected the C2-arylation product could be obtained in modest yield; however when the tosyl-protected indole was used isolation of the C3-arylation product was achieved (Scheme 2.3). This methodology was also found to be applicable to the direct arylation of pyrroles.<sup>35</sup>

**Scheme 2.3.** Ohta's regioselective direct arylation of indoles.



Sames has more recently reported indole direct arylation protocols employing both palladium<sup>36</sup> and rhodium<sup>37</sup> as catalysts. The reactions proved to be more selective for C2-arylation though variation of the steric bulk of the arylhalide provided low ratios of C3 : C2-arylated products (Scheme 2.4). Sanford has reported a very mild C2-selective arylation of indoles utilizing her Pd(II)/Pd(IV) methodology (Scheme 2.5), which could also be extended

<sup>34</sup> Akita, Y.; Itagaki, Y.; Takizawa, S.; Ohta, A. *Chem. Pharm. Bull.* **1989**, *37*, 1477.

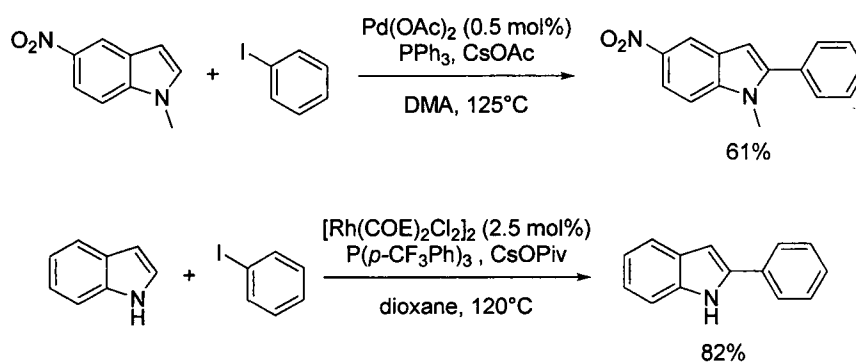
<sup>35</sup> Aoyagi, Y.; Inoue, A.; Koizumi, I.; Hashimoto, R.; Tokunaga, K.; Gohma, K.; Komatsu, J.; Sekine, K.; Miyafuji, A.; Kunoh, J.; Honma, R.; Akita, Y.; Ohta, A. *Heterocycles* **1992**, *33*, 257.

<sup>36</sup> (a) Lane, B. S.; Brown, M. A.; Sames, D. *J. Am. Chem. Soc.* **2005**, *127*, 8050. (b) Lane, B. S.; Sames, D. *Org. Lett.* **2004**, *6*, 2897. (c) Touré, B. B.; Lane, B. S.; Sames, D. *Org. Lett.* **2006**, *8*, 1979.

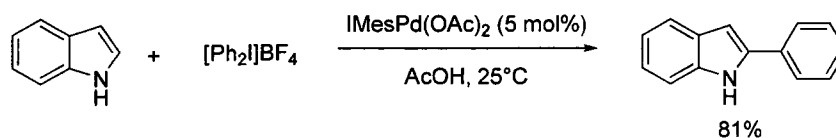
<sup>37</sup> Wang, X.; Lane, B. S.; Sames, D. *J. Am. Chem. Soc.* **2005**, *127*, 4996.

to C2-selective arylation of pyrroles.<sup>38</sup> Gaunt has more recently employed copper-catalysis for the direct arylation of indoles. An Ar-Cu(III)-species is formed *in situ via* oxidation of a Cu(I)-catalyst by a hypervalent iodine reagent, which is also the source of the aryl group that is transferred in the process (Scheme 2.6).<sup>39</sup> The authors postulate that the *N*-acetyl group may have a directing effect and favor a C3,C2-copper migration resulting in the complementary regioselectivity observed for the two different protocols (Scheme 2.6).

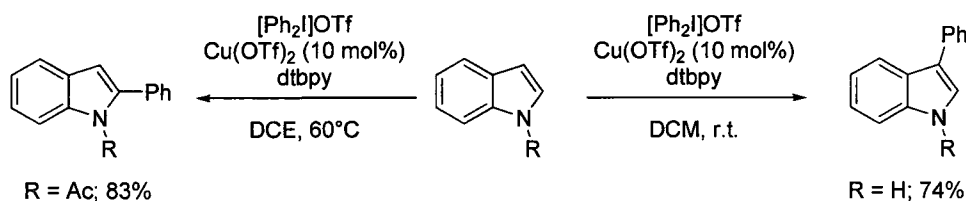
**Scheme 2.4.** Sames' C2-selective direct arylation of indole catalyzed by palladium and rhodium.



**Scheme 2.5.** Sanford's direct arylation of indoles *via* Pd(II)/Pd(IV) manifold.



**Scheme 2.6.** Gaunt's copper-catalyzed direct arylation of indoles.



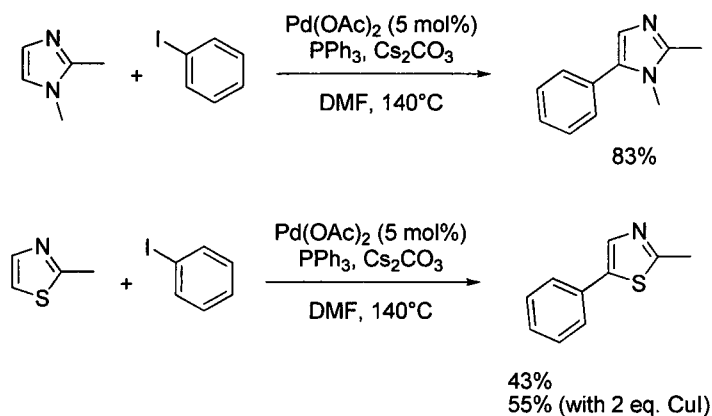
**Other  $\pi$ -rich heterocycles in direct arylation.** Oxazoles, thiazoles, and imidazoles have all been used extensively in direct arylation reactions. Miura has pioneered the use of many  $\pi$ -rich heterocycles in direct arylation reactions.<sup>3</sup> C5-Arylation was achieved in the direct arylation of imidazoles and thiazoles and in some cases increased yields were obtained

<sup>38</sup> Deprez, N. R.; Kalyani, D.; Krause, A.; Sanford, M. S. *J. Am. Chem. Soc.* **2006**, *128*, 4972

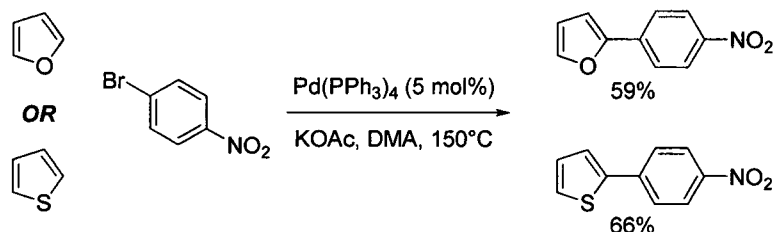
<sup>39</sup> Phipps, R. J.; Grimster, N. P.; Gaunt, M. J. *J. Am. Chem. Soc.* **2008**, *130*, 8172.

by the addition of CuI (Scheme 2.7). Numerous other researchers have worked on the direct arylation of  $\pi$ -rich 5-membered heterocycles as well as their derivatives and the reader is directed to comprehensive reviews on the subject.<sup>26c,d</sup> Ohta, and others, have developed conditions for the successful direct arylation of thiophene, furan, and their benzo-derivatives (Scheme 2.8).<sup>40</sup>

**Scheme 2.7.** Miura's direct arylation of imidazole and thiazole.



**Scheme 2.8.** Ohta's direct arylation of furan and thiophene.



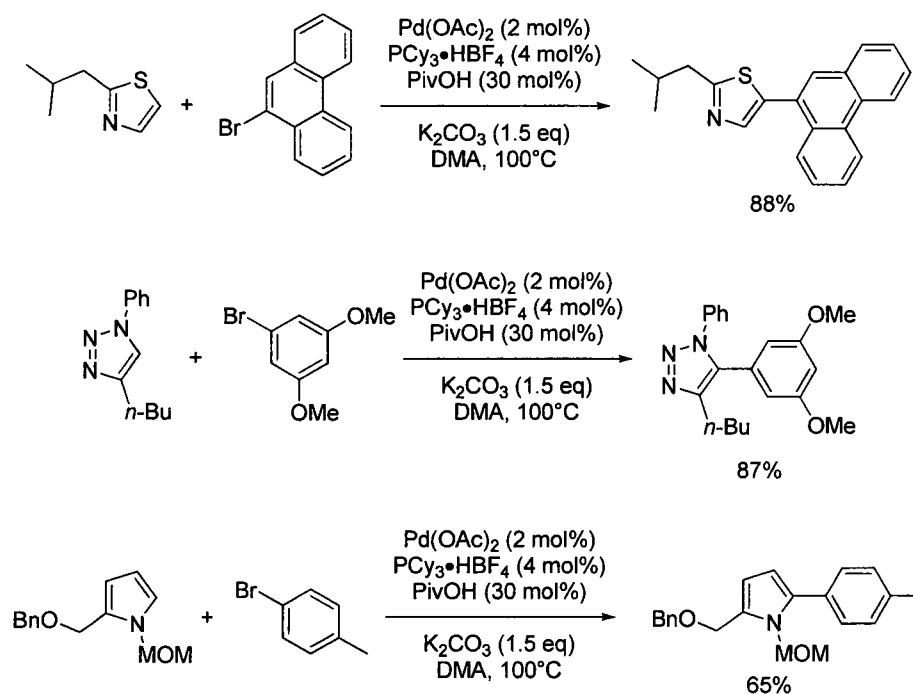
**Development of general reaction conditions for direct arylation of heterocycles.** It is evident from the preceding sections that there are a large number of reaction conditions for the direct arylation of  $\pi$ -rich heterocycles. Pursuant to the goal of recognizing a common mechanism for direct arylation, Fagnou has developed a set of conditions for a wide range of  $\pi$ -rich heterocycles with two main objectives.<sup>41</sup> First amongst these targets was for the reaction conditions to be as generally applicable as possible, reaching a wide range of heterocycles, and second, for the stoichiometry of the coupling partners to be as close to

<sup>40</sup> Ohta, A.; Akita, Y.; Ohkuwa, T.; Chiba, M.; Fukunaga, R.; Miyafuji, A.; Nakata, T.; Tani, N.; Aoyagi, Y. *Heterocycles* **1990**, *31*, 1951. For numerous other examples of direct arylation of furans and thiophenes, see ref. 7c,d.

<sup>41</sup> Liégault, B.; Lapointe, D.; Caron, L.; Vlassova, A.; Fagnou, K. *J. Org. Chem.* **2009**, *74*, 1826.

unity in all cases. Based on previous chemistry from this group the use of catalytic quantities of pivalic acid was instituted<sup>8b</sup> and found to be instrumental in obtaining high conversion for an expansive set of heterocycles. These conditions, for the most part, feature low catalyst loading (1 – 2 mol% Pd(OAc)<sub>2</sub>), relatively mild conditions (100 °C) and a 1 : 1 stoichiometry of the two coupling partners. Additionally, the heterocycles that have been found to be responsive to these conditions include: (benzo)thiophenes, (benzo)furans, pyrroles, indolazines, imidazoles, thiazoles, oxazoles, as well as various triazoles and reactions proceed in moderate to excellent yields (Scheme 2.9).

**Scheme 2.9.** General conditions for the direct arylation of heterocycles.



### 2.1.2. Direct Arylation of $\pi$ -Deficient Heterocycles.

More challenging, and scarce in the literature, is the direct arylation of  $\pi$ -deficient heterocycles, such as pyridine. However, given the high occurrence of the 2-arylpyridine motif in pharmaceutically relevant compounds much research in traditional cross-coupling methodology has been dedicated towards this class of compound. 2-Halopyridines have been used in these types of reactions; 2-metallopyridines, on the other hand, have seen little use due to the instability of these organometallics. For example, the instability of 2-

pyridylboronic acids has limited their use in Suzuki cross-couplings, an issue that has only recently been addressed through the use of pyridylboronates.<sup>42</sup> In addition to the synthetic issues that may accompany the use of an organometallic cross-coupling partner, the need for dual substrate pre-activation introduces additional waste to the overall process, since both the organometallic and the aryl halide must be independently prepared prior to cross-coupling (Scheme 2.1). Thus, direct arylation could serve as a potential solution to the 2-metalloazine problem by replacing the organometallic with a simple arene.<sup>43</sup> Additionally, this strategy becomes even more attractive when the organometallic species is difficult to prepare or is unstable under cross-coupling conditions.

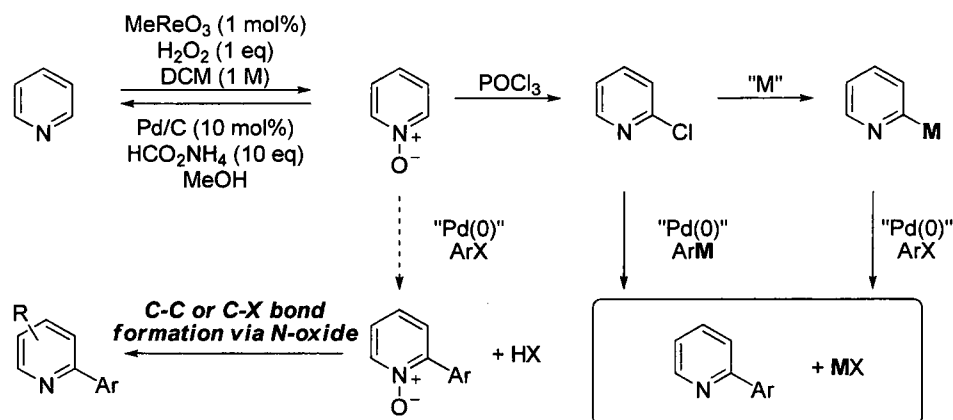
Our group has reported, over the past few years, a direct arylation strategy that employs the bench stable and increasingly commercially available azine and azole *N*-oxides as surrogates for 2-metalloazines and azoles.<sup>16a,b,c,e</sup> Such a strategy, though still requiring an activation step, would minimize the number of synthetic steps associated with this process. As illustrated in Scheme 2.10, the installation of both halide and organometallic functional groups adjacent to the nitrogen atom typically passes through an *N*-oxide species. Thus, improved efficiency would be obtained if the *N*-oxide itself could be employed in a cross-coupling process. Furthermore, since the *N*-oxide moiety would not be consumed in the cross-coupling step, it could subsequently be used to introduce further functionality on the azine core following the formation of the biaryl carbon-carbon bond. This section of the introduction will highlight advances made by other groups in the arylation/functionalization of the 2-position of the pyridine core, as well as our own contribution to this area *via* the azine *N*-oxide strategy.

---

<sup>42</sup> (a) Billingsley, K. L.; Buchwald, S. L. *Angew. Chem. Int. Ed.* **2008**, *47*, 4695. (b) Yang, D. X.; Colletti, S. L.; Wu, K.; Song, M.; Li, G. Y.; Shen, H. C. *Org. Lett.* **2009**, *11*, 381.

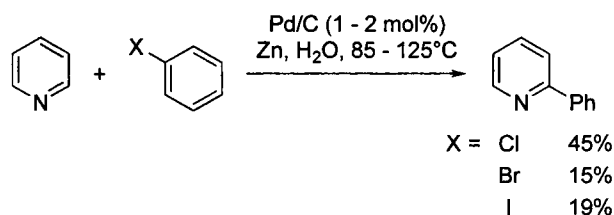
<sup>43</sup> For a review on cross-coupling methodologies involving metalloazines and alternatives to these processes, please see: Campeau, L.-C.; Fagnou, K. *Chem. Soc. Rev.* **2007**, *36*, 1058.

**Scheme 2.10.** General strategy for *N*-oxide utility in pyridine arylation and functionalization.



**Direct arylation of “free” pyridine.** A low-yielding, but regioselective, arylation of “free” pyridine catalyzed by Pd/C was reported by Sasson and co-workers in 2000.<sup>44</sup> The authors suggested a radical mechanism due to inhibition of the reaction when 2,6-di-*tert*-butyl-4-methylphenol (BHT), a radical trap, was added to the reaction mixture. Arylchlorides, bromides, and iodides were all compatible in the reaction, though arylchlorides afforded the highest yields (Scheme 2.11).

**Scheme 2.11.** Direct arylation of pyridine catalyzed by Pd/C.



More recently, Bergman and Ellman have reported the regioselective alkylation<sup>45</sup> and arylation<sup>46</sup> of pyridine and its derivatives under Rh(I)-catalysis without recourse to pyridine pre-activation. Both pyridines and quinolines efficiently undergo alkylation; however pyridines require a substituent at the 6-position, with unsubstituted pyridine being alkylated

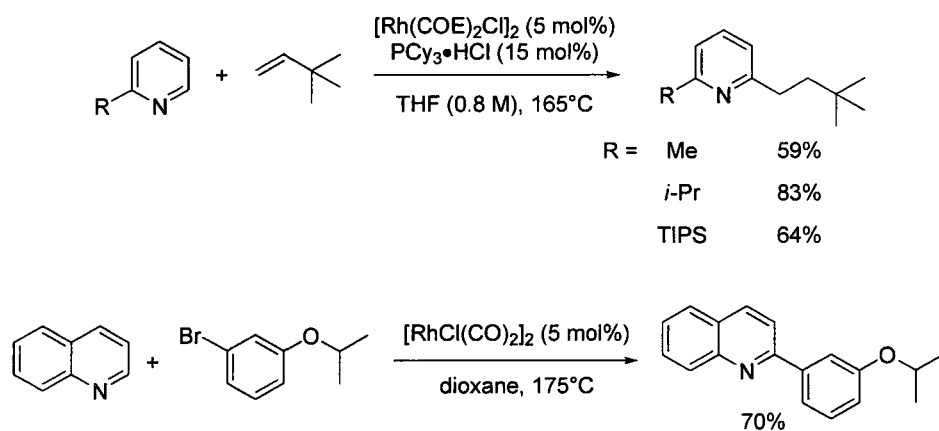
<sup>44</sup>Mukhopadhyay, S.; Rothenberg, G.; Gitis, D.; Baidossi, M.; Ponde, D. E.; Sasson, Y. *J. Chem. Soc., Perkin Trans. 2* **2000**, 1809.

<sup>45</sup>Lewis, J. C.; Bergman, R. G.; Ellman, J. A. *J. Am. Chem. Soc.* **2007**, *129*, 5332.

<sup>46</sup>Berman, A. M.; Lewis, J. C.; Bergman, R. G.; Ellman, J. A. *J. Am. Chem. Soc.* **2008**, *130*, 14926.

in < 5% yield under the standard reaction conditions. Formation of a Rh-NHC complex was implicated in the mechanism of C-H bond cleavage and this is in accordance with the observation that substitution at the 6-position of pyridine was necessary for reactivity.<sup>47</sup> In their arylation chemistry, it was also observed that substitution at the 6-position was necessary for reactivity of pyridines and that the reaction was highly concentration dependant with increased yields obtained at higher concentrations. Additionally, optimal results were obtained when 6 equivalents of the heterocycle were used in the reaction (Scheme 2.12).

**Scheme 2.12.** Direct alkylation/arylation of pyridines and quinoline *via* Rh(I)-catalysis.



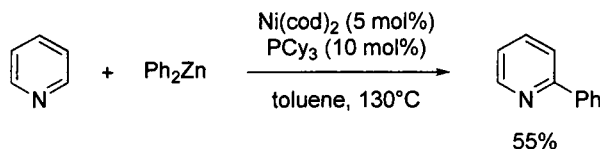
Very recently in the literature, Chatani and co-workers have reported a nickel catalyzed protocol for the direct arylation of pyridines with phenylzinc compounds (Scheme 2.13).<sup>48</sup> The reaction was proposed to proceed *via* the 1,2-addition of the arylorganometallic to the azine, followed by re-aromatization of the azine. A complete mechanistic evaluation has not yet been presented though preliminary studies suggest that the arylzinc reagent serves as both the arene source and the oxidant, generating metallic zinc in the process. Additionally, no product was observed in the absence of the nickel catalyst. Interestingly,

<sup>47</sup> (a) Alvarez, E.; Conejero, S.; Paneque, M.; Petronilho, A.; Poveda, M. L.; Serrano, O.; Carmona, E. *J. Am. Chem. Soc.* **2006**, *128*, 13060. (b) Esteruelas, M. A.; Fernandez-Alvarez, F. J.; Onate, E. *J. Am. Chem. Soc.* **2006**, *128*, 13044. (c) Canac, Y.; Soleilhavoup, M.; Conejero, S.; Bertrand, G. *J. Organomet. Chem.* **2004**, *689*, 3857.

<sup>48</sup>Tobisu, M.; Hyodo, I.; Chatani, N. *J. Am. Chem. Soc.* **2009**, *131*, 12070.

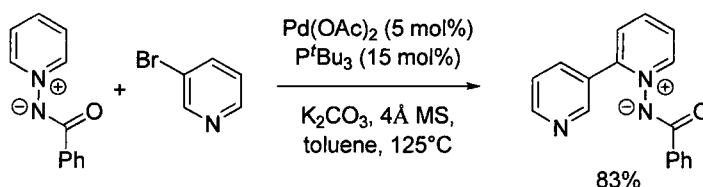
there has been a recent report of a metal free, base promoted regioselective arylation of azines at the 2-position with arylbromides and iodides.<sup>49</sup>

**Scheme 2.13.** Direct arylation of pyridine *via* 1,2-addition/oxidation protocol.



**Direct arylation of “activated” pyridine.** In 2008 Charette and co-workers reported the regioselective direct arylation of *N*-iminopyridinium ylides with a variety of arylbromides and heteroaryl bromides (Scheme 2.14).<sup>50</sup> In their initial report, the authors propose that the amide functionality of the pyridinium ylide acts as a strong Lewis base to complex and direct palladium to regioselectively cleave the C-H bond at the 2-position of pyridine. Furthermore, the N-N bond of the *N*-iminopyridinium ylide may be reductively cleaved to provide the free 2-arylpyridine, or alternatively the pyridine ring bearing the benzoylamide may be functionalized by Grignard addition or fully reduced to the piperidine derivative. Prior to this report by the Charette group, our group had investigated pyridine *N*-oxides as 2-metallopyridine surrogates and in 2005 reported the successful cross-coupling of pyridine *N*-oxides with a variety of arylbromides (Scheme 2.15).<sup>16a</sup> This chemistry was later elaborated to include a variety of substituted pyridine *N*-oxides,<sup>16e</sup> diazine *N*-oxides,<sup>16b</sup> as well as azole *N*-oxides (Scheme 2.16).<sup>16c,e</sup> Additionally, the *N*-oxide methodology was exploited in the expedient synthesis of a potent sodium channel inhibitor and a Tie2 tyrosine kinase inhibitor.<sup>16e</sup>

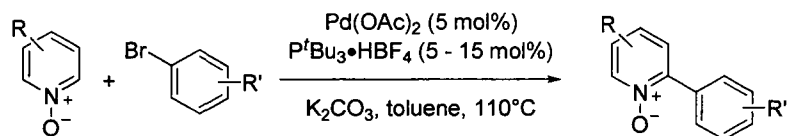
**Scheme 2.14.** Direct arylation of *N*-iminopyridinium ylides.



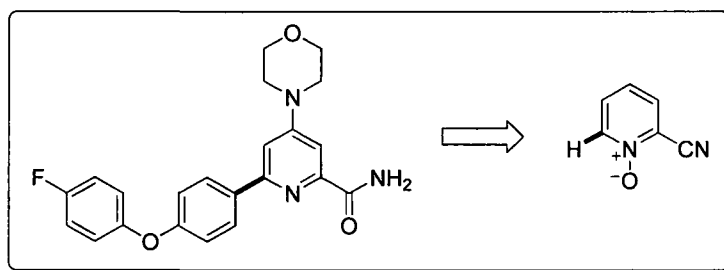
<sup>49</sup>Yanagisawa, S.; Ueda, K.; Taniguchi, T.; Itami, K. *Org. Lett.* **2008**, *10*, 4673.

<sup>50</sup>Larivée, A.; Mousseau, J. J.; Charette, A. B. *J. Am. Chem. Soc.* **2008**, *130*, 52. A later publication by the same group related their findings on the site-selectivity in *sp*<sup>2</sup> vs *sp*<sup>3</sup> arylation of *N*-iminopyridinium ylides, please see: Mousseau, J. J.; Larivée, A.; Charette, A. B. *Org. Lett.* **2008**, *10*, 1641.

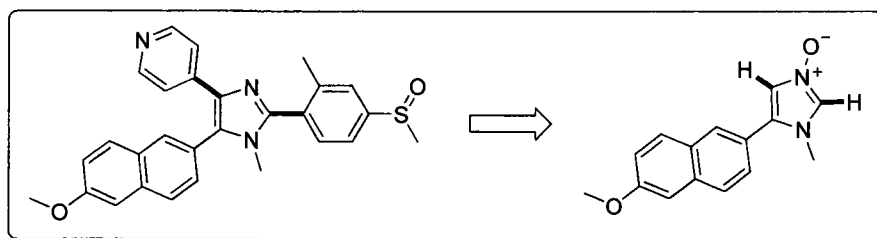
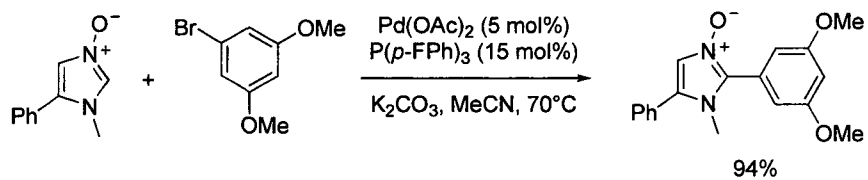
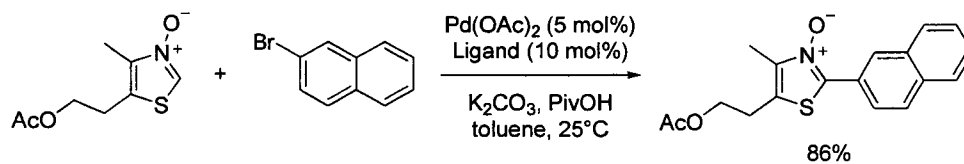
**Scheme 2.15.** Direct arylation of azine *N*-oxides.



R = 4-CO <sub>2</sub> Me	R' = 4'-OMe	88%
4-OMe	4'-Me	80%
2-CN	4'-OMe	81%
3-Ph	3',5'-Me	80%
3-F	3',5'-Me	78%



**Scheme 2.16.** Direct arylation of azole *N*-oxides.



### 2.1.3. Mechanistic Consideration in Direct Arylation of Azine *N*-Oxides.

The mechanistic possibilities available to palladium in its reactions with aromatic C-H bonds were detailed in Chapter 1 (*vide supra*). The new reactivity observed and the accessibility of the products, as a result of this reactivity, is often of greater importance than the mechanism with which the reaction takes place. That being said, mechanistic knowledge can greatly aid in reaction optimization, catalyst design, and in the facilitation of future reaction development.

Relevant to the work presented in this thesis is the mechanism of direct arylation of pyridine *N*-oxides. Competition experiments and the presence of a DKIE were used as initial mechanistic probes for this process. The competition between an electron-rich and electron-deficient pyridine *N*-oxide resulted in the electron-deficient pyridine *N*-oxide providing the exclusive product of the reaction. As well, a DKIE of 4.7 was observed. These mechanistically suggestive experiments preclude the involvement of an electrophilic aromatic substitution pathway. Following this, a computational analysis was carried out on the four potential mechanisms outlined in Chapter 1.<sup>51</sup> The lowest energy pathway was found to be the CMD transition state in which the bromide ligand on palladium acts as an internal base deprotonating pyridine *N*-oxide (Figure 2.2). This calculated transition state was further validated by the very close correlation between experimental and computational results. The relative rates of reaction between two electronically different pyridine *N*-oxides was consistently computationally predicted by invoking a CMD transition state and in all cases the more electron-deficient pyridine *N*-oxide was formed in great amounts (Figure 2.3).<sup>52</sup> The slight bias of the reaction for the 4-methoxypyridine *N*-oxide over 4-methylpyridine *N*-oxide may be rationalized by the  $\sigma$ -withdrawing nature of the methoxy-group to the 2-position of the aromatic ring. These results may be related to the discussion of the nature of the CMD transition state in that pyridine *N*-oxide has a relatively low barrier to distortion ( $E_{dist}$ ) and is not energetically compensated by a strong energy of interaction ( $E_{int}$ ) (*vide supra*). The calculated transition state was also effective in predicting the relative

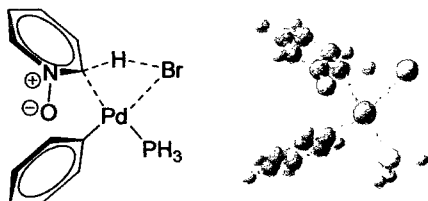
---

<sup>51</sup> The computational work was initiated by Louis-Charles Campeau and was re-investigated at a higher level of theory by Serge Gorelsky, Gorelsky, S.; Campeau, L.-C.; Fagnou, K. *unpublished results*.

<sup>52</sup> Experimental results obtained by Louis-Charles Campeau (Campeau, L.-C. *Ph.D Thesis*, University of Ottawa, 2007) and computational results obtained by Serge Gorelsky (Gorelsky, S.; Fagnou, K.. *unpublished results*).

rates of reaction for two positions within the same molecule (Figure 2.4). The nature of the substituent at the 3-position, with respect to both sterics and electronic, has a dramatic influence over the reaction regioselectivity and this is computationally predicted using a CMD transition state.<sup>53</sup> Additional correlation between experimental and computational results comes from an Arrhenius plot.<sup>54</sup> The energy of activation was calculated for the CMD transition state and found to be 15.5 kcal/mol. This is in strong agreement with an experimentally derived value from an Arrhenius plot of 19.7 kcal/mol. Further correlation with a weak  $E_{int}$  was derived from a Hammett plot.<sup>55</sup> The Hammett correlation was obtained using 4-substituted pyridine *N*-oxides and, plotting the natural logarithm of the ratio of initial rates against the  $\sigma_{meta}$ -values, a  $\rho$ -value of +1 was revealed. The positive nature of the  $\rho$ -value indicates the development of a negative charge on the aromatic system at the transition state of the C-H bond cleavage. These results correlate well with a relatively low  $E_{dist}$  (36.8 kcal/mol) in the activation-strain analysis of the CMD transition state for pyridine *N*-oxide,<sup>9</sup> and are also indicative of a late transition state.

**Figure 2.2.** Lowest energy transition state calculated for pyridine *N*-oxide direct arylation.



<sup>53</sup> Experimental results obtained by Louis-Charles Campeau (published in ref. 15e) and computational results obtained by Serge Gorelsky (Gorelsky, S.; Fagnou, K.. *unpublished results*).

<sup>54</sup> Experimental result for the Arrhenius plot obtained by Ho-Yan Sun and computational result obtained by Serge Gorelsky, Sun, H.-Y.; Gorelsky, S.; Fagnou, K.. *unpublished results*.

<sup>55</sup> The Hammett plot was obtained by Ho-Yan Sun; Sun, H.-Y.; Fagnou, K. *unpublished results*.

**Figure 2.3.** Experimental and computational results for competition experiments between electronically different pyridine *N*-oxides (computational result shown above the arrow, experimental result shown below the arrow).

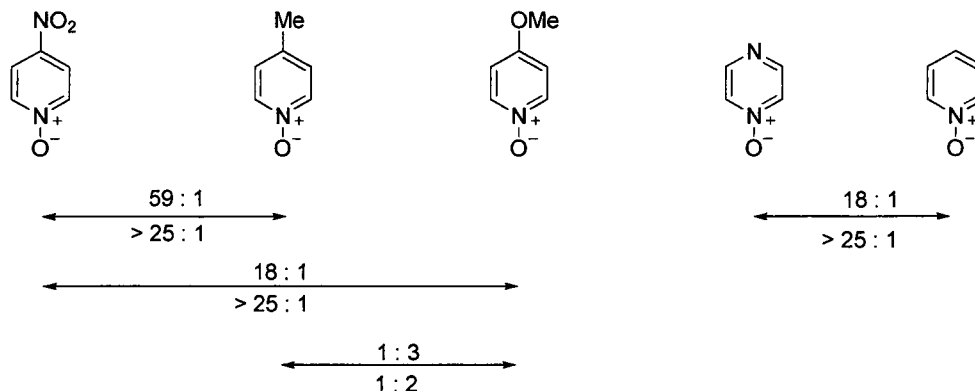


**Figure 2.4.** Experimental and computational results for regioselectivities in the direct arylation of 3-substituted pyridine *N*-oxides.

	Ph	MeO <sub>2</sub> C	MeO	O <sub>2</sub> N	NC	F
Calculated (PMe <sub>3</sub> )	1 : 11	1 : 4	6 : 1	9 : 1	4 : 1	76 : 1
Experiment (P <sup>t</sup> Bu <sub>3</sub> )	1 : 10	1 : 7	1 : 1	4 : 1	10 : 1	25 : 1
Experiment (P <sup>t</sup> Bu <sub>2</sub> Me)	—	—	5 : 1	6 : 1	15 : 1	—

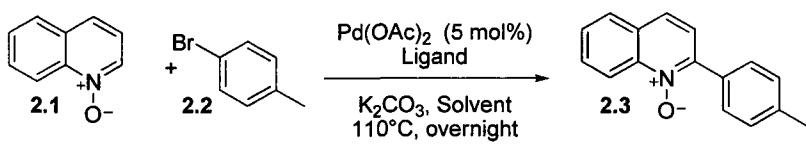
## 2.2. Results and Discussion

### 2.2.1. Reaction Development and Investigation of Aryl Halide Compatibility in the Direct Arylation of Quinoline and Isoquinoline *N*-Oxide.

**Quinoline *N*-Oxide.** Following the development of the original conditions for the direct arylation of pyridine *N*-oxide,<sup>16a</sup> a secondary reaction optimization with quinoline *N*-oxide **2.1**, a substrate which gave lower yields under the initially described conditions (Table 2.1, entry 1), was undertaken. This work was performed under slightly modified conditions to facilitate a rapid evaluation of the important reaction parameters: in sealed vials heated in an aluminum block with mesitylene as the solvent in place of toluene to reduce solvent volatility at elevated temperature. Under these conditions, it was determined that reducing

the ligand: Pd ratio from 3 : 1 to 1 : 1 resulted in an increase in yield of the 2-arylquinoline *N*-oxide **2.3** from 65% to 91% (Table 2.1, entries 2 – 4). Upon returning to a more traditional reaction set up (round-bottom flask with a reflux condenser heated in an oil bath with toluene as the solvent) a slight decrease in the yield to 77% was noted, though this still represents a marked increase from the initially reported conditions (Table 2.1, entries 1 and 5). A scan of other trialkyl phosphine ligands revealed that the yield could be improved from 77% to 96% by replacing the more sterically encumbered tri-*t*-butylphosphonium tetrafluoroborate as the pre-ligand with di-*t*-butylmethylphosphonium tetrafluoroborate in a 1 : 1 ligand : Pd ratio (Table 2.1, entries 5 – 7). Under these conditions, the amount of *N*-oxide **2.1** can also be reduced while maintaining synthetically useful isolated yields. For example, the use of 2 equivalents of *N*-oxide **2.1** results in an 85% isolated yield of **2.3**, while the use of a slight excess of the *N*-oxide (1.1 equivalents) provides 67% isolated yield (Table 2.1, entries 8 and 9). Other solvents, such as dioxane and acetonitrile, can also be employed at refluxing temperatures to provide the 2-arylquinoline *N*-oxide in good yields (Table 2.1, entries 10 and 11).

**Table 2.1.** Reaction development for the direct arylation of quinoline *N*-oxide.<sup>a</sup>

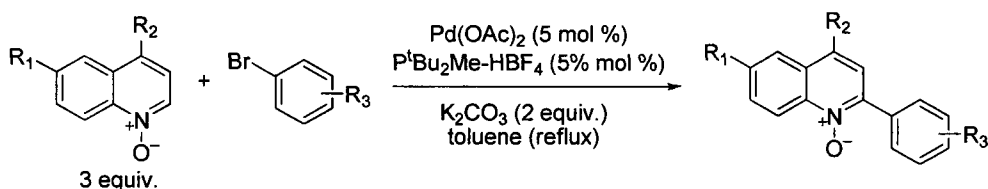


Entry	Equiv. <i>N</i> -Oxide	Pre-ligand	Ligand: Pd Ratio	Solvent	Yield(%) <sup>b</sup>
1	3	P <sup>t</sup> Bu <sub>3</sub> -HBF <sub>4</sub>	3:1	PhMe	34
2	3	P <sup>t</sup> Bu <sub>3</sub> -HBF <sub>4</sub>	3:1	Mesitylene	65
3	3	P <sup>t</sup> Bu <sub>3</sub> -HBF <sub>4</sub>	2:1	Mesitylene	88
4	3	P <sup>t</sup> Bu <sub>3</sub> -HBF <sub>4</sub>	1:1	Mesitylene	91
5	3	P <sup>t</sup> Bu <sub>3</sub> -HBF <sub>4</sub>	1:1	PhMe	77
6	3	PCy <sub>3</sub> -HBF <sub>4</sub>	1:1	PhMe	50
7	3	P <sup>t</sup> Bu <sub>2</sub> Me-HBF <sub>4</sub>	1:1	PhMe	96(96)
8	2	P <sup>t</sup> Bu <sub>2</sub> Me-HBF <sub>4</sub>	1:1	PhMe	86(85)
9	1.1	P <sup>t</sup> Bu <sub>2</sub> Me-HBF <sub>4</sub>	1:1	PhMe	(67)
10	3	P <sup>t</sup> Bu <sub>2</sub> Me-HBF <sub>4</sub>	1:1	Dioxane	82
11	3	P <sup>t</sup> Bu <sub>2</sub> Me-HBF <sub>4</sub>	1:1	MeCN	75

<sup>a</sup>Conditions: 4-bromotoluene (1 eq, 0.3 M), quinoline *N*-oxide (3 eq), Pd(OAc)<sub>2</sub> (5 mol%), ligand (5 - 15 mol%), K<sub>2</sub>CO<sub>3</sub> (2 eq), toluene, 110°C, 16 hours. <sup>b</sup> <sup>1</sup>H NMR yield, isolated yield in parentheses.

Additional examples of direct arylation of quinoline *N*-oxides are included in Table 2.2. The reaction is compatible with a range of functional groups and substitution patterns on the aryl bromide and both electron-donating and electron-withdrawing groups are tolerated on the quinoline *N*-oxide. Alkyl substitution in the *para*, *ortho*, and *meta*-positions is tolerated on the arylbromide (Table 2.2, entries 2, 5, 8). Activated and unactivated aryl bromides are also compatible in the reaction (Table 2.2, entries 3, 4, 7). If the arene bears both a chloride and a bromide substituent, the reaction takes place selectively at the aryl bromide (Table 2.2, entry 6). Naphthyl bromides also react cleanly providing the 2-(1-naphthyl)quinoline *N*-oxide or 2-(2-naphthyl)quinoline *N*-oxides in good yield (Table 2.2, entries 9 and 10). 5-Methoxy substituted quinoline *N*-oxide participates in these reactions with a range of aryl bromides (Table 2.2, entries 11 – 14) as does an electron-deficient *N*-oxide (Table 2.2, entry 15).

**Table 2.2.** Compatible aryl halides in the direct arylation of quinoline *N*-oxide.<sup>a</sup>



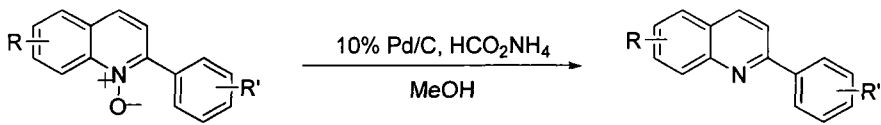
Entry	Product	Yield <sup>b</sup>	Entry	Product	Yield <sup>b</sup>
1		R=H 89	9		73
2		R= <sup>t</sup> Bu 94	10 <sup>c</sup>		83
3		R=OMe 88	11		R=H 72
4		R=CO <sub>2</sub> Et 61	12		R=Me 85
5 <sup>c</sup>		R=Me 80	13		R=OMe 77
6 <sup>c</sup>		R=Cl 70	14		R=Cl 55
7		87	15		91
8		92			

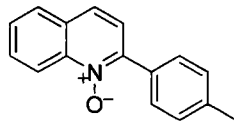
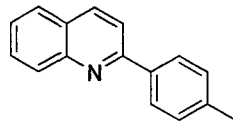
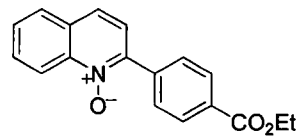
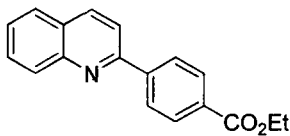
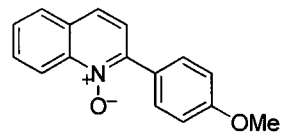
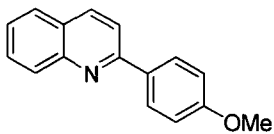
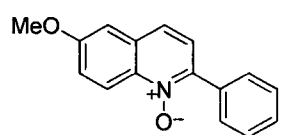
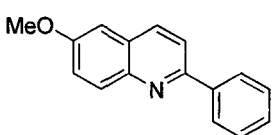
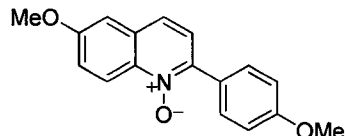
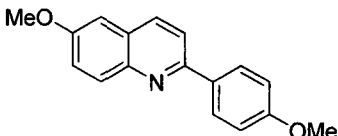
<sup>a</sup>Conditions: Quinoline *N*-oxide (3 eq), bromoarene (1 eq, 0.3 M), Pd(OAc)<sub>2</sub> (5 mol%), P<sup>t</sup>Bu<sub>2</sub>Me-HBF<sub>4</sub> (5 mol%), K<sub>2</sub>CO<sub>3</sub> (2 eq.), toluene, reflux, 16 hours. <sup>b</sup>Isolated yield. <sup>c</sup>Addition of Ag<sub>2</sub>CO<sub>3</sub> (0.5 eq).

The utility of the direct arylation methodology for azine *N*-oxides relies on the ability either to employ the *N*-oxide moiety in other types of functionalization or to easily induce *N*-oxide deoxygenation under mild conditions subsequent to direct arylation. For the latter, two sets of conditions were typically employed based on the substrate undergoing reduction. Quinoline *N*-oxides can be readily reduced to the corresponding 2-arylquinoline by Pd/C with ammonium formate or under a hydrogen atmosphere. Reactions are run at room temperature, proceed in relatively short reaction times (often complete within a few hours), and provide the products in good to excellent yields (Table 2.3). This protocol is not compatible with some functional groups such as aryl halides however. In these cases use of Zn dust in aqueous ammonium chloride/THF can selectively achieve deoxygenation without inducing hydrodechlorination (Table 2.5, entry 7).

***Isoquinoline N-Oxide.*** Use of the *N*-oxide cross-coupling strategy can also offer advantages to the use of traditional cross-coupling techniques when non-symmetrical substrates bearing two potential sites for reaction are employed. Traditional techniques rely on the availability of regioisomerically pure haloazines or azine organometallics that may be difficult to prepare. To ascertain whether the *N*-oxide cross-coupling strategy could provide a solution in some of these cases, isoquinoline *N*-oxide **2.4** was employed as a test substrate. Under our previously reported reaction conditions<sup>16a</sup> the arylation of **2.4** provides a regioisomeric product ratio of 1.7 : 1 (**2.5a** : **2.5b**, Table 2.4). Our previous work in regioselective intramolecular direct arylation of simple arenes prompted us to consider a ligand effect.<sup>15e</sup> We were pleased to find that, on changing the ligand from tri-*tert*-butylphosphine to tri-cyclohexylphosphine to di-*tert*-butylmethylphosphine the yield remained high and the regioselectivity could be improved from 1.7: 1 to 7.5: 1 to 12.8: 1, respectively. In these cases, contrary to reactions employing *N*-oxides that do not possess two different regioisomeric sites for reaction, we found that the use of a ligand to metal ratio of 2: 1 provided the most reproducible results.

**Table 2.3.** Selected examples in the reduction of 2-arylquinoline *N*-oxides.<sup>a</sup>



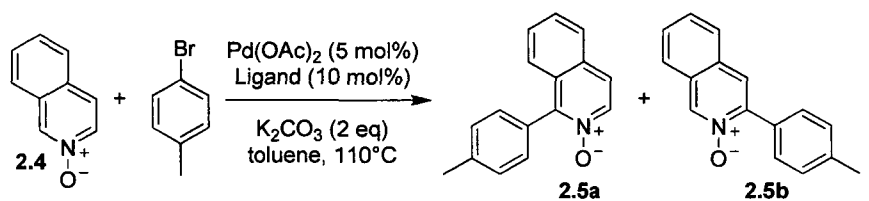
Entry	N-Oxide	Product	Yield <sup>b</sup>
1			94
2			80
3			93
4			93
5			79

<sup>a</sup>Conditions: *N*-oxide (1 eq), 10% Pd/C (10 mol% Pd), ammonium formate (10 eq), methanol (0.1 M), room temperature. <sup>b</sup>Isolated yields are reported.

Aspects of regioselectivity were investigated with isoquinoline *N*-oxide and a number of different aryl bromides with various functional groups and substitution patterns (Table 2.5). During the course of these studies it was determined that the *N*-oxide regioisomeric products were often inseparable by silica gel flash chromatography. For this reason, the *N*-oxide products were isolated as a mixture and subjected to de-oxygenation reaction conditions. Conveniently, the free bases exhibit sufficient chromatographic separation to permit facile separation of the two isomers. While 3 equivalents of the *N*-oxide are regularly employed and give excellent yields of the major regioisomer (Table 2.5, entry 1), good to excellent yields are still obtained with 1.1 and 2 equivalents of isoquinoline *N*-oxide (Table 2.5, entries 2 and 3). *Meta*-substitution as well as activated and unactivated aryl bromides

may be employed providing products in excellent yields and regioselectivities ranging from 16: 1 to 12: 1 for the 1-arylisquinoline *N*-oxides (Table 2.5, entries 4 – 6). A chloride substituent may also be present on the aryl bromide and the product can be obtained in good yield with high regioselectivity (Table 2.5, entry 7). In this case, the use of zinc powder in an aqueous THF/ammonium chloride solution is employed instead of Pd/C in the presence of ammonium formate to minimize undesired reduction of the aryl chloride moiety.<sup>56</sup>

**Table 2.4.** Ligand effects on the regioselectivity of the direct arylation of isoquinoline *N*-oxide.<sup>a</sup>



Entry	Pre-ligand	2.5a:2.5b <sup>b</sup>	Conversion (%) <sup>c</sup>
1	P <sup>t</sup> Bu <sub>3</sub> -HBF <sub>4</sub>	1.7:1	>99
2	PCy <sub>3</sub> -HBF <sub>4</sub>	7.5:1	90
3	PMe <sup>t</sup> Bu <sub>2</sub> -HBF <sub>4</sub>	12.8:1	>99

<sup>a</sup>Conditions: 4-Bromotoluene (1 eq, 0.3 M), *N*-oxide (3 eq), Pd(OAc)<sub>2</sub> (5 mol%), ligand (10 mol%), K<sub>2</sub>CO<sub>3</sub> (2 eq), toluene, 110°C, 16 hours. <sup>b</sup>Isomeric ratio determined from <sup>1</sup>H NMR spectrum. <sup>c</sup>Conversion determined by integration against an internal standard (trimethoxybenzene) in the <sup>1</sup>H NMR spectrum.

<sup>56</sup> For reduction with Pd/C/ammonium formate see: Balicki, R. *Synthesis* **1989**, 645. For reduction with Zn/ammonium chloride see: Aoyagi, Y.; Abe, T.; Ohta, A. *Synthesis* **1997**, 891.

**Table 2.5.** Regioselectivity and scope in the direct arylation of isoquinoline *N*-oxide.<sup>a</sup>

Entry	Aryl Bromide	Yield <sup>c</sup> of <b>2.5a'</b> + <b>2.5b'</b>	Ratio <sup>d</sup> of <b>2.5a'</b> : <b>2.5b'</b>	Yield <sup>c</sup> of <b>2.6</b>
1		98%	13.5 : 1	80%
2		91% <sup>e</sup>	14.4 : 1	—
3		71% <sup>f</sup>	39.6 : 1	—
4		92%	12.4 : 1	73%
5		95%	15.8 : 1	83%
6		96%	13.5 : 1	83%
7		63%	14.1 : 1	85%

<sup>a</sup>Conditions: Aryl bromide (1 eq), isoquinoline *N*-oxide (3 eq), Pd(OAc)<sub>2</sub> (5 mol%), P<sup>t</sup>Bu<sub>2</sub>Me-HBF<sub>4</sub> (10 mol%), K<sub>2</sub>CO<sub>3</sub> (2 eq), toluene (0.3 M), 110 °C, 16 hours. <sup>b</sup>Entries 1, 4 - 6: Mixture of **2.5a** and **2.5b** (1 eq), ammonium formate (14 eq), 10% wt. Pd/C (0.1 eq of Pd), MeOH (0.1 M), 40 °C, 2 - 5 hours. Entry 5: Mixture of **2.5a** and **2.5b** (1 eq), zinc dust (10 eq), THF/NH<sub>4</sub>Cl(aq, sat) (1:1 vol/vol, 0.033 M), r.t., 1 hour. <sup>c</sup>Isolated yield. <sup>d</sup>Determined by <sup>1</sup>H NMR spectroscopy. <sup>e</sup>2 equivalents of isoquinoline *N*-oxide was used. <sup>f</sup>1.1 equivalents of isoquinoline *N*-oxide was used.

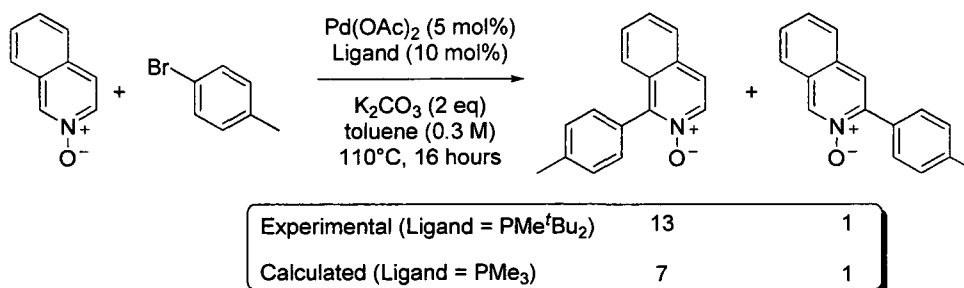
### 2.2.2. Correlation to a CMD Pathway.

An in depth mechanistic evaluation of the direct arylation of azine *N*-oxides has been carried out by Ho-Yan Sun<sup>57</sup> and a brief discussion here is relevant. As previously described, a CMD transition state was found to be operative for the direct arylation of pyridine *N*-oxides. When this transition state is invoked, the experimentally observed regioselectivity for isoquinoline *N*-oxide direct arylation is accurately predicted by computational methods (Scheme 2.17).<sup>58</sup> While a large ligand effect was noted experimentally for this process, in all cases the 1-position was the major regioisomer, in accordance with computational prediction.

<sup>57</sup> Sun, H.-Y.; Fagnou, K. *unpublished results*.

<sup>58</sup> Gorelsky, S.; Fagnou, K. *unpublished results*.

**Scheme 2.17.** Experimental and calculated results for regioselectivity.



## 2.3. Outlook and Perspectives

The field of direct arylation has been expanding rapidly, particularly in the past 5 years, and will continue to expand to accommodate the growing need for reaction efficiency and functional group compatibility. Though still in a relative state of infancy in comparison with other reaction classes, the utility of direct arylation is evident by its use in the synthesis of natural products<sup>59</sup> and pharmalogically relevant compounds<sup>60</sup> – this reaction class has already seen use on kilo-scale in process chemistry.<sup>61</sup> While a single, unifying mechanism for direct arylation has not been generally accepted, the ability of a CMD transition state to accurately describe many experimentally observed results from a wide array of arenes continues to push this mode of C-H bond cleavage to the forefront of mechanistic proposals.

<sup>59</sup> For representative examples from the literature, see: (a) Rhazinilam: Bowie, A. L.; Hughes, C. C.; Trauner, D. *Org. Lett.* **2005**, *7*, 5207. (b) Mastigophorene A and B: Bringmann, G.; Pabst, T.; Henschel, P.; Kraus, J.; Peters, K.; Peters, E.-M.; Rycroft, D. S.; Connolly, J. D. *J. Am. Chem. Soc.* **2000**, *122*, 9127. (c) Korupensamines: Bringmann, G.; Ochse, M. *Synlett* **1998**, 1294 and Bringmann, G.; Ochse, M.; Götz, R. *J. Org. Chem.* **2000**, *65*, 2069.

<sup>60</sup> For representative examples from the literature, see: (a) Muscimol: Nakamura, N.; Tajima, Y.; Sakai, K. *Heterocycles* **1982**, *17*, 235. (b) Paullone: Avila-Zárraga, J. G.; Lujan-Montelongo, A.; Covarrubias-Zúñiga, A.; Romero-Ortega, M. *Tetrahedron Lett.* **2006**, *47*, 7987.

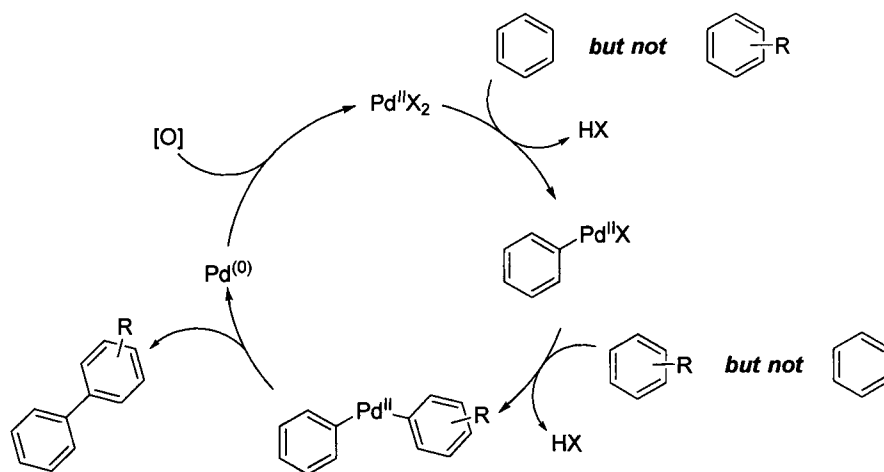
<sup>61</sup> (a) Gauthier, D. R., Jr.; Limanto, J.; Devine, P. N.; Desmond, R. A.; Szumigala, R. H., Jr.; Foster, B. S.; Volante, R. P. *J. Org. Chem.* **2005**, *70*, 5938. (b) Jensen, M. S.; Hoerrner, R. S.; Li, W.; Nelson, D. P.; Javadi, G. J.; Dormer, P. G.; Cai, D.; Larsen, R. D. *J. Org. Chem.* **2005**, *70*, 6034. (c) Cameron, M.; Foster, B. S.; Lynch, J. E.; Shi, Y.-J.; Dolling, Y.-H. *Org. Process Res. Dev.* **2006**, *10*, 398.

# Palladium(II) Catalyzed Oxidative Cross-Coupling of Unactivated Arenes

## 3.1. Introduction

The importance of the biaryl motif and the avenues available for its construction *via* traditional palladium-catalyzed cross-coupling and direct arylation were largely dealt with in Chapter 2 (*vide supra*). While direct arylation introduces a significant advantage over traditional methods it still employs one pre-activated coupling partner. Thus, an even more efficient route to biaryls would be the oxidative cross-coupling of two simple arenes (Scheme 3.1). However, this introduces an additional level of complexity to the reaction. The catalyst must display orthogonal reactivity with each of the arenes at distinct steps within the catalytic cycle in order to achieve successful cross-coupling.

**Scheme 3.1.** General catalytic cycle of the oxidative cross-coupling of two simple arenes.



An assessment of the oxidative cross-coupling literature quickly illustrates the challenges of obtaining a successful cross-coupling of two simple arenes. The necessary mechanistic dichotomy of palladium to react differently with two arenes requires them to have distinct physical properties. While the oxidative *homo-coupling* of many arenes under transition metal catalysis<sup>62</sup> or under the action of super-stoichiometric quantities of single electron-oxidants<sup>63</sup> has been reported, only in the past two years have successful oxidative *cross-couplings* of two simple arenes under catalytic conditions been realized.<sup>64</sup> Additionally, a survey of these reports can allow for a separation of compatible arenes into three groups: Type I, Type II, and Type III arenes (Figure 3.1), and a description of these three groups follows. This introduction serves to review the pertinent literature and to establish a useful classification system for simple arenes which may assist in the further

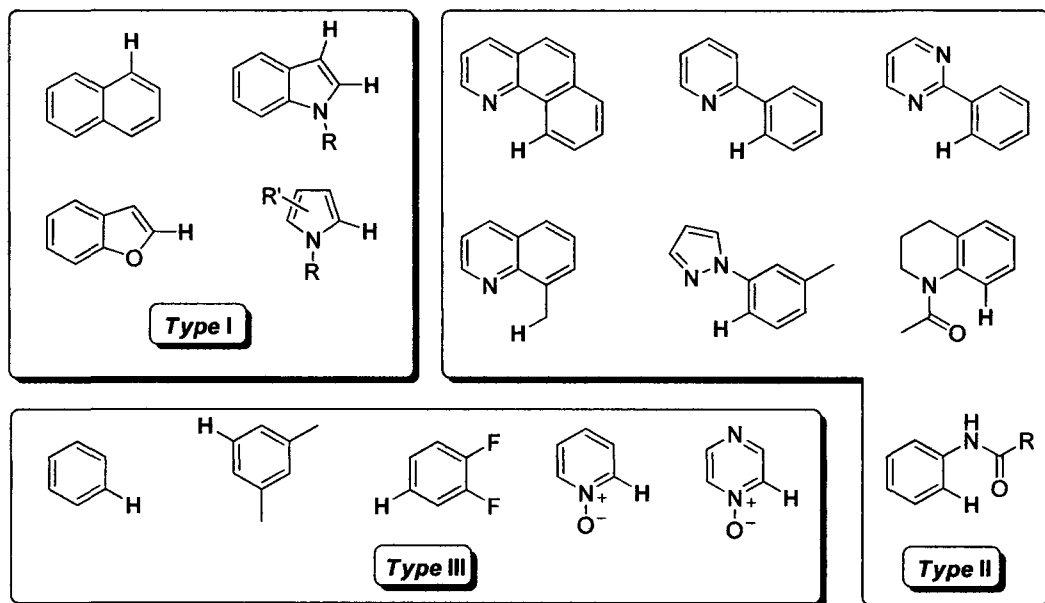
<sup>62</sup> For lead references please see: (a) van Helden, R.; Verberg, G. *Rec. Trav. Chim. Pays-Bas*. **1965**, *84*, 1263. (b) Davidson, J. M.; Triggs C. *Chem. Ind.* **1966**, 475.

<sup>63</sup> The homo-coupling of electron-rich arenes, such as binaphthol, by single electron-oxidants has been extensively reviewed and will not be discussed. For additional reading on this subject, see: *Modern Arene Chemistry*; Astruc, D., Ed.; Wiley-VCH: Weinheim, **2002**.

<sup>64</sup>(a) Rong, Y.; Li, R.; Lu, W. *Organometallics* **2007**, *26*, 4376. (b) Stuart, D. R.; Fagnou, K. *Science* **2007**, *316*, 1172. (c) Stuart, D. R.; Villemure, E.; Fagnou, K. *J. Am. Chem. Soc.* **2007**, *129*, 12072. (d) Dwight, T. A.; Rue, N. R.; Charyk, D.; Josselyn, R.; DeBoef, B. *Org. Lett.* **2007**, *9*, 3137. (e) Hull, K. L.; Sanford, M. S. *J. Am. Chem. Soc.* **2007**, *129*, 11904. (f) Xia, J.-B.; You, S.-L. *Organometallics*, **2007**, *26*, 4869. (g) Potavathri, S.; Dumas, A. S.; Dwight, T. A.; Naumiec, G. R.; Hammann, J. M.; DeBoef, B. *Tetrahedron Lett.* **2008**, *49*, 4050. (h) Li, B.-J.; Tian, S.-L.; Fang, Z.; Shi, Z.-J. *Angew. Chem. Int. Ed.* **2008**, *47*, 1115. (i) Brasche, G.; Garcia-Fortanet, J.; Buchwald, S. L. *Org. Lett.* **2008**, *10*, 2207. (j) Cho, S. H.; Hwang, S. J.; Chang, S. *J. Am. Chem. Soc.* **2008**, *130*, 9254. (k) Hull, K. L.; Sanford, M. S. *J. Am. Chem. Soc.* **2009**, *131*, 9651.

development of broadly applicable conditions for the oxidative cross-coupling of simple arenes.

**Figure 3.1.** Classification of arenes in oxidative homo-coupling and cross-coupling of simple arenes.



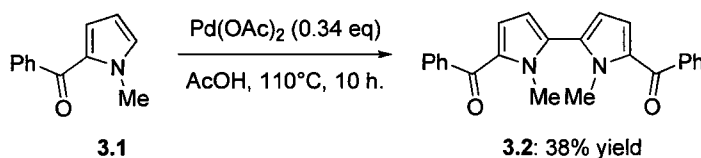
Type I arenes are those that display an inherent increased nucleophilicity over benzene itself and the particular C-H bond that is regioselectively cleaved in an oxidative cross-coupling is shown in blue (Figure 3.1). Type II arenes are those that bear Lewis basic functionality and therefore direct the metal to regioselectively cleave a particular C-H bond in the substrate (shown in blue, Figure 3.1). Type III arenes (only selected examples are shown in Figure 3.1), for the most part, have the unifying characteristic that they may be used as a bulk solvent in the reaction and these arenes show the poorest regioselectivities in oxidative homo-coupling and cross-coupling (*vide infra*). The azine *N*-oxides shown as Type III arenes are exceptions to this general classification and will be discussed in more detail (*vide infra*). This classification system is solely based on observations of the inherent physical properties of the individual substrates and does not suggest a particular mechanism for C-H bond cleavage, individual mechanistic analysis for each of the arenes must be conducted to determine this parameter of the reactivity.<sup>65</sup>

<sup>65</sup> The only in-depth mechanistic analysis to appear in the literature has been reported by Sanford, see ref. 63k.

### 3.1.1. Oxidative Homo-coupling of Type I or Type III Arenes

*Using stoichiometric palladium.* The earliest example of the oxidative coupling of simple arenes was the homo-coupling of benzene (Type III arene) to biphenyl under the action of stoichiometric palladium(II) chloride in the presence of sodium acetate and acetic acid.<sup>62a</sup> Shortly after, an improved system employing palladium acetate in the presence of perchloric acid was reported by Davidson and Triggs.<sup>62b</sup> Fujiwara also found that an olefin-palladium chloride complex in stoichiometric amounts could mediate the oxidative coupling of benzene to biphenyl.<sup>66</sup> Type I arenes, specifically 2-benzoyl-1-methylpyrrole (**3.1**), may also be dimerized to form 2,2'-bipyrrole (**3.2**) with substoichiometric amounts of palladium acetate, though conversions of ~ 1 turnover were obtained (Scheme 3.2).<sup>67</sup>

**Scheme 3.2.** Homo-coupling of pyrroles (Type I arene).



*Using catalytic palladium.* More recently, catalytic versions of this reaction have appeared in the literature.<sup>68</sup> Type III arenes, such as benzene, have been oxidatively homo-coupled by palladium acetate catalyst in the presence of O<sub>2</sub> (10 atm) and a manganese(VI) cocatalyst, although homo-coupling was also accompanied by benzene oxidation.<sup>69</sup> Multi-catalytic systems that utilize more than one metal cocatalyst as oxidants and molecular oxygen as the terminal oxidant have also been reported. Sasson has described the use of Zr(IV), Mn(II), and Co(II) as cocatalysts in the presence of O<sub>2</sub> in the palladium chloride-catalyzed homo-coupling of benzene to afford biphenyl in 89% yield.<sup>70</sup> Heteropoly acids have also been used as oxidants (often in conjunction with O<sub>2</sub>) in this chemistry and innovations in this area have been reported independently and concurrently by Kozhevnikov

<sup>66</sup> Fujiwara, Y.; Moritani, I.; Ikegami, K.; Tanaka, R.; Teranishi, S. *Bull. Chem. Soc. Jpn.* **1970**, *43*, 863.

<sup>67</sup> Itahara, T. *J. Chem. Soc. Chem. Comm.* **1980**, 49.

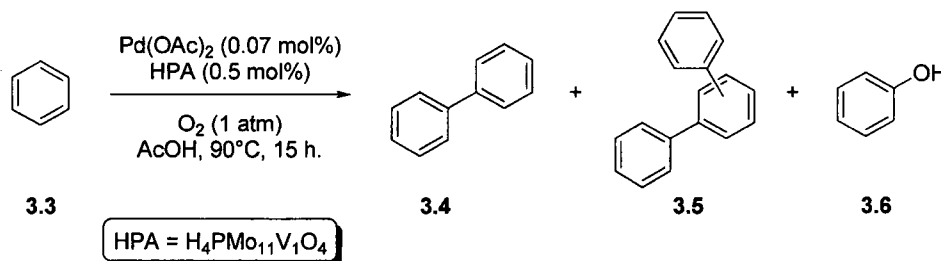
<sup>68</sup> For leading references into catalytic variants of homo-coupling of Type I arenes please see: Iataaki, H.; Yoshimoto, H. *J. Org. Chem.* **1973**, *38*, 76.

<sup>69</sup> Okamoto, M.; Yamaji, T. *Chem. Lett.* **2001**, 212.

<sup>70</sup> Mukhopadhyay, S.; Rothenberg, G.; Lando, G.; Agbaria, K.; Kazanci, M.; Sasson, Y. *Adv. Synth. Catal.* **2001**, *343*, 455.

and Ishii.<sup>71</sup> Benzene, **3.3**, (Type III arene) was homo-coupled to form biphenyl, **3.4**, with catalyst turnover mediated by the heteropoly acid,  $\text{H}_4\text{PMo}_{11}\text{V}_1\text{O}_4$ , and molecular oxygen as the terminal oxidant (Scheme 3.3). The side products of oligomerization, **3.5**, and benzene oxidation, **3.6**, were minimized in this chemistry and it was noted that in the absence of heteropoly acid biphenyl was formed stoichiometrically based on palladium.

**Scheme 3.3.** Homo-coupling of benzene (Type III arene) by catalytic palladium.



Catalytic palladium has also been used in the homo-coupling of Type I arenes. An early example by Kozhevnikov demonstrated the dimerization of furans by palladium(II) salts and copper(II) acetate as the oxidant.<sup>72</sup> The conditions described, however, provided low turnover numbers in the dimerization of thiophenes.<sup>72b</sup> In recent years a successful dimerization of thiophenes was reported by Mori and coworkers (Scheme 3.4).<sup>73</sup> 2-Substituted thiophenes, such as **3.7**, homo-couple at the 5-position in the presence of  $\text{AgF}$  as an activator and it was later found that the yields of homo-coupling may be improved when two equivalents of  $\text{AgNO}_3$  and  $\text{KF}$  are used.<sup>74</sup> Earlier this year the You group reported a highly regioselective homo-coupling of indolazines catalyzed by palladium acetate (5 mol%) and employing a copper(II) oxidant ( $\text{Cu}(\text{OAc})_2$ ).<sup>75</sup> Impressively, this methodology was used in the macrocyclization of 19-membered cyclophane, **3.10**, by intramolecular oxidative coupling of bis-indolazine, **3.9** (Scheme 3.5).

<sup>71</sup> (a) Burton, H. A.; Kozhevnikov, I. V. *J. Mol. Catal. A* **2002**, *185*, 285. (b) Yokoto, T.; Sakaguchi, S.; Ishii, Y. *Adv. Synth. Catal.* **2002**, *344*, 849.

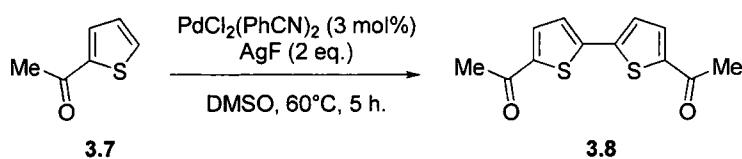
<sup>72</sup> (a) Kozhevnikov, I. V. *React. Kinet. Catal. Lett.* **1976**, *5*, 415. (b) Kozhevnikov, I. V. *React. Kinet. Catal. Lett.* **1976**, *4*, 451. (c) Kozhevnikov, I. V. *React. Kinet. Catal. Lett.* **1977**, *6*, 401.

<sup>73</sup> Masui, K.; Ikegami, H.; Mori, A. *J. Am. Chem. Soc.* **2004**, *126*, 5074.

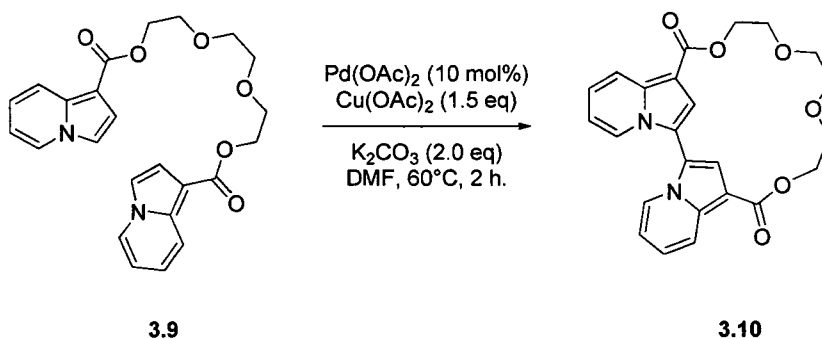
<sup>74</sup> (a) Kobayashi, K.; Sugie, A.; Takahashi, M.; Masui, K.; Mori, A. *Org. Lett.* **2005**, *7*, 5083. (b) Takahashi, M.; Masui, K.; Sekiguchi, H.; Kobayashi, N.; Mori, A.; Funahashi, M.; Tamaoki, N. *J. Am. Chem. Soc.* **2006**, *128*, 10930.

<sup>75</sup> Xia, J.-B.; Wang, X.-Q.; You, S.-L. *J. Org. Chem.* **2009**, *74*, 456.

**Scheme 3.4.** Homo-coupling of thiophenes (Type I arene) by catalytic palladium.



**Scheme 3.5.** Cyclophane formation *via* intramolecular oxidative homo-coupling of indolazines (Type I arene).

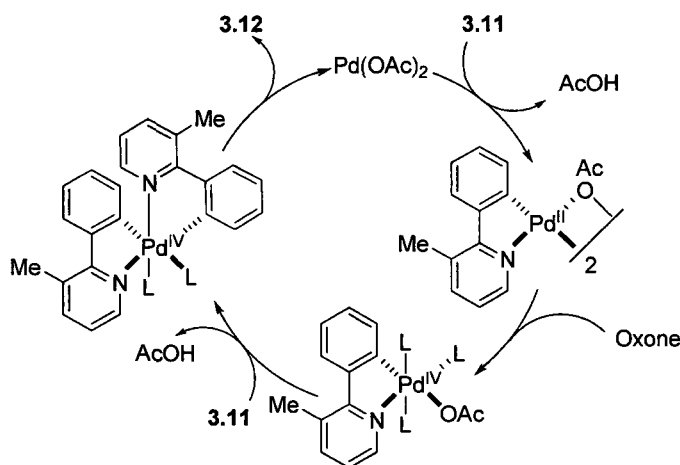
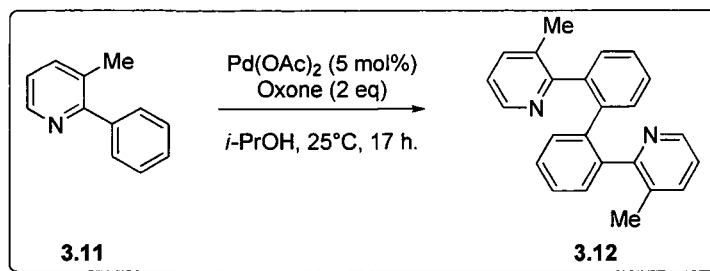


### 3.1.2. Oxidative Homo-coupling of Type II Arenes

The sole example of homo-coupling of a Type II arene was reported by Sanford in 2006.<sup>76</sup> In this case 2-arylpyridines, **3.11**, are regioselectively homo-coupled by a catalytic amount of palladium acetate in the presence of oxone (2 equiv.) to afford homo-coupled products, **3.12**, in moderate to excellent yield. Extensive mechanistic studies *via* stoichiometric experiments resulted in the following catalytic cycle in which carbon-carbon bond reductive elimination from palladium(IV) was proposed (Scheme 3.6).

<sup>76</sup> Hull, K. L.; Lanni, E. L.; Sanford, M. S. *J. Am. Chem. Soc.* **2006**, *128*, 14047.

**Scheme 3.6.** Proposed catalytic cycle for the homo-coupling of 2-arylpyridines (Type II arenes).



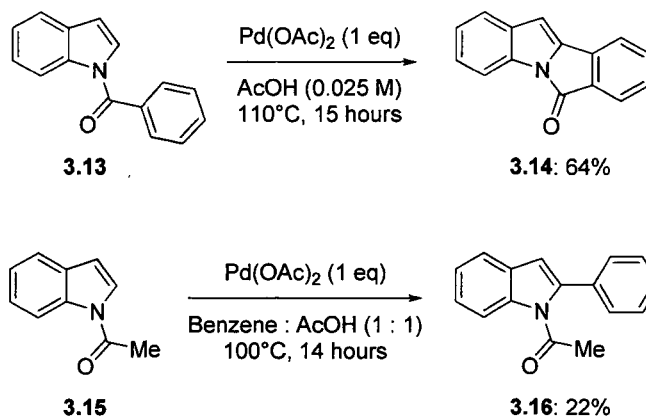
### 3.1.3. Oxidative Cross-coupling between Type I and Type III Arenes

While the intermolecular oxidative cross-coupling of simple arenes represents a significant challenge due to competitive homo-coupling of each of the two arenes; intramolecular oxidative coupling is a convenient medium in which to probe potential reaction conditions for this type of reactivity. Itahara was successful in this arena in the intramolecular oxidative ring closure of *N*-benzoylindoles, **3.13**, mediated by stoichiometric palladium acetate (Scheme 3.7).<sup>77</sup> Itahara's research in intramolecular oxidative ring closure led to the discovery of an oxidative cross-coupling between *N*-acetylindole, **3.15**, (Type I arene) and benzene (Type III arene) to yield a 2-phenyl-*N*-acetylindole, **3.16**, although in very low isolated yield and use of stoichiometric palladium acetate.<sup>78</sup>

<sup>77</sup> (a) Itahara, T. *Synthesis* **1979**, 151. (b) Itahara, T. *Heterocycles* **1986**, 24, 2557.

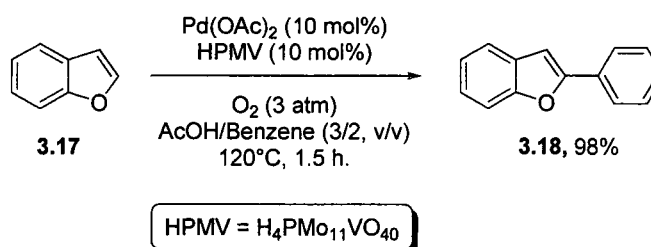
<sup>78</sup> (a) Itahara, T. *J. Chem. Soc., Chem. Comm.* **1981**, 254. (b) Itahara, T. *J. Org. Chem.* **1985**, 50, 5272.

**Scheme 3.7.** Intra- and intermolecular oxidative cross-coupling between Type I and III arenes mediated by stoichiometric palladium.



The previous two years have witnessed extensive growth in this field. In 2006 Lu reported the oxidative cross-coupling of naphthalene (Type I arene) and benzene (Type III arene).<sup>64a</sup> Although, the yield and catalyst turn-over numbers (TON) are low this constituted one of the first examples of a successful oxidative cross-coupling of simple arenes. While our own contributions<sup>64b,c</sup> are detailed in the subsequent sections (*vide infra*) DeBoef used a similar strategy in the cross-coupling of a Type I arene, benzofuran, **3.17**, with a Type III arene, benzene (Scheme 3.8).<sup>64d,g</sup> In the initial report<sup>64d</sup> both electron-rich indoles and benzofurans (both Type I arenes) are regioselectively cross-coupled with benzene (Type III arene), or its derivatives. In a subsequent report<sup>64g</sup> an observation correlating regioselectivity with the choice of oxidant was made and corroborates the observations reported herein (*vide infra*).

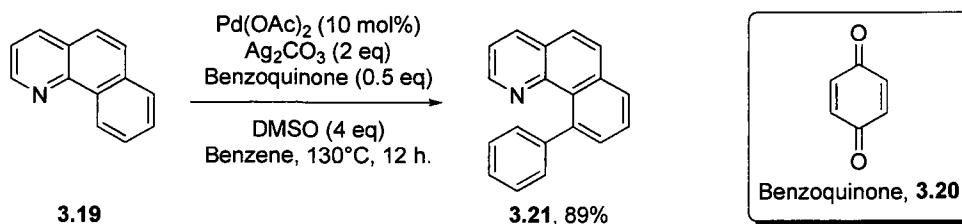
**Scheme 3.8.** Oxidative cross-coupling of benzofuran (Type I arene) and benzene (Type III arene).



### 3.1.4. Oxidative Cross-coupling between Type II and Type III Arenes.

The majority of approaches to oxidative cross-coupling have employed Type II arenes, those arenes containing Lewis basic functionality, to obtain high regioselectivity. Hull and Sanford reported the first example in this variant in which benzo[*h*]quinoline, **3.19**, (Type II arene) was regioselectively coupled to benzene, **3.3**, and its derivatives (Type III arenes) catalyzed by Pd(OAc)<sub>2</sub> (10 mol%) and in the presence of Ag<sub>2</sub>CO<sub>3</sub> (2 equiv.), benzoquinone, (**3.20**, 0.5 equiv.), and DMSO (4 equiv.) (Scheme 3.9).<sup>64e</sup> In this chemistry it was observed that the site of reactivity of the benzo[*h*]quinoline, **3.19**, was governed by the directing ability of the Lewis basic nitrogen and was exclusive to this position. However, the regioselectivity at the Type III arene was much less selective and much less predictable. Through careful optimization, specifically the steric properties of the benzoquinone ligand/oxidant, an increase in *meta*-selectivity was observed when mono-substituted Type III arenes were employed. In depth mechanistic analysis was carried out on this reaction and recently reported in the literature.<sup>64k</sup> The mode of C-H bond cleavage at the benzo[*h*]quinoline was not investigated, though the mechanism of related cyclometallations with palladium have been reported previously to proceed *via* a CMD transition state (*vide supra*).<sup>79</sup> The C-H bond cleavage at the Type III arene was the subject of their investigation. All mechanistic data pointed toward the involvement of a CMD pathway; and an S<sub>E</sub>Ar mechanism was ruled out consistent with their previous observation of *meta* selectivity in the arylation of anisole.

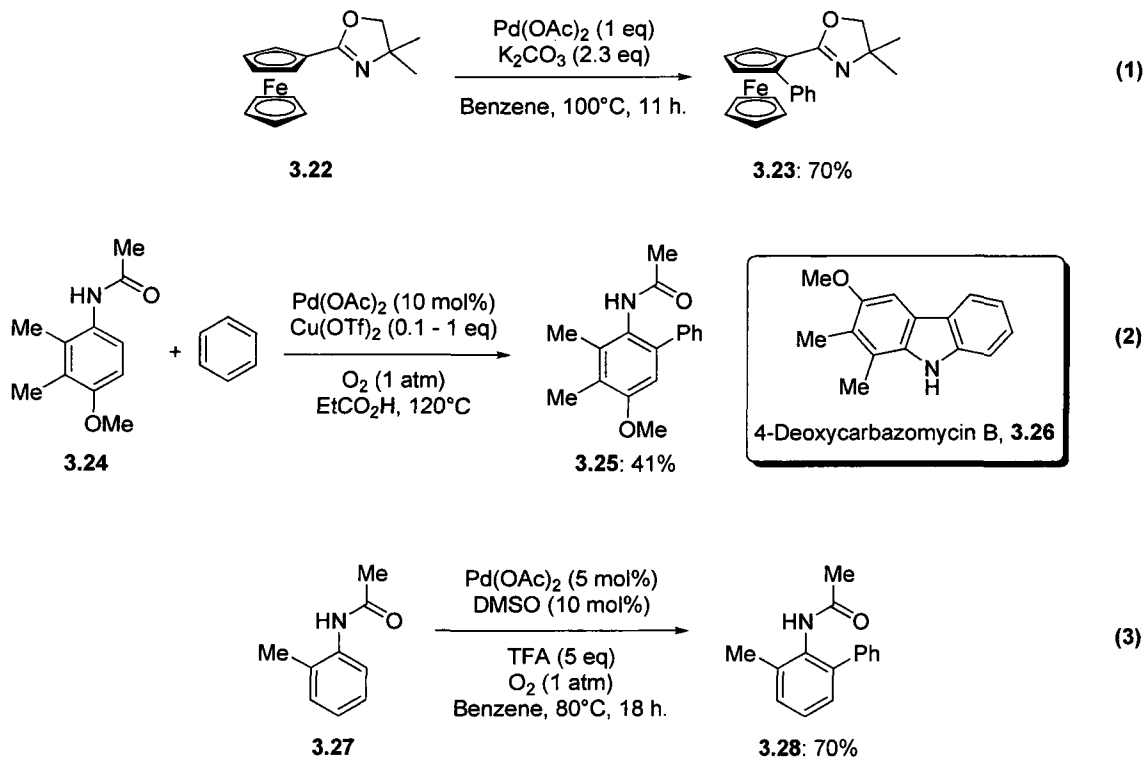
**Scheme 3.9.** Oxidative cross-coupling between benzo[*h*]quinoline (Type II arene) and benzene (Type III arene).



<sup>79</sup> For experimental work on the mechanism of cyclopalladation of *N,N*-dimethylbenzylamine, see: (a) Ryabov, A. D.; Sakodinskaya, I. K.; Yatsimirsky, A. K. *J. Chem. Soc., Dalton Trans.* **1985**, 2629. For computational work on the mechanism of cyclopalladation of *N,N*-dimethylbenzylamine, see: (b) Davies, D. L.; Donald, S. M. A.; Macgregor, S. A. *J. Am. Chem. Soc.* **2005**, *127*, 13754.

Shortly thereafter, a number of other reports employing Type II arenes appeared in the literature. Xia and You reported the use of oxazoline as a directing group in the oxidative cross-coupling of ferrocenyl oxazoline, **3.22** (Type II arene) and benzene (Type III arene) (Scheme 3.10, equation 1).<sup>64f</sup> The reaction displayed a deuterium kinetic isotope effect (KIE) of 1.8 for the C-H bond cleavage at benzene. Shi and Buchwald have both used amides as directing groups in this chemistry.<sup>64h,i</sup> The first report of oxygen being used as the terminal oxidant in an oxidative cross-coupling of a Type II arene, acetanilide, **3.24**, and benzene and its derivatives (Type III arenes) was made by Shi. This chemistry proceeds in moderate to excellent yield and was applied to the synthesis of 4-deoxycarbazomycin B, **3.26**, a degradation product of the natural product carbazomycin B (Scheme 3.10, equation 2). In Buchwald's innovation the direct oxidation of Pd(0) by molecular oxygen is reported and this metal free oxidation system represents a significant advantage over the previously reported systems. This system also utilized *N*-acetanilides, **3.27**, (Type II arenes) and benzene (Type III arene) or its derivatives (Scheme 3.10, equation 3). In the later two reports, reactions involving benzene derivatives were regioselective for reaction at the more sterically accessible C-H bond, though only moderate selectivity was observed.

**Scheme 3.10.** Oxidative cross-coupling between other Type II arenes and benzene (Type III arene).



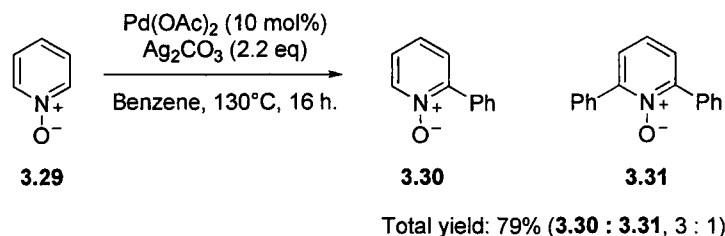
### 3.1.5. Oxidative Cross-Coupling between Type III Arenes.

Chang has reported the only example of oxidative cross-coupling of two different Type III arenes.<sup>64j</sup> In this case pyridine *N*-oxide **3.29** is successfully cross-coupled with benzene and its derivatives (Scheme 3.11). These reactions are highly regioselective for the two position of pyridine *N*-oxide and moderately selective for the most sterically accessible C-H bond of the Type III arene. The mono-arylation product, **3.30**, was accompanied by a diarylation product, **3.31**, when possible. Chang and co-workers suggest that the *N*-oxide moiety facilitates regioselective C-H bond cleavage by acting as a Lewis base, thus classifying it as a Type II arene. However, computational data from the Fagnou group has ruled out any involvement of the *N*-oxide moiety acting as a directing group in pyridine *N*-oxide direct arylation<sup>80</sup> and therefore **3.29** is not classed as a Type II arene here.

<sup>80</sup> Gorelsky, S.; Fagnou, K. *unpublished results*.

Additionally, **3.29** is more electron-deficient than benzene and thus could not be described as a Type I arene.

**Scheme 3.11.** Oxidative cross-coupling between pyridine *N*-oxide (Type II arene) and benzene (Type III arene).

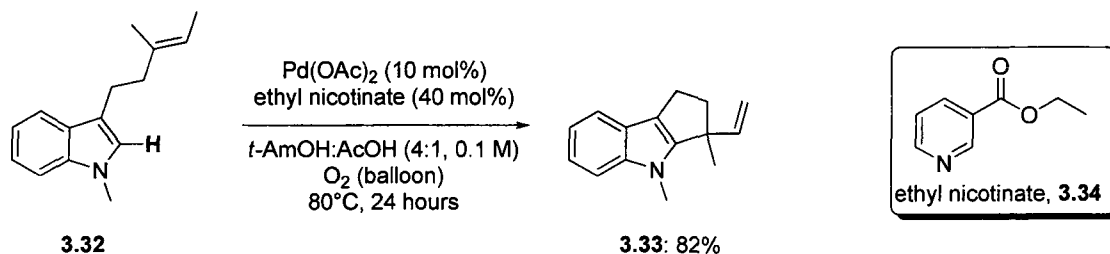


## 3.2. Results and Discussion

### 3.2.1. Reaction Development and Investigation of Functional Group Compatibility.

**Intramolecular Oxidative Cross-Coupling.** Our investigation into a catalytic intramolecular oxidative coupling of simple arenes, *N*-benzoylindole, was inspired by Itahara's work on the same transformation mediated by stoichiometric palladium (Scheme 3.7).<sup>77</sup> Insights reported by Stoltz on palladium catalyzed transformations of indoles, namely intramolecular aerobic annulation of indole *via* oxidative Heck reaction (Scheme 3.12) was also instructive in the development of this chemistry.<sup>81</sup>

**Scheme 3.12.** Indole annulation *via* oxidative Heck reaction.



<sup>81</sup> Ferreira, E. M.; Stoltz, B. M. *J. Am. Chem. Soc.* **2003**, *125*, 9578.

Selected data from the optimization of the intramolecular oxidative ring closure of *N*-benzoylindole, **3.13**, are presented in Table 3.1. As stated previously inspiration came from Stoltz's report that pyridine ligands were beneficial in indole annulations<sup>82</sup> and modification of the conditions (20 mol% Pd, 3-CNpy as ligand) reported therein resulted in 30% GCMS conversion (Table 3.1, entry 1). A later report by the same author<sup>83</sup> led to the introduction of acetate additives (NaOAc) which provided a modest increase in conversion (33%) (Table 3.1, compare entries 1 and 2). It was then found that both the catalyst loading of the ligand and palladium could be reduced to 20 mol % and 10 mol %, respectively, providing a marked increase in conversion to 47% (Table 3.1, entries 3 and 4). A further amplification in conversion (61%) was observed when the more electrophilic palladium source, Pd(TFA)<sub>2</sub> was employed (Table 3.1, entry 5). Additionally, a 1 : 1 ratio of Pd : ligand proved optimal further augmenting the conversion to 71% (Table 3.1, entry 6). Following this result the beneficial effects of pivalic acid/pivalate<sup>8b</sup> on the reaction was investigated by replacement of acetic acid for pivalic acid and sodium acetate for potassium pivalate and the conversion was increased to 78% (Table 3.1, entry 7). A series of other pyridine derivatives were also evaluated as potential ligands and it was observed that 3-nitropyridine was most effective resulting in a GCMS conversion of 87% (Table 3.1, entries 7 – 10). Furthermore, it should be noted that only modest conversion (44%) is observed in the absence of ligand (Table 3.1, entry 11). Complete conversion was finally obtained by use of CsOPiv as additive (Table 3.1, entry 12), and it is postulated that this is due to the increased solubility of the base when the cesium analogue is used.

Application of the optimal reaction conditions resulted in a 74% isolated yield of the tetracyclic indole product, **3.14** (Scheme 3.13, equation 1). Moreover, the reaction conditions were compatible with the formation of carbazole, **3.36** *via* oxidative ring closure of diphenylamine, **3.35**, which was observed to proceed in 87% GCMS conversion (Scheme 3.13, equation 2). The further development of this chemistry was conducted by a post-doctoral fellow, Benoît Liégault, with an emphasis on the preparation of electron-rich

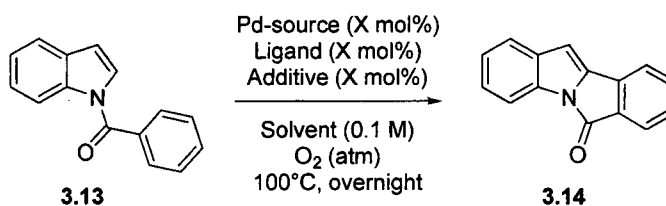
---

<sup>82</sup> Pyridine-palladium systems have also been useful catalysts in alcohol oxidation: (a) Nishimura, T.; Onoue, T.; Ohe, K.; Uemura, S. *J. Org. Chem.* **1999**, *64*, 6750-6755; oxidative ring cleavage: (b) Nishimura, T.; Ohe, K.; Uemura, S. *J. Am. Chem. Soc.* **1999**, *121*, 2645-2646; oxidative amination: (c) Fix, S. R.; Brice, J. L.; Stahl, S. S. *Angew. Chem., Int. Ed.* **2002**, *41*, 164-166; and Waker-type cyclizations: (d) Trend, R. M.; Ramtohl, Y. K.; Ferreira, E. M.; Stoltz, B. M. *Angew. Chem., Int. Ed.* **2003**, *42*, 2892-2895.

<sup>83</sup> Zhang, H.; Ferreira, E. M.; Stoltz, B. M. *Angew. Chem. Int. Ed.* **2004**, *43*, 6144.

carbazoles and application of the methodology to the synthesis of the carbazole natural products murrayafoline A, mukonine, and clausenine.<sup>84</sup>

**Table 3.1.** Optimization for the intramolecular oxidative ring closure of *N*-benzoylindole, **3.13**.<sup>a</sup>

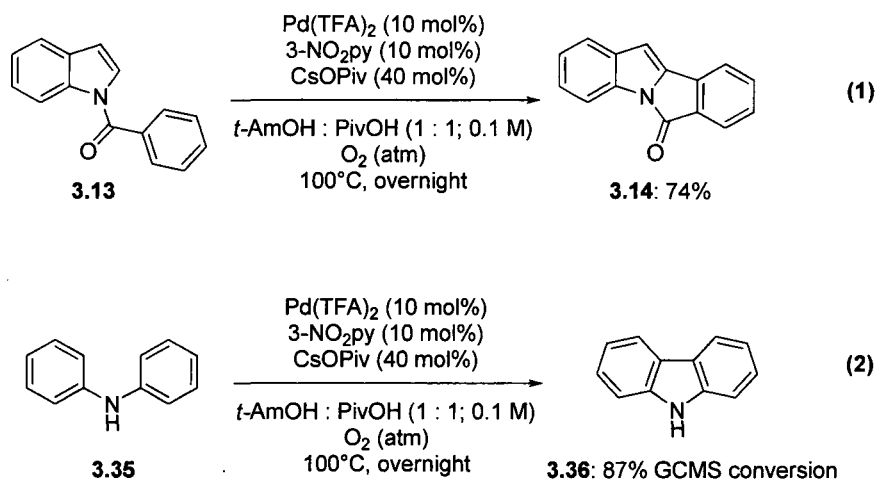


Entry	Pd (mol %)	Ligand (mol %)	Additive (mol %)	Solvent	Conv (%) <sup>b</sup>
1	Pd(OAc) <sub>2</sub> (20)	3-CNpy (40)	—	<i>t</i> -AmOH:AcOH (4:1)	30
2	Pd(OAc) <sub>2</sub> (20)	3-CNpy (40)	NaOAc (40)	<i>t</i> -AmOH:AcOH (4:1)	33
3	Pd(OAc) <sub>2</sub> (20)	3-CNpy (20)	NaOAc (40)	<i>t</i> -AmOH:AcOH (4:1)	48
4	Pd(OAc) <sub>2</sub> (10)	3-CNpy (20)	NaOAc (40)	<i>t</i> -AmOH:AcOH (4:1)	47
5	Pd(TFA) <sub>2</sub> (10)	3-CNpy (20)	NaOAc (40)	<i>t</i> -AmOH:AcOH (4:1)	61
6	Pd(TFA) <sub>2</sub> (10)	3-CNpy (10)	NaOAc (40)	<i>t</i> -AmOH:AcOH (4:1)	71
7	Pd(TFA) <sub>2</sub> (10)	3-CNpy (10)	KOPiv (40)	<i>t</i> -AmOH:PivOH (4:1)	78
8	Pd(TFA) <sub>2</sub> (10)	4-CNpy (10)	KOPiv (40)	<i>t</i> -AmOH:PivOH (4:1)	64
9	Pd(TFA) <sub>2</sub> (10)	3-CO <sub>2</sub> Mepy (10)	KOPiv (40)	<i>t</i> -AmOH:PivOH (4:1)	71
10	Pd(TFA) <sub>2</sub> (10)	3-NO <sub>2</sub> py (10)	KOPiv (40)	<i>t</i> -AmOH:PivOH (4:1)	87
11	Pd(TFA) <sub>2</sub> (10)	—	KOPiv (40)	<i>t</i> -AmOH:PivOH (4:1)	44
12	Pd(TFA) <sub>2</sub> (10)	3-NO <sub>2</sub> py (10)	CsOPiv (40)	<i>t</i> -AmOH:PivOH (4:1)	99

<sup>a</sup>Conditions: **3.13** (1 eq, 0.1 M), PdX<sub>2</sub> (X mol%), ligand (X mol%), additive (X mol%), *t*-AmOH : RCO<sub>2</sub>H (4 : 1), 100°C, 12 - 16 hours. <sup>b</sup>Determined by GCMS, based on substrate consumption.

<sup>84</sup> Liégault, B.; Lee, D.; Heustis, M. P.; Stuart, D. R.; Fagnou, K. *J. Org. Chem.* **2008**, *73*, 5022.

**Scheme 3.13.** Application of optimized reaction conditions.

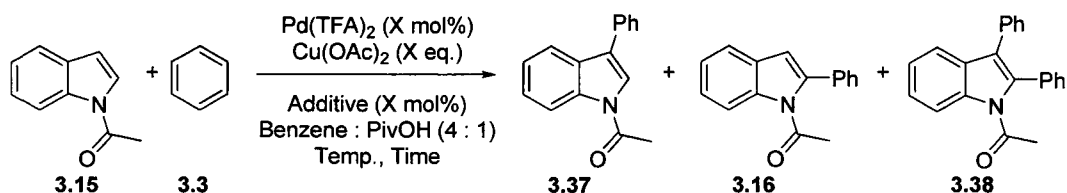


***Intermolecular Oxidative Arylation of Indoles: First Generation Conditions.***

Itahara also pioneered the intermolecular oxidative cross-coupling of two unactivated arenes mediated by stoichiometric palladium salts (Scheme 3.7) (*vide supra*).<sup>78</sup> In his report the reaction of *N*-acetylindole, **3.15**, and benzene, **3.3**, resulted in an isolated yield of 22% for the C2-phenylated indole, **3.16**, though no discussion of the possible regioisomeric product distribution was presented. *N*-Acetylindole, **3.15**, was thus a suitable choice for an investigation into the catalytic oxidative cross-coupling of unactivated arenes.<sup>64b</sup> Under slightly modified conditions (benzene : PivOH, 4 : 1) the 2-phenylated indole, **3.16**, was obtained in 13% GCMS yield with the C3-phenylated isomer, **3.37**, constituting the major product of the reaction (55% GCMS yield, Table 3.2, entry 1) in our hands. It was observed, however, that under catalytic conditions (10 mol % Pd), employing Cu(OAc)<sub>2</sub> as a terminal oxidant, the regioselectivity of the reaction was greatly improved (C3 : C2, 27 : 1), though the conversion of starting materials to products suffered (Table 3.2, entry 3). Complete conversion could be re-established by allowing the reaction to proceed for 48 hours although this also increased the proportion of C2,C3-diphenylated indole (Table 3.2, entry 4). The relative amount of the unwanted diarylated product could be effectively reduced by use of 3-nitropyridine as ligand and CsOPiv (in sub-stoichiometric quantities) while maintaining the high level of conversion previously observed (Table 3.2, entry 5). Microwave irradiation was investigated to reduce reaction times and was found to be quite capable in this process (Table 3.2, entry 6) providing the C3-phenylated indole in 87% isolated yield. While the

catalyst loading of Pd(TFA)<sub>2</sub> could, in fact, be lowered (Table 3.2, entry 7 and 8), the conversion suffered and product isolation was hampered for this particular substrate. Therefore, the optimal conditions used to investigate the scope of the reaction employed 10 mol % Pd(TFA)<sub>2</sub> (Table 3.2, entry 6).

**Table 3.2.** Optimization for the C3 Oxidative Arylation of N-Acetylindoles.<sup>a</sup>



Entry	Mol% Pd	Equiv. Cu	Additives (mol%)	Temp. (°C)	Time (h)	Conv. <sup>b</sup>	Ratio <sup>c</sup>	% Yield <sup>e</sup>
1	100	—	none	110	24	>99	4.4:1:2.6	55
2	100	2	none	110	24	>99	3.1:1:5.4	35
3	10	3	none	110	24	67	27:1:0.28	64
4	10	3	none	110	48	>99	27:1:1.2	92
5	10	3	3-NO <sub>2</sub> pyridine (10) CsOPiv (40)	110	48	>99	17:1:0.23	93
6	10	3	3-NO <sub>2</sub> pyridine (10) CsOPiv (40)	140 <sup>e</sup>	5	>99	8.9:1:0.26	88(87)
7	5	3	3-NO <sub>2</sub> pyridine (5) CsOPiv (40)	140 <sup>e</sup>	5	92	13.8:1:0.24	84
8	2	3	3-NO <sub>2</sub> pyridine (2) CsOPiv (40)	140 <sup>e</sup>	5	66	27:1:0	63
9	0	3	3-NO <sub>2</sub> pyridine (10) CsOPiv (40)	110	24	0	—	0

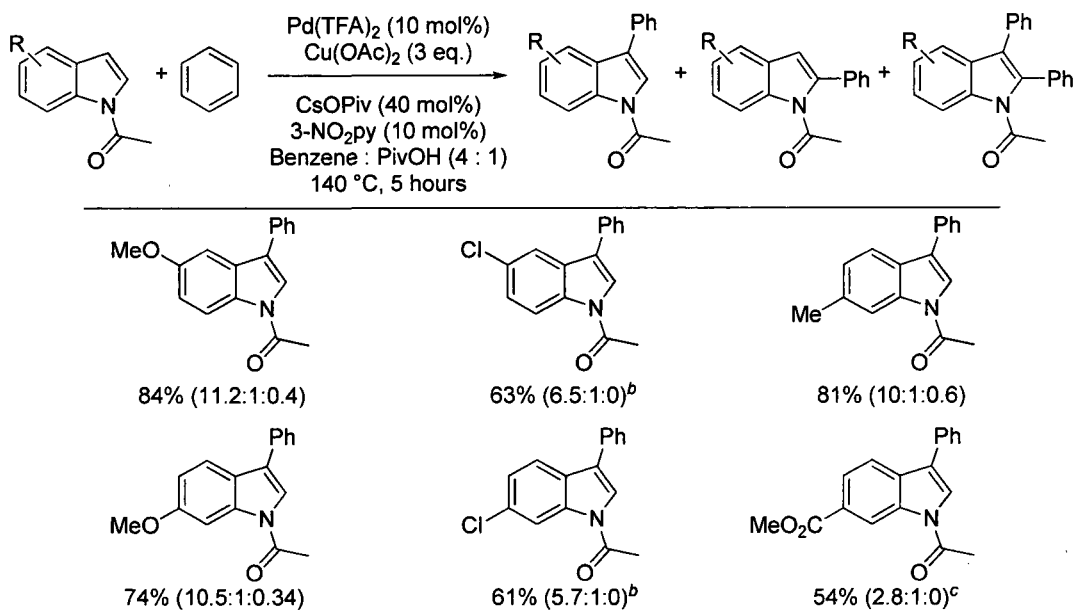
<sup>a</sup>Conditions: **3.15** (1 eq, 0.3 M), Pd(TFA)<sub>2</sub> (X mol%), Cu(OAc)<sub>2</sub> (2 - 3 eq), additive (see above), Benzene : PivOH (4 : 1), temperature (see above), time (see above). <sup>b</sup>Determined by GCMS. <sup>c</sup>Ratio of **3.37** : **3.16** : **3.38**.

<sup>d</sup>Reaction was conducted in microwave-reactor. <sup>e</sup>Yield of **3.37** determine by GCMS, isolated yield in parentheses.

Under the optimized conditions (Table 3.2, entry 6) the generality of the reaction was investigated with respect to both the indole (Table 3.3) and the arene coupling partner (Table 3.4). Substitution at both C5 and C6 was tolerated in the form of electron-donating groups (methoxy), halides (Cl), alkyl groups (methyl) and electron-withdrawing groups (CO<sub>2</sub>Me) providing the C3-phenylated indole in moderate (54%) to good (84%) isolated yield. C3 : C2 regioselectivity ranged from 3 : 1 (6-CO<sub>2</sub>Me) to 11 : 1 (5-OMe) with the C5- and C6-Cl providing 6.5 : 1 and 5.7 : 1 regioselectivities, respectively. It should also be noted that the halide functionality were not compatible with the microwave conditions due to a competing

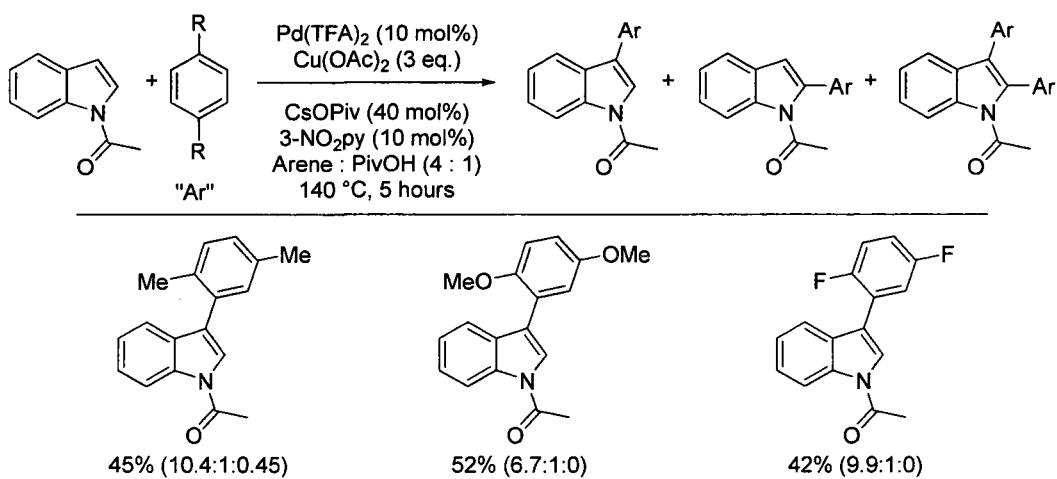
hydro-dehalogenation process. Therefore, these substrates were heated thermally in Schlenk tubes.

**Table 3.3.** Scope of compatible functionality on indole in the C3 oxidative arylation of *N*-acetylindoles.<sup>a</sup>



<sup>a</sup>Conditions: Indole (1 eq, 0.3 M), Pd(TFA)<sub>2</sub> (10 mol%), Cu(OAc)<sub>2</sub> (3 eq), 3-nitropyridine (10 mol%), CsOPiv (40 mol%), Benzene : PivOH (4 : 1), 140 °C, 5 hours. <sup>b</sup>Heated thermally at 110 °C for 16 hours. <sup>c</sup>Pd(TFA)<sub>2</sub> (20 mol%), 3-nitropyridine (20 mol%). <sup>d</sup>Isolated yields are reported above; ratios are GCMS ratios.

**Table 3.4.** Scope of compatible arenes in the C3 oxidative arylation of *N*-acetylindole.<sup>a</sup>

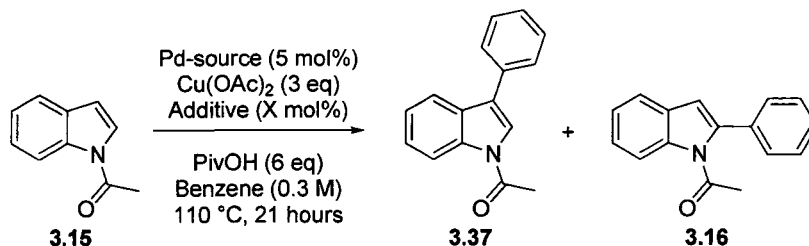


<sup>a</sup>Conditions: Indole (1 eq, 0.3 M), Pd(TFA)<sub>2</sub> (20 mol%), Cu(OAc)<sub>2</sub> (3 eq), 3-nitropyridine (20 mol%), CsOPiv (40 mol%), Benzene : PivOH (4 : 1), 140 °C, 5 hours. <sup>b</sup>Isolated yields are reported above; ratios are GCMS ratios.

In order to avoid issues of regioselectivity 1,4-symmetrically disubstituted arenes were selected as coupling partners in our first report of this chemistry (Table 3.4). Again moderate to good regioselectivities were obtained and moderate yields of the C3-arylated products were achieved for electron-rich (R = OMe), neutral (R = Me) and electron-deficient (R = F) arenes (Table 3.4).

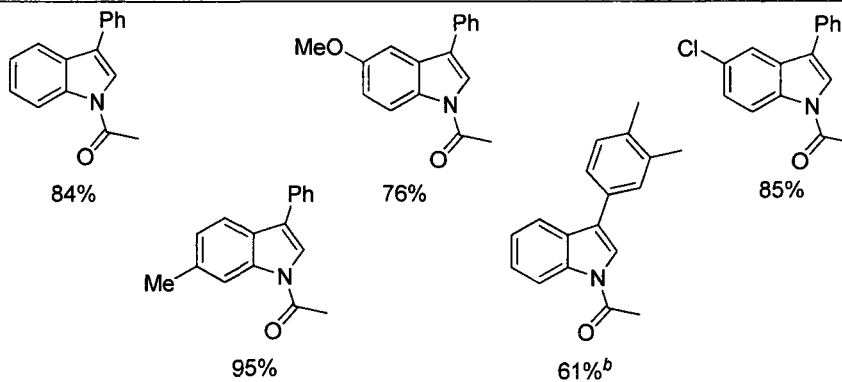
***Intermolecular Oxidative Arylation of Indoles: Second Generation Conditions.*** A secondary investigation into the various reaction parameters governing reactivity provided conditions under thermal heating for the C3 oxidative arylation of *N*-acetylindoles and selected results are presented in Table 3.5. Most influential on the reaction outcome was the palladium source with Pd(acac)<sub>2</sub> providing the highest GCMS yield (62%) of the C3-phenylated product (Table 3.5, entry 1 – 3). Following this it was found that when using Pd(acac)<sub>2</sub> the ligand 3-nitropyridine was not necessary and in its absence the GCMS yield was increased to 84% (Table 3.5, entry 4). The proportion of added acid (PivOH) and base (CsOPiv) also affected the reactivity with the relative amount of acid having the greatest influence, providing both increased yield (26% - 95%) and improved C3-selectivity (14 : 1 to 20 : 1) (Table 3.5, entries 5 – 8). A small number of indoles and arenes were selected to validate the second generation conditions and uniformly good isolated yields could be obtained for the C3-arylated *N*-acetylindole (Table 3.5).

**Table 3.5.** Optimization for the thermal C3 oxidative arylation of *N*-acetylindoles and representative examples.<sup>a</sup>



Entry	Pd-source	Additive (mol%)	PivOH (eq)	Ratio <sup>b</sup>	Yield <sup>c</sup>
1	Pd(TFA) <sub>2</sub>	3-NO <sub>2</sub> py (5) CsOPiv (40)	6	11 : 1	42%
2	Pd(acac) <sub>2</sub>	3-NO <sub>2</sub> py (5) CsOPiv (40)	6	10 : 1	62%
3	PdCl <sub>2</sub>	3-NO <sub>2</sub> py (5) CsOPiv (40)	6	only C3	10%
4	Pd(acac) <sub>2</sub>	CsOPiv (40)	6	13 : 1	84%
5	Pd(acac) <sub>2</sub>	—	0	only C3	26%
6	Pd(acac) <sub>2</sub>	—	1	14 : 1	88%
7	Pd(acac) <sub>2</sub>	—	3	15 : 1	91%
8	Pd(acac) <sub>2</sub>	—	6	20 : 1	95%(84%)

<sup>a</sup>Conditions: **3.15** (1 eq, 0.3 M), PdX<sub>2</sub> (5 mol%), Cu(OAc)<sub>2</sub> (3 eq), additive (see above), PivOH (X eq), 110 °C, 21 hours. <sup>b</sup>Ratio of **3.37** : **3.16**, determined by GCMS. <sup>c</sup>Yield of **3.37** determine by GCMS, isolated yield in parentheses.



<sup>a</sup>Conditions: Indole (1 eq, 0.3 M), Pd(acac)<sub>2</sub> (5 mol%), Cu(OAc)<sub>2</sub> (3 eq), PivOH (6 eq), Benzene, 110 °C, 21 hours. <sup>b</sup>Pd(acac)<sub>2</sub> (10 mol%). <sup>c</sup>Isolated yields are reported above.

### *Intermolecular Oxidative Arylation of Indoles: Third Generation Conditions.*

During the course of our investigation into the oxidative arylation of *N*-acetylindoles, one of the reaction parameters examined was the nature of the oxidant. At this stage an interesting

inversion in regioselectivity (C3 : C2; 8.9 : 1 to 1 : 4) was observed when silver acetate was employed (Table 3.6, entries 1 and 2). A further increase in the C2 selectivity of the reaction was observed when the acetyl group was replaced by a pivaloyl group. It may be counter-intuitive that an increase in steric congestion (change of methyl to *tert*-butyl) resulted in an increase in C2-selectivity (*ortho*). However, this substrate modification may have an influence over the inherent physical properties of the substrate (*vide infra*) (Table 3.6, entry 3).<sup>85</sup> Removal of both ligand, 3-nitropyridine, and substoichiometric base, CsOPiv, additive resulted in a beneficial effect on both the conversion and the regioselectivity, as had been previously observed in the thermal C3 oxidative arylation of *N*-acetylindole (*vide supra*). Furthermore, this catalyst system proved to be much more reactive and the reaction was complete within 3 hours (Table 3.6, entry 4) these conditions were reported as the optimal set of conditions and used to explore the generality of the reaction.<sup>64c</sup>

**Table 3.6.** Optimization for the C2 oxidative arylation of *N*-pivaloylindoles.<sup>a</sup>

Entry	Mol% Pd	Oxidant (eq)	Additive (mol%)	Indole	Time (h)	Conv. <sup>c</sup>	Ratio <sup>d</sup>
1 <sup>b</sup>	10	Cu(OAc) <sub>2</sub> (3)	3-NO <sub>2</sub> pyridine (10) CsOPiv (40)	<b>3.15a</b>	5	100	8.9:1:0.26
2	10	AgOAc (2.2)	3-NO <sub>2</sub> pyridine (10) CsOPiv (40)	<b>3.15a</b>	24	32	1:4:0
3	10	AgOAc (2.2)	3-NO <sub>2</sub> pyridine (10) CsOPiv (40)	<b>3.15b</b>	24	78	1:8.7:0.3
4	5	AgOAc (3)	none	<b>3.15b</b>	3	99	1:25:0.7
5	2	AgOAc (3)	none	<b>3.15b</b>	15	87	1:14:0.4

<sup>a</sup>Conditions: **3.15a** or **3.15b** (1 eq, 0.3 M), Pd(TFA)<sub>2</sub> (X mol%), Oxidant (see above), additive (see above), PivOH (6 eq), Benzene, 110 °C, time (see above). <sup>b</sup>Microwave heating used, see Table 4.2, entry 6. <sup>c</sup>Determined by GCMS.

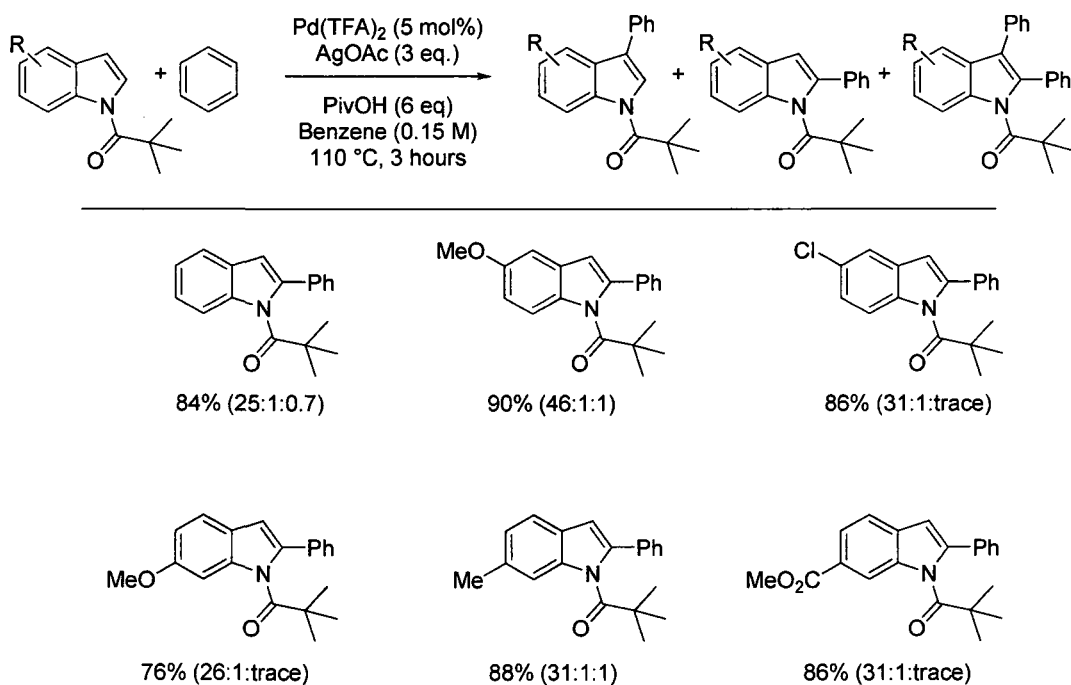
<sup>d</sup>Ratio of **3.37** : **3.16** : **3.38**, determined by GCMS.

The reaction displayed uniformly good yields (76 – 90%) and high C2 selectivity (>25 : 1) for a range of substituted indoles including electron-rich groups (5-OMe and 6-

<sup>85</sup> For examples where substrate or solvent modification can result in a dramatic change in selectivity, see: (a) Grimster, N. P.; Gauntlett, C.; Godfrey, C. R. A.; Gaunt, M. J. *Angew. Chem., Int. Ed.* **2005**, *44*, 3125. (b) Beck, E. M.; Grimster, N. P.; Hatley, R.; Gaunt, M. J. *J. Am. Chem. Soc.* **2006**, *128*, 2528. See also ref. 35.

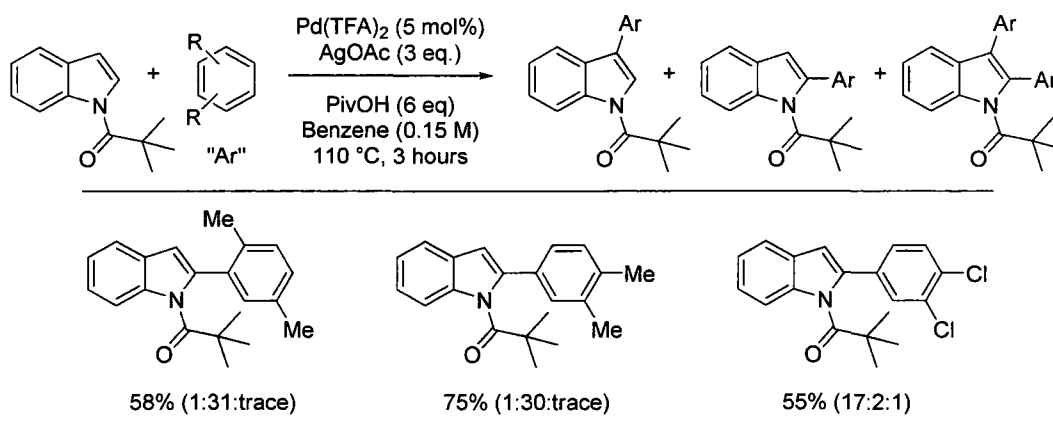
OMe), halides (5-Cl) and electron-withdrawing groups (6-CO<sub>2</sub>Me) (Table 3.7). Arenes other than benzene were also evaluated as potential coupling partners in this chemistry as well. It was found in this case that when symmetrically *ortho*-disubstituted arenes were used, the reaction was regioselective for the least sterically encumbered C-H bond of the arene (Table 3.8). This allows some predictive ability in substrate selection but may also have mechanistic implications as well (*vide infra*). This chemistry was also validated in the oxidative cross-coupling of pyrrole substrates with benzene and *ortho*-xylene.<sup>64c</sup>

**Table 3.7.** Scope of compatible functionality on indole in the C2 oxidative arylation of *N*-pivaloylindoles.<sup>a</sup>



<sup>a</sup>Conditions: Indole (1 eq, 0.15 M), Pd(TFA)<sub>2</sub> (5 mol%), AgOAc (3 eq), PivOH (6 eq), Benzene, 110 °C, 3 hours. <sup>b</sup>Isolated yields are reported above; ratios are GCMS ratios.

**Table 3.8.** Scope of compatible arenes in the C2 oxidative arylation of *N*-pivaloylindole.<sup>a</sup>



<sup>a</sup>Conditions: Indole (1 eq, 0.15 M),  $\text{Pd}(\text{TFA})_2$  (10 mol%),  $\text{AgOAc}$  (3 eq),  $\text{PivOH}$  (6 eq), Arene, 110 °C, 3 hours. <sup>b</sup>Isolated yields are reported above; ratios are GCMS ratios.

### 3.2.2. Kinetics and Mechanistic Evaluation for the Oxidative Cross-Coupling of *N*-Acetyl and *N*-Pivaloylindole with Unactivated Arenes.

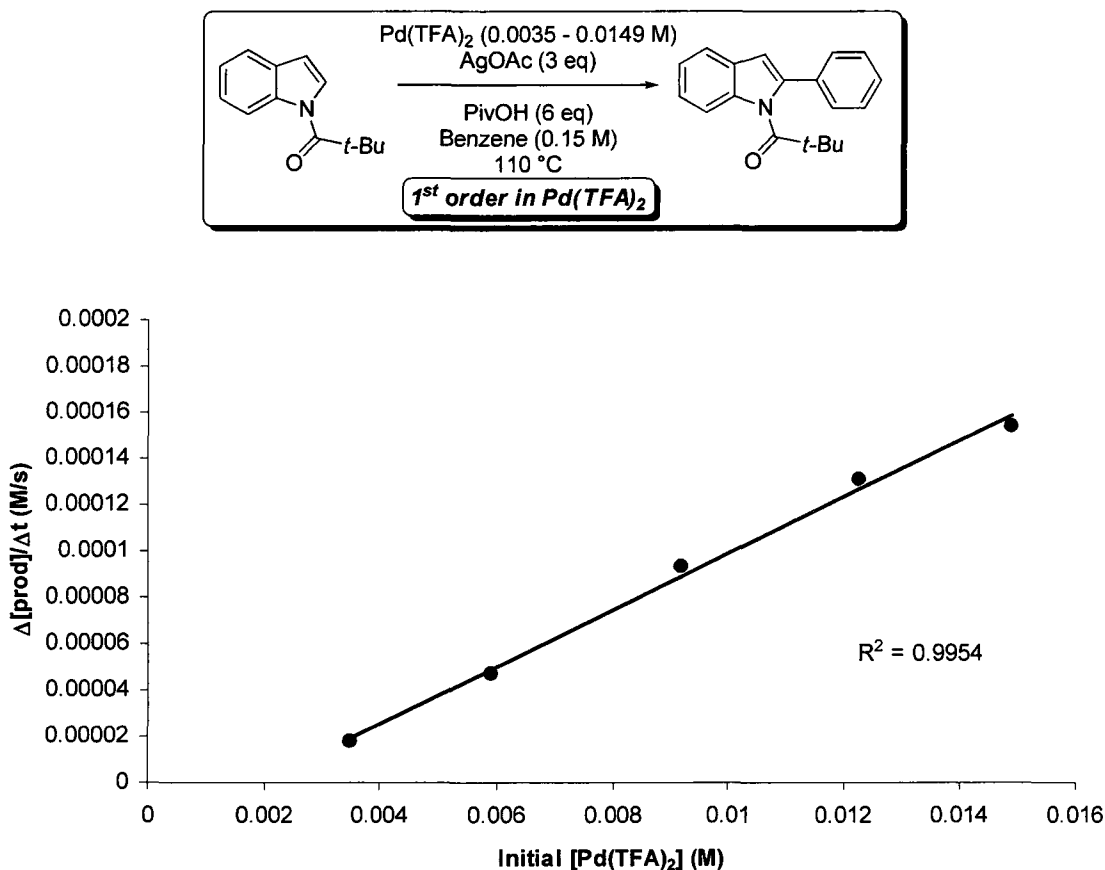
The intricate details of the catalytic cycle necessary for the efficient cross-coupling of two simple arenes were probed by a mechanistic analysis of the oxidative arylation of *N*-acetyl and *N*-pivaloylindoles. Kinetic studies, as well as free-energy correlations and DKIE were used in this process.

**Order of reagents.** The order of each reagent was determined by the method of initial rates. The formation of product was monitored by removing aliquots of the reaction mixture at specified time intervals and determining conversion of starting material to product by GCMS (conversions were < 20%). The conversion of product was then converted to a relative concentration and the initial rate was determined from the slope of a linear plot of concentration of product ([prod]) against time (s). This was done for a number (4 – 10) of different initial concentrations of a given reagent while holding all other reagent concentrations constant; and each reagent was examined in this way.<sup>86</sup> The order in each reagent was determined by plotting the initial rate ( $\Delta[\text{prod}]/\Delta t$ ) against initial concentrations (initial [reagent]) and examining the dependence of the rate on concentration. Under the

<sup>86</sup> See supporting information (Chapter 5) for a sample plot.

standard reaction conditions<sup>87</sup> for oxidative C2-arylation of *N*-pivaloylindole with benzene, the reaction displayed first order dependence in both palladium trifluoroacetate and benzene, and zero order dependence in *N*-pivaloylindole, silver acetate, and pivalic acid (Figure 3.2 – Figure 3.6). Similar trends were observed for the oxidative C3-arylation of *N*-acetylindole with benzene under standard second generation conditions.<sup>88</sup> These results point toward a mechanism with a rate determining C-H bond cleavage taking place at benzene.

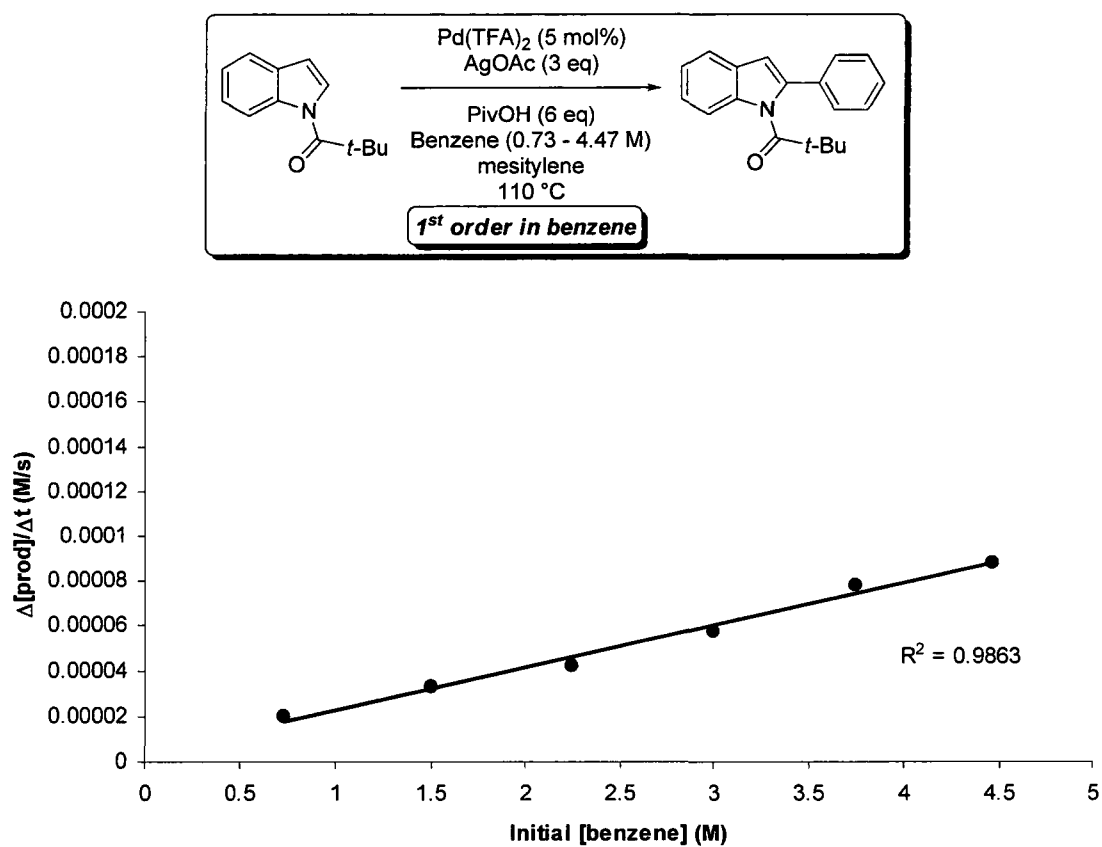
**Figure 3.2.** Initial rate vs. initial concentration of Pd(TFA)<sub>2</sub>.



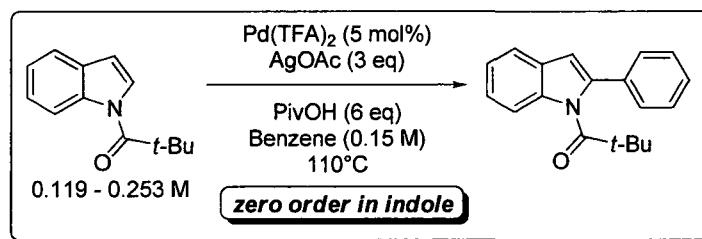
<sup>87</sup> Standard reaction conditions for the oxidative C2-arylation of *N*-pivaloylindole are: *N*-pivaloylindole (1 equiv., 0.15 M), Pd(TFA)<sub>2</sub> (5 mol%, 0.0075 M), AgOAc (3 equiv., 0.45 M), PivOH (6 equiv., 0.90 M), benzene (67 equiv., ~10 M).

<sup>88</sup> Standard second generation conditions for the oxidative C3-arylation of *N*-acetylindole are: *N*-acetylindole (1 equiv., 0.3 M), Pd(acac)<sub>2</sub> (5 mol%, 0.015 M), Cu(OAc)<sub>2</sub> (3 equiv., 0.9 M), PivOH (6 equiv., 1.8 M), benzene (~30 equiv.).

**Figure 3.3.** Initial rate vs. initial concentration of benzene.



**Figure 3.4.** Initial rate vs. initial concentration of *N*-pivaloylindole.



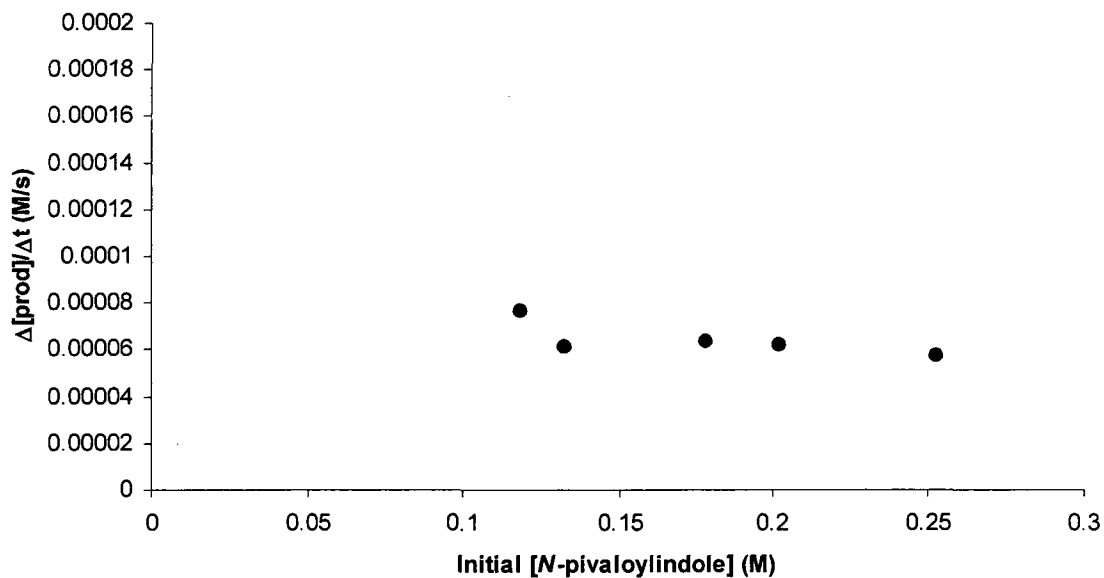


**Figure 3.5.** Initial rate vs. initial concentration of silver acetate.

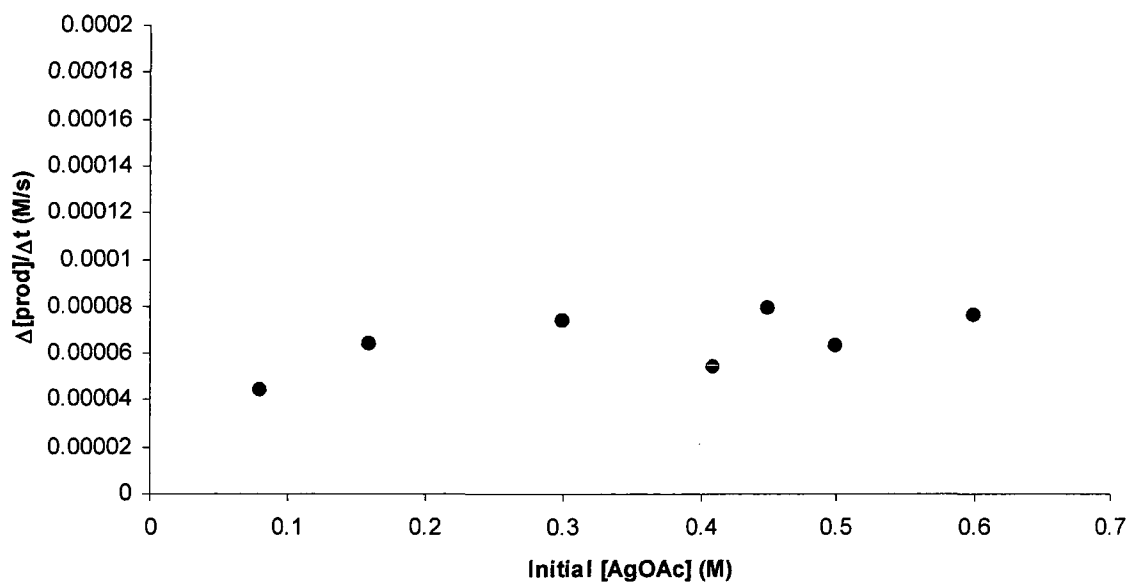
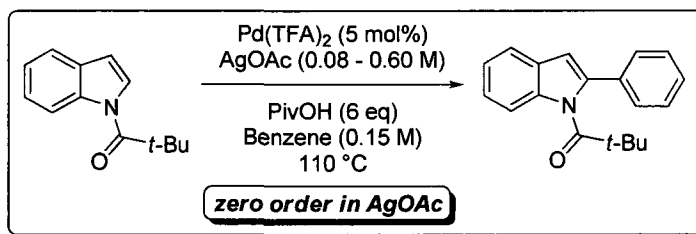
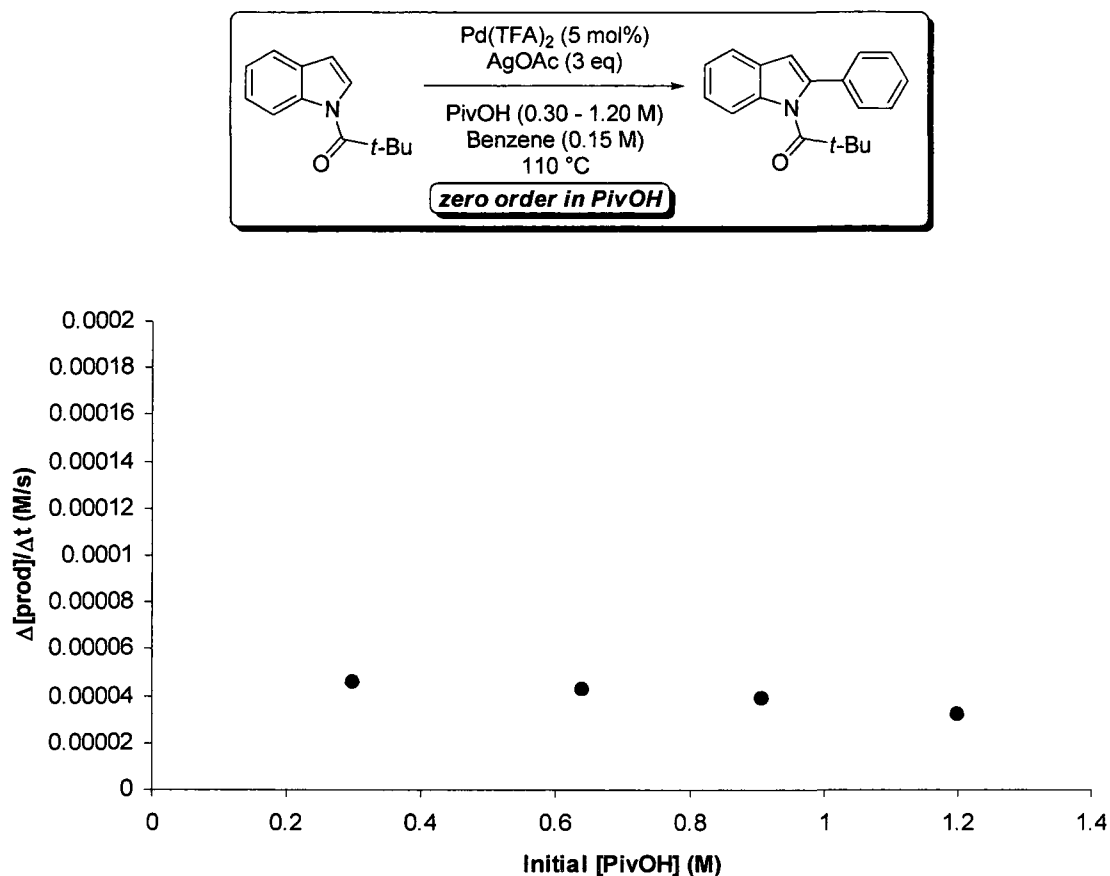


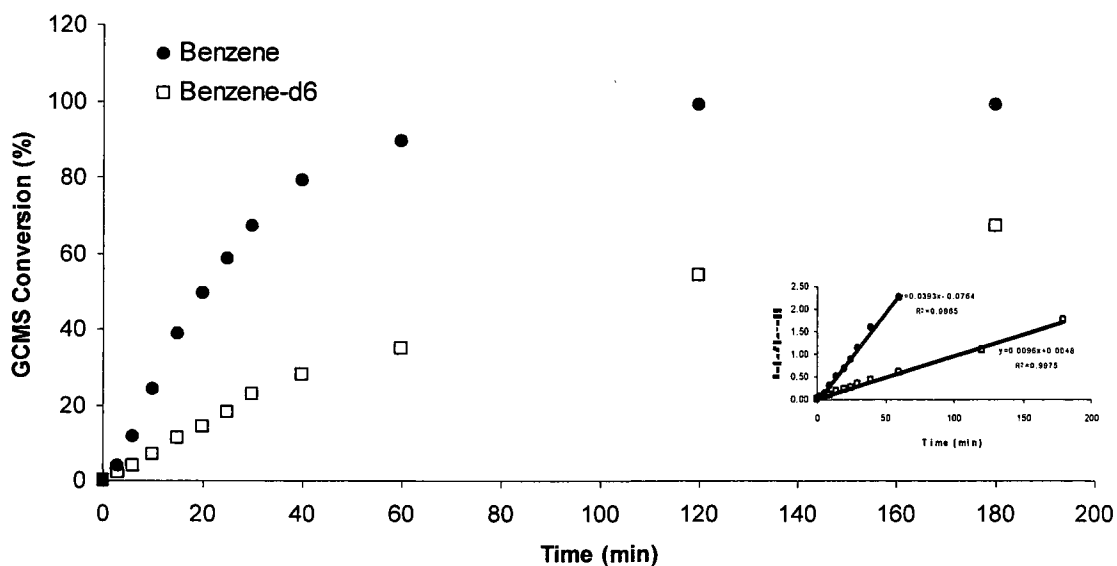
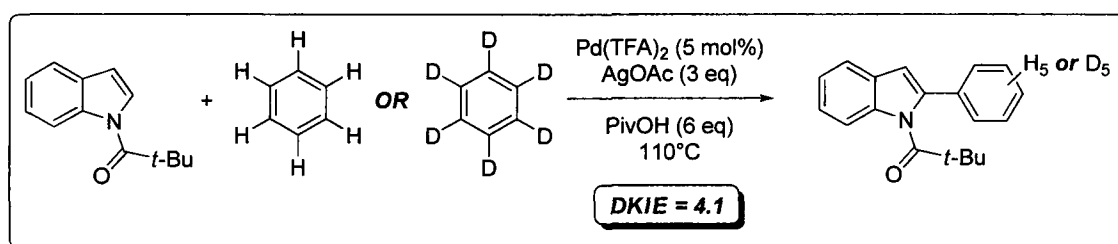
**Figure 3.6.** Initial rate vs. initial concentration of pivalic acid.



**Deuterium kinetic isotope effect (DKIE) at benzene.** The hypothesis that benzene palladation was rate determining in the catalytic cycle was corroborated by the presence of a DKIE. The rate of product formation was determined for separate reactions employing benzene or benzene-*d*<sub>6</sub> by removing aliquots at specific time intervals and measuring the conversion by GCMS analysis. The exponential conversion vs. time plot was made linear by plotting the natural logarithm of conversion against time. The ratio of *k*<sub>H</sub> over *k*<sub>D</sub>, obtained from the slopes of the linear plots, provided the DKIE. A visible rate difference was observed for these two reactions in the oxidative C2-arylation of *N*-pivaloylindole (Figure 4.10) yielding a primary DKIE of 4.1. Likewise, the oxidative C3-arylation of *N*-acetylindole displayed a significant primary DKIE of 4.2 when separate reactions were run with benzene and benzene-*d*<sub>6</sub> and the data treated in a similar manner. The presence of a significant DKIE for the palladation of benzene, when obtained in this way, not only suggests a kinetically significant event in the catalytic cycle but also carries with it

mechanistic implications as to the mode of C-H bond cleavage. Comparatively, the arylation of benzene with arylbromides under palladium(0) catalysis has been shown experimentally to exhibit a significant DKIE of 5.5.<sup>89</sup> Furthermore, as described previously, it has been found computationally that the palladation of benzene proceeds through a CMD pathway to forge the palladium-carbon bond. Thus, the significant DKIE (4.1 and 4.2) obtained here for both sets of arylation protocols (C2 and C3) suggest a similar mechanism being operative for the palladation of benzene.

**Figure 3.7.** Product formation vs time (DKIE).



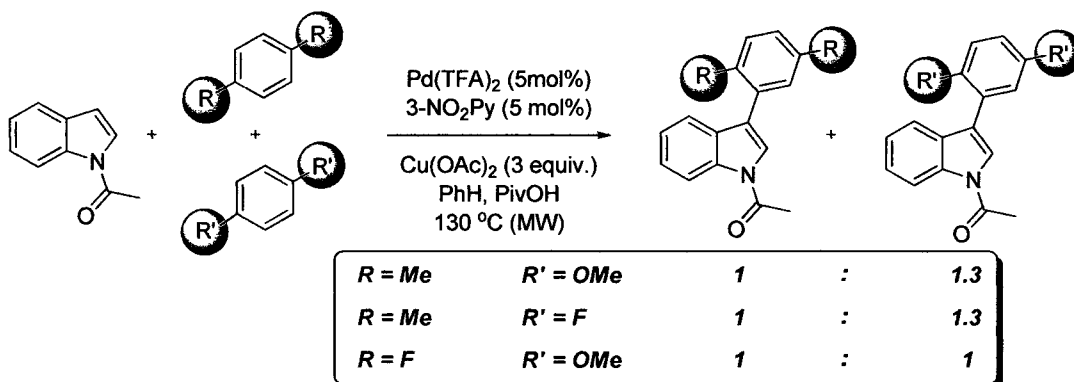
**Competition experiments of electronically and sterically diverse arenes.**

Competition experiments were used to definitively discount an  $\text{S}_{\text{E}}\text{Ar}$ -type process for C-H

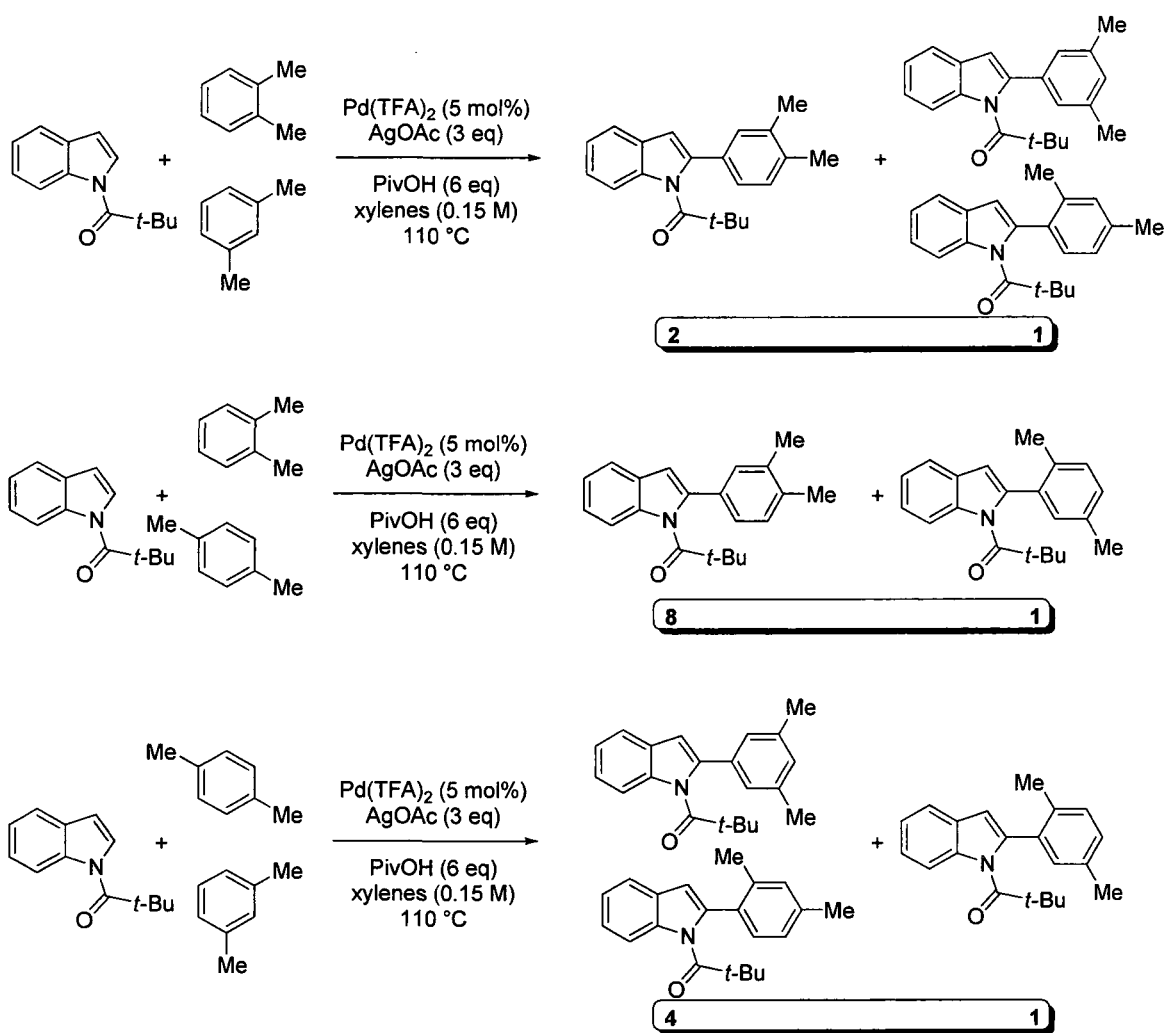
<sup>89</sup> See reference 8b. Other significant DKIE have been observed for the direct arylation of pentafluorobenzene (KIE = 3.0; see ref. 8a) and pyridine *N*-oxide (KIE = 4.7; ref. 15a). These three reactions were found computationally to proceed *via* a CMD pathway.

bond cleavage at benzene (Scheme 3.14).<sup>11</sup> The electron-deficient *p*-difluorobenzene reacted with equal ability to the electron-rich *p*-dimethoxybenzene, a result that conflicts with the expected outcome of a reaction operating under an S<sub>E</sub>Ar mechanism. While the electronic nature of the arene appears to have little effect on the course of the reaction, the steric environment of the arene does appear to have a significant influence (Scheme 3.15). When competition experiments were performed with the xylene series of arenes on the oxidative C2-arylation of *N*-pivaloylindole the arene with the greater number of positions with no *ortho*-substituents consistently reacted preferentially with *N*-pivaloylindole. More specifically, the xylene series had a relative reactivity order of *ortho*-xylene > *meta*-xylene > *para*-xylene; and in all cases (where applicable) the major regioisomer of reaction was at the most sterically accessible position. *Ortho*-xylene displayed particularly high regioselectivity in that essentially none of the regioisomer of reaction adjacent to the methyl groups was observed. Others have observed a similar reactivity pattern for 1,2-disubstituted arenes and also found that mono-substituted arenes react regioselectively at the *meta*-position regardless of the electronic nature of the arene, a result that conflicts with an S<sub>E</sub>Ar mechanism.<sup>64e,k</sup>

**Scheme 3.14.** Competition experiments for electronically dissimilar arenes.

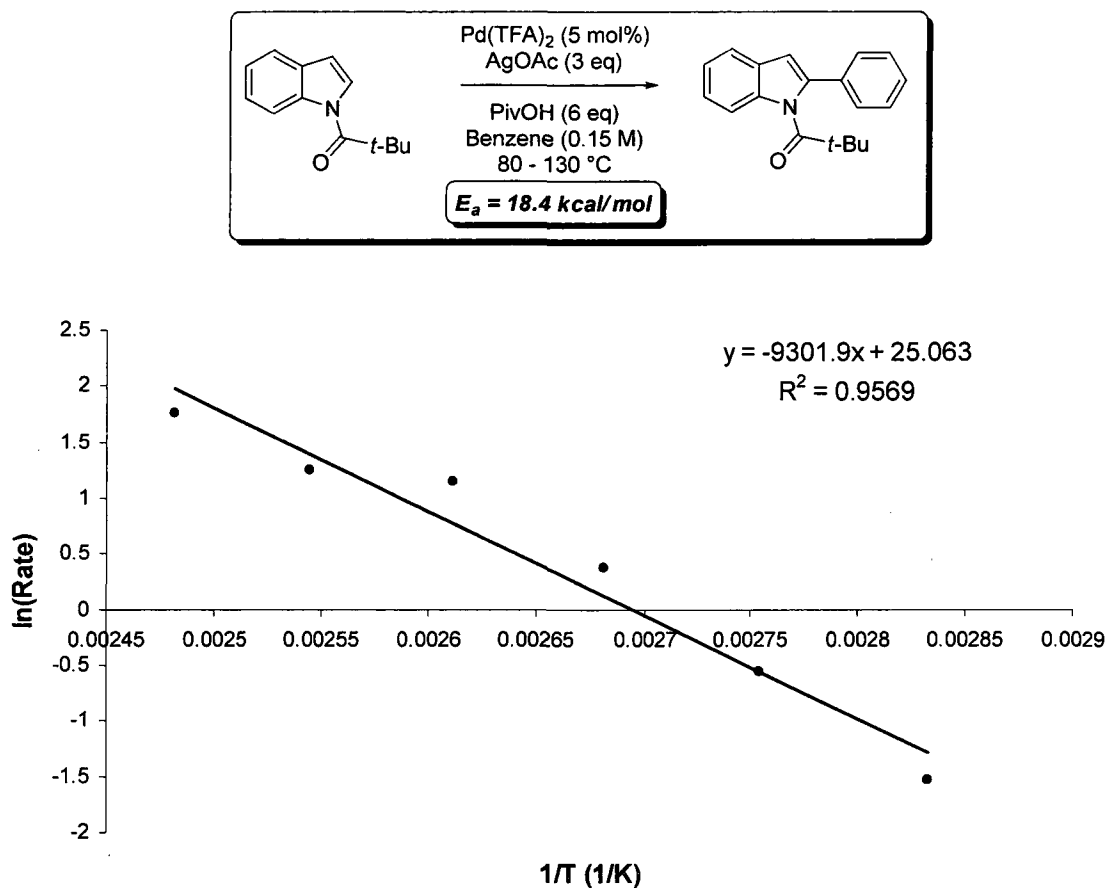


**Scheme 3.15.** Competition experiments for the xylene series.



**Arrhenius plot.** To further probe the mechanism of benzene palladation, an Arrhenius plot was generated by measuring the initial rate of the reaction at a number of different temperatures (80 – 130°C) (Figure 3.8). The natural logarithm of the initial rate was plotted against the inverse of the absolute temperature (Kelvin) and the slope of the free-energy relationship provided a value of 18.4 kcal/mol for the activation energy ( $E_a$ ). This value correlates well with the value obtained for the arylation of benzene with arylbromides under palladium(0) catalysis (25.1 kcal/mol).<sup>9</sup> Thus, the results presented above, taken together, advocate for a rate determining C-H bond cleavage at benzene passing through a CMD transition state.

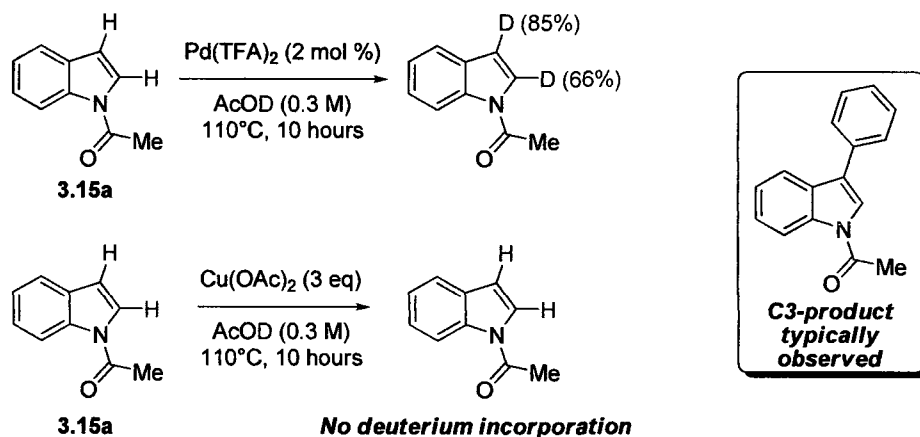
**Figure 3.8.** Arrhenius plot for the C2 arylation of *N*-pivaloylindole.



**Regioselectivity at indole.** As stated previously the reaction rate was zero-order in indole under the standard conditions. However, an intriguing inversion of indole regioselectivity was observed depending on the choice of oxidant and indole nitrogen protecting group and thus this process was investigated. The method of initial rates could not be used because the reaction rate showed no dependence on the concentration of indole and therefore single-pot competition experiments were used to interrogate this region of the catalytic cycle. This investigation was conducted in an effort to determine the source of regioselectivity at indole, however, with every experiment conducted this goal seemed more and more elusive. Nonetheless, some interesting observations have been made and will be disclosed in the forthcoming sections.

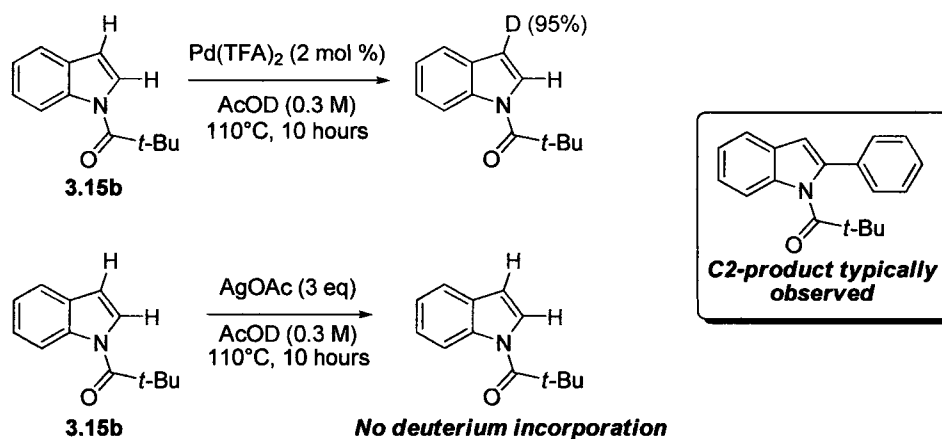
**Involvement of the oxidant in the regioselectivity.** A scenario that was first considered was the involvement of copper-indoyl and silver-indoyl species with orthogonal regioselectivity. However, if present these transient species would be highly reactive and very difficult to isolate or characterize. Therefore, to investigate their short-lived existence deuterium was used as an isotopic probe. It was presumed that a highly reactive organometallic species would deuterio-demetallate in the presence of acetic acid-*OD* and therefore deuterium would be placed at the position of metallation (Scheme 3.16 and Scheme 3.17). These data provide two interesting and important pieces of information. The first being that no deuterium is incorporated into the indole in the presence of either only  $\text{Cu}(\text{OAc})_2$  or  $\text{AgOAc}$  and therefore precludes the involvement of a copper-indoyl or silver-indoyl species. The second relates to the levels of deuterium incorporation at the C2 and C3 positions for the both *N*-acetylintole, **3.15a**, and *N*-pivaloylintole, **3.15b**. In the presence of palladium and acetic acid-*OD*, **3.15a** undergoes deuterium incorporation at both C2 (66%) and C3 (85%) even though high regioselectivity ( $\sim 15 : 1$ ) is observed for C3 arylation. This suggests that while palladium spends time on both carbons the C3 position is selectively arylated. An equally interesting, though confounding, result was observed in the case of deuterium incorporation into **3.15b** in the presence of palladium and acetic acid-*OD*. Deuterium is exclusively, and near quantitatively, incorporated into the C3 position (95%), where as arylation predominates at the C2 position ( $>25 : 1$ ).<sup>90</sup>

**Scheme 3.16.** Deuterium incorporation experiments on *N*-acetylintole.



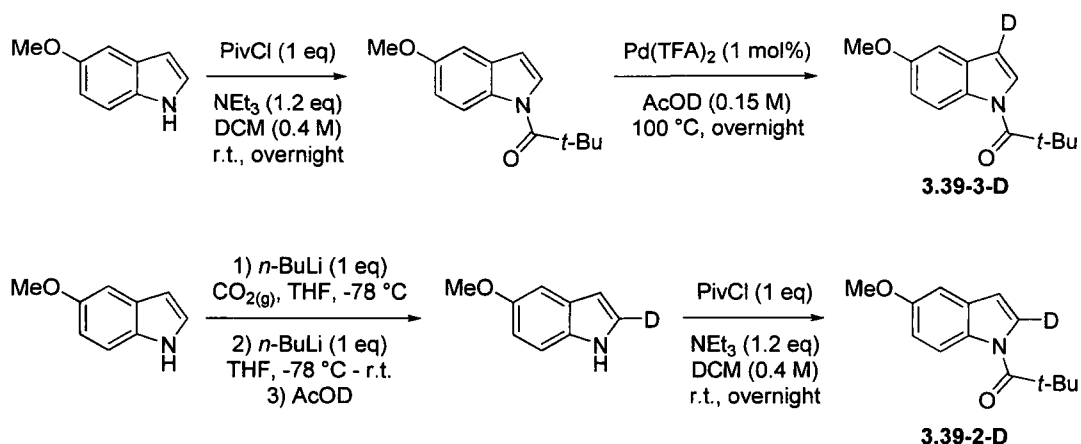
<sup>90</sup> In both cases, **3.15a** and **3.15b**, no deuterium is incorporated in the absence of palladium(II) trifluoroacetate.

**Scheme 3.17.** Deuterium incorporation experiments on *N*-pivaloylindole.

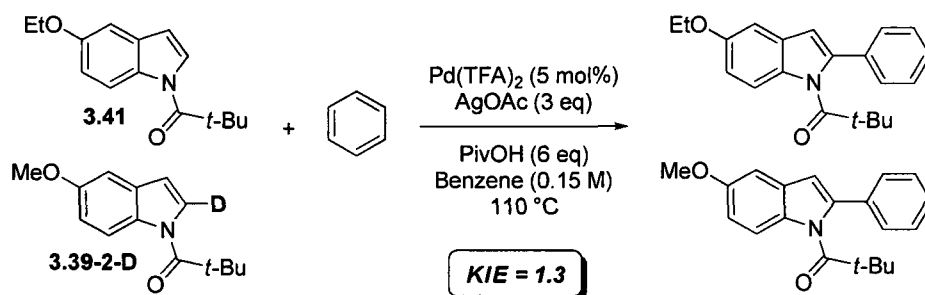


**DKIE at indole via competition experiments.** The level and position of deuterium incorporation on *N*-acetyl and *N*-pivaloylindole lead to the use of competition experiments to probe the presence of a DKIE at indole. This was done in order to apply an additional level of scrutiny to the palladation of indole and provide further insight into the mechanism of this process. Due to the ease of substrate preparation the oxidative C2-arylation of *N*-pivaloylindole was used in this investigation. Substrates tagged with a methoxy group were selectively deuterated at either the C3 or C2 position (Scheme 3.18). Competition experiments were run between each of the regioselectively deuterated substrates and an electronically equivalent non-deuterated substrate tagged with an ethoxy group. The competitions were run to ~ 10% conversion to stay under pseudo-first order conditions and the integration of the two product peaks in the GCMS chromatogram were compared to determine the DKIE. A secondary DKIE of 1.3 was observed when **3.39-2-D** was placed in a competition with **3.41** (Scheme 3.19). *Surprisingly, however, there was a primary DKIE of 3.2 observed at C3 even though arylation takes place at C2* (Scheme 3.20). Evidently, a more complex situation takes place in the indole metallation step. Additionally, and of mechanistic importance, it was noted in the competition of **3.41** with **3.39-3-D** that the C3 deuterium of **3.39-3-D** was quantitatively lost in the product even at very low conversion (< 10%, Scheme 3.20).

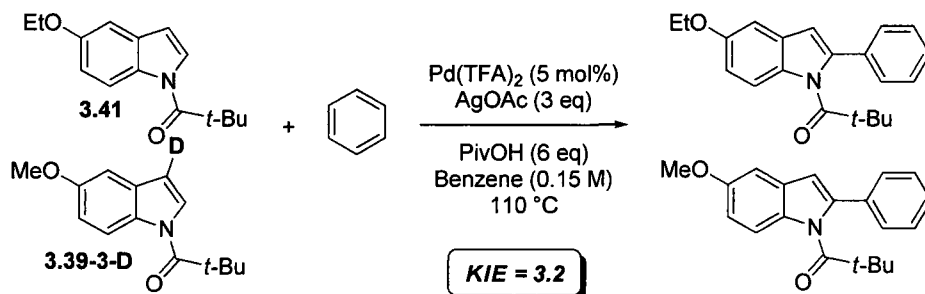
**Scheme 3.18.** Preparation of deuterium labeled 5-methoxy-*N*-pivaloylindoles.



**Scheme 3.19.** Competition experiments between 3.41 and 3.39-2-D.



**Scheme 3.20.** Competition experiments between 3.41 and 3.39-3-D.



**Deuterium erosion experiments.** The observation of quantitative loss of deuterium at C3 in the C2-arylated indole product (Scheme 3.20) could be of great mechanistic significance. Thus, the reaction of *N*-pivaloylindole-C3-*d* was monitored over time in order to further probe this observation. Aliquots were taken at specific time intervals and analyzed by GCMS. The intensity of the mass peaks (*M* and *M*+1) corresponding to the non-deuterated and deuterated starting material (and product) were compared to provide a relative percentage of deuterium at the C3 position. The relative percentage of deuterium was plotted

against time (Figure 3.9). Four different experiments were run in order to reveal different aspects of the reaction. First, in the absence of Pd(TFA)<sub>2</sub> no loss of deuterium was observed at C3 (Figure 3.9, trace ×) and therefore an operative background loss of deuterium can be dismissed. However, under the standard reaction conditions deuterium in the starting material is depleted (Figure 3.9, trace ●). This is likely due to an evolving competition between the deuterated starting material and the non-deuterated material being produced as the reaction proceeds, and as described previously (*vide supra*) the catalyst showed a bias for reaction with the non-deuterated substrate (DKIE = 3.2). Thus, as the reaction proceeds the percent deuterium in the starting material (●) was artificially high as a result of a bias of the catalyst for the non-deuterated substrate produced during the reaction. Most informative from these experiments was the percent deuterium in the product under the standard reaction conditions (Figure 3.9, trace □). Even at very low conversion deuterium is near quantitatively absent from the product and only leaches slightly into the product (~ 14% deuterium) over time. A control experiment was performed to ensure that the immediate loss in deuterium in the product of the reaction was not an artifact of the reaction conditions (Figure 3.9, trace ▲).<sup>91</sup> As shown in the graph in Figure 3.9 the product added to the reaction tagged with a methylester exhibits ~75% deuterium incorporation at very low conversion (initial deuterium incorporation was 95%); whereas the product formed during the reaction contains ~5% deuterium (initial deuterium incorporation in the starting material was > 95%). Thus, these results point toward a scenario in which the C3-deuterium is lost as a function of the mechanism of indole palladation, and exclude the possibility of deuterium loss in the product as an artifact of the reaction conditions.

<sup>91</sup> The following compound, , was added to a typical reaction mixture (Figure 3.9) and the level of deuterium

loss monitored by GCMS, as described previously.

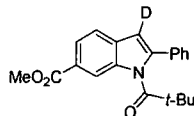
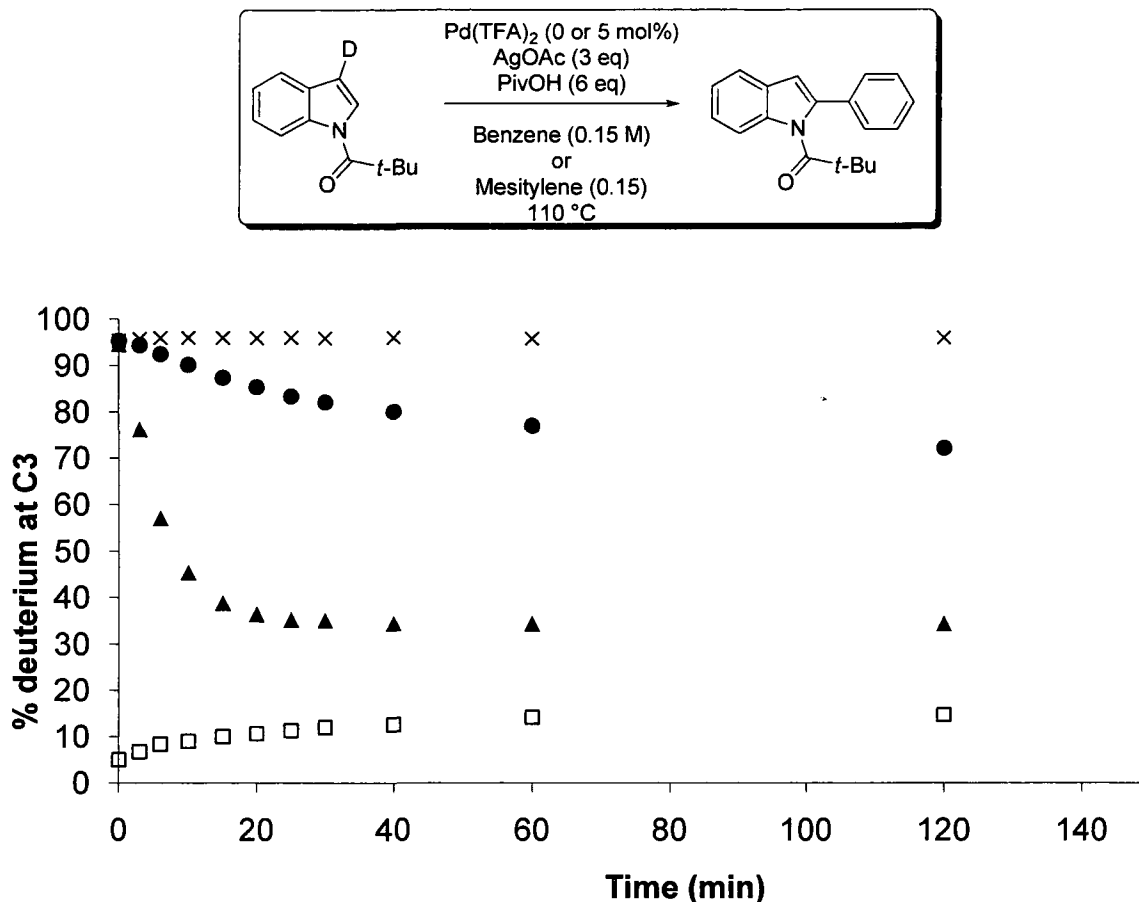


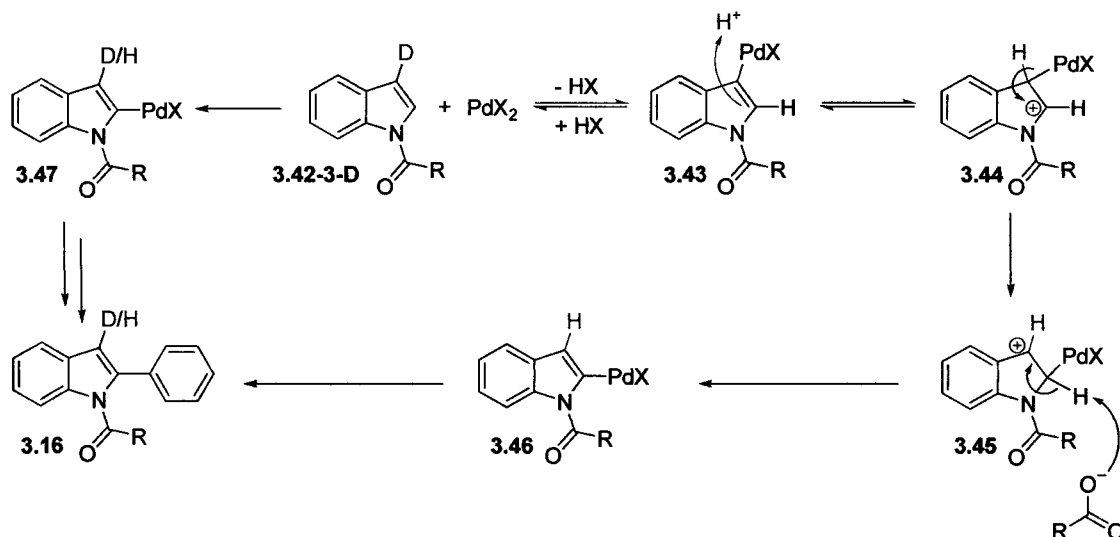
**Figure 3.9.** Deuterium loss as a function of time.



**C3,C2-Palladium migration as a possible mechanism.** Sames<sup>36a</sup> and Gaunt<sup>39</sup> have both observed that the C2/C3 selectivity for related transition metal catalyzed reactions at indole may be influenced by reaction conditions and the steric/electronic nature of the nitrogen protecting group. Proposals from both of these groups for the observed variation in C2/C3 regioselectivity have involved a C3,C2-metal migration, and therefore this scenario was considered here as well. In this context the experimental observations made here, with respect to the reactivity and isotopic labeling experiments on indole, are consistent with this process (Scheme 3.21). **3.42-3-D** could undergo a reversible palladation at C3 accounting for the observed loss in deuterium at this position. In addition to a reversible C3 palladation **3.42-3-D** could also undergo palladation (irreversible in the case of *N*-pivaloylindole) at C2 to form **3.47** followed by reaction with benzene and formation of **3.16**. However, this pathway is inconsistent with the quantitative loss of deuterium in the product at low conversion. If this were the case it would be expected that **3.42-3-D** and **3.16** would have

similar levels of deuterium at the C3 position at any time during the reaction. Alternatively, during the reversible C3-palladation of **3.42-3-D** the Wheland intermediate, obtained after protonation, could go through a C3,C2-palladium migration to afford **3.45**. Compound **3.45**, containing a C3-carbocation, could then be re-aromatized by deprotonation at C2 and following reaction with benzene, give the product, **3.16**. This scenario is consistent with the very low percentage of deuterium at the C3-position in the product essentially at the outset of the reaction. When Wheland intermediate **3.44** is formed the C3 position is exclusively protonated (not deuterated), and thus after migration to form **3.45**, the high level of protonation (low percentage of deuterium) is reflected in the product, **3.16**.

**Scheme 3.21.** Plausible mechanism for the C2 arylation of *N*-pivaloylindole.



**Hammett correlation.** A Hammett correlation was conducted to assess the hypothesis of a C3,C2-palladium migration. As presented in Figure 3.10 an electron-donating group should promote the C3,C2-palladium migration by stabilization of a C3-carbocation; whereas an electron-withdrawing group should destabilize the C3-carbocation intermediate. Though the correlation could not be obtained through the direct measurement of initial rates, as described earlier, competition experiments between C6-substituted *N*-pivaloylindoles and unsubstituted *N*-pivaloylindole could be carried out to observe a possible electronic influence on the reaction. The Hammett correlation was obtained by plotting the natural logarithm of the product ratio of the competition experiment against the  $\sigma_{\text{para}}$ -values of the C6-

substituents.<sup>92</sup> Treatment of the data in this way provided a  $\rho$ -value of -1.8 which is indicative of buildup of positive charge near the aromatic ring (Figure 3.11). A Hammett plot was also obtained for the oxidative arylation of *N*-acetylindoles *via* competition with a series of 6-substituted *N*-acetylindoles and a similar  $\rho$ -value (-1.9) was obtained. These data are suggestive of a C3,C2-migration and formation of a benzylic carbocation in both the oxidative arylation of *N*-acetyl and *N*-pivaloylindole. However, the negative  $\rho$ -value may also be due to a favorable  $E_{\text{int}}$  value in the context of a CMD transition state for C3 palladation. This possibility would also correlate well with the significant DKIE of 3.2.

**Figure 3.10.** Influence of C6-substitution on C3,C2-palladium migration.

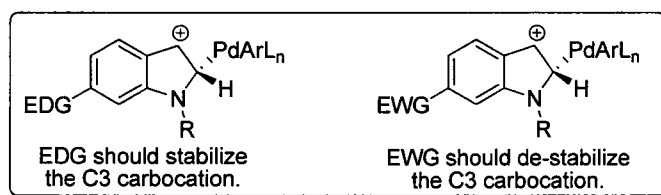
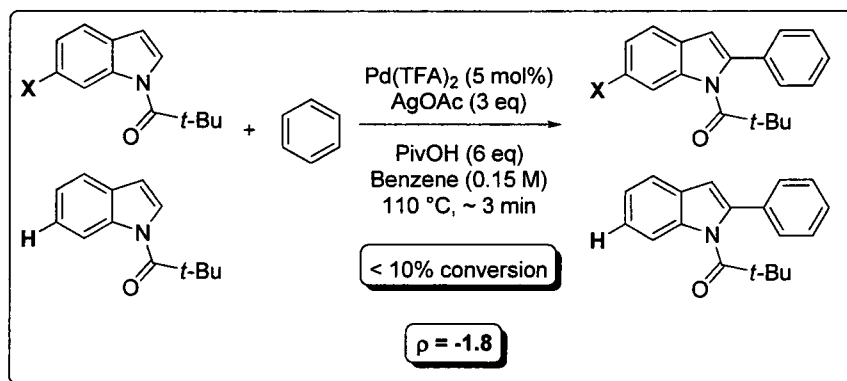
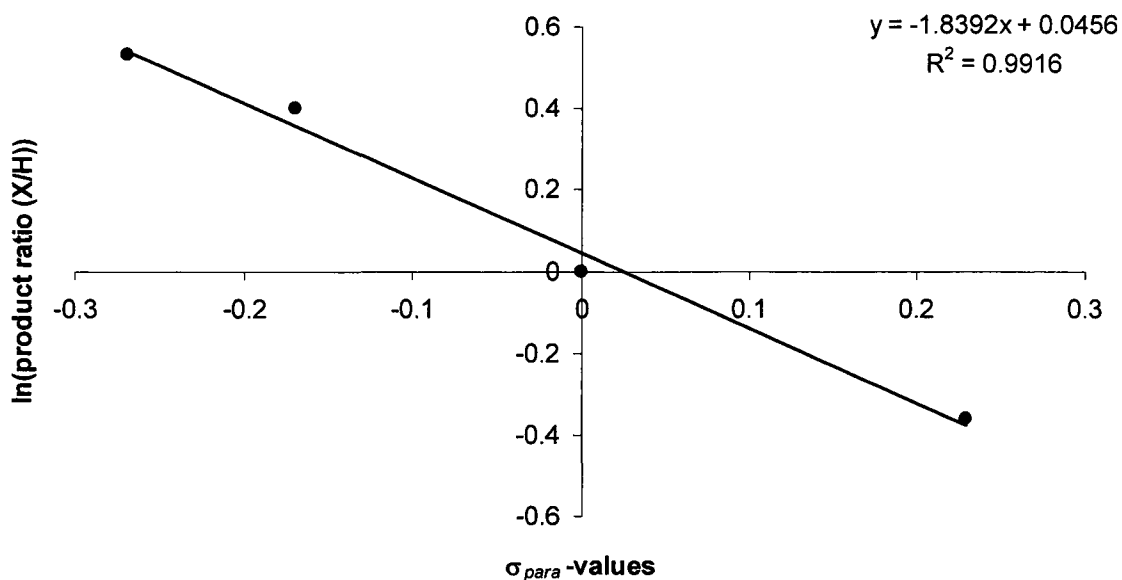


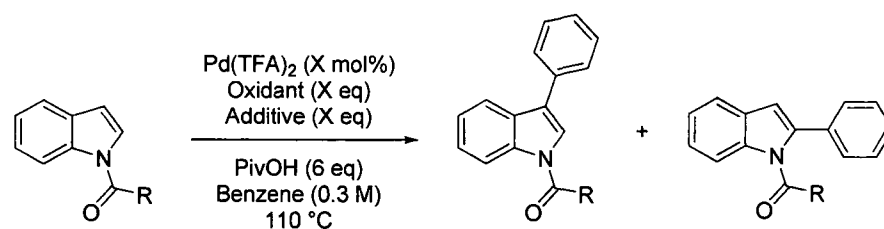
**Figure 3.11.** Hammett correlation for 6-X-*N*-pivaloylindoles.



<sup>92</sup> The  $\sigma_{\text{para}}$ -values were used from the following compilation: Hansch, C.; Leo, A.; Taft, R. W. *Chem. Rev.* **1991**, *91*, 165.



**Differences between *N*-acetylindole and *N*-pivaloylindole.** While these results are intriguing they fail to explain the vastly different regioselectivity obtained for oxidative arylation of *N*-acetylindole and *N*-pivaloylindole. A number of experiments were conducted with a focus on regioselectivity of the reactions based on both oxidants and additives that may simulate a part of the oxidant (counterion) without the ability to do redox chemistry (Table 3.9). These results show that in the presence of stoichiometric palladium, both *N*-acetyl and *N*-pivaloylindole have a propensity to undergo arylation at C3 (Table 3.9, entries 1 and 4). Under catalytic conditions in the presence of  $\text{Cu}(\text{OAc})_2$  as oxidant C3 arylation is favored for both reactions (Table 3.9, entries 2 and 5), with the *N*-acetylindole being much more C3 selective. However, when  $\text{AgOAc}$  is used as the oxidant the regioselectivity is inverted so that C2 arylation is preferred, much more so in the case of *N*-pivaloylindole (Table 3.9, entries 3 and 6). A final experiment, which employs  $\text{CsOAc}$  as an additive in the absence of any oxidant revealed a strong bias for C2 arylation (Table 3.9, entry 7) suggesting an influence of the source of added acetate not the metal to which it is bound. Thus, perhaps the source (different counterion) of added acetate modulates the relative basicity of the reaction mixture affecting the protonation/deprotonation events necessary for a successful C3,C2-palladium migration.

**Table 3.9.** Acetate assisted regioselectivity of *N*-acetyl and *N*-pivaloylindoles.<sup>a</sup>

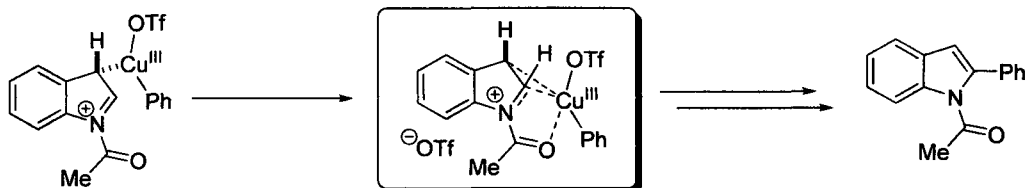
Entry	R	mol % Pd	Oxidant (eq)	Additive (eq)	Ratio <sup>b</sup>
1	Me	100	—	—	4.4 : 1
2	Me	10	Cu(OAc) <sub>2</sub> (3)	—	27 : 1
3	Me	10	AgOAc (3)	—	1 : 3.3
4	<i>t</i> -Bu	100	—	—	3.7 : 1
5	<i>t</i> -Bu	5	Cu(OAc) <sub>2</sub> (3)	—	2.1 : 1
6	<i>t</i> -Bu	5	AgOAc (3)	—	1 : 25
7	<i>t</i> -Bu	20	—	CsOAc (2)	1 : 99

<sup>a</sup>Conditions: Indole (1 eq, 0.3 M), Pd(TFA)<sub>2</sub> (X mol%), Oxidant (see above), Additive (see above), PivOH (6 eq), Benzene, 110 °C, 3 hours. <sup>b</sup>Ratio of C3 : C2 product.

**Amide conformations of *N*-acetyl and *N*-pivaloylindole.** In Gaunt's copper-catalyzed direct arylation of indole<sup>39</sup> he postulates that the ability of the acetyl carbonyl to coordinate copper promotes a C3,C2-copper migration resulting in a regioselective C2-arylation (Scheme 3.22). In the chemistry presented in the preceding sections *N*-acetylindole underwent C3-arylation while the more sterically encumbered *N*-pivaloylindole was arylated regioselectively in the C2 position. While the nature of the reaction conditions for the two protocols described herein are slightly different, and undoubtedly this may be a significant source for regio-differentiation (Table 3.9, and relevant discussion), it is also recognized<sup>93</sup> that the inherent differences in amide conformation for the two substrates (*N*-acetyl and *N*-pivaloylindole) may also influence this process.

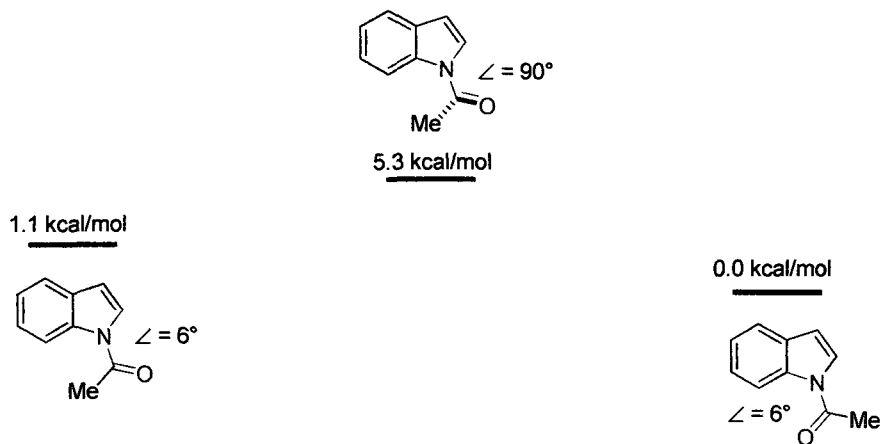
<sup>93</sup> My entire thesis committee and particularly Prof. André Beauchemin is acknowledged for insightful and fruitful discussions on this concept.

**Scheme 3.22.** Gaunt's Proposed Intermediate for Acetate Assisted C2-Arylation.



When energy minimizations<sup>94</sup> were run on selected amide conformations of *N*-acetylindole it was found that the lowest energy conformer contained the acetyl carbonyl directed away from the C2-position and the position of a migrating metal. Moreover, the second lowest energy conformer (with the acetyl carbonyl directed towards the C2-position), at a relative energy of 1.1 kcal/mol, had the acetyl carbonyl in the plane of the heterocycle and not bent out of plane at the proper angle to accept an incoming copper during migration (as is shown in Gaunt's model, Scheme 3.22). In order to shift the acetyl group out of plane, such that a proper orientation may be adopted to coordinate a migrating metal this comes at an energy cost of  $\sim 5$  kcal/mol.

**Figure 3.12.** Relative Energies of Selected Amide Conformations of *N*-Acetylindole.

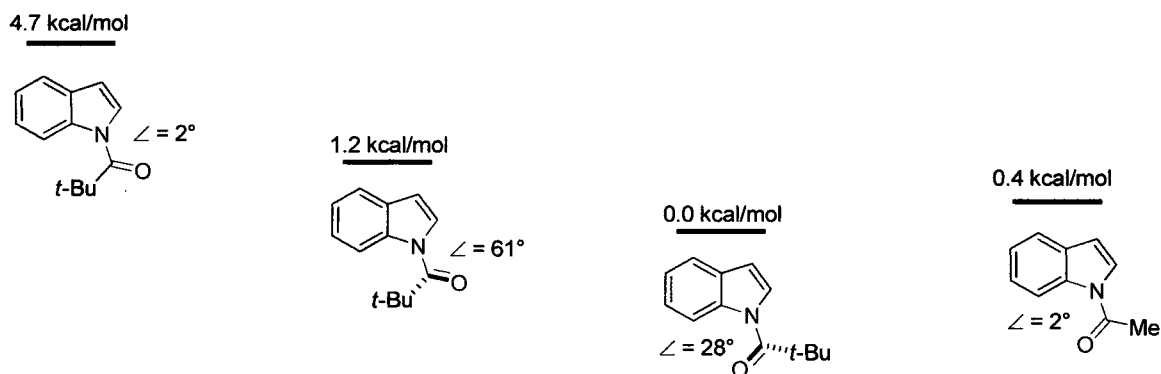


The results previously described for the relative energies of the amide conformations of *N*-acetylindole are in stark contrast to those obtained for *N*-pivaloylindole. When similar energy minimizations were run for *N*-pivaloylindole the lowest energy conformer was one in

<sup>94</sup> Energy minimizations were run as an MM2 calculation using ChemBio3D Ultra v. 12 and the relative energies determined by setting the lowest energy conformer to 0.0 kcal/mol.

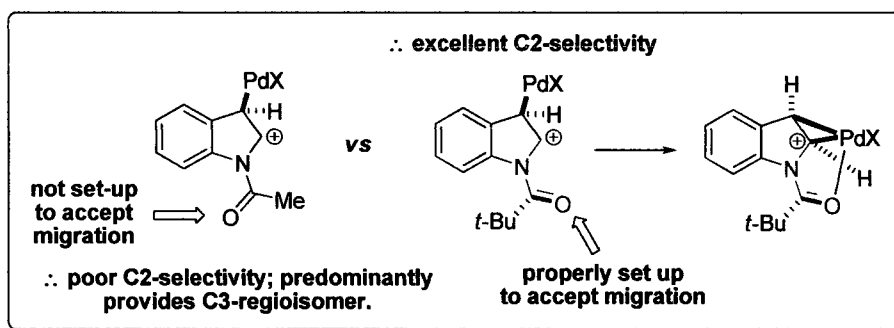
which the pivaloyl moiety was 28° out of plane with the aromatic system and the carbonyl of the acetyl directed toward the benzene portion of the heterocycle. However, a relatively low energy conformer (1.2 kcal/mol) with the acetyl carbonyl directed toward the C2 position and the pivaloyl moiety twisted 61° out of plane is set up very nicely to accept a migrating metal, such as palladium. The highest energy conformer in this case was one of the “in-plane” conformers in which the bulky *tert*-butyl group is pointed toward the benzene moiety of the heterocycle.

**Figure 3.13.** Relative Energies of Selected Amide Conformations of *N*-Pivaloylindole.



Thus, while other factors, such as the source of acetate (Table 3.9) must also be considered in the cause of such disparate regioselectivity for *N*-acetyl and *N*-pivaloylindole the results presented here suggest that amide conformation is also a contributing important factor (Figure 3.14)

**Figure 3.14.** Differences in Amide Conformation for *N*-Acetyl and *N*-Pivaloylindole As It Relates to Regioselectivity.



### 3.3. Outlook and Perspectives

Highly regioselective arylation has been achieved for Type I and Type II arenes, however, the continuing challenge in oxidative cross-coupling chemistry is associated with Type III arenes both in stoichiometry and regioselectivity. Type III arenes are commonly used as bulk solvent and are present in approximately 30 – 60 fold excess relative to the other coupling partner. Buchwald has made the most significant advance in this area by developing conditions which allow for the use of 11 equivalents of benzene but may go as low as 4 equivalents and still obtain 78% GC yield of the cross-coupled product.<sup>64i</sup> Regioselectivity is a larger hurdle to overcome and represents perhaps the most important challenge due the difficulty related with separation of arene regioisomers. Sanford has made exciting progress in this field by variation of the steric requirement of the benzoquinone ligand, though in this case conversion to product suffered. While this is an important advance it has little relevance where the modulation of benzoquinone is not applicable. The large number of publications (11) on the intermolecular oxidative cross-coupling of unactivated arenes over the past two years is strong evidence that this young, but important, area of research is sure to witness exciting growth in the years ahead.

# Rhodium(III) Catalyzed Oxidative Preparation of Indoles and Pyrroles

## 4.1. Introduction

Indole is the most abundant heterocycle in nature and has been termed a “privileged motif” in medicinal chemistry (Figure 4.1).<sup>95</sup> As such, much attention has been given to the development of methods for the synthesis of indoles by the synthetic community dating back over 125 years. There are at least 17 “named” reactions alone dedicated to the preparation of indoles with a plethora of additional methods developed towards this end.<sup>96</sup> Numerous books and reviews have been devoted to the subject of their classical synthesis and thus they

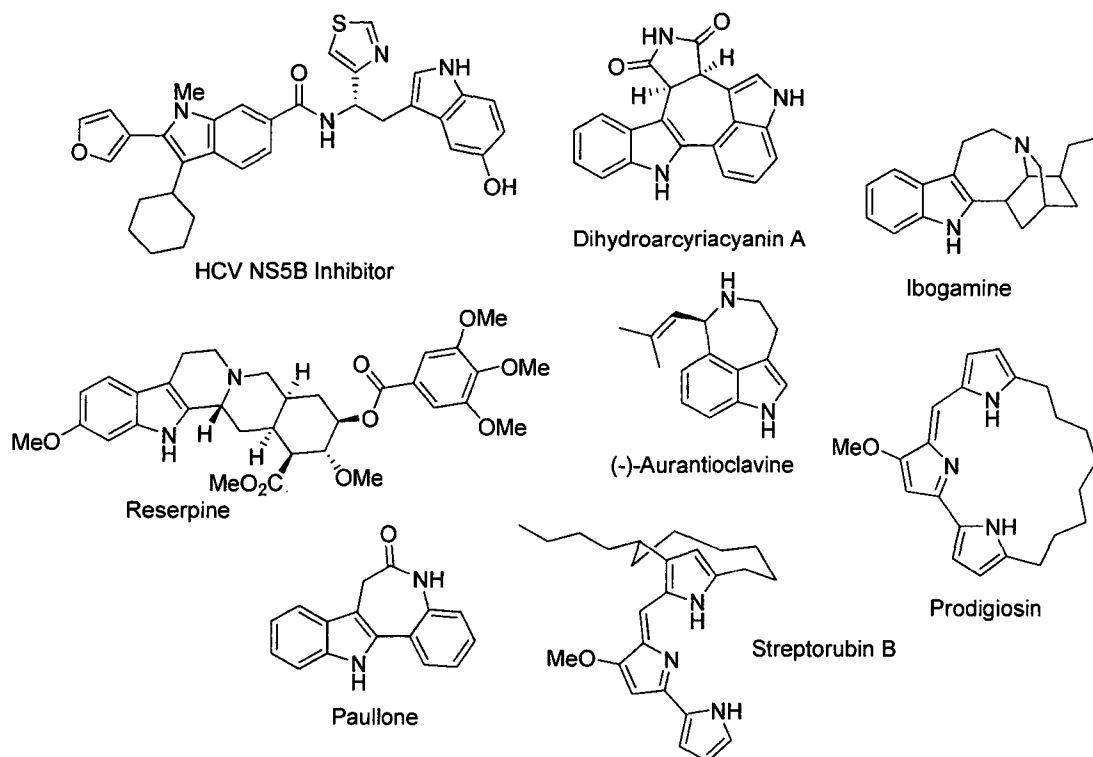
---

<sup>95</sup> (a) A Beilstein search for indoles with biological activity yielded > 45,000 results. (b) de Sá Alves, F. R.; Barreiro, E. J.; Fraga, C. A. M. *Mini-Reviews in Medicinal Chemistry*, **2009**, *9*, 782.

<sup>96</sup> The 17 “named” indole syntheses referred to, in no particular order, are: Batcho-Leimgruber, Reissert, Hegedus, Fukuyama, Sugawara, Bischler, Gassman, Fischer, Japp-Klingemann, Buchwald, Larock, Bartoli, Castro, Hemetsberger, Mori-Ban, Madelung, and Nenitzescu. Sundberg, R. J. *Indoles*. Academic Press Ltd.: San Diego, 1996.

will not be re-iterated here;<sup>97</sup> furthermore, transition metal-catalysis has been heavily exploited in the synthesis of indoles and these efforts have also been heavily documented in the literature.<sup>98</sup>

**Figure 4.1.** Representative indoles and pyrroles in nature and medicinal chemistry.



Despite the recent advances, most of these techniques rely heavily on substrate pre-activation, and very few employ readily available anilines as starting materials. Transition

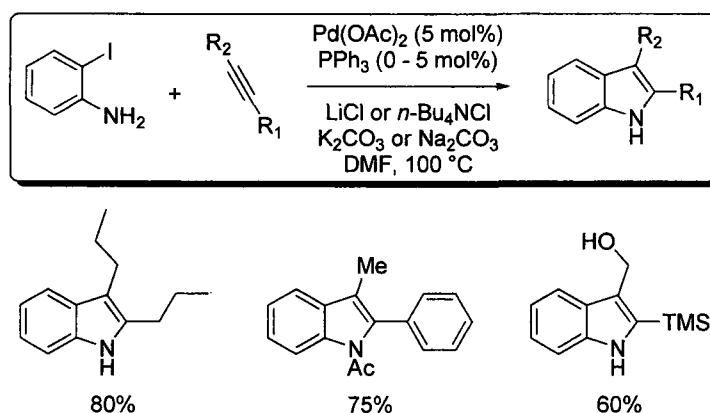
<sup>97</sup> For reviews on indole synthesis, see: (a) Gribble, G. W. *J. Chem. Soc. Perkin Trans. 1* **2000**, 1045. (b) Alonso, F.; Beletskaya, I. P.; Yus, M. *Chem. Rev.* **2004**, *104*, 3079. (c) Nakamura, I.; Yamamoto, Y. *Chem. Rev.* **2004**, *104*, 2127. (d) Cacchi, S.; Fabrizi, G. *Chem. Rev.* **2005**, *105*, 2873. For recent individual accounts, see: (e) Shen, M.; Leslie, B. E.; Driver, T. G. *Angew. Chem., Int. Ed.* **2008**, *47*, 5056. (f) Takaya, J.; Udagawa, S.; Kusama, H.; Iwasawa, N. *Angew. Chem., Int. Ed.* **2008**, *47*, 4906. (g) Pei, T.; Chen, C.-Y.; Dormer, P. G.; Davies, I. W. *Angew. Chem., Int. Ed.* **2008**, *47*, 4231. (h) Alex, K.; Tillack, A.; Schwarz, N.; Beller, M. *Angew. Chem., Int. Ed.* **2008**, *47*, 2304.

<sup>98</sup> For a review, see: (a) Zeni, G.; Larock, R. C. *Chem. Rev.* **2004**, *104*, 2285. For selected individual accounts, see: (b) Tida, H.; Yuasa, Y.; Kibayashi, C. *J. Org. Chem.* **1980**, *45*, 2938. (c) Sakamoto, T.; Nagano, T.; Kondo, Y.; Yamanaka, H. *Synthesis* **1990**, 215. (d) Larock, R. C.; Yum, E. K. *J. Am. Chem. Soc.* **1991**, *113*, 6689. (e) Koerber-Ple, K.; Massiot, G. *Synlett* **1994**, 759. (f) Chen, C. Y.; Lieberman, D. R.; Larsen, R. D.; Verhoeven, T. R.; Reider, P. J. *J. Org. Chem.* **1997**, *62*, 2676. (g) Larock, R. C.; Yum, E. K.; Refvik, M. D. *J. Org. Chem.* **1998**, *63*, 7652. (h) Yamazaki, K.; Nakamura, Y.; Kondo, Y. *J. Org. Chem.* **2003**, *68*, 6011. (i) Watanabe, T.; Arai, S.; Nishida, A. *Synlett* **2004**, 907. (j) Nazare, M.; Schneider, C.; Lindenschmidt, A.; Will, D. W. *Angew. Chem., Int. Ed.* **2004**, *43*, 4526. (k) Jia, Y.; Zhu, J. *J. Org. Chem.* **2006**, *71*, 7826. (l) Leogane, O.; Lebel, H. *Angew. Chem., Int. Ed.* **2008**, *47*, 350.

metal catalyzed processes<sup>98</sup> are illustrative, commonly requiring *ortho*-halogenated anilines as starting materials thus adding cost<sup>99</sup> and reducing the breadth of readily available starting materials. The Larock indole synthesis<sup>100</sup> is the most commonly used transition metal-catalyzed indole forming reaction, finding extensive use in both medicinal chemistry and total synthesis,<sup>101</sup> and has set the bar for *intermolecular* processes of this type for the past 18 years.

**Larock indole synthesis.** This indole synthesis efficiently couples *ortho*-iodoanilines with internal alkynes under palladium-catalysis (Scheme 4.1). The mechanism is proposed to

**Scheme 4.1.** Larock indole synthesis.



proceed *via* (1) oxidative addition of Pd(0) to the *ortho*-iodoaniline; (2) alkyne coordination to Pd; (3) *syn*-addition across the alkyne; and (4) C-N bond reductive elimination to provide the indole product and the active Pd(0) catalyst; however, no in-depth mechanistic studies on this reaction have been reported to date (Scheme 4.2). The highlights of this approach are its

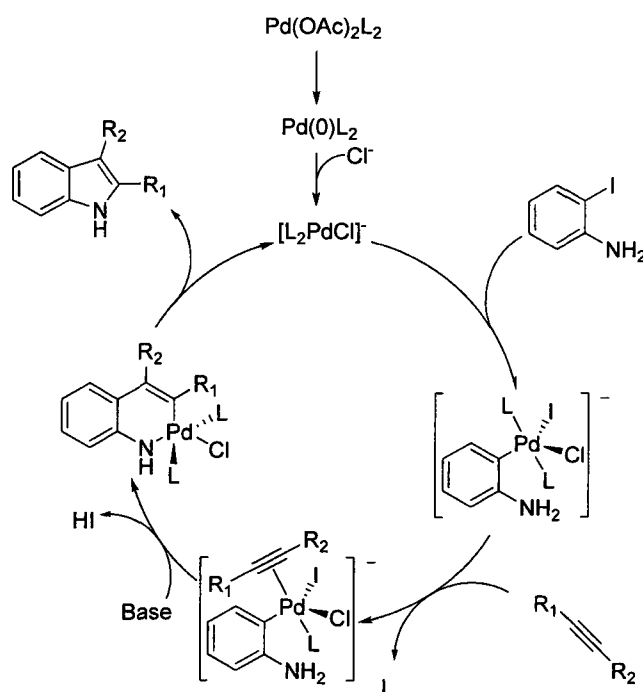
<sup>99</sup> For example, 4-methoxyaniline is \$49.26/mol where as 2-iodo-4-methoxyaniline is \$87, 150/mol.

<sup>100</sup> Larock, R. C.; Yum, E. K. *J. Am. Chem. Soc.* **1991**, *113*, 6639.

<sup>101</sup> For representative examples of the Larock indole synthesis in medicinal chemistry, please see: (a) Lanter, J. C. *et. al. Bioorg. Med. Chem. Lett.* **2007**, *17*, 2545. (b) Watterson, S. H. *et. al. Bioorg. Med. Chem. Lett.* **2003**, *13*, 1273. (c) Curtis, N. R.; Kulagowski, J. J.; Leeson, P. D.; Ridgill, M. P.; Emms, F.; Freedman, S. B.; Patel, S.; Patel, S. *Bioorg. Med. Chem. Lett.* **1999**, *9*, 585. (d) Ujjainwalla, F.; Walsh, T. F. *Tetrahedron Lett.* **2001**, *41*, 6441. For representative examples of the Larock indole synthesis in total synthesis, please see: (e) Newhouse, T.; Lewis, C. A.; Baran, P. S. *J. Am. Chem. Soc.* **2009**, *131*, 6360. (f) Newhouse, T.; Baran, P. S. *J. Am. Chem. Soc.* **2008**, *130*, 10886.

convergent nature and high functional group compatibility. Drawbacks of this approach, however, are the high cost and low availability of substituted *ortho*-iodoanilines, and as a result the substrate scope with respect to the aniline coupling partner is limited to variation of the nitrogen protecting group. Additionally, the super-stoichiometric quantities of alkyne often employed (up to 5 equivalents of alkyne are often necessary) represents a disadvantage of this methodology. Thus, there exists a niche in transition metal-catalyzed indole forming reactions yet to be filled – the employment of simple anilines in convergent, oxidative processes.

**Scheme 4.2.** Proposed mechanism of Larock indole synthesis.



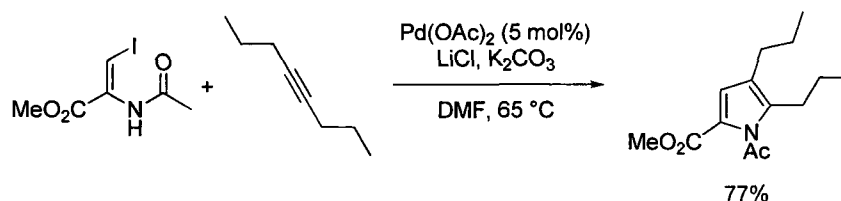
While closely related to the indole, pyrroles have not enjoyed the continued attention of the synthetic community despite their prevalence in pharmaceuticals<sup>102</sup> and materials science.<sup>103</sup> A significant number of classical pyrrole syntheses exist, however their transition

<sup>102</sup> (a) Thompson, R. B. *FASEB J.* **2001**, *15*, 1671. (b) Muchowski, J. M. *Adv. Med. Chem.* **1992**, *1*, 109. (c) Cozzi, P.; Mongelli, N. *Curr. Pharm. Des.* **1998**, *4*, 181. (d) Fürstner, A.; Szillat, H.; Gabor, B.; Mynott, R. *J. Am. Chem. Soc.* **1998**, *120*, 8305.

<sup>103</sup> Skotheim, T. A., Elsenbaumer, R. L., Reynolds, J. R., Eds. *Handbook of Conducting Polymers*, 2nd ed.; Marcel Dekker: New York, 1998.

metal-catalyzed counter parts are lacking relative to indole syntheses.<sup>104</sup> Similar to transition metal-catalyzed indole syntheses the processes that have been reported for pyrroles typically employ pre-activated substrates. This is well illustrated by a report from researchers at Wyeth who have developed a pyrrole synthesis from iodoacrylates and internal alkynes analogous to the Larock indole synthesis (Scheme 4.3).<sup>104j</sup>

**Scheme 4.3.** Palladium catalyzed formation of pyrroles from iodoacrylates.



A major advance in indole and pyrrole syntheses would, thus, be the development of oxidative processes that employ simple anilines (or enamides) as starting materials and readily couple with a two carbon fragment (an alkyne) of appropriate oxidation state to form theazole ring. The first portion of this introduction will present recent advances from the literature employing transition metal-catalyzed oxidative approaches toward indoles and indolines. The second portion will elaborate on the use of rhodium(III) as an oxidant in organic synthesis.

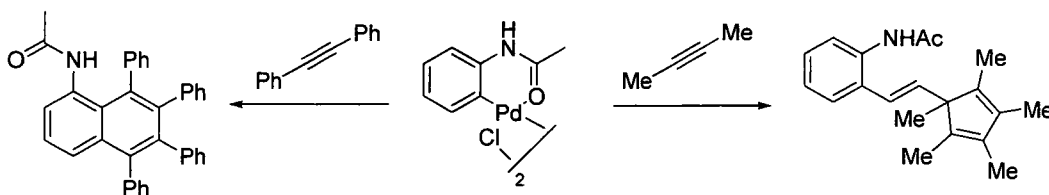
#### 4.1.1. Transition Metal-Catalyzed Oxidative Approaches in Indole Synthesis.

Early work by Heck and Dupont to effect the annulation of cyclopalladated species with alkynes have generally resulted in multiple insertion products or cyclization back onto

<sup>104</sup> For transition metal-catalyzed pyrrole syntheses, see : (a) Kel'in, A. V.; Sromek, A. W.; Gevorgyan, V. *J. Am. Chem. Soc.* **2001**, *123*, 2074. (b) Gabriele, B.; Salerno, G.; Fazio, A. *J. Org. Chem.* **2003**, *68*, 7853. (c) Takaya, H.; Kojima, S.; Murahashi, S.-I. *Org. Lett.* **2001**, *3*, 421. (d) Lee, C.-F.; Yang, L.-M.; Hwu, T.-Y.; Feng, A. S.; Tseng, J.-C.; Luh, T.-Y. *J. Am. Chem. Soc.* **2000**, *122*, 4992. (e) Merlic, C. A.; Baur, A.; Aldrich, C. C. *J. Am. Chem. Soc.* **2000**, *122*, 7398. (f) Braun, R. U.; Zeitler, K.; Müller, T. J. *Org. Lett.* **2001**, *3*, 3297. (g) Nishibayashi, Y.; Yoshikawa, M.; Inada, Y.; Milton, M. D.; Hidai, M.; Uemura, S. *Angew. Chem., Int. Ed.* **2003**, *42*, 2681. (h) Deng, G. S.; Jiang, N.; Ma, Z. H.; Wang, J. B. *Synlett* **2002**, 1913. (i) Wang, Y.; Zhu, S. *Org. Lett.* **2003**, *5*, 745. (j) Dieter, R. K.; Yu, H. *Org. Lett.* **2001**, *3*, 3855. (j) Crawley, M. L.; Goljer, I.; Jenkins, D. J.; Mehlmann, J. F.; Nogle, L.; Dooley, R.; Mahaney, P. E. *Org. Lett.* **2006**, *8*, 5837.

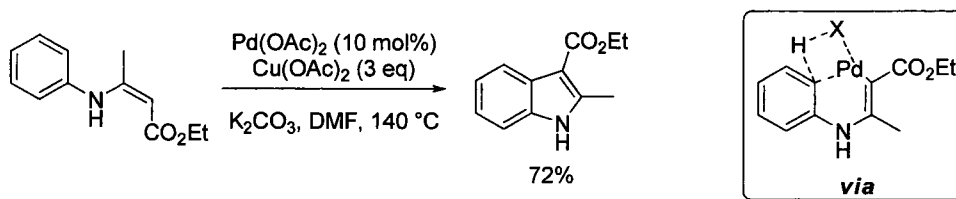
the pre-existing arene (Scheme 4.4).<sup>105</sup> However, the past year and a half have witnessed significant growth in the field of oxidative indole and indoline synthesis.

**Scheme 4.4.** Observed products from multiple alkyne insertion.



In 2008 Glorius and co-workers reported the oxidative intramolecular cyclization of *N*-arylenamines catalyzed by palladium(II) (Scheme 4.5).<sup>106</sup> The reaction displayed good substrate scope on the aryl moiety though in all cases the resulting indole contains a C3 carbonyl substituent. While the optimized conditions were developed for an intramolecular process, the reaction may be rendered intermolecular by a one-pot reaction of a simple aniline with a  $\beta$ -ketoester, followed by palladium-catalyzed oxidative cyclization with no loss in yield. The cyclization onto the aryl unit was proposed to proceed *via* a CMD transition state based on the reactivity profile of electronically different arenes and presence of a significant primary DKIE of 4.6.

**Scheme 4.5.** Oxidative intramolecular cyclization of *N*-arylenamines.

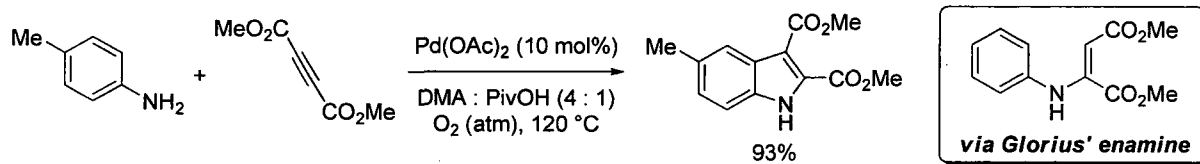


<sup>105</sup> (a) Dupont, J.; Pfeffer, M.; Daran, J.-C.; Gouteron, J. J. *Chem. Soc., Dalton Trans.* **1988**, 2421. (b) Wu, G.; Rheingold, A.L.; Heck, R.F. *Organometallics* **1986**, 5, 1922.

<sup>106</sup> Wurtz, S.; Rakshit, S.; Neumann, J. J.; Droge, T.; Glorius, F. *Angew. Chem., Int. Ed.* **2008**, 47, 7230.

Very recently, a palladium-catalyzed oxidative coupling of simple anilines with acetylenedicarboxylate esters was reported by Jiao and co-workers (Scheme 4.6).<sup>107</sup> The reaction proceeds in moderate to excellent yield and displays broad applicability with respect to the aniline moiety. Additionally, the use of molecular oxygen as the stoichiometric oxidant is advantageous in this process and the authors report the relevance of the method to the synthesis of a 5-HT<sub>3</sub> receptor antagonist and an inhibitor of PDE-IV and TXA<sub>2</sub>. However, the substrate scope with respect to the alkyne is limited to alkynes bearing two electron-withdrawing groups and when unsymmetrical alkynes are used, such as 3-phenylpropionitrile, low yields (20%) are obtained.

**Scheme 4.6.** Jiao's intermolecular coupling of anilines with acetylenedicarboxylate esters.



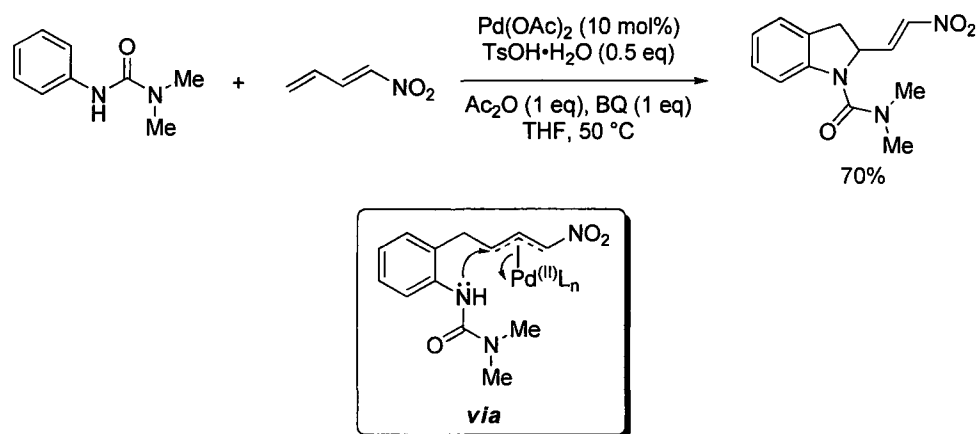
An oxidative transition metal-catalyzed approach has been exploited in the construction of the indoline core, as well. Lloyd-Jones and Booker-Milburn reported the palladium-catalyzed oxidative carboamination of 1,3-dienes with *N*-arylureas (Scheme 4.7).<sup>108</sup> The reaction is proposed to proceed *via* urea-directed palladation of the arene, followed by carbo-palladation of the terminal alkene of the 1,3-diene forging a C-C bond and a  $\pi$ -allyl palladium(II) species. C-N bond formation then takes place by nucleophilic attack of the aniline nitrogen atom on the  $\pi$ -allyl palladium. Additionally, the active catalyst is proposed to be a palladium-tosylate generated *in situ* from palladium acetate and *p*-toluenesulfonic acid. Moderate to excellent yields are obtained for a variety of substituted *N*-arylureas under relatively mild conditions (50 °C, 4 hours), however the 1,3-dienes are

<sup>107</sup> Shi, Z.; Zhang, C.; Li, S.; Pan, D.; Ding, S.; Cui, Y.; Jiao, N. *Angew. Chem. Int. Ed.* **2009**, *48*, 4572. For a low yield precedent to this reaction, please see: Sakakibara, T.; Tanaka, Y.; Yamasaki, S. *Chem. Lett.* **1986**, 797.

<sup>108</sup> Houlden, C. E.; Bailey, C. D.; Ford, J. G.; Gagné, M. R.; Lloyd-Jones, G. C.; Booker-Milburn, K. I. *J. Am. Chem. Soc.* **2008**, *130*, 10066.

limited to those containing an electron-withdrawing group and are otherwise unsubstituted.<sup>109</sup>

**Scheme 4.7.** Oxidative carboamination of 1,3-dienes.



#### 4.1.2. Rhodium(III) as an Oxidant in Organic Synthesis.

Palladium(II) has seen extensive use as an oxidant in organic synthesis and its use in this capacity has been largely documented in the literature.<sup>110</sup> Rhodium(III), on the other hand, has seen relatively little use as an oxidant in organic synthesis and its has been primarily limited to oxidative heterocycle synthesis<sup>111</sup> and oxidative carbonylation.<sup>112</sup>

**Oxidative synthesis of heterocycles.** Rhodium(III) has served as an oxidant in the transformation of aromatic amino-alcohols to five, six, and seven membered ring lactams *via* sequential alcohol oxidation, hemi-aminal formation and finally hemi-aminal oxidation

<sup>109</sup> Glorius has recently disclosed an impressive oxidative amination of unactivated C-H bonds at *sp*<sup>3</sup>-centers *via* palladium-catalysis to form indolines, see: Neumann, J. J.; Rakshit, S.; Dröge, T.; Glorius, F. *Angew. Chem. Int. Ed.* **2009**, *48*, 6892.

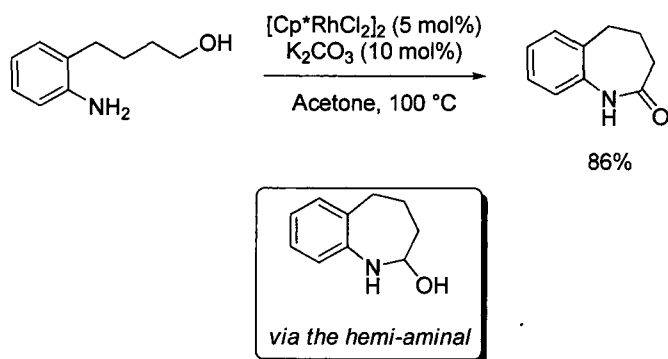
<sup>110</sup> For reviews on Pd(II) as an oxidant in organic synthesis, please see: (a) Stahl, S. S. *Angew. Chem. Int. Ed.* **2004**, *43*, 3400. (b) Gligorich, K. M.; Sigman, M. S. *Chem. Commun.* **2009**, 3854. (c) Sigman, M. S.; Schultz, M. J. *Org. Biomol. Chem.* **2004**, *2*, 2551. (d) Stoltz, B. M. *Chem. Lett.* **2004**, *33*, 362.

<sup>111</sup> For examples of rhodium(III)-catalyzed heterocycle synthesis, see: (a) Ueura, K.; Satoh, T.; Miura, M. *Org. Lett.* **2007**, *9*, 1407. (b) Ueura, K.; Satoh, T.; Miura, M. *J. Org. Chem.* **2007**, *72*, 5362. (c) Umeda, N.; Tsurugi, H.; Satoh, T.; Miura, M. *Angew. Chem. Int. Ed.* **2008**, *47*, 4019. (d) Li, L.; Brennessel, W. W.; Jones, W. D. *J. Am. Chem. Soc.* **2008**, *130*, 12414. (e) Li, L.; Brennessel, W. W.; Jones, W. D. *Organometallics*, **2009**, *28*, 3492. (f) Fujita, K.-I.; Takahashi, Y.; Owaki, M.; Yamamoto, K.; Yamaguchi, R. *Org. Lett.* **2004**, *6*, 2785.

<sup>112</sup> (a) Grushin, V.V.; Marshall, W.J.; Thorn, D.L. *Adv. Syn. Catal.* **2001**, *343*, 161. (b) Zakzeski, J.; Behn, A.; Head-Gordon, M.; Bell, A. T. *J. Am. Chem. Soc.* **2009**, *131*, 11098.

(Scheme 4.8).<sup>111f</sup> As observed in other heterocycles syntheses (*vide infra*) the optimal rhodium source was the (pentamethylcyclopentadienyl)rhodium dichloride dimer,  $[\text{Cp}^*\text{RhCl}_2]_2$ . This method provides efficient access to amides directly from the coupling of aromatic amines and alcohols and appeared to be an attractive approach to the azepine lactam ring of Paullone (*vide infra*).<sup>113</sup>

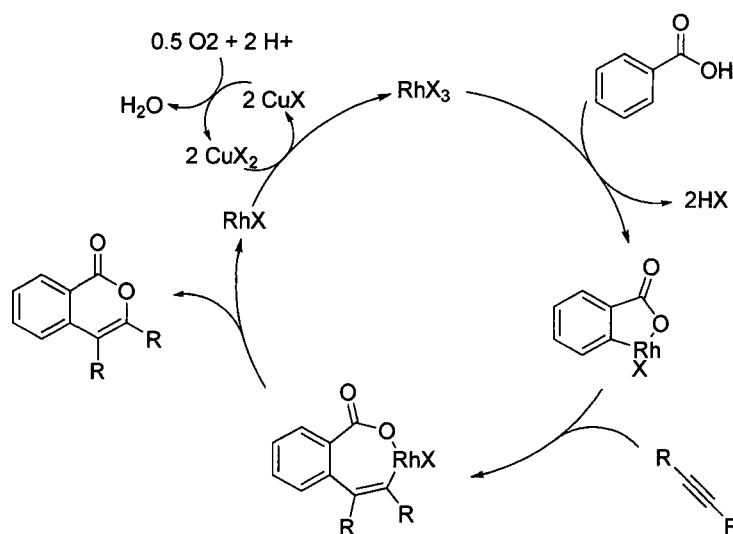
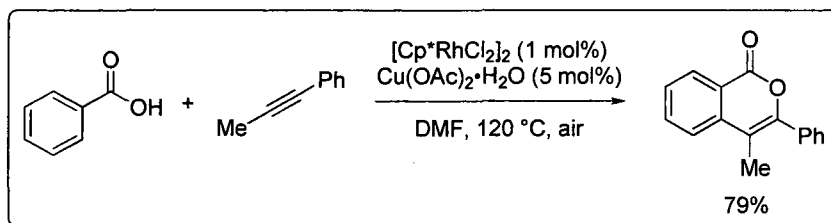
**Scheme 4.8.** Rhodium(III)-catalyzed formation of lactams from aromatic amino-alcohols.



More relevant to the work presented herein is the annulation of benzoic acids with internal alkynes catalyzed by the  $[\text{Cp}^*\text{RhCl}_2]_2$  complex reported by Satoh and Miura (Scheme 4.9).<sup>111a</sup> The authors report good substrate scope for the benzoic acid coupling partner, however, in this account the alkyne coupling partner is primarily limited to symmetrical alkynes. Interestingly, in the two examples in which unsymmetrical internal alkynes were used the aryl substituent is located on the carbon next to the oxygen in the isocoumarin product. The following mechanism was proposed by Satoh and Miura (Scheme 4.9).<sup>111a</sup> The carboxylic acid functionality directs the rhodium to cyclometallate the arene ring forming a 5-membered metallacycle. Carbo-rhodation of the internal alkyne results in a seven-membered metallacycle which then undergoes C-O bond reductive elimination. The rhodium(I) produced in the reductive elimination is then re-oxidized to the catalytically active rhodium(III) with two equivalents of copper(II). This work served as a principal source of inspiration for the potential of rhodium(III) in the annulation of acetanilides with internal alkynes.

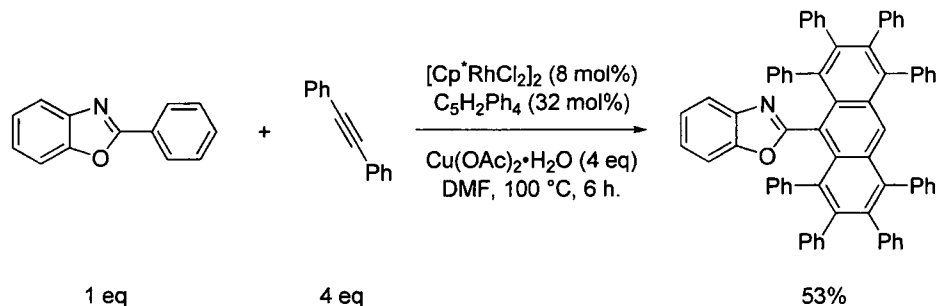
<sup>113</sup> In our synthesis of Paullone (*vide infra*) a completely different route was taken to close the azepine lactone ring.

**Scheme 4.9.** General reaction and mechanism for annulation of benzoic acid by internal alkynes.

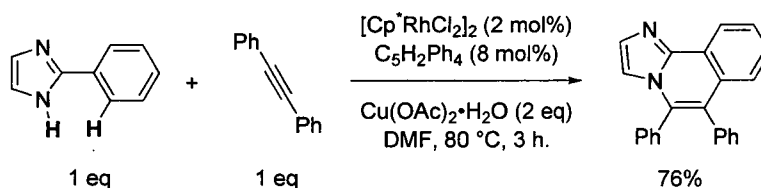


More recently, the same authors have reported the formation of naphthyl- and anthrylazoles *via* rhodium-catalyzed cleavage of multiple C-H bonds in the reaction of phenylazoles with internal alkynes (Scheme 4.10).<sup>111c</sup> These densely arylated arenes were prepared to investigate their spectroscopic (fluorescence) properties. The authors found that the fluorescence spectra were enhanced by the azole ring which also served as a directing group in the formation of these polyaromatic compounds. An interesting observation, and a significant source of inspiration to us, was the reaction of 2-phenyl-1*H*-imidazole with one equivalent of internal alkyne leading to the formation of imidazoisoquinoline. This provided evidence of a C-N bond reductive elimination from rhodium(III) (Scheme 4.11).

**Scheme 4.10.** Formation of polyaromatic compounds *via* rhodium(III)-catalysis.

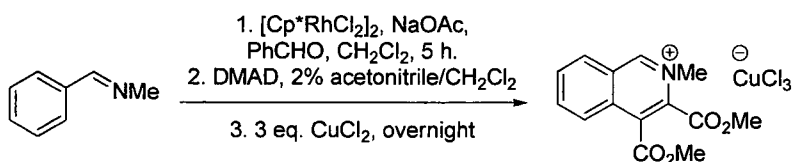


**Scheme 4.11.** Evidence for C-N bond reductive elimination from a rhodium(III) center.



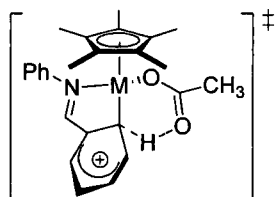
Jones has also made recent contributions to the development of oxidative formation of heterocycles mediated by  $[\text{Cp}^*\text{RhCl}_2]_2$ .<sup>111d,e</sup> His group's work has primarily been the investigation of stoichiometric cyclometallation reactions of rhodium(III) with *N*-substituted aldimines and ketimines, subsequent reaction of these metallocycles with internal alkynes, and the Cu(II)-assisted formation of isoquinoline salts. While each of these reactions have been placed under individual mechanistic scrutiny, a one-pot procedure that provides access to isoquinoline salts directly from aromatic aldimines (or ketimines) has also been reported.<sup>111d</sup> The authors particularly noted that different solvent conditions necessary for each of the three steps has thus far thwarted the development of a reaction that is catalytic in rhodium.

**Scheme 4.12.** Jones' one-pot procedure for the preparation of isoquinoline salts.



The Jones group has also carried out mechanistic investigations for C-H bond cleavage in the stoichiometric cyclometallation of 2-phenylpyridines and phenyl imines with  $[\text{Cp}^*\text{RhCl}_2]_2$  (and its iridium analogue).<sup>111e</sup> The authors found that the reaction proceeded faster for substrates (imines) bearing electron donating groups and that the reaction had a DKIE effect of  $\sim 5$ . Their mechanistic investigation pointed toward a concerted mechanism with the transition state shown in Figure 4.2. The proposal of a highly ordered transition state is supported by computational work conducted by Davies and Macgregor for the cyclometallation of *N,N*-dimethylbenzylamine by both palladium(II) acetate and more relevantly,  $[\text{Cp}^*\text{IrOAc}]^+$ .<sup>13,14</sup> Davies and Macgregor also observed a rate enhancement for electron-rich substrates; however, the aforementioned computational work found that there was no evidence for any contribution of a Wheland intermediate. This suggests, therefore, that the nucleophilic component of these arenes is important such that  $E_{int}$  is likely a dominant term in the C-H bond cleaving mechanism. Jones also found that the regioselectivity of the reaction was unaffected by temperature and solvent polarity.

**Figure 4.2.** Proposed transition state for Jones cyclorhodation of *N*-phenyl imines.

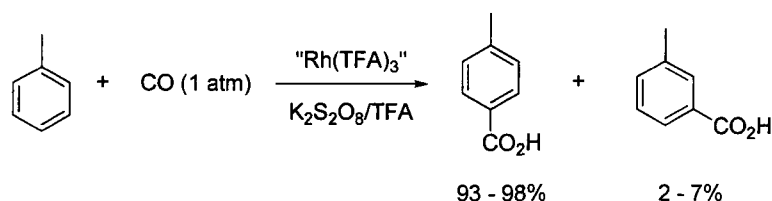


**Oxidative carboxylation of arenes.** Subsequent to Fujiwara's report on the palladium catalyzed oxidative carboxylation of arenes,<sup>114</sup> rhodium catalyzed approaches were developed. Of particular interest was the large scale production of *p*-toluic acid, a precursor to terephthalic acid and other bifunctionalized arenes with various large-scale industrial applications. While the arene substrate is also used as the solvent, this is of no consequence for the carboxylation of inexpensive arenes, such as benzene and toluene, used in the bulk preparation of industrially useful compounds. Additionally, high catalyst turn-

<sup>114</sup> For a review on the palladium catalyzed oxidative carboxylation of arenes, please see: (a) Fujiwara, K.; Takaki, K.; Taniguchi, Y. *Synlett* **1996**, 591.

over numbers, and therefore yields based on catalyst, are observed. Grushin, at Dupont de Nemours & Co., has reported a highly selective Rh(III)-catalyst system for this process which described the active species to be “Rh(TFA)<sub>3</sub>”.<sup>115</sup> A particularly impressive aspect of this chemistry was the high *para*-selectivity that was observed, typically >10 : 1 (*para* : *meta*) (Scheme 4.13).

**Scheme 4.13.** Grushin's Rh(III)-catalyzed oxidative carboxylation of toluene.



Bell and co-workers have recently identified the ionic ligand environment on rhodium to have a significant influence on both the activity and selectivity in oxidative carboxylation.<sup>116</sup> When conjugate bases of acids with pK<sub>a</sub> values ranging from 0 – 0.5 serve as the ligands the highest activity is observed; likewise, the highest *para/meta*-isomer ratios are observed at pK<sub>a</sub> value of 0 and drop off significantly when the acid pK<sub>a</sub> is both less than or greater than 0. Computational data outlined an electrophilic-type (S<sub>E</sub>Ar-type) mechanism that was also influenced by the pK<sub>a</sub> of the anionic ligand, with charge stabilization of the *para*-carbon facilitated by ligands characterized by lower pK<sub>a</sub>'s.

## 4.2. Results and Discussion

### 4.2.1. Rhodium(III)-Catalyzed Annulation of Acetanilides with Internal Alkynes: Reaction Development and Scope

***Rhodium(III)-catalyzed annulation of acetanilides to form indoles: first generation conditions.*** Based on the known ability of *N*-acetylanilines to undergo *ortho*-metallation,<sup>117</sup>

<sup>115</sup> Grushin, V. V.; Marshall, W. J.; Thorn, D. L. *Adv. Synth. Catal.* **2001**, *343*, 161.

<sup>116</sup> Zakzeski, J.; Behn, A.; Head-Gordon, M.; Bell, A. T. *J. Am. Chem. Soc.* **2009**, *131*, 11098.

<sup>117</sup> For recent examples in direct arylation see: (a) Kalyani, D.; Deprez, N.R.; Desai, L.V.; Sanford, M.S. *J. Am. Chem. Soc.*, **2005**, *127*, 7330. (b) Daugulis, O.; Zaitsev, V.G. *Angew. Chem. Int. Ed.* **2005**, *44*, 4046. For

and the ease with which *N*-acetyl indoles may be deprotected, *N*-acetylaniline **4.1a** was selected along with 1-phenyl-1-propyne **4.2a** for reaction development. Extensive experimentation with a variety of palladium(II) catalysts<sup>118</sup> failed to produce indole **4.3a**, instead giving small amounts of Heck and multiple Heck-type additions. Similarly, Wilkinson's catalyst, which has been shown to induce similar reactivity with 1,2-diaryldiazines,<sup>119</sup> gave none of the desired product. A promising lead was obtained with [Cp\*RhCl<sub>2</sub>]<sub>2</sub> in conjunction with a stoichiometric copper(II) oxidant - a catalyst system recently employed by Satoh and Miura<sup>111a,b</sup> and by Jones<sup>111c,d</sup> for other reactions initiated *via* cyclometallation.<sup>120</sup> Under these conditions, small amounts of **4.3a** (approx. 3% yield) could be detected by GCMS analysis of the crude reaction mixture (Table 4.1, entry 1). Continued optimization revealed that the presence/absence of chloride anions and the choice of solvent exert a dramatic impact on reaction outcome.<sup>121</sup> For example, the addition of silver triflate to sequester the chloride ligands increases the yield five-fold (Table 4.1, entry 2). A solvent screen revealed that the yield could be further increased to 55% by using *t*-AmOH as solvent (Table 4.1, entry 6) and a second assay of silver salts revealed that, with 10 mol% silver hexafluoroantimonate, a 79% isolated yield of **4.3a** could be obtained as one regioisomer<sup>122</sup> (Table 4.1, entry 9). The reaction time could also be significantly shortened since **4.3a** can be isolated in 65% yield even after five minutes of reaction (Table 4.1, entry 10). Conversely, if one equivalent of LiCl is added to the reaction mixture, product formation is completely inhibited; adding additional weight to the observation that chloride anions exert a negative impact on catalyst activity (Table 4.1, entry 11).

---

recent examples in oxidative Heck reactions see: (c) Boele, M.D.K.; Strijdonck, G.P.F.; de Vries, A.H.M.; Kamer, P.C.J.; de Vries, J.G.; van Leeuwen, P.W.N.M. *J. Am. Chem. Soc.* **2002**, *124*, 1586. (d) Zaitsev, V.G.; Daugulis, O. *J. Am. Chem. Soc.* **2005**, *127*, 4156. For recent examples in oxidative biaryl formation see: (e) Li, B.-L.; Tian, S.-L.; Fang, Z.; Shi, Z.-J. *Angew. Chem. Int. Ed.* **2008**, *47*, 1115. (f) Brasche, G.; Garcia-Fortanet, J.; Buchwald, S.L. *Org. Lett.* **2008**, *10*, 2207.

<sup>118</sup> Only unreacted acetanilide **4.1a** and trace amounts of a multiple alkyne insertion product previously observed by Heck appeared in the GCMS trace.

<sup>119</sup> Aulwurm, U.R.; Melchinger, J.U.; Kisch, H. *Organometallics* **1995**, *14*, 3385.

<sup>120</sup> For the use of this complex in the cleavage of other strong bonds, see: Taw, F. L.; Mueller, A. H.; Bergman, R. G.; Brookhart, M. *J. Am. Chem. Soc.* **2003**, *125*, 9808

<sup>121</sup> A similar effect has been observed in rhodium catalyzed carbonylation reactions see ref 18a.

<sup>122</sup> In the reaction yielding **3a** the regioselectivity is > 40 : 1 by GCMS.

**Table 4.1** Reaction development in the rhodium(III)-catalyzed synthesis of indoles.<sup>a</sup>

Reaction scheme: Acetanilide (4.1a) + Alkyne (4.2a)  $\xrightarrow[\text{Solvent (0.2 M), 120 }^\circ\text{C, Time}]{[\text{Cp}^*\text{RhCl}_2]_2 \text{ (2.5 mol\%)} + \text{Additive (X mol\%)}, \text{Cu(OAc)}_2 \cdot \text{H}_2\text{O (2.1 eq)}$  Indole (4.3a)

Entry	Additive (mol%)	Solvent	Time (hours)	GCMS Yield (%)
1	none	DMF	16	3
2	AgOTf (10)	DMF	16	15
3	AgOTf (10)	DMA	16	18
4	AgOTf (10)	NMP	16	0
5	AgOTf (10)	mesitylene	16	40
6	AgOTf (10)	<i>t</i> -AmOH	16	55
7	AgBF <sub>4</sub> (10)	<i>t</i> -AmOH	16	53
8	AgSbF <sub>6</sub> (10)	<i>t</i> -AmOH	16	74
9	AgSbF <sub>6</sub> (10)	<i>t</i> -AmOH	1	86, 79 <sup>b</sup>
10	AgSbF <sub>6</sub> (10)	<i>t</i> -AmOH	0.1	65 <sup>b</sup>
11	LiCl (100)	<i>t</i> -AmOH	16	< 1%

<sup>a</sup>Conditions: Acetanilide (1 eq, 0.2 M), alkyne (1.1 eq), [Cp\*RhCl<sub>2</sub>]<sub>2</sub> (2.5 mol%), additive, Cu(OAc)<sub>2</sub>·H<sub>2</sub>O (2.1 eq), solvent, 120 °C, specified time. <sup>b</sup>Isolated yield.

**Rhodium(III)-catalyzed annulation of acetanilides to form indoles: second generation conditions.** Having previously established reaction conditions to affect the desired oxidative coupling of acetanilides and internal alkynes to afford highly functionalized indoles<sup>123</sup> we sought to improve on those conditions. Our main goal in re-optimization was the use of a co-catalytic quantity of Cu(OAc)<sub>2</sub> in conjunction with an oxygen atmosphere as the terminal oxidant. For practical purposes the effects of temperature on the reaction yield was first investigated and it was found that at 60 °C under extended reaction times (6 hours) 90% isolated yield of the desired indole **4.3a** was obtained (Table 4.2, entry 1 and 2). The catalyst loading of Cu(OAc)<sub>2</sub> was then examined and while 10 mol% Cu(OAc)<sub>2</sub> provided a moderate <sup>1</sup>H NMR yield (55%), 20 mol% of the co-oxidant afforded an additional increase in the yield (81%) (Table 4.2, entries 3 – 5). The <sup>1</sup>H NMR yield of **4.3a** was further increased to 93% (90% isolated yield) by employing a dicationic rhodium complex, [Cp\*Rh(MeCN)<sub>3</sub>][SbF<sub>6</sub>]<sub>2</sub>, as opposed to its *in situ* formation by addition of both rhodium catalyst, [Cp\*RhCl<sub>2</sub>]<sub>2</sub>, and the necessary silver salt, AgSbF<sub>6</sub>. With these

<sup>123</sup> Stuart, D.R.; Bertrand-Laperle, M.; Burgess, K.M.N.; Fagnou, K. *J. Am. Chem. Soc.* **2008**, *130*, 16474.

conditions in hand the amount of  $\text{Cu}(\text{OAc})_2$  was reduced by ten-fold and the reaction temperature was reduced by 60 °C. Additionally, it should be noted that catalyst turnover is also possible in the absence of copper with oxygen acting as the sole oxidant (Table 4.2, entry 7). While the  $^1\text{H}$  NMR yield was low (22%, TON = 4) this provides evidence for the potential of rhodium oxidase chemistry as a viable tool in organic synthesis.

**Table 4.2.** Re-optimization of the reaction conditions for the annulation of acetanilides with internal alkynes.<sup>a</sup>

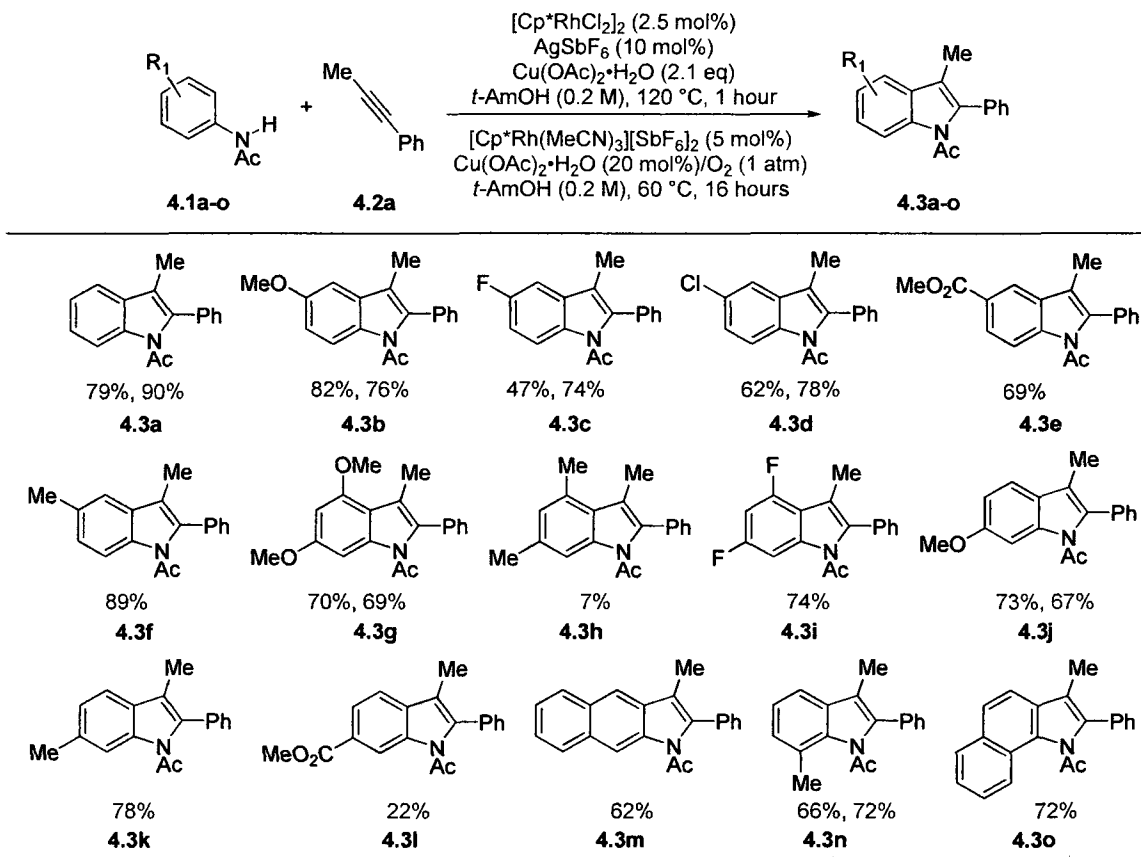
Entry	Catalyst	$\text{Cu}(\text{OAc})_2$	Temp.	Time (h)	$^1\text{H}$ NMR Yield <sup>c</sup>
1	$[\text{Cp}^*\text{RhCl}_2]_2$ (2.5) $\text{AgSbF}_6$ (10)	210 <sup>b</sup>	120 °C	1	86(79)
2	$[\text{Cp}^*\text{RhCl}_2]_2$ (2.5) $\text{AgSbF}_6$ (10)	210 <sup>b</sup>	60 °C	6	92(90)
3	$[\text{Cp}^*\text{RhCl}_2]_2$ (2.5) $\text{AgSbF}_6$ (10)	10	60 °C	6	55
4	$[\text{Cp}^*\text{RhCl}_2]_2$ (2.5) $\text{AgSbF}_6$ (10)	10	60 °C	22	68
5	$[\text{Cp}^*\text{RhCl}_2]_2$ (2.5) $\text{AgSbF}_6$ (10)	20	60 °C	22	81
6	$[\text{Cp}^*\text{Rh}(\text{MeCN})_3]$ $[\text{SbF}_6]_2$ (5)	20	60 °C	22	93(90)
7	$[\text{Cp}^*\text{Rh}(\text{MeCN})_3]$ $[\text{SbF}_6]_2$ (5)	—	60 °C	22	22

<sup>a</sup>Conditions: Acetanilide (1 eq, 0.2 M), alkyne (1.1 eq), catalyst,  $\text{Cu}(\text{OAc})_2 \cdot \text{H}_2\text{O}$  (X eq),  $\text{O}_2$  balloon (if applicable), *t*-AmOH, temperature, specified time. <sup>b</sup>No balloon of  $\text{O}_2$  used. <sup>c</sup>Isolated yields in parentheses.

**Reaction scope with respect to acetanilide and alkyne.** The generality of the reaction was then probed under both first and second generation conditions with respect to both the acetanilide and the alkyne. When various acetanilides were examined, yields were comparable or better under the second generation conditions (for example compare 79% and 90% for first and second generation conditions, respectively, Table 4.3, **4.3a**). Of particular note is the multitude of 5-, 6-, and 7-substituted indoles that may be produced in this reaction. *Para*-substituted acetanilides bearing electron-donating, electron-withdrawing, and halo substituents afford the corresponding 5-substituted indoles in good yields (Table 4.3,

**4.3b – 4.3f).** *Meta*-substitution is tolerated in the case of both symmetrical and unsymmetrical acetanilides. Electron-rich and electron-poor di-*meta*-substituted acetanilides give 4,6-di-substituted indoles in good yields (Table 4.3, **4.3g** and **4.3i**). However, the reaction is particularly sensitive to sterics as 3,5-dimethylacetanilide provides only 7% isolated yield of **4.3h**. *Meta*-substituted acetanilides react with good regioselectivity and allow the isolation of 6-substituted indoles as a single regioisomer in good yield. When the substituent is electron-donating (Table 4.3, **4.3j**) or alkyl (Table 4.3, **4.3k**) the products are obtained in good yields; however the presence of a 3-methyl ester on the acetanilide (Table 4.3, **4.3l**) results in a poor yield of the indole product due to an unfavourable electronic environment of the acetanilide. Additionally, benzo fused acetanilides provide the corresponding indole in good yield (Table 4.3, **4.3m**). *Ortho*-substitution is also tolerated yielding 7-methyl or benzo[g] indoles (Table 4.3, **4.3n** and **4.3o**).

**Table 4.3.** Acetanilide applicability under both first and second generation conditions.<sup>a</sup>



<sup>a</sup>Conditions: First generation (red): Acetanilide (1 eq, 0.2 M), alkyne (1.1 eq), [Cp\*RhCl<sub>2</sub>]<sub>2</sub> (2.5 mol%), AgSbF<sub>6</sub> (10 mol%), Cu(OAc)<sub>2</sub>·H<sub>2</sub>O (2.1 eq), *t*-AmOH, 120 °C, 1 - 3 hours. Second generation (blue): Acetanilide (1 eq, 0.2 M), alkyne (1.1 eq), [Cp\*Rh(MeCN)<sub>3</sub>][SbF<sub>6</sub>]<sub>2</sub> (5 mol%), Cu(OAc)<sub>2</sub>·H<sub>2</sub>O (20 mol%), O<sub>2</sub> balloon, *t*-AmOH, 60 °C, 20 hours.

<sup>b</sup>Isolated yields are reported above.

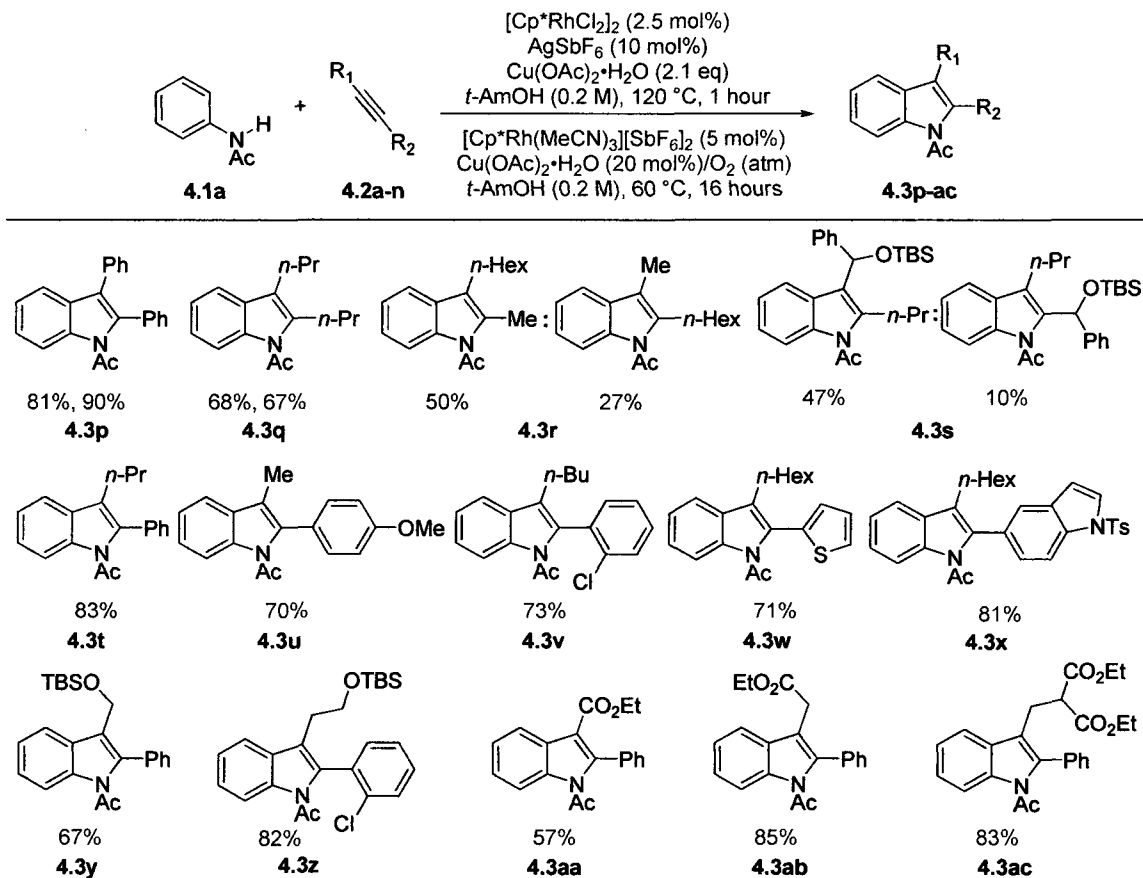
A range of alkynes have also been found to be compatible under the second generation conditions. Both aryl/aryl and alkyl/alkyl symmetrically substituted internal alkynes produce 2,3-di-substituted indoles in good to excellent yield (Table 4.4, **4.3p** and **4.3q**). However, when unsymmetrical alkyl/alkyl substituted internal alkynes are employed in the reaction mixtures of C2/C3 indole regioisomers are obtained (Table 4.4, **4.3r** and **4.3s**). Of particular interest is that there is any regioselectivity at all between a primary and methyl carbon (1.8 : 1) in the case of **4.3r** with the larger primary carbon taking the C3 position in the major regioisomer. More pronounced regioselectivity is observed between a secondary and primary carbon (4.7 : 1) again with the larger secondary carbon at the C3 position of the major isomer which is obtained in moderate yield (Table 4.4, **4.3s**). As previously observed, alkyl/aryl internal alkynes react with near exclusive regioselectivity (>

40 : 1) placing the  $sp^2$  carbon at the C2 position of indole. Though this electronic effect has not yet been rationalized, the high level of regioselectivity has been exploited in the synthesis of Paullone (*vide infra*). A number of different groups, including electron-donating groups and halides are compatible on the aryl moiety (Table 4.4, **4.3t** – **4.3v**). Unsaturated heterocycles, such as thiophene and indole, may also serve as the aryl moiety providing a heterobiaryl linkage at the C2 position of indole in good yield (Table 4.4, **4.3w** and **4.3x**). Additional functionality on the alkyl moiety of alkyl/aryl internal alkynes was also investigated. Unprotected propargyl alcohols were unreactive when subjected to the reaction conditions and thus a scan of common protecting groups was conducted to allow for the use of this important class of compound in the reaction (Table 4.5). It was found that, without any further optimization to the reaction conditions, the *tert*-butyldimethylsilyl (TBS) protecting group afforded the highest yield of the desired indole while minimizing the formation of an undesired solvolysis side product (Table 4.5, entry 4). Control experiments on both the alkyne coupling partner and the indole product have shown that the solvolysis product is formed only after indole formation has occurred by reaction of the solvent with the indole product. Furthermore, presence of the rhodium catalyst is not necessary for the formation of the solvolysis side product which is observed when the indole product alone is heated in *tert*-amyl alcohol.<sup>124</sup> Thus, TBS-protected propargyl and homopropargyl alcohols react in good yield (Table 4.4, **4.3y** and **4.3z**), as well do propionate esters, homo-propargyl esters and a diethylmalonate moiety at the homo-propargylic position (Table 4.4, **4.3aa** – **4.3ac**). Of particular note is the reaction of the homo-propargyl ester in the reaction. These compounds are extremely sensitive to base readily undergoing isomerization to the allenic esters; however, in this case no such isomerization is observed and clean reaction takes place. High yielding removal of the acetyl group was observed when the *N*-acetylindoles were subjected to basic reaction conditions (Table 4.6).

---

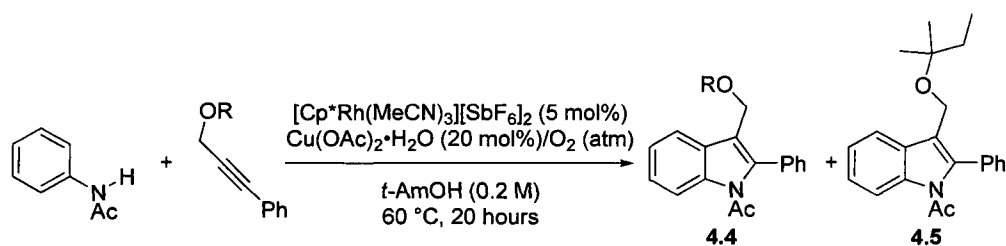
<sup>124</sup>See supporting information for details of control experiments and characterization of solvolysis side products.

**Table 4.4.** Alkyne applicability under both first and second generation conditions.<sup>a</sup>



<sup>a</sup>Conditions: First generation (red): Acetanilide (1 eq, 0.2 M), alkyne (1.1 eq), [Cp\*RhCl<sub>2</sub>]<sub>2</sub> (2.5 mol%), AgSbF<sub>6</sub> (10 mol%), Cu(OAc)<sub>2</sub>·H<sub>2</sub>O (2.1 eq), *t*-AmOH, 120 °C, 1 - 3 hours. Second generation (blue): Acetanilide (1 eq, 0.2 M), alkyne (1.1 eq), [Cp\*Rh(MeCN)<sub>3</sub>][SbF<sub>6</sub>]<sub>2</sub> (5 mol%), Cu(OAc)<sub>2</sub>·H<sub>2</sub>O (20 mol%), O<sub>2</sub> balloon, *t*-AmOH, 60 °C, 20 hours. <sup>b</sup>Isolated yields are reported above.

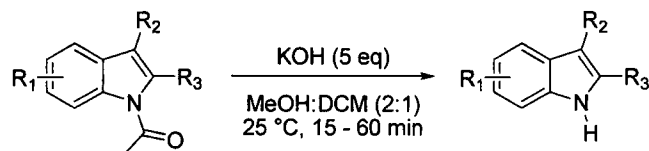
**Table 4.5.** Determination of optimal protecting groups for propargyl alcohols.<sup>a</sup>



Entry	R-group	Isolated yield 4.4 (%)	Isolated yield 4.5 (%)
1	H	—	—
2	Ac	16	59
3	Bn	35	11
4	TBS	67	11
5	TIPS	35	17

<sup>a</sup>Conditions: Acetanilide (1 eq, 0.2 M), alkyne (1.1 eq), [Cp\*Rh(MeCN)<sub>3</sub>][SbF<sub>6</sub>]<sub>2</sub> (5 mol%), Cu(OAc)<sub>2</sub>·H<sub>2</sub>O (20 mol%), O<sub>2</sub> balloon, *t*-AmOH, 60 °C, 20 hours.

**Table 4.6.** Removal of acetyl group.<sup>a</sup>

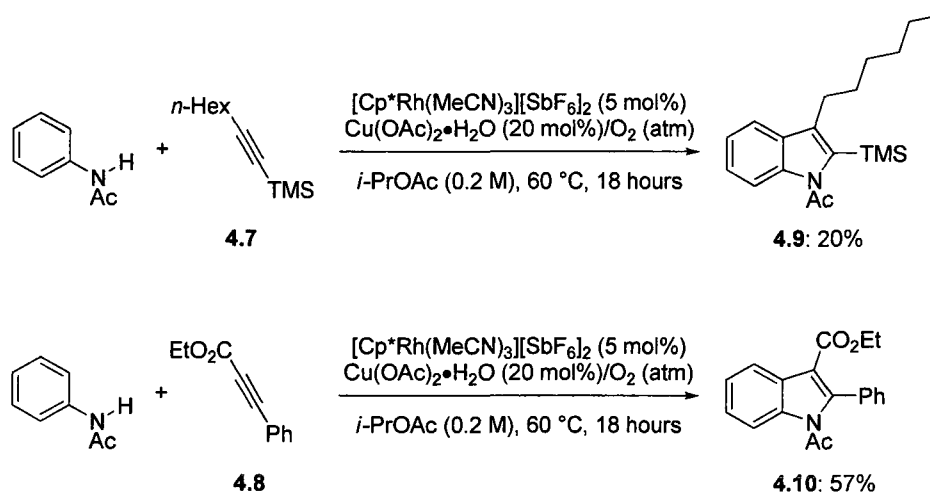


Entry	<i>N</i> -acetylindole	<i>N</i> -H-indole	Yield <sup>b</sup>
1			90%
2			97%
3			98%

<sup>a</sup>Conditions: *N*-Acetylindole (1 eq, 0.13 M), MeOH:DCM (2:1), KOH (5 eq), room temperature, 15 min - 1 hour. <sup>b</sup>Isolated yields are reported above.

**Incompatible alkynes and promising leads.** The inability to utilize terminal alkynes<sup>125</sup> led to the investigation of appropriately substituted alkynes that would be compatible under the reaction conditions and allow for removal of one of the groups yielding a C3 or C2-unsubstituted indole. A number of different alkynes were investigated and those protected with a silyl group, **4.7**, or an ethyl ester, **4.8**, proved to be most promising (Scheme 4.14). Though a brief optimization was carried out and resulted in the conditions shown below (Scheme 4.14) the isolated yield of **4.9** could not be increased above ~ 20%.<sup>126</sup> The regioselectivity of **4.9** was confirmed by 2-D NMR (COSY and NOESY) spectroscopy.<sup>127</sup> Alkyne **4.8** was, however, more promising providing the desired indole in 57% under the second-generation conditions with no additional optimization.<sup>128</sup> The regioselectivity was confirmed by derivatization (removal of the acetyl group) and comparison of the spectral data with the corresponding literature values.<sup>127</sup> The C3 ethyl ester provides an additional handle for functional group interconversions (aldehyde/alcohol), derivatization (decarboxylative cross-coupling) or cleavage.

**Scheme 4.14.** Compatibility of protected alkynes in the annulation of acetanilides.



<sup>125</sup> The use of terminal alkyne led to alkyne dimerization as the major product and no formation of the desired indole.

<sup>126</sup> The optimization included the silyl derivatives (TMS, TIPS, and TBS), solvent, and stoichiometry. This chemistry has not been further investigated.

<sup>127</sup> Please see Chapter 5 (supporting information) for more details.

<sup>128</sup> This chemistry has since been further optimized by an undergraduate student, Kevin Burgess.

It was found in our initial studies that internal alkynes substituted with an alkyl and an aryl substituent coupled to acetanilides with high regioselectivity (> 40 : 1, GCMS) with the aryl group taking the C2-position of indole. This appears to be an electronic effect (*vide infra*) though a thorough understanding of this regioselectivity has not yet been gained. Nevertheless, high regioselectivities were observed over a significant range of alkyl and aryl substitution (Table 4.4).

The use of nonsymmetrical alkyl/alkyl internal alkynes as coupling partners resulted in poor C2/C3 regioselectivity in the indole product. Moreover, the chromatographic separation of the two regioisomers was challenging and therefore this prompted the consideration of the regioselective outcome when an enyne, such as **4.11**, was employed as a coupling partner (Scheme 4.15). The observation that  $sp^2$ -hybridized carbons (phenyl) are placed regioselectively at the C2 position of indole suggested this approach may provide access to single C2/C3 alkyl/alkyl regioisomers after alkene hydrogenation. Additionally, the resulting C2-alkene could be used as a handle for further functional group manipulation (Scheme 4.15). When enyne **4.11** was used as the alkyne coupling partner indole **4.12** was obtained and isolated in low yield, though more importantly as a *single regioisomer*. The regioselectivity was confirmed by 2-D NMR (COSY and NOESY) spectroscopy.<sup>129, 130</sup> This result also suggests an electronic influence for the regioselectivity in which the  $sp^2$ -hybridized alkene is placed at the C2-position of indole. Also, this innovation allows for the preparation of nonsymmetrical C2/C3-alkyl/alkyl substituted indoles (after hydrogenation) as *single regioisomers*.

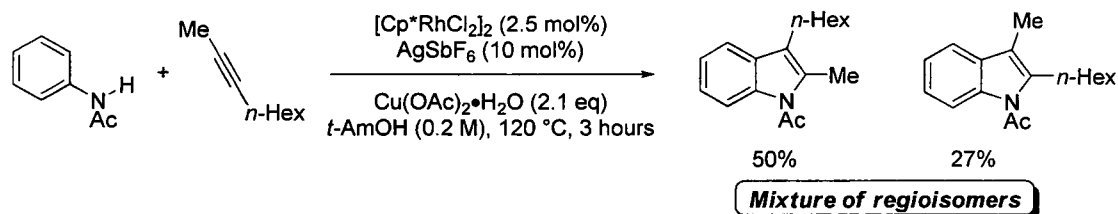
---

<sup>129</sup>Please see Chapter 5 (supporting information) for the synthesis and characterization data of enyne **4.11** and characterization data for indole, **4.12**.

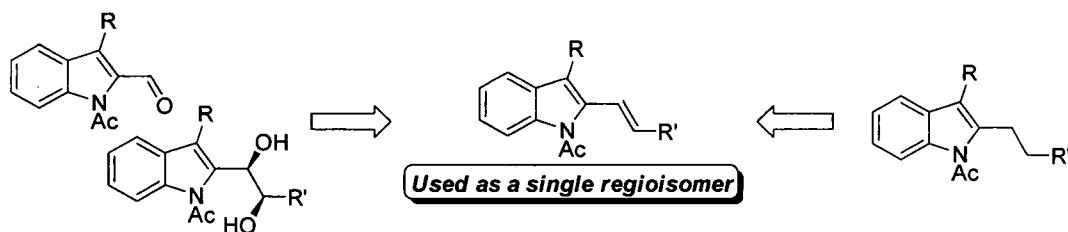
<sup>130</sup>This chemistry was further optimized by M.Sc. candidate Malcolm Heustis.

### Scheme 4.15. Regioselectivity for annulation of acetanilides with enyne substrates.

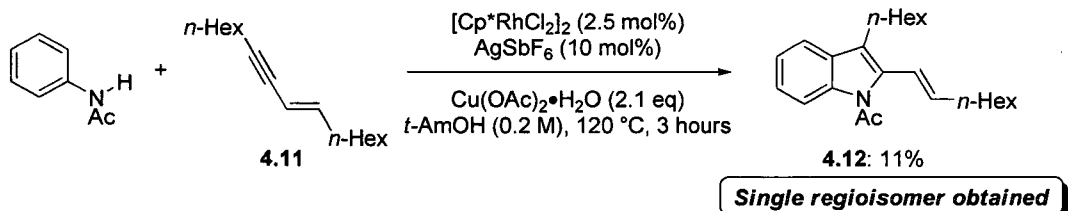
**Current regioselectivity:**



**Potential applicability of enyne annulation:**



**Promising lead result with enynes:**



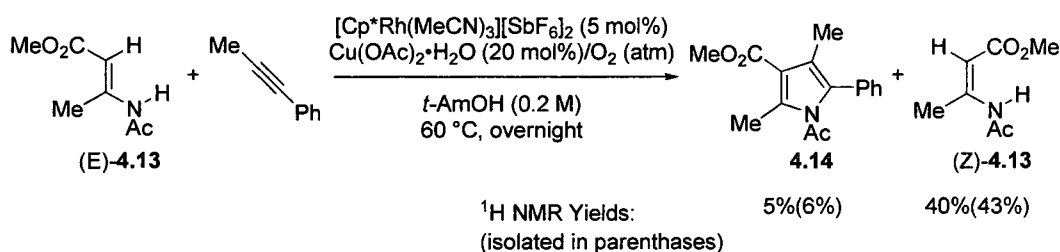
## 4.2.2. Rhodium(III)-Catalyzed Annulation of Enamides with Internal Alkynes: Reaction Development and Scope

**Reaction development.** With an interest in the application of rhodium(III)-catalysis to the synthesis of other unsaturated heterocycles, isoquinoline<sup>131</sup> and pyrrole syntheses were investigated. Compound **4.13** was selected as a model substrate in reaction development for the preparation of pyrroles due to its ease of synthesis. In this case it was envisioned that the proper enamide geometry must be used and conserved throughout the reaction. Enamide (E)-**4.13** was prepared and subjected to the second generation reaction conditions for indole formation (Scheme 4.16). This resulted in only 5% yield (by <sup>1</sup>H NMR spectroscopy) of the desired pyrrole **4.14** along with 40% of the enamide geometrical isomer, (Z)-**4.13**. To test

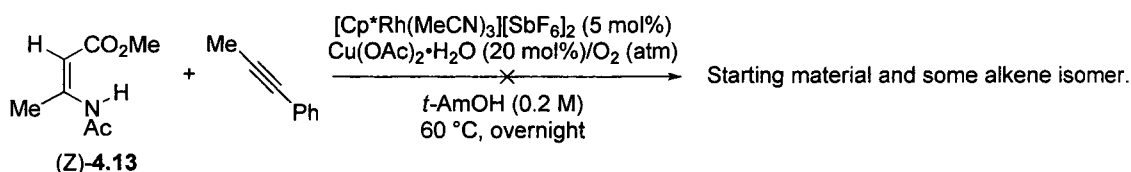
<sup>131</sup> The preparation of isoquinoline *via* annulation of *tert*-butyl benzaldimine with internal alkynes was investigated by Nicolas Guimond, see: Guimond, N.; Fagnou, K. *J. Am. Chem. Soc.* **2009**, *131*, 12050.

the hypothesis that (Z)-4.13 of the enamide is inactive under the reaction conditions and that its competing formation limits the amount of desired pyrrole product formed, this enamide was prepared and used in the reaction. However, in this case no pyrrole product was formed and only a small amount of (E)-4.13 was observed (Scheme 4.17). Control experiments revealed that the presence of rhodium was the major source of enamide isomerization and therefore experiments were done to quantify the amount of isomerization under modified reaction conditions when each of the individual enamide geometrical isomers were used (Scheme 4.18). Pure (E)- and (Z)-4.13 enamides were subjected to modified reaction conditions<sup>132</sup> and both resulted in ~ 15 : 85 ratio of E : Z isomers. While this particular enamide was unsuccessful in the preparation of tetrasubstituted pyrroles investigation into the use of other substituted enamides is ongoing in our laboratory.

**Scheme 4.16.** Formation of a tetrasubstituted pyrrole with (E)-4.13.

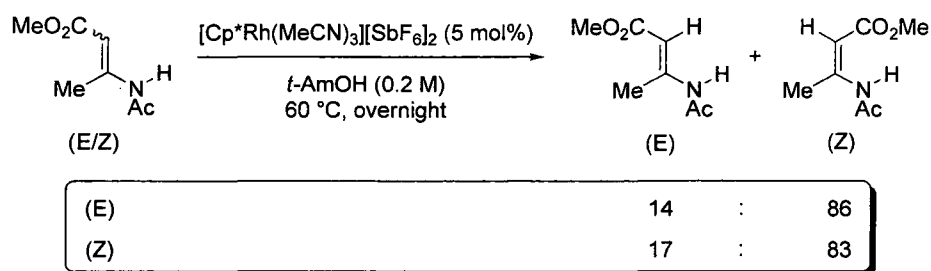


**Scheme 4.17.** Use of (Z)-4.13 in the formation of tetrasubstituted pyrroles.



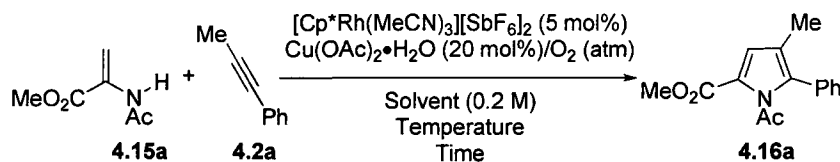
<sup>132</sup> The modified reaction conditions did not contain any  $\text{Cu}(\text{OAc})_2$  or alkyne.

**Scheme 4.18.** Evaluation of enamide isomerization by  $^1\text{H}$  NMR spectroscopy.



Having observed the challenges of alkene isomerization in our previous attempt at the synthesis of pyrroles, a substrate that would not be fraught with these concerns was prepared (**4.15a**). Application of the second generation conditions to the coupling of **4.15a** with 1-phenyl-1-propyne **4.2a** afforded the trisubstituted pyrrole in 98% GCMS yield (Table 4.7, entry 1). Pleased with this result we realized the opportunity to develop more mild conditions for this annulation process. Our primary goal was to conduct the reaction at ambient temperature.<sup>133</sup> It was found that at 60 °C these reactions proceeded at a much faster rate than the indole-forming reaction and that they were complete within 4 hours, providing 93% GCMS yield of the desired pyrrole (Table 4.7, entry 2). However, when the reaction was performed at 30 °C in *t*-AmOH the yield dropped significantly (37% GCMS yield) even after extended reaction times (24 hours, Table 4.7, entry 3). This result was likely due to the insolubility of many of the reaction components in *t*-AmOH at this temperature. Conversely, use of acetone as the reaction solvent at 21 °C yielded 87% GCMS yield and 81% isolated yield of the pyrrole product (Table 4.7, entry 4). Transition metal catalyzed reactions which take place at C-H bonds are rare at this temperature and therefore this constitutes a significant advance in the development of mild conditions for this class of reaction. It should be noted that in the absence of rhodium catalyst no reaction was observed.

<sup>133</sup> Room temperature in the lab in which these reactions were conducted was  $21 \pm 2^\circ\text{C}$ .

**Table 4.7.** Reaction development in the rhodium(III)-catalyzed synthesis of pyrroles.<sup>a</sup>

Entry	Solvent	Temp.	Time (h)	Yield <sup>b</sup>
1	<i>t</i> -AmOH	60 °C	16	98(85)
2	<i>t</i> -AmOH	60 °C	4	93
3	<i>t</i> -AmOH	30 °C	24	37
4	acetone	21 °C	18	87(81)

<sup>a</sup>Conditions: **4.15a** (1 eq, 0.2 M), 1-phenylpropyne (1.1 eq),  $[\text{Cp}^*\text{Rh}(\text{MeCN})_3][\text{SbF}_6]_2$  (5 mol %),  $\text{Cu}(\text{OAc})_2 \cdot \text{H}_2\text{O}$  (20 mol %),  $\text{O}_2$  (balloon), solvent (specified above), temperature (specified above), time (specified above). <sup>b</sup>Yields are GCMS yields relative to trimethoxybenzene as an internal standard; isolated yields in parentheses.

**Reaction scope.** Investigation of the generality of the reaction with respect to the alkyne and enamide **4.15a** proved reasonably broad (Table 4.8). Internal alkynes symmetrically substituted with both alkyl (*n*-Pr) and aryl (Ph) groups provided trisubstituted pyrroles in good isolated yield (83% and 89%, respectively, Table 4.8, **4.16b** and **4.16c**). When alkyl/aryl substituted internal alkynes were employed good yields were obtained for the respective products with regioselectivity consistent with that previously observed by us and others.<sup>134</sup> Other aromatics, such as indole, may serve as the aryl moiety on the alkyne to provide unsymmetrical heterocyclic biaryls in good yield (70%, indole; Table 4.8, **4.16d**). More diverse functionality is also tolerated on the alkyl moiety of the alkyne. Propiolates are well tolerated (82%, **4.16e**), as well are protected propargyl alcohols (81%, **16f**), homopropargyl esters (79%, **4.16g**) and propargyl amines protected as a phthalimide (77%, **4.16h**) (Table 4.8). Additionally, as previously observed, enamide **4.15a** proved more reactive than acetanilide and thus reacted well with previously stubborn substrates. Silyl-substituted alkynes performed well in the reaction with no additional optimization, though isolation of the product was complicated by co-elution of an unidentified side-product from the column.

<sup>134</sup> Crawley, M. L.; Goljer, I.; Jenkins, D. J.; Mehlmann, J. F.; Nogle, L.; Dooley, R.; Mahaney, P. E. *Org. Lett.* **2006**, *8*, 5837.

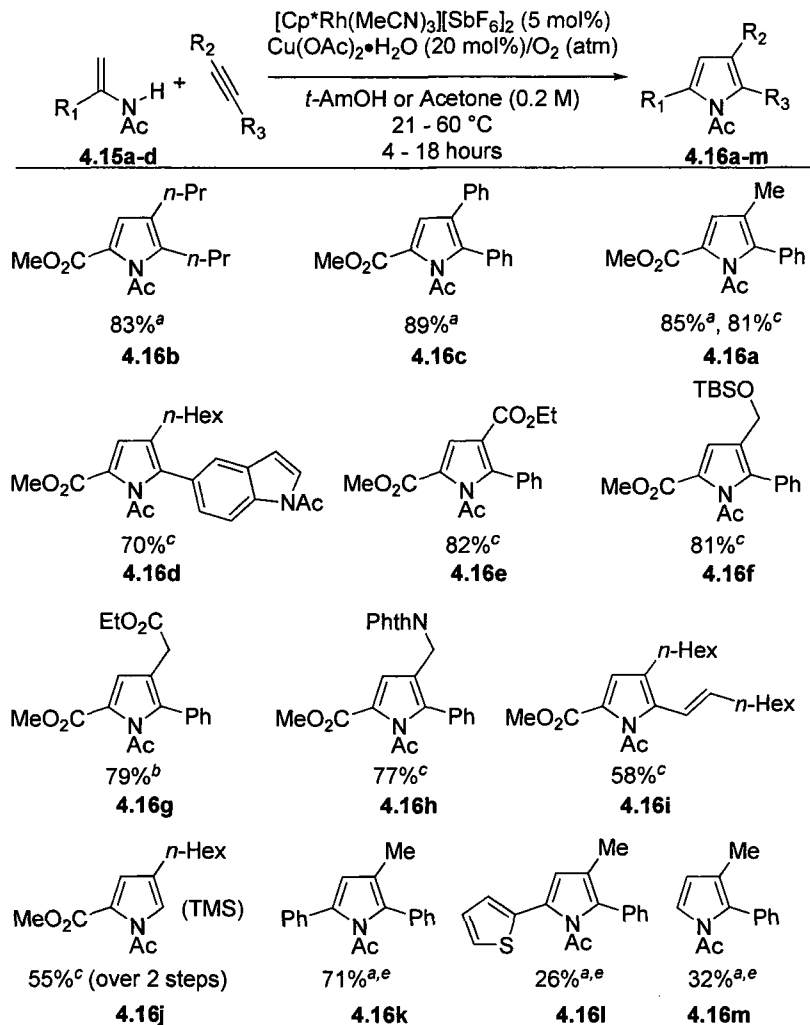
This was remedied by treatment of the crude reaction mixture with TBAF to cleave the TMS group *in situ*, providing the C4-alkylated pyrrole in 55% isolated yield over two steps (Table 4.8, **4.16j**). Alkylation of pyrrole by other means (Friedel-Crafts) typically takes place at the C2 position and therefore this represents a useful complimentary process to access this challenging substrate class. An enyne was also assessed as coupling partner with the goal of obtaining a pyrrole substituted regioselectively at the C2 and C3 position with differing alkyl groups (58%, **4.16i**). As with TMS-substituted alkynes, these alkynes proved to be much more compatible with enamides than with acetanilides as evidenced by the much better yield obtained in this case<sup>135</sup> (Table 4.8).<sup>130</sup> The regioselectivity of pyrrole **4.16i** and **4.16j** were both determined by 2-D NMR (COSY and NOESY).<sup>136</sup> Other trisubstituted pyrroles were investigated with phenyl-substituted enamide and when two equivalents of this enamide were employed a 71% isolated yield of the trisubstituted pyrrole was obtained (Table 4.8, **4.16k**). However, when the phenyl-substituent of the enamide was replaced by a thiophenyl-substituent under the same reaction conditions the yield was significantly reduced and the heterobiaryl was isolated in 26% yield (Table 4.8, **4.16l**). The preparation of this substrate class is being further investigated in our laboratory due to its applicability in materials chemistry. *N*-Vinylacetamide was also tested as a potential substrate to access 1,2-substituted pyrroles, a preparatively difficult substrate class. An isolated yield of 32% of the *N*-acetyl-2-methyl-1-phenylpyrrole **4.16m** was obtained. In these reactions complete consumption of the enamide was observed, even in reactions employing excess enamide. Further experiments to identify reaction parameters capable of coupling this specific enamide are underway in our laboratory.

---

<sup>135</sup> Compare 58% isolated yield for the pyrrole with 11% isolated yield for the indole (*vide supra*).

<sup>136</sup> Please see Chapter 5 (supporting information) for details.

**Table 4.8.** Reaction scope under optimized conditions.<sup>a</sup>



<sup>a</sup>Conditions: 4.15a-d (1 eq, 0.2 M), alkyne (1.1 eq), [Cp\*Rh(MeCN)<sub>3</sub>][SbF<sub>6</sub>]<sub>2</sub> (5 mol%), Cu(OAc)<sub>2</sub>·H<sub>2</sub>O (20 mol%), O<sub>2</sub> (balloon), *t*-AmOH, 60 °C, 16 hours. <sup>b</sup>Allowed to react for 4 hours. <sup>c</sup>Acetone used as the solvent at 21 °C for 18 hours. <sup>d</sup>Isolated yields given above. <sup>e</sup>Two equivalents of enamide used.

### 4.2.3. Synthesis of Paullone

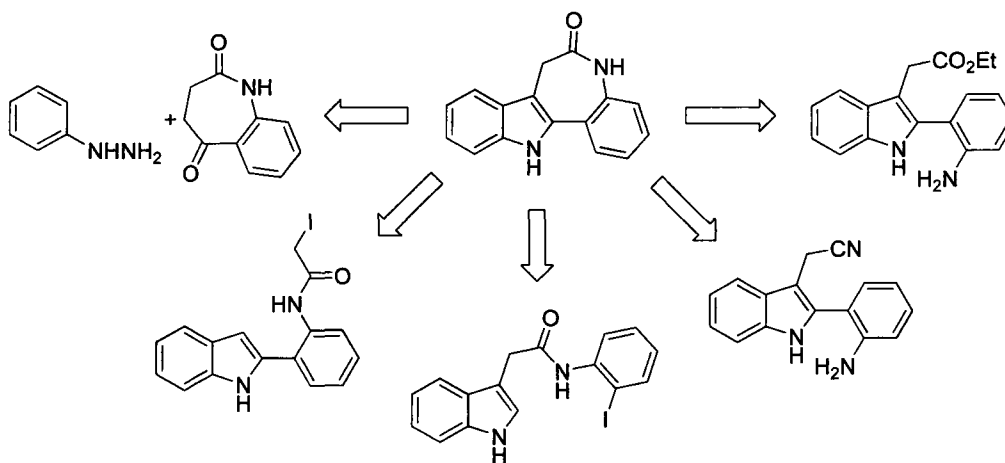
**General background.** Cyclin dependant kinases (CDK's) are key to the regulation of cell cycle progression and consequently deregulation of their activity has been closely linked to tumor growth.<sup>137</sup> As such, inhibitors of this class of kinase have been of great interest as therapeutic agents against cancer. The Paullone family of compounds was originally

<sup>137</sup> Sausville, E.A.; Zaharevitz, D.; Gussio, R.; Meijer, L.; Louarn-Leost, M.; Kunick, C.; Schultz, R.; Lahusen, T.; Headlee, D.; Stinson, S.; Arbuck, S.G.; Senderowicz, A. *Pharmacol. Ther.* **1999**, *82*, 285.



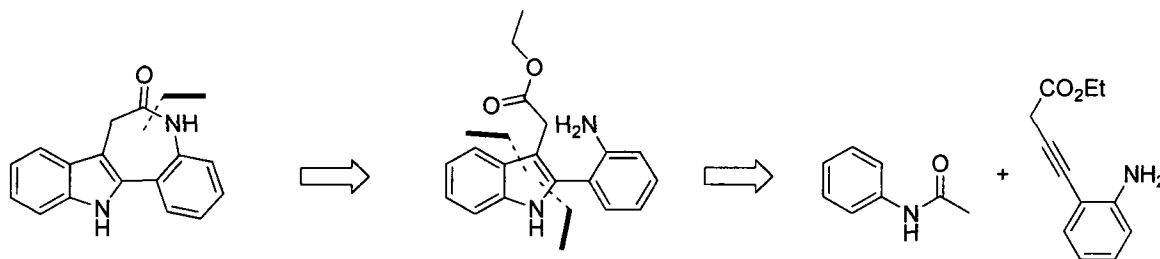
the construction of indoles with high regioselectivity would serve well in a cost effective and rapid synthesis of Paullone.

**Scheme 4.19.** Retrosynthetic avenues for the construction of the Paullone core.



**Retrosynthesis.** The high regioselectivity observed for the formation of C2-arylindoles and the high functional group compatibility observed in the rhodium-catalyzed coupling of acetanilides with internal alkynes prompted us to consider an efficient route to Paullone. This synthetic route employs fewer steps than the majority of other syntheses therefore increasing the efficiency with which the desired compound could be prepared. Additionally, the functional group compatibility enjoyed by the acetanilide and alkyne suggest that analogue synthesis would be readily facilitated by this path. The retrosynthetic route is displayed in Scheme 4.20. The azepine lactone could be closed by intramolecular nucleophilic addition of the aniline moiety on the pendant homo-benzylic ester following a literature procedure. The required indole could be formed by rhodium-catalyzed oxidative coupling of acetanilide with a functionalized internal alkyne.

**Scheme 4.20.** Our retrosynthetic analysis of the Paullone core.



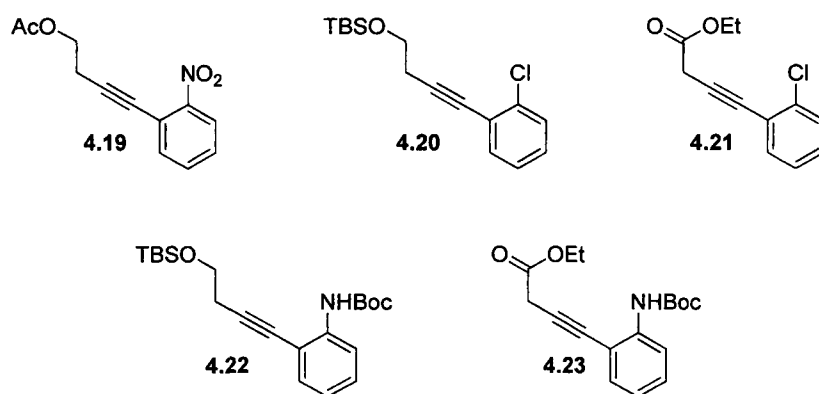
**Initial experiments to probe viability of retrosynthesis.** Initial experiments were conducted to probe potential functionality on the alkyne that could serve as homo-propargylic ester and aniline surrogates. A number of alkynes were prepared and tested under the second generation coupling conditions (Figure 4.4). A protected homo-propargylic alcohol was the simplest proxy for a homo-propargylic ester and was the first functional group tested in a number of alkynes (**4.19**, **4.20**, and **4.22**, Figure 4.4). A nitro group was investigated as a latent amino moiety. However, alkyne **4.19** failed to provide any of the desired indole under the second generation conditions.<sup>144</sup> An aryl chloride could be elaborated to an aniline *via* Buchwald-Hartwig amination and therefore this functionality was next put to the test (alkyne **4.20** and **4.21**, Figure 4.4). While these two alkynes provided the desired indole under the second generation conditions in 82% and 54% isolated yield, respectively all attempts to convert the chloride to an amino group failed.<sup>145</sup> A more direct route involved the use of protected aniline (alkyne **4.22** and **4.23**, Figure 4.4). The structural similarity of the NHBoc protected aniline to acetanilide represents a significant issue in chemoselectivity. Rhodium may be directed by either the carbonyl group of the acetanilide or the Boc-protected aniline; however, control experiments showed that the NHBoc group does not participate in the reaction and furthermore that it does not inhibit the reactivity of the acetanilide. Additionally, alkyne **4.22** participated well in the reaction under the second generation conditions to provide the desired indole in 79% isolated yield. Unfortunately, this route suffered from issues of protecting group manipulations and was also plagued with additional redox steps in the oxidation of the homo-benzylic alcohol to the homo-benzylic ester. The most direct route would employ alkyne **4.23** adorned with an *N*-Boc-protected

<sup>144</sup> Control experiments revealed that it was the nitro group that inhibited product formation not the acetyl-protected homo-propargylic alcohol.

<sup>145</sup> De-acetylation of the indole was the major product isolated from these reactions.

aniline and a homo-propargylic ester, which, after deprotection, marriage of these two groups would provide the azepine lactone ring. Gratifyingly, alkyne **4.23** performed well in the reaction under the second generation conditions producing the desired indole in 71% isolated yield. Thus, **4.23** was chosen as the alkyne which would be utilized in the synthesis of Paullone.

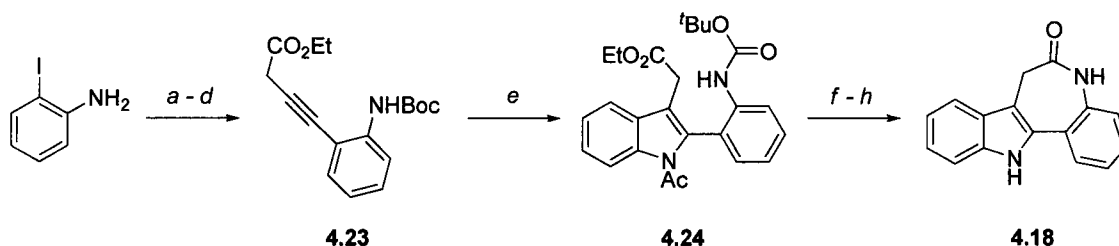
**Figure 4.4.** Potential alkynes for the synthesis of Paullone.



**Synthesis of Paullone.** Preparation of the internal alkyne, **4.23**, was carried out over 4 steps with only one chromatographic purification. The amino-group of *ortho*-iodoaniline was protected as its *N*-boc derivative in essentially quantitative yield, and the crude product may be used directly for further manipulations. A palladium-catalyzed Sonagashira reaction followed this in order to couple trimethylsilylacetylene and *ortho*-iodo-*N*-bocaniline. The crude TMS-protected alkyne was subjected to the action of TBAF to provide the free terminal alkyne to be used crude in a copper-catalyzed coupling with ethyl diazoacetate. This 4 step sequence provided internal alkyne **4.23** in an overall yield of 46% and featured only chromatographic purification after the fourth step. The key indole forming step was then accomplished by an oxidative coupling of acetanilide and internal alkyne **4.23** to furnish the highly functionalized indole **24** in 71% isolated yield. It was then found that the order of protecting group manipulations was essential for successful completion of the synthesis. Treatment of the **4.24** with TFA smoothly removed the *N*-Boc protecting group; however, it was observed that the acetyl group was transposed to the aniline moiety when treated with the basic conditions necessary for deacetylation. Thus, the acetyl group was first removed

under basic conditions followed by exposure of the crude reaction mixture to trifluoroacetic acid to cleave the *N*-Boc-group from the aniline moiety. The final azepine ring closure was carried out on the globally deprotected indole by treatment of the crude product with DBU in DMF at 150°C to provide Paullone in 33% isolated yield over the final three steps.<sup>146</sup> The overall synthetic sequence employs 8 distinct steps with need for only 3 chromatographic purifications in which the target molecule may be isolated in an overall yield of 11% (average of 76% yield/step).

**Scheme 4.21.** Final synthetic route to Paullone.



<sup>a</sup>Conditions: (a) *ortho*-iodoaniline (1 eq, 0.34 M), Boc<sub>2</sub>O (1 eq), NaHMDS (2 eq), THF, r.t., 2 hours. (b) trimethylsilylacetylene (1 eq, 1 M), Pd(PPh<sub>3</sub>)<sub>2</sub>Cl<sub>2</sub> (3 mol%), CuI (6 mol%), NEt<sub>3</sub> (4 eq), DMF, 50 °C, 3 hours. (c) TBAF (1.2 eq, 0.4 M), THF, 0 - 25 °C, 2 hours. (d) Ethyl diazoacetate (1.05 eq, 0.8 M), CuI (10 mol%), MeCN, r.t., 12 hours. (e) acetanilide (1 eq, 0.2 M), **4.23** (1.1 eq), [Cp\**Rh*(MeCN)<sub>3</sub>][SbF<sub>6</sub>]<sub>2</sub> (5 mol%), Cu(OAc)<sub>2</sub>·H<sub>2</sub>O (20 mol%), *t*-AmOH, 60 °C, 20 hours. (f) K<sub>2</sub>CO<sub>3</sub> (10 eq), MeOH : DCM (1 : 1), r.t., 12 hours. (g) TFA (0.1 M), r.t., 30 min. (h) DBU (1.2 eq), DMF (0.1 M), 150 °C, 19 hours.

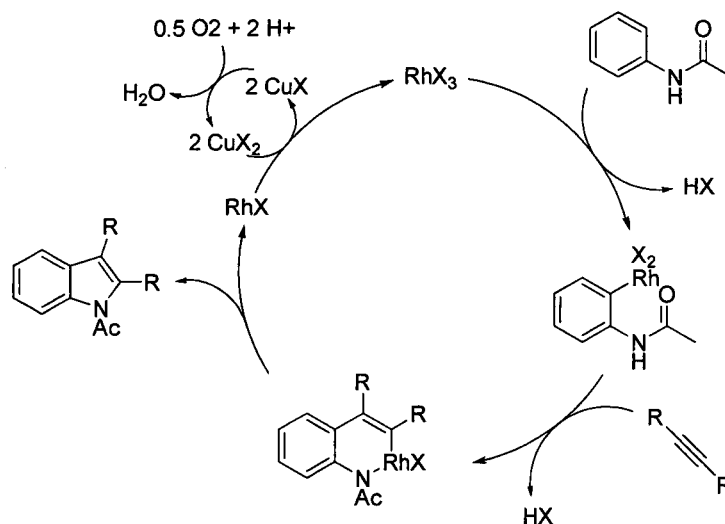
#### 4.2.4. Kinetic and Mechanistic Analysis of the Rhodium(III)-Catalyzed Annulation of Acetanilides with Internal Alkynes.

**Mechanistic overview.** Literature precedent suggests a number of possible mechanisms for the annulation of acetanilides with internal alkynes and a basic catalytic cycle representing these possibilities is presented in Scheme 4.22.<sup>111</sup> An in-depth mechanistic investigation was conducted to identify the most relevant mechanistic scenario and to address the current limitations of the methodology. The mechanism of the reaction was probed by kinetic analysis (determination of the order of reagents), isotopic labeling, and

<sup>146</sup> Please see Chapter 5 (supporting information) for characterization data of all intermediates in the synthesis. Literature references for the following steps of Scheme 4.21, please see: step (a) Kelly, T. A.; McNeil, D. W. *Tetrahedron Lett.* **1994**, *35*, 9003. Step (b) Hiroya, K.; Itoh, S.; Sakamoto, T. *J. Org. Chem.* **2004**, *69*, 1126. Step (c) Mitsumori, S.; Tsuru, T.; Honma, T.; Hiramatsu, Y.; Okada, T.; Hashizume, H.; Inagaki, M.; Arimura, A.; Yasui, K.; Asanuma, F.; Kishino, J.; Ohtani, M. *J. Med. Chem.* **2003**, *46*, 2436. Step (d) Suárez, A.; Fu, G. C. *Angew. Chem. Int. Ed.* **2004**, *43*, 3580. Step (h) please see: Henry, N.; Blu, J.; Bénétou, V.; Mérour, J.-Y. *Synthesis* **2006**, 3895.

free-energy correlations. The absence of an induction period enabled the use of the method of initial rates to obtain the majority of the kinetic information.

**Scheme 4.22.** Basic mechanism for the annulation of acetanilides with internal alkynes.

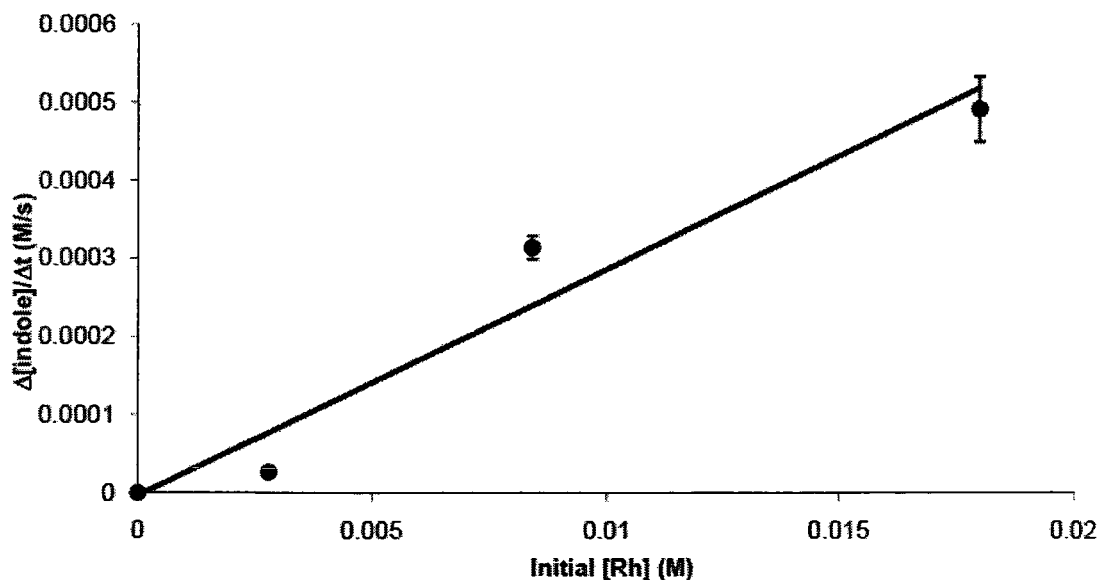
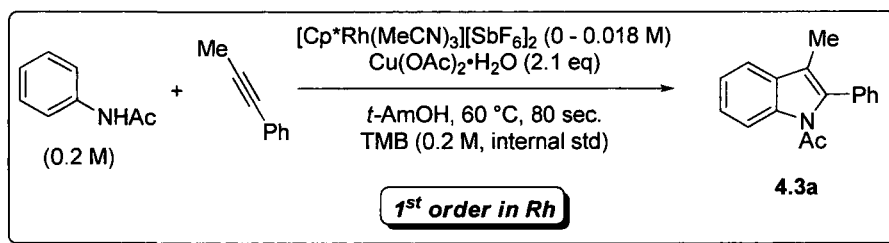


**Order of reagents.** Our analysis of the reaction mechanism commenced with the determination of the order of each of the primary reaction components (catalyst, acetanilide, alkyne, and oxidant). As previously mentioned the method of initial rates was used and for ease of reaction set up and analysis the following procedure was carried out. The acetanilide, alkyne, oxidant (copper(II) acetate), internal standard (trimethoxybenzene) and solvent (*t*-AmOH) were added to a vial which was sealed and heated to 60 °C for ~ 2 minutes to ensure complete dissolution of the acetanilide (note: copper(II) acetate was not completely soluble at this temperature). An acetone solution of [Cp\**Rh*(MeCN)<sub>3</sub>][SbF<sub>6</sub>]<sub>2</sub> was added *via* microsyringe to initiate the reaction and signify time zero ( $t = 0$ ). Aliquots (~ 10 – 20 μL) were then removed at 20 second intervals for the first 80 seconds of the reaction (~ 10% conversion). Each aliquot was diluted with ethyl acetate and extracted with a saturated solution of ammonium chloride to remove inorganic materials. The organic layer was then analyzed by GCMS and the relative concentration of indole formed was determined from a calibration curve (see Chapter 5 – Supporting Information for more details). The slope of the concentration versus time plot provided the initial rate (M/s) of the reaction and this was

done for at least four different concentrations of each reagent. The initial rate (M/s) was plotted against the initial concentration (M) to reveal the order of the reaction in each reagent.

When this procedure was carried out with varying concentrations of  $[\text{Cp}^*\text{Rh}(\text{MeCN})_3][\text{SbF}_6]_2$  a linear plot of initial rate versus initial concentration was obtained indicating that the reaction was *first order in rhodium* (Figure 4.5). As expected, this implies that one molecule of the rhodium catalyst is involved in the rate determining step of the catalytic cycle.

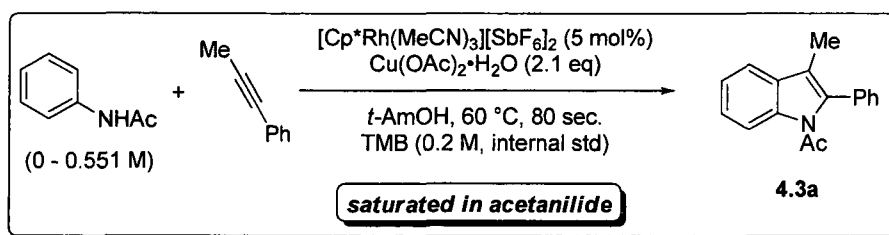
**Figure 4.5.** Initial rate versus initial concentration of rhodium.



Analysis of the dependence of the initial reaction rate on the concentration of acetanilide revealed an initial first order dependence followed by a plateau region and the data adhered to an equation describing simple saturation kinetics (Figure 4.6). A Lineweaver-Burke plot was obtained by taking the initial portion of the data in Figure 4.6

and plotting the inverse of both the initial rate and the concentration; a linear plot thus confirms the compliance of the reaction profile to saturation kinetics (Figure 4.7). These first two pieces of data together point toward a rate limiting step involving both catalyst and acetanilide, and further the observed saturation in acetanilide concentration supports a pre-equilibrium between this species and the catalyst. The potential reversibility of the cyclorhodation was probed by an isotopic labeling experiment as shown in Scheme 4.23. When acetanilide- $d_5$  was subjected to the first generation reaction conditions and the reaction allowed to proceed to  $\sim 50\%$  conversion a significant loss of deuterium was observed in the remaining starting material (Scheme 4.23). This data confirms a reversible rhodation of acetanilide.

**Figure 4.6.** Initial rate versus initial concentration of acetanilide.



$$\text{Data fit to: } y = \frac{ax}{bx + c}$$

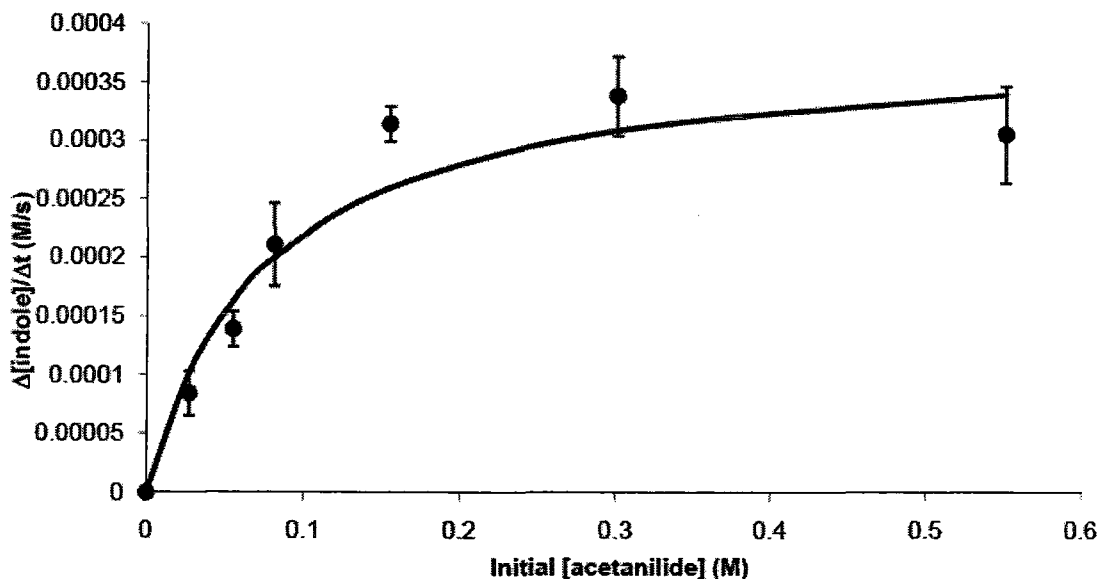
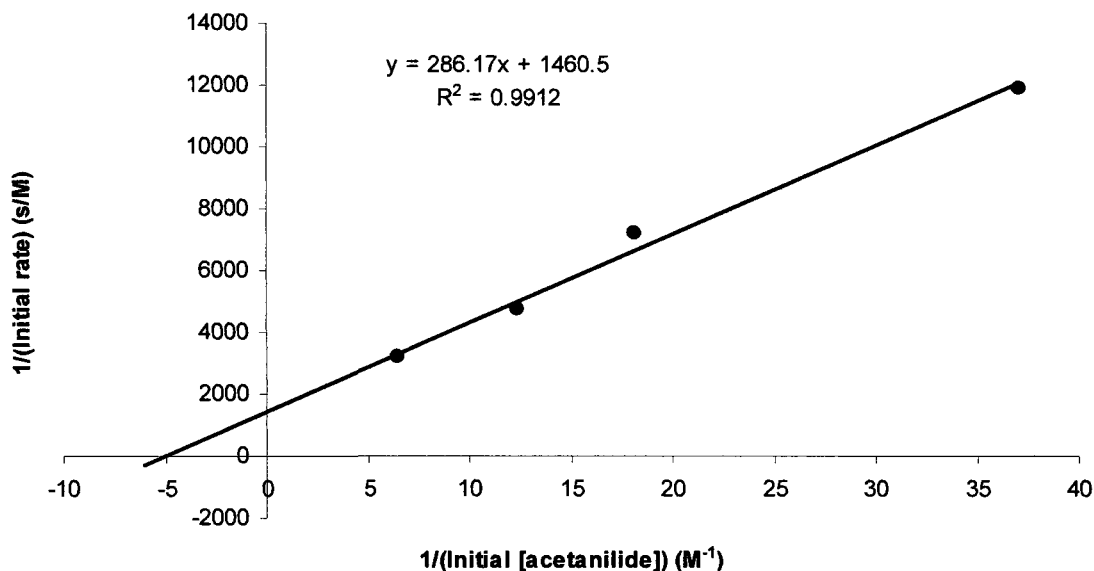
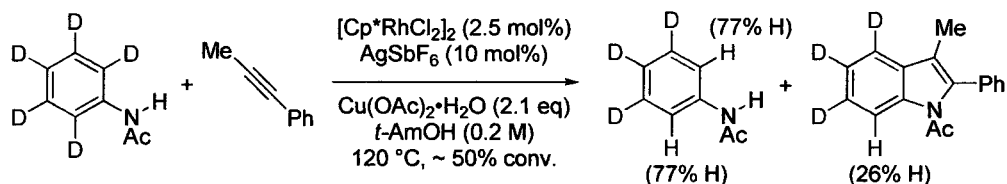


**Figure 4.7.** Lineweaver-Burke plot acetanilide concentration.



**Scheme 4.23.** Investigating the reversibility of acetanilide cyclorhodation.



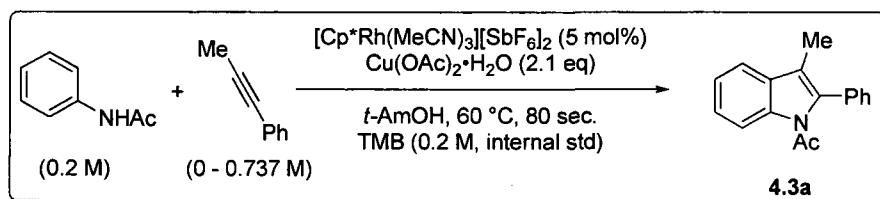
A more complex situation was observed when the initial rate was measured for a number of initial concentrations of alkyne (Figure 4.8). Upon initial addition of alkyne an increase in reaction rate is observed, however at high alkyne concentration (~ 20 : 1, alkyne : rhodium) the plot shows an inhibition of the rate of reaction. The data set was fit to the equation above the graph (depicted by the curve in Figure 4.8). A similar relationship between reaction rate and pyridine or triethylamine concentration has been observed by Stahl<sup>147</sup> and Sigman,<sup>148</sup> respectively, for the palladium catalyzed aerobic oxidation of alcohols. Each of the authors attributes this relationship to a pre-equilibrium involving the

<sup>147</sup> Steinhoff, B. A.; Guzei, I. A.; Stahl, S. S. *J. Am. Chem. Soc.* **2004**, *126*, 11268.

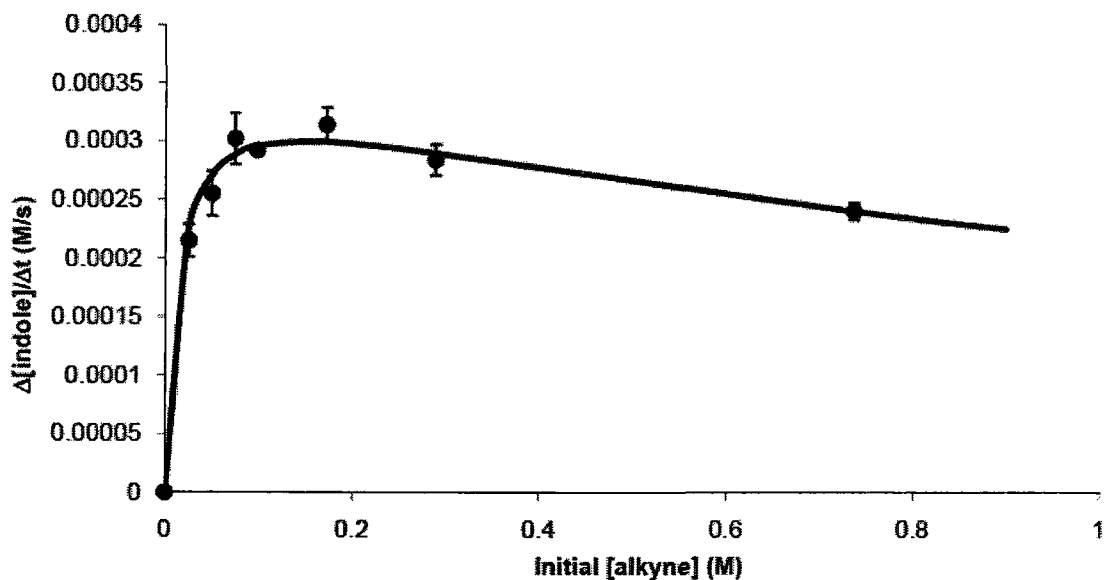
<sup>148</sup> Schultz, M. J.; Adler, R. S.; Zierkiewicz, W.; Privalov, T.; Sigman, M. S. *J. Am. Chem. Soc.* **2005**, *127*, 8499.

formation of palladium-amine coordination complexes of varying stoichiometry (Scheme 4.24). The excellent fit of the experimental data to the aforementioned equation strongly suggests that a similar scenario may be operative in this case as well, though at this time it is speculative as to which rhodium species may undergo cyclorhodation of the acetanilide. Experimental evidence for this will be elaborated on in a subsequent section (*vide infra*).

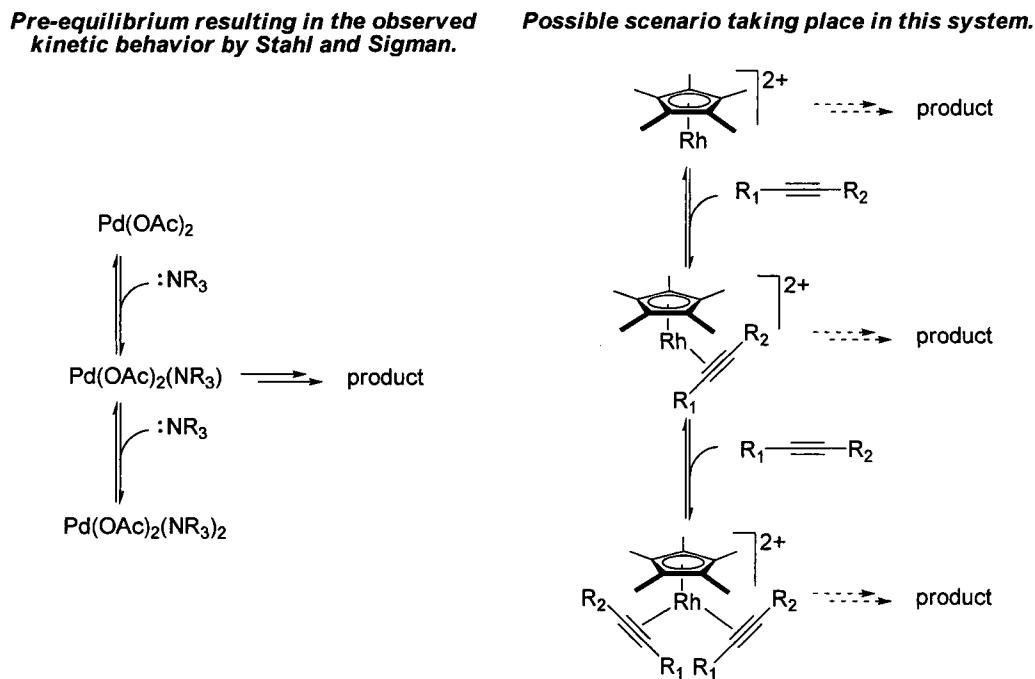
**Figure 4.8.** Initial rate versus initial concentration of alkyne.



$$\text{Data fit to: } y = \frac{ax}{bx^2 + cx + d}$$

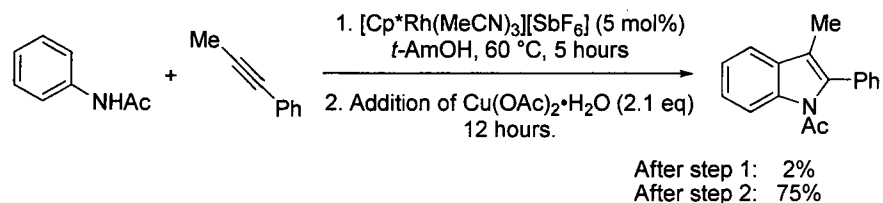


**Scheme 4.24.** Literature precedent and rationale for the kinetic behavior observed for alkynes.



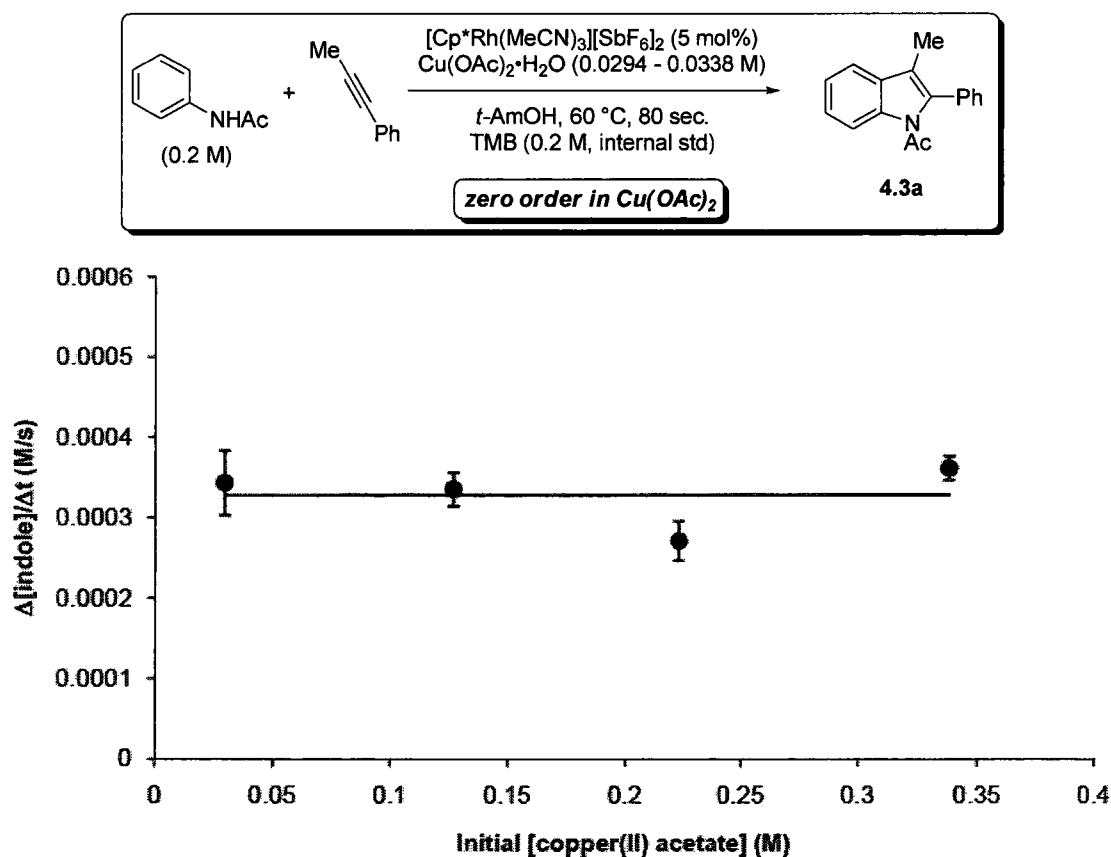
Finally, the dependence of the reaction rate on the oxidant, copper(II) acetate, concentration was investigated. The linear plot with a slope of zero indicates that the rate of the reaction is independent of oxidant concentration and suggests that copper does not play a role in the formation of the indole product and therefore should not appear in the rate law (Figure 4.9). Furthermore, though Jones has proposed an oxidatively induced reductive elimination of rhodacycles mediated by copper(II) in the formation of isoquinoline salts<sup>111d</sup> independent experimentation found that this was not operative in this case (Scheme 4.25). Under modified

**Scheme 4.25.** Investigation of an oxidatively induced reductive elimination.



first generation conditions, in the absence of copper(II) acetate, formation of product is still observed thus obviating the need for copper(II) in this process. However, catalyst re-oxidation does not take place and so the yield remains below the catalyst loading (5%) until the addition of copper(II) acetate, at which time the yield is increased to 75% (GCMS yield).

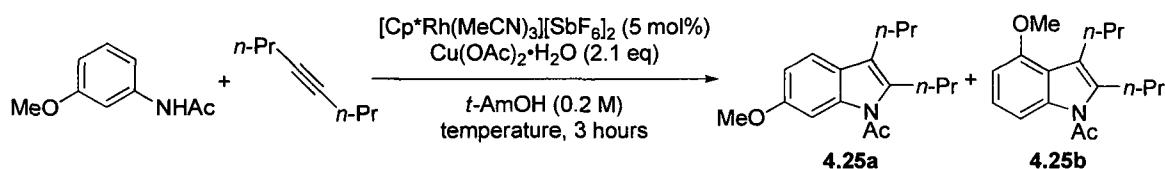
**Figure 4.9.** Initial rate versus initial concentration of copper(II) acetate.



**Mechanistic implications in acetanilide regioselectivity.** An area of significant interest to us is the ability to selectively obtain one (or very high levels of a) single regioisomer at the acetanilide in cases where regioselectivity may be an issue. It was previously observed that the reaction was extremely sensitive to sterics as 3,5-dimethylacetanilide provided only 7% isolated yield of the desired indole and that 3-methylacetanilide reacted to provide only a single acetanilide regioisomer (Table 4.3, **4.3h**

and **4.3k**). These results are in accord with those described by Jones in the cyclorhodation of *N*-phenyl benzaldimine.<sup>111e</sup> However, when other less sterically encumbered substituents, such as methoxy and fluoro, were present in the 3-position on the acetanilide mixtures of regioisomers resulted. A number of different reaction parameters (temperature, alkyne structure, and alkyne concentration) were examined in order to determine how the regioselectivity maybe influenced. We also reasoned that gaining an understanding of the effect of the alkyne on acetanilide regioselectivity may provide insight as to the specific rhodium species involved in the cyclorhodation of acetanilide (*vide supra*).

**Table 4.9.** Effect of temperature on acetanilide regioselectivity.<sup>a</sup>



Entry	Temperature (°C)	Ratio (4.25a : 4.25b) <sup>b</sup>
1	60	10 : 1
2	70	9.8 : 1
3	80	10.1 : 1
4	90	10.1 : 1
5	100	9.9 : 1
6	110	10.4 : 1
7	120	10.9 : 1

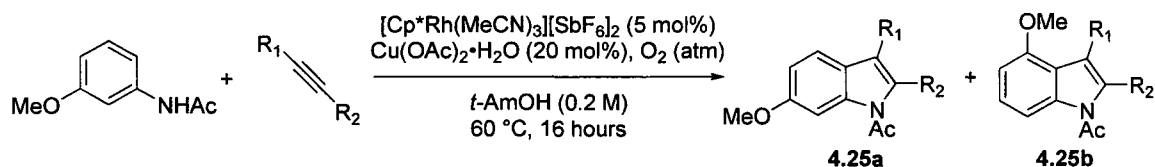
<sup>a</sup>Conditions: acetanilide (0.1 mmol, 0.2 M, 1 eq), alkyne (0.11 mol, 1.1 eq), [Cp<sup>\*</sup>Rh(MeCN)<sub>3</sub>][SbF<sub>6</sub>]<sub>2</sub> 5 mol%, Cu(OAc)<sub>2</sub>·H<sub>2</sub>O (0.21 mmol, 2.1 eq), *t*-AmOH, temperature (see above), 3 hours. <sup>b</sup>Ratio determined by <sup>1</sup>H NMR spectroscopy (average of 3 runs).

When 3-methoxyacetanilide was reacted with 4-octyne under slightly modified reaction conditions over a wide temperature range (60 – 120°C) essentially no change in regioselectivity was observed (Table 4.9)<sup>149</sup> and therefore precluded the opportunity to obtain thermodynamic parameters, such as  $\Delta\Delta G^\ddagger$ ,  $\Delta\Delta H^\ddagger$  and  $\Delta\Delta S^\ddagger$ .

<sup>149</sup> This reflects the results observed by Jones in the cyclorhodation and iridation of *N*-phenyl benzaldimine. Please see ref. 17e.

When acetanilide regioselectivity was, however, investigated with respect to both the identity and relative concentration of the alkyne an interesting relationship which has direct mechanistic consequences was discovered. The identity of the alkyne influenced the acetanilide regioselectivity such that increasing the steric bulk of the alkyne (Me(*A*-value = 1.74) → Ph(*A*-value = 2.8))<sup>150</sup> reduced the occurrence of reaction at the more sterically accessible position (Table 4.10). Thus, this steric requirement dictates that the rhodium species that undergoes cyclorhodation of acetanilide is not coordinated by an alkyne, and therefore is the species [Cp\*Rh<sup>(III)</sup>]. This also suggests that the regioselectivity at the acetanilide is governed by the relative rates of the reversibility of cyclorhodation and alkyne insertion ( $k_3, k_{-3}, k_{3'}, k_{-3'}, k_4, k_{4'}$ ). In this way, the diaryl substituted alkyne reacts much faster than the dialkyl substituted alkyne such that  $k_4, k_{4'} \gg k_{-3}, k_{-3'}$ , and therefore the product regioselectivity more closely reflects the original acetanilide metallation regioselectivity or rather the ratio of  $k_3/k_{3'}$ . (Scheme 4.26). To test the hypothesis that aryl substituted alkynes react faster than alkyl substituted alkynes a competition experiment was performed in which 4-octyne, **4.26**, and 1,2-diphenylacetylene, **4.27**, were added to the same reaction flask and the product distribution determined by GCMS (Scheme 4.27). A 3:1 ratio of the **4.28** : **4.29** was observed confirming that aryl substitution on the alkyne induces faster reaction with the rhodacycle than alkyl substitution.

**Table 4.10.** Effect of alkyne identity on acetanilide regioselectivity.

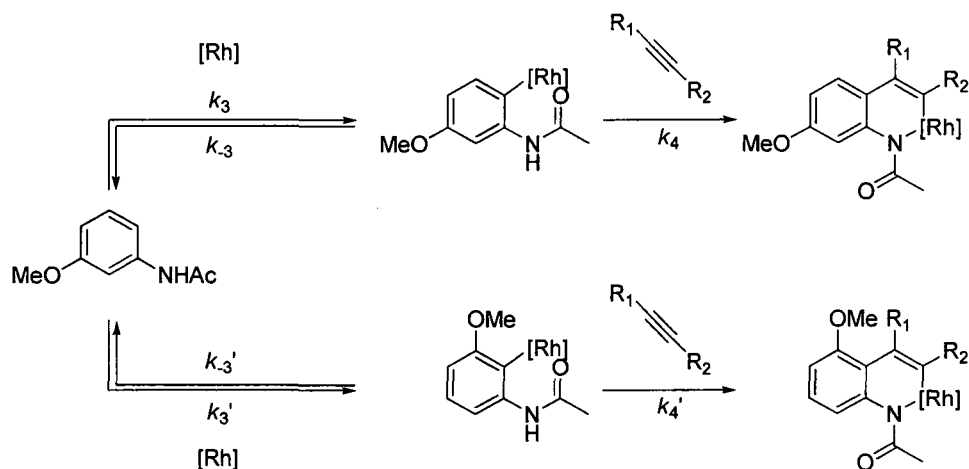


Entry	R <sub>1</sub>	R <sub>2</sub>	Ratio ( <b>4.25a</b> : <b>4.25b</b> ) <sup>b</sup>
1	<i>n</i> -Pr	<i>n</i> -Pr	9.4 : 1
2	Me	Ph	4.8 : 1
3	Ph	Ph	3.1 : 1

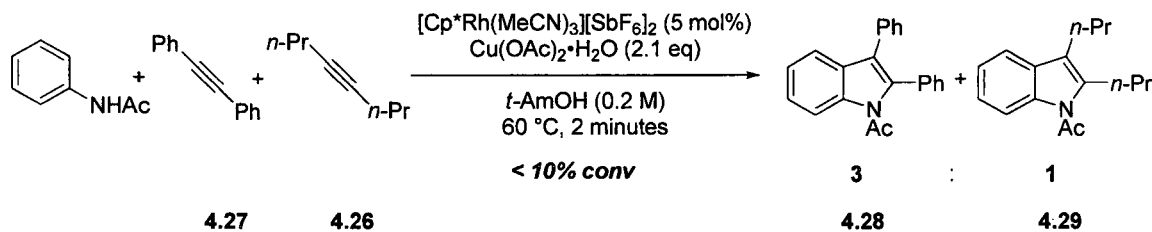
<sup>a</sup>Conditions: acetanilide (0.1 mmol, 0.2 M, 1 eq), alkyne (0.11 mol, 1.1 eq), [Cp\*Rh(MeCN)<sub>3</sub>][SbF<sub>6</sub>]<sub>2</sub> (5 mol%), Cu(OAc)<sub>2</sub>·H<sub>2</sub>O (20 mol%), *t*-AmOH, O<sub>2</sub> (atm) 60 °C, 16 hours. <sup>b</sup>Ratio determined by <sup>1</sup>H NMR spectroscopy (average of 3 runs).

<sup>150</sup> Anslyn, E.; Dougherty, D. A. *Modern Physical Organic Chemistry* (University Science Books, 2006).

**Scheme 4.26.** Mechanistic rationale for alkyne influence over acetanilide regioselectivity.



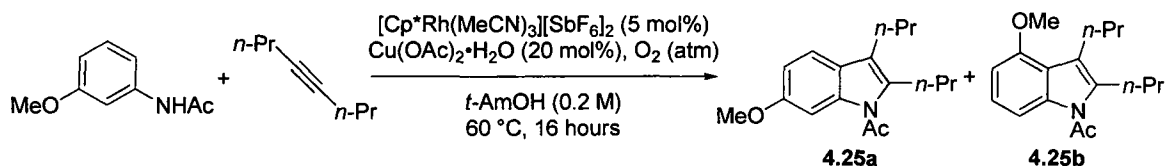
**Scheme 4.27.** Competition experiment between electronically different alkynes.



Additionally, the influence of the alkyne concentration on acetanilide regioselectivity was explored over a range of 0.3 – 9 equivalents of alkyne relative to acetanilide. It was found that when a large excess of alkyne was present the regioselectivity at acetanilide dropped significantly (compare entries 1 and 9, Table 4.11). Again, this behavior reflects a mechanistic scenario in which the regioselectivity is decreased when  $k_4, k_4' \gg k_3, k_3'$  as would be the case at high alkyne concentration (Scheme 4.26). Thus, the regioselectivity of the acetanilide is governed by Curtin-Hammett kinetics. These observations may assist in the development of reaction conditions capable of providing high yields of a single regioisomer in cases plagued by low regioselectivity by maintaining a low alkyne concentration *via* syringe pump addition. Additionally, these observations provide mechanistic insight in that the rhodium species that undergoes cyclometallation is

[Cp\*Rh<sup>(III)</sup>] and that the rhodacycle undergoes alkyne coordination followed by 1,2-migratory insertion of the carbon-rhodium bond across the alkyne.

**Table 4.11.** Influence of alkyne equivalents on acetanilide regioselectivity.



Entry	Alkyne equivalents	Ratio (4.25a : 4.25b) <sup>b</sup>
1	0.3	13.3 : 1
2	0.6	11.9 : 1
3	1.1	10.5 : 1
4	3.0	9.7 : 1
5	6.0	8.9 : 1
6	9.0	3.2 : 1

<sup>a</sup>Conditions: acetanilide (0.1 mmol, 0.2 M, 1 eq), alkyne (0.11 mol, 1.1 eq), [Cp\*Rh(MeCN)<sub>3</sub>][SbF<sub>6</sub>]<sub>2</sub> (5 mol%), Cu(OAc)<sub>2</sub>·H<sub>2</sub>O (20 mol%), O<sub>2</sub> (atm), *t*-AmOH, 60 °C, 16 hours. <sup>b</sup>Ratiodetermined by <sup>1</sup>H NMR spectroscopy.

**Isolation and characterization of a reaction side product.** Over the course of reaction optimization, certain solvents<sup>151</sup> gave rise to a significant side product **4.30** with a mass of 251 amu, as observed in the GCMS trace (Scheme 4.28). The target indole of our optimization had a mass of 249 amu and so it was postulated that this side product may be a reaction intermediate *en route* to the product. Isolation and subsection of **4.30** to structural inspection by 1D NMR spectroscopic (<sup>1</sup>H and <sup>13</sup>C NMR) means revealed the general carbon framework and relative number of chemically and magnetically inequivalent protons and carbons. The regioselectivity and stereochemistry of **4.30** was revealed by 2D NMR spectroscopy (COSY, Figure 4.10 and NOESY, Figure 4.11). Correlation between the broad singlet at 2.19 ppm and the broad singlet at 6.49 ppm in the COSY spectrum (D in Figure 4.10) of **4.30** revealed that these two signals couple to one another with a very small coupling constant owing to the broad nature of the peaks. Additionally, this correlation

<sup>151</sup> The solvents in which the side product was observed the most were the chlorinated solvents, dichloroethane and dichloromethane.

differentiates the two upfield singlets and allows assignment of the singlet at 2.11 ppm as the acetyl methyl group, the singlet at 2.19 ppm as the allylic methyl group, as well as the singlet at 6.49 ppm as the vinylic proton. Most informative in the NOESY spectrum (Figure 4.11) were the correlations between the allylic methyl group and the doublet at 7.19 ppm (C, Figure 4.11) as well as the multiplet at 7.37 ppm (A, Figure 4.11). Further confirmation of the regio- and stereochemistry in **4.30** was the correlation between the vinylic proton at 6.49 ppm and the multiplet at 7.37 ppm (D, Figure 4.11).

**Scheme 4.28.** Potential structures of the observed side product.

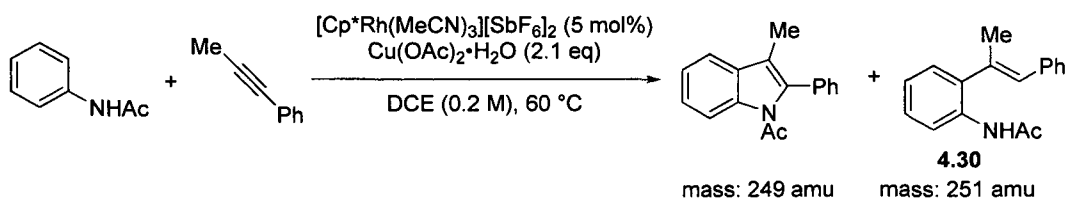


**Figure 4.10.** COSY Correlations of Compound **4.30**.

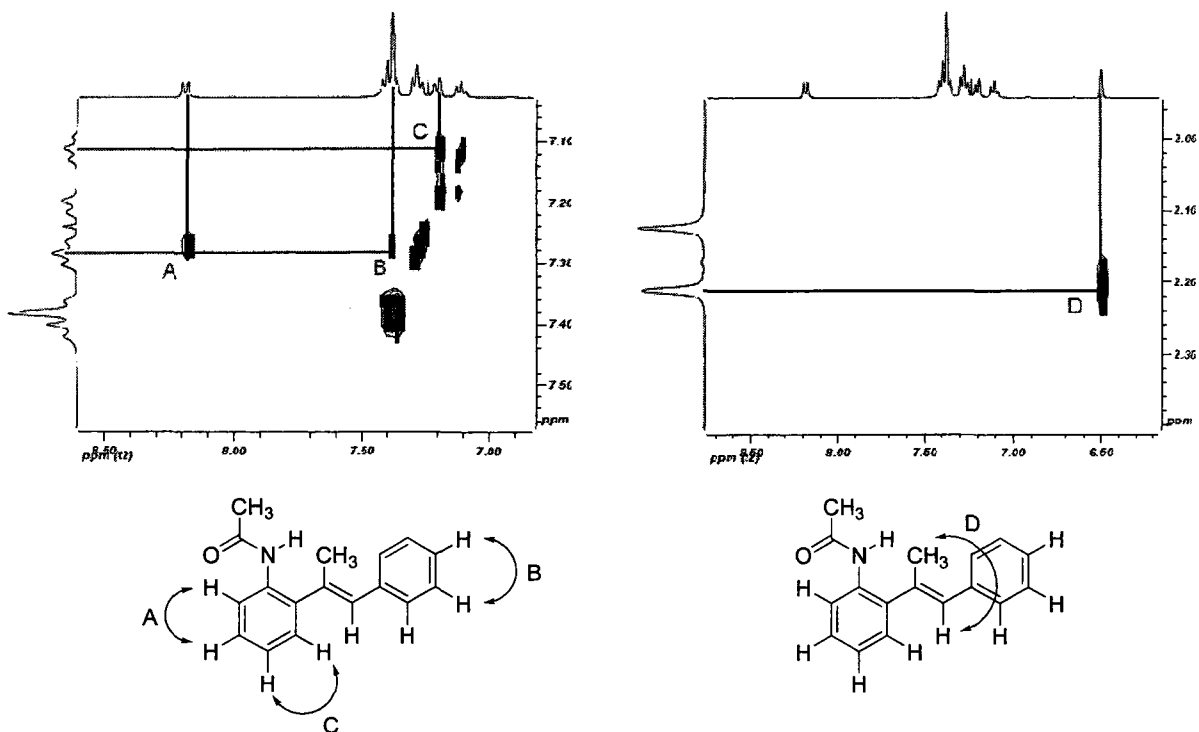
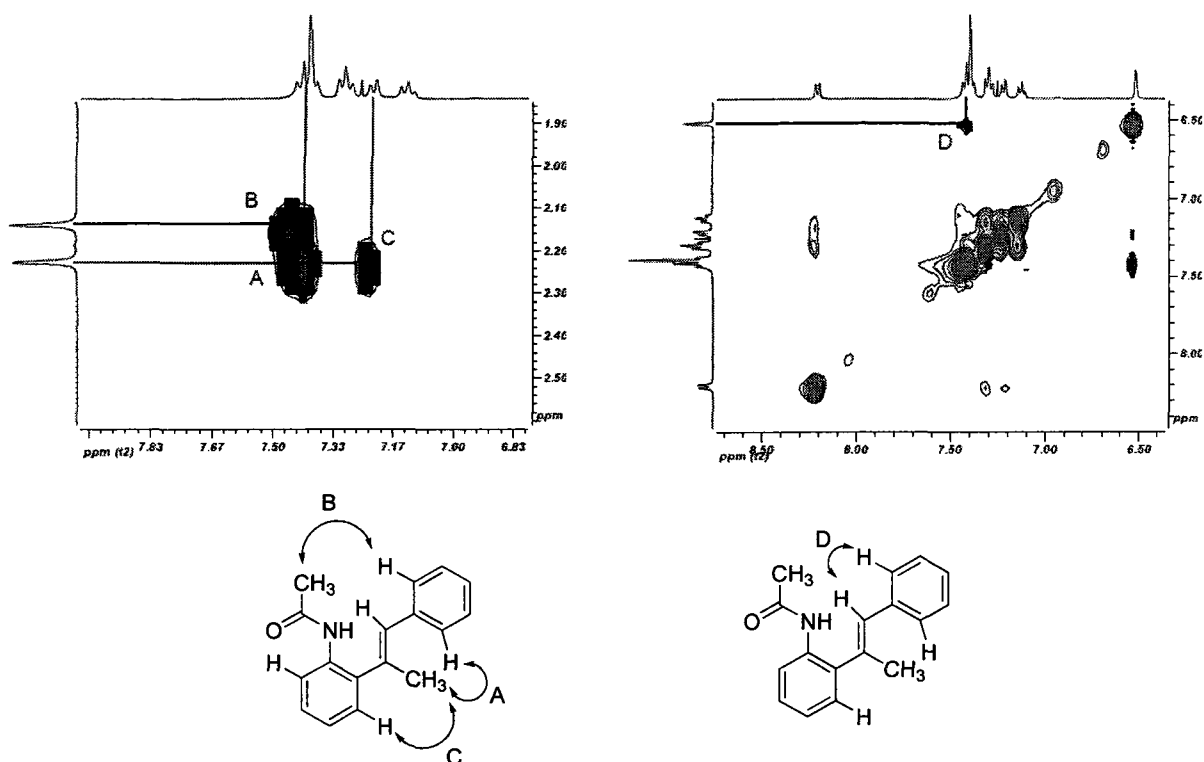
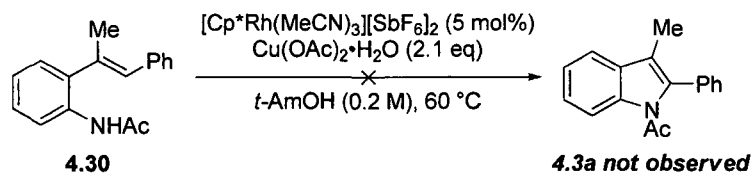


**Figure 4.11.** NOESY Correlations of Compound **4.30**.

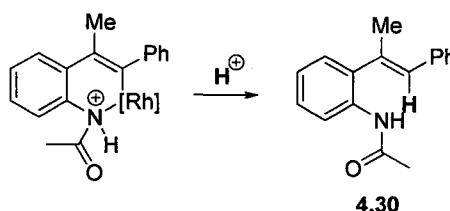


Having established the structural identity of the isolated side product it was realized that this compound may not be an innocent side product but rather a productive intermediate in the catalytic cycle. To test this hypothesis a sample of **4.30** was placed under the optimized reaction conditions and it was found that no indole product was observed. Thus, **4.30** may be considered to form in the catalytic cycle as a side product but not go on to generate the desired indole. However, we were interested in the mechanism of formation of **4.30** and that it was formed in greater quantities in certain solvents, namely the chlorinated solvents dichloroethane and dichloromethane. Chlorinated solvents are known to decompose to form HCl and therefore the increased acidity of these solvents may promote protoderhodation of a productive organometallic intermediate in the catalytic cycle (Scheme 4.30).

**Scheme 4.29.** Testing the hypothesis that **4.30** is an intermediate in the catalytic cycle.

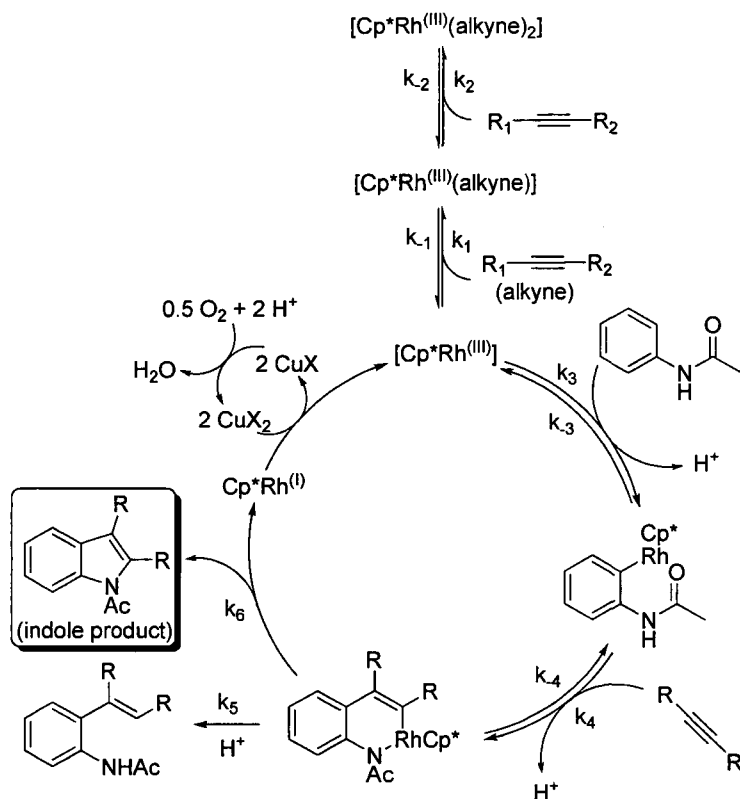


**Scheme 4.30.** Proposed formation of **4.30** via proto-derhodation.



**Derivation of a rate law and experimental and simulated verification.** Based on the experimental data describing the contribution of each of the primary reaction components to the rate of reaction, the isolation and structural characterization of a “hydroarylation” side product, and the effect of alkyne on acetanilide regioselectivity, the following catalytic cycle is proposed (Scheme 4.31). Linked with this mechanistic proposal is one caveat – the reversibility of the alkyne insertion ( $k_4/k_{-4}$ ) on the acetanilide derived rhodacycle. While this step is likely not reversible, the assumption was made to aid in the derivation of a rate law and it was found through simulation of the data that this admonition was inconsequential (*vide infra*). Thus, the following rate law was derived from the catalytic cycle and is consistent with all experimental data thus far obtained.

**Scheme 4.31.** Proposed catalytic cycle based on experimental evidence.



rate

$$= \frac{k_6 K_{eq4} K_{eq3} [Rh]_t [acetanilide] [alkyne]}{[acid]^2 (1 + K_{eq1} [alkyne] + K_{eq2} K_{eq1} [alkyne]^2 + K_{eq3} \frac{[acetanilide]}{[acid]} + K_{eq4} K_{eq3} \frac{[acetanilide] [alkyne]}{[acid]^2})}$$

$$rate_{Rh} = a[Rh]_t + b$$

$$rate_{acetanilide} = \frac{a[acetanilide]}{b[acetanilide] + c}$$

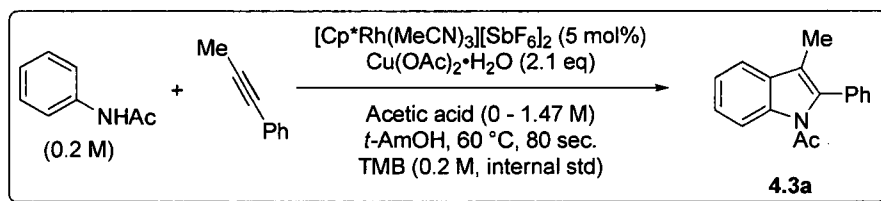
$$rate_{alkyne} = \frac{a[alkyne]}{b[alkyne]^2 + c[alkyne] + d}$$

$$rate_{acid} = \frac{a}{b[acid]^2 + c[acid] + d}$$

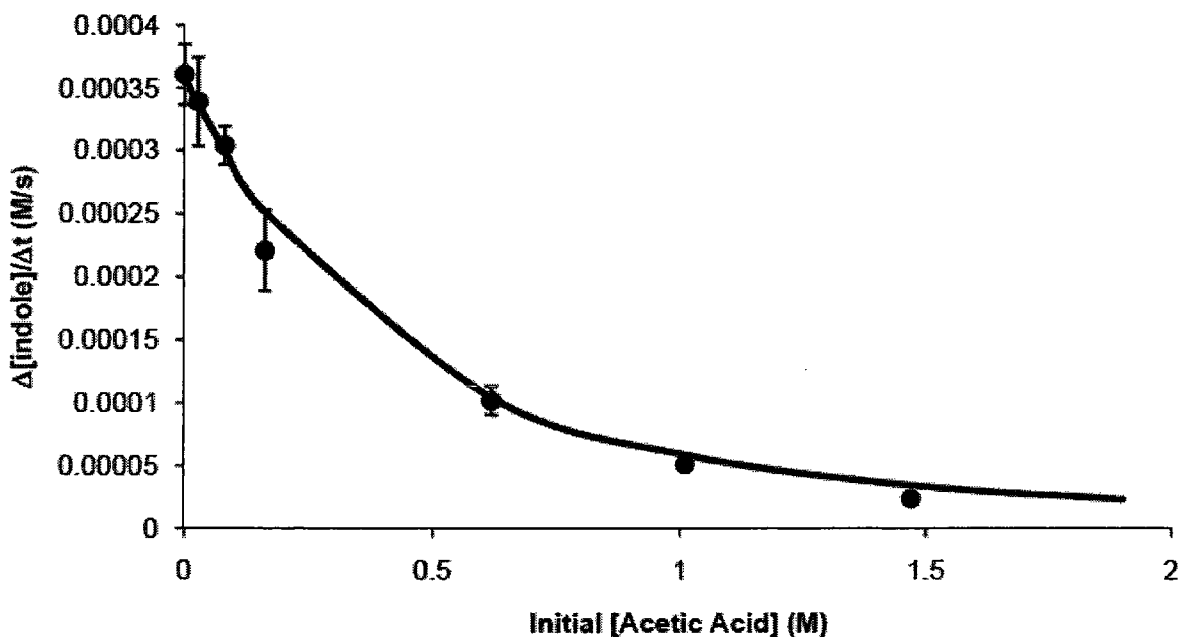
When each of the species present in the rate law is extracted to see how their concentrations individually affect the rate it is observed that each of these equations matches the equations to which the data was fit in the preceding sections. Notably, the concentration

of the copper(II) oxidant is absent from the rate law and correlates well with the observed independence of the initial rate with changes in the initial concentration of copper(II) acetate. Interestingly, however, an acid component with an inhibitory effect on the rate is present in the rate law. In order to test the validity and the predictive ability of the derived rate law acetic acid was added to the reaction mixture over a concentration range of 0 – 1.47 M and its effect on the initial rate of the reaction was observed (Figure 4.12). The experimental data was fit to the equation shown above the graph (equivalent to the previously described equation) and therefore experimentally authenticates the derived rate law and credits the ability of the rate law to predict experimental outcomes.

**Figure 4.12.** Initial rate versus initial concentration of acetic acid.

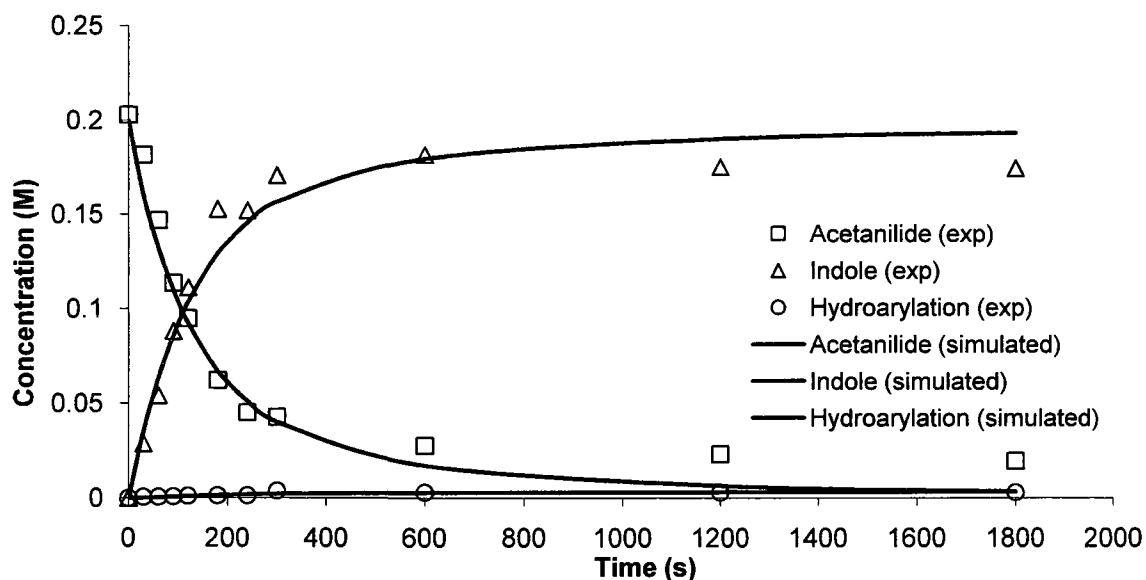


$$\text{Data fit to: } y = \frac{a}{bx^2 + cx + d}$$



Kinetic modeling software, Copasi (COMplex PATHway SIMulator)<sup>152</sup>, was used as well to corroborate the proposed catalytic cycle and the formation of the “hydroarylation” side product. The experimental data (acetanilide, □; indole, Δ; hydroarylation, ○) is plotted with the simulated data (—) and an excellent correlation is observed, particularly early in the reaction. Simulations in which both reversible and irreversible (shown) alkyne insertion into the acetanilide derived rhodacycle were performed and gave essentially the same data. Therefore, the simulated data adds additional validation to the proposed catalytic cycle.

**Figure 4.13.** Experimental and simulated data for the proposed catalytic cycle.

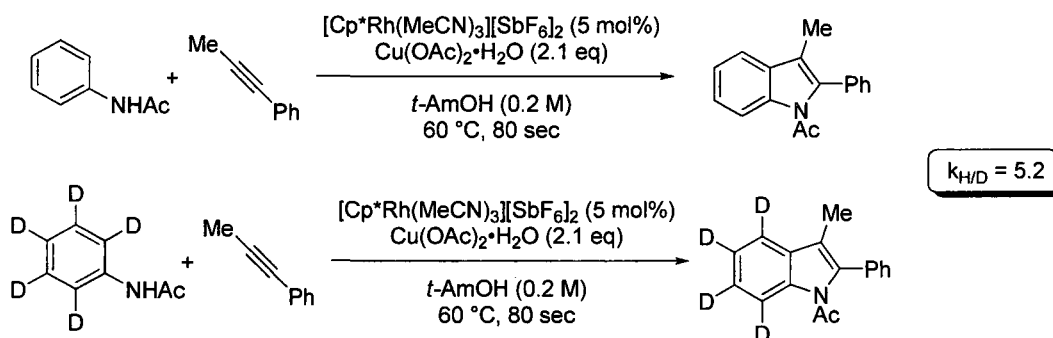


**Mechanism of C-H bond cleavage.** A central part of our group’s research is the development of transition metal catalyzed reactions which take place at C-H bonds and more directly the mechanism with which C-H bonds are cleaved. Having established an intimate knowledge of the catalytic cycle focus was then directed toward determining the mechanism of C-H bond cleavage and C-Rh bond formation. Deuterium kinetic isotope effects, Hammett correlation, and an Arrhenius plot were used investigate this process.

<sup>152</sup> Copasi v. 4.5 was used in this study. Copasi may be downloaded from [www.copasi.org/tiki-index.php](http://www.copasi.org/tiki-index.php). For a report describing the use of Copasi, please see: Hoops, S.; Sahle, S.; Gauges, R.; Lee, C.; Pahle, J.; Simus, N.; Singhal, M.; Xu, L.; Mendes, P.; Kummer, U. *Bioinformatics* **2006**, *22*, 3067.

**Deuterium kinetic isotope effect.** As previously described (*vide supra*), the presence (or absence) of a DKIE can often be indicative of the mechanism of C-H bond cleavage. The existence of a DKIE was probed by measuring the initial rate of reaction for acetanilide and acetanilide- $d_5$  in separate reaction flasks. Though the C-H bond cleavage was shown to be reversible (*vide supra*) this is of no consequence under the reaction conditions used for this experiment. Very short reaction times ( $\sim 80$  seconds) were used in the measurement of initial rates and under these conditions no loss of deuterium was observed for acetanilide- $d_5$ . Thus, when the experiment was carried out a significant primary DKIE = 5.2 was observed. This is consistent with the results of Jones (DKIE > 5) in the cyclorhodation of *N*-phenylbenzylimine with  $[\text{Cp}^*\text{RhCl}_2]_2$ .<sup>11e</sup> Additionally, when measured in this way (separate reaction flasks) the presence of a DKIE also corroborates our earlier finding that cleavage of the C-H bond (rhodacycle formation) is the rate determining step of the catalytic cycle.

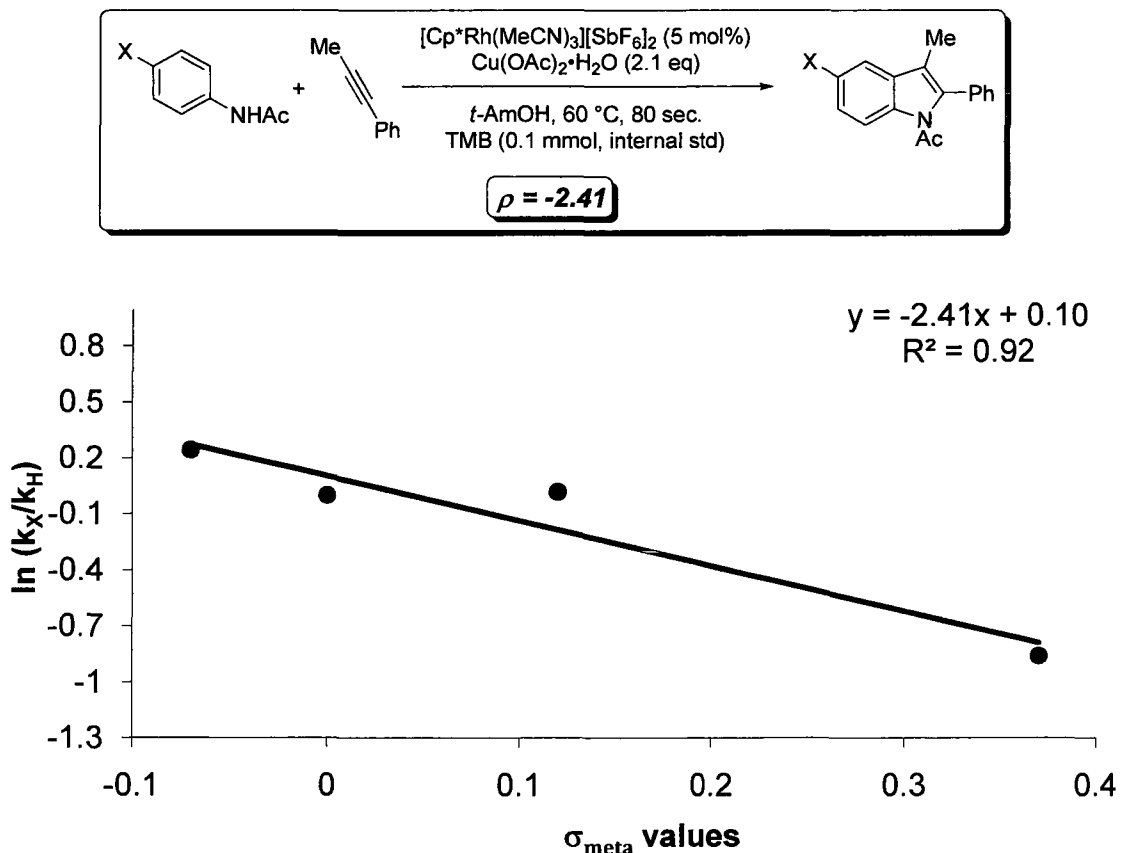
**Scheme 4.32.** Determination of a deuterium kinetic isotope effect.



**Hammett correlation and competition experiments.** While the presence of a significant primary DKIE is suggestive of a CMD pathway a Hammett correlation was performed to probe the electronic bias of the acetanilide and to further interrogate the identity of the transition state of C-H bond cleavage. The initial reaction rate was measured for a number of *para*-substituted acetanilides and these rates compared with the initial rate of reaction for unsubstituted acetanilide ( $X = \text{H}$ ; Figure 4.14). A  $\rho$ -value = -2.41 was obtained from the linear free energy relationship. While a negative  $\rho$  value is suggestive of a developing positive charge (Wheland intermediate in  $\text{S}_{\text{E}}\text{Ar}$ ) on the aromatic system, the absolute value of 2.41 is relatively small for an  $\text{S}_{\text{E}}\text{Ar}$  process.<sup>19</sup> In the context of a CMD

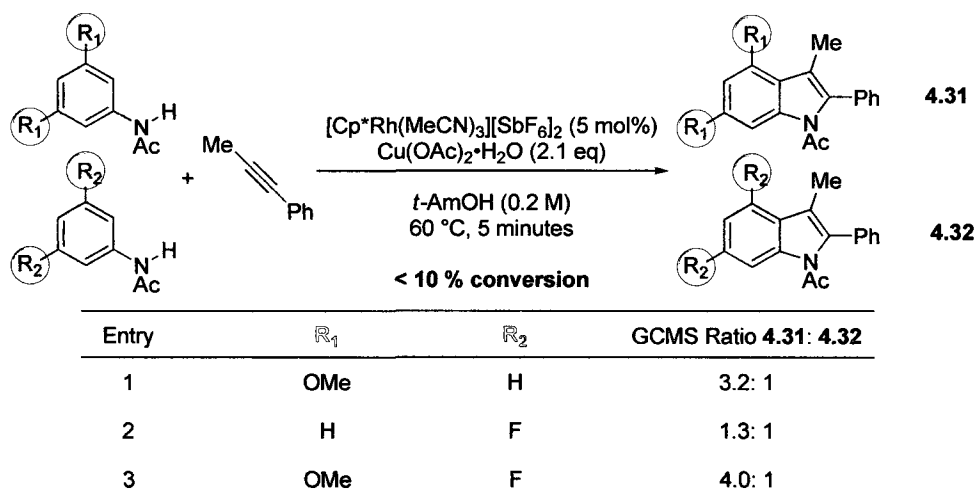
transition state this relationship may more accurately describe the important nucleophilic component of the arene metal interaction ( $E_{int}$ ). These results also mirror those obtained by Jones<sup>11e</sup> in the cyclorhodation of *N*-phenylbenzylimine with  $[\text{Cp}^*\text{RhCl}_2]_2$  and the computational work by Davies and Macgregor<sup>13,14</sup> on the CMD transition state for related processes with palladium(II) and iridium(III). It should be noted that in this Hammett correlation ( $R^2 = 0.92$ ) the natural logarithm of the ratio of initial rates was plotted against the  $\sigma_{meta}$ -values to reflect the *meta*-relationship between the X-substituent and the site of reaction. Moreover, when the natural logarithm of the ratio of initial rates was plotted against the  $\sigma_{para}$ -values a poor correlation was observed ( $R^2 = 0.75$ ). This implies that the electronic influence of the X-substituent has a stronger correlation with the *meta*-carbon than with increasing the Lewis basicity of the anilide moiety and thus increasing its ability to coordinate rhodium.

**Figure 4.14.** Hammett correlation for *para*-substituted acetanilides.



Competition experiments were also conducted to determine the electronic influence of X-substituents *para* to the site of reactivity. Because of the high sensitivity of the reaction to sterics and the issues of regioselectivity that this would cause (*vide supra*) a Hammett correlation could not be conducted using 3-X-acetanilides. Therefore symmetrical substrates, 3,5-di-X-acetanilides, were employed in single pot competition experiments in this study (Scheme 4.33). It can be observed that in each case the electron-rich substrate reacts preferentially with the catalyst, again corroborating that a strong nucleophilic component of the arene is important in the mechanism of C-H bond cleavage.

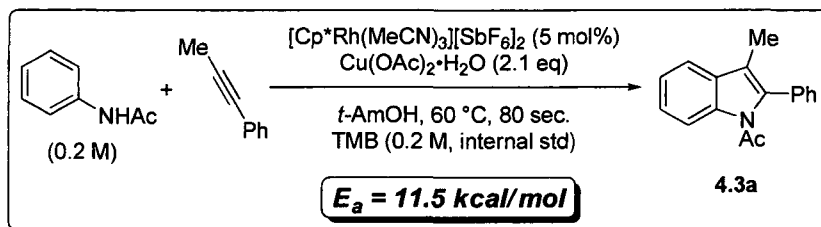
**Scheme 4.33.** Competition experiments of 3,5-disubstituted acetanilides.



**Arrhenius plot.** Another linear free energy relationship was utilized to explore the energetics of the transition state of the rate determining step – C-H bond cleavage. An Arrhenius plot was obtained by measuring the initial rate at a number of different temperatures and plotting the natural logarithm of the initial rate against the inverse of the absolute temperature (Figure 4.15). The activation energy ( $E_a$ ) may be calculated from the slope of the plot in Figure 4.15 and was determined to be 11.5 kcal/mol. Computationally, the  $E_a$  of the CMD transition state has been determined for a number of different arenes with palladium(II) and found to range from 5.8 kcal/mol (thiazole *N*-oxide) to 25.1 kcal/mol (benzene).<sup>9</sup> Therefore, the value obtained in this study of 11.5 kcal/mol is within the range observed for a CMD transition state over a diverse set of arenes, as well the relatively low  $E_a$

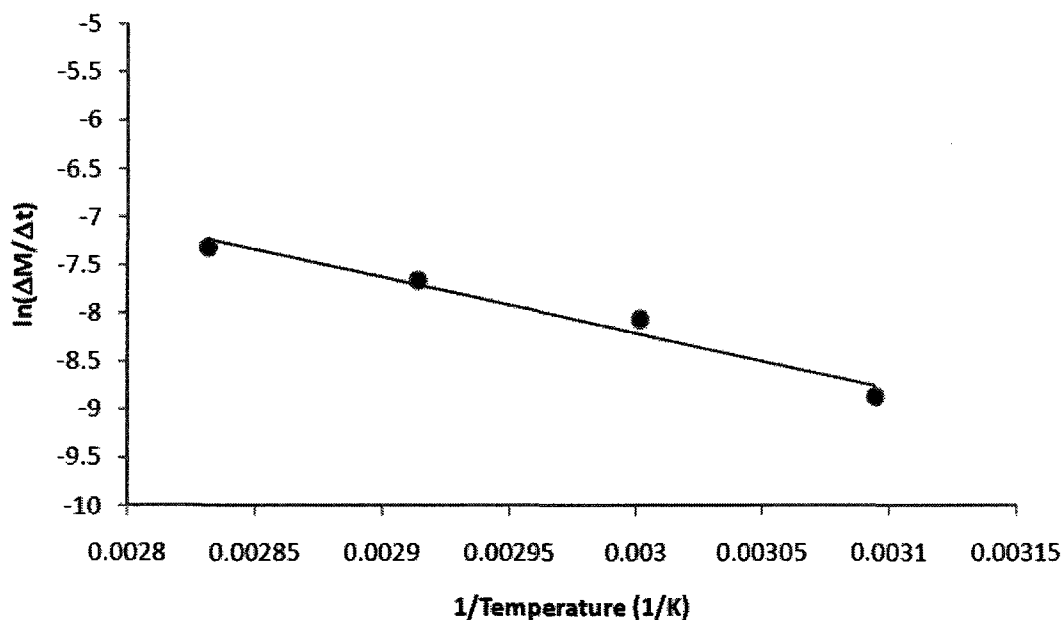
supports our ability to conduct the reaction under particularly mild conditions (60 °C or 21 °C over 5 days).

**Figure 4.15.** Arrhenius plot for the rhodium catalyzed annulation of acetanilides with internal alkynes.



$$\text{Arrhenius equation: } k = Ae^{\frac{-E_a}{RT}}$$

$$\therefore \ln(k) = \frac{-E_a}{R} \times \frac{1}{T} + \ln(A)$$



Thus, the experimental data described in this chapter accurately portray C-H bond cleavage via a CMD transition state. Therefore, further reaction development and substrate selection should be done with these mechanistic findings in mind.

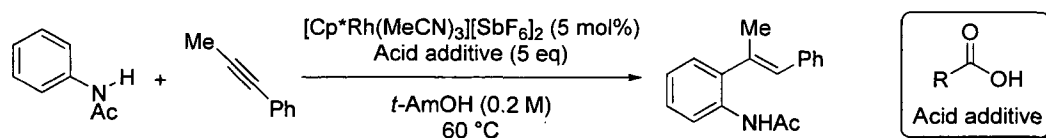
#### 4.2.5. Optimization of an Alkyne Hydroarylation Protocol

Realizing the difficulty associated with the preparation of geometrically pure, highly substituted alkenes<sup>153</sup> combined with the observation that **4.30** is obtained as a *single regio- and stereoisomer* the optimization of its formation was explored. As described previously it was postulated that the product arose from protonation of an organometallic species with acid produced during the reaction. Therefore, to probe this hypothesis and further promote this process a number of carboxylic acid additives were investigated with varying degrees of acid strength ( $pK_a$ ). It was found that relatively strong organic acids ( $pK_a < 1$ ) resulted in very low yields of the alkyne hydroarylation product and that significant amounts of starting acetanilide remained in the reaction mixture (Table 4.12, entry 1 and 2). Under these strongly acidic conditions proto-derhodation of the initial organometallic species **4.33** generated simply results in re-generation of starting material. However, under more mild acidic conditions ( $pK_a > 1$ ) a significant portion of the alkyne hydroarylation product is formed (Table 4.12, entry 3 – 7) with pivalic acid providing the highest level of **4.30** by <sup>1</sup>H NMR spectroscopy (Table 4.12, entry 7). These results suggest that strongly acidic additives ( $pK_a < 1$ ) promote the proto-derhodation of **4.33** to re-generate the starting acetanilide. While employing less acidic additives ( $pK_a > 1$ ) the organo-rhodium species **4.33** may irreversibly react with the alkyne to produce **4.34** which then may undergo proto-derhodation to provide **4.30** (Scheme 4.34).

---

<sup>153</sup> Flynn, A. B.; Ogilvie, W. W. *Chem. Rev.* **2007**, *107*, 4698.

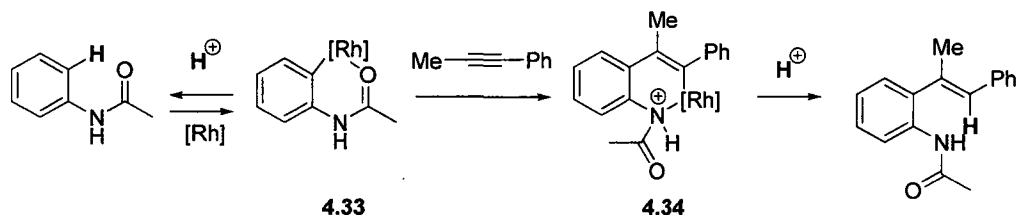
**Table 4.12.** Dependence of acid strength on yield of alkyne hydroarylation product.<sup>a</sup>



Entry	Acid R-group	pK <sub>a</sub>	<sup>1</sup> H NMR Yield (%) <sup>b</sup>
1	CF <sub>3</sub>	-0.25	7
2	CCl <sub>3</sub>	0.65	14
3	CHCl <sub>2</sub>	1.29	42
4	CH <sub>2</sub> Cl	2.86	51
5	CH <sub>2</sub> I	3.12	53
6	CH <sub>3</sub>	4.76	49
7	C(CH <sub>3</sub> ) <sub>3</sub>	5.10	54

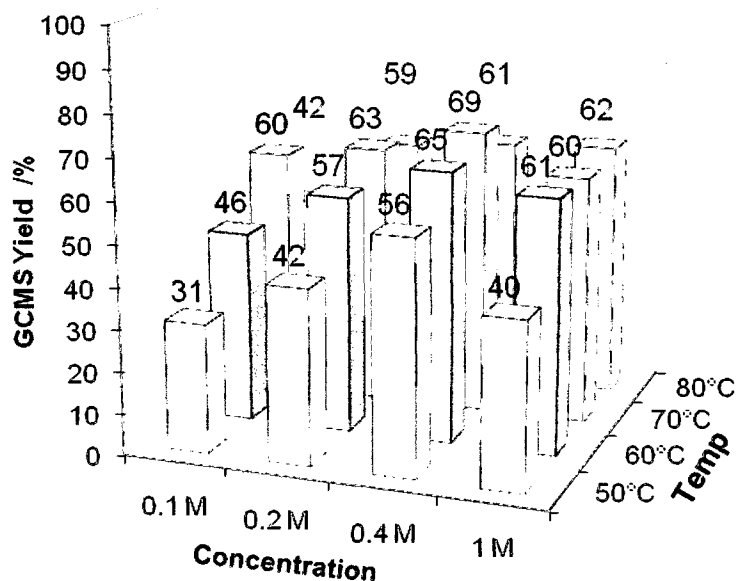
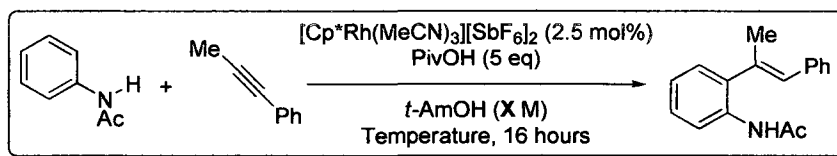
<sup>a</sup>Conditions: acetanilide (1 eq, 0.2 M), alkyne (1.1 eq),  $[\text{Cp}^*\text{Rh}(\text{MeCN})_3][\text{SbF}_6]_2$  (5 mol%), acid additive (5 eq), *t*-AmOH, 60 °C, 16 hours. <sup>b</sup>Verses an internal standard (trimethoxybenzene).

**Scheme 4.34.** Formation of hydroarylation product over starting materials.



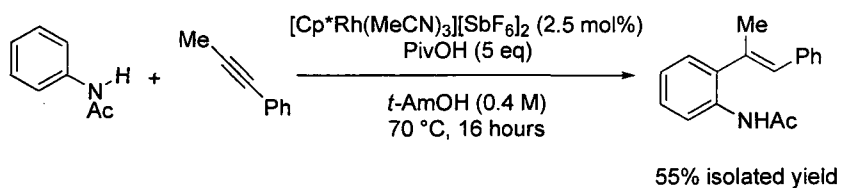
The use of 2.5 mol % rhodium was found to have no deleterious effect on the yield of the product and therefore this catalyst loading was used for the remainder of the optimization. Additionally, *t*-AmOH was found to be the optimal solvent. Both concentration and temperature were investigated with respect to the yield of **4.30** (Figure 4.16). The reactions were analyzed *via* GCMS against an internal standard and the local maximum for this data set appeared at a concentration of 0.4 M and a temperature of 70 °C yielding 69% of the desired alkyne hydroarylation product (Figure 4.16).

**Figure 4.16.** Effect of concentration and temperature on hydroarylation.



After much optimization the highest crude ( $^1\text{H}$  NMR or GCMS) yield obtained in the reaction was 69%. This is largely due to two reasons. First, this reaction does not undergo any redox chemistry (rhodium stays at the 3+ oxidation state) and therefore a terminal oxidant ( $\text{Cu}(\text{OAc})_2$ ) is not necessary or employed. Second, small amounts ( $\sim 5\%$ ) of indole side product are produced in the reaction resulting in the production of rhodium(I). Rhodium(I) is an inactive form of the catalyst in this reaction and the absence of an oxidant to re-generate the catalytically active rhodium(III) effectively shuts down the reaction. However, introduction of copper(II) acetate to the reaction did not increase the yield of the desired product. The application of the optimized conditions resulted in a 55% isolated yield of the desired alkyne hydroarylation product (Scheme 4.35). Additionally, other internal alkynes (4-octyne) failed to provide any of the desired product under the optimized reaction conditions. This protocol may also be applied to an intramolecular variant of the reaction providing access to interesting bicyclic frameworks.

**Scheme 4.35.** Intermolecular hydroarylation of alkynes.



### 4.3. Outlook and Perspectives

The innovations described herein should provide ample opportunity for the construction of highly substituted and diverse indole and pyrrole containing compounds. Additionally, the mechanistic conclusions should aid in the development of future rhodium(III)-catalyzed reactions at C-H bonds of both aromatic and vinylic substrates. The literature has seen a recent surge of activity in the development of oxidative approaches to pharmaceutically relevant heterocycles and this should continue to accommodate both the need for functional group compatibility and mild reaction conditions.

# Supporting Information

## 5.1. General Methods

All reagents and solvents were purchased from commercial sources and used without further purification, unless otherwise stated. HPLC grade THF, Et<sub>2</sub>O, benzene, toluene, and DCM were purified *via* MBraun SP Series solvent purification system. THF used in reactions with *n*-BuLi, *t*-BuLi, or NaH was freshly distilled from Na/benzophenone before every use. Triethylamine was freshly distilled from NaOH before every use. All other reaction solvents used were HPLC grade (minimum). Palladium(II) acetate was purchased from Pressure Chemicals, palladium(II) trifluoroacetate was purchased from Strem, and palladium(II) acetylacetonate was purchased from Aldrich. Rhodium trichloride was purchased from Pressure Chemicals and [Cp\*RhCl<sub>2</sub>]<sub>2</sub> was either purchased from Strem or synthesized by literature methods.<sup>111f</sup> [Cp\*Rh(MeCN)<sub>3</sub>][SbF<sub>6</sub>] was synthesized by literature methods.<sup>154</sup> Trialkylphosphonium tetrafluoroborate salts were either purchased from Strem or synthesized by literature methods.<sup>155</sup> All palladium(0) catalyzed reactions were run under an inert (argon) atmosphere and set up accordingly. All oxidative reactions (primarily

<sup>154</sup> White, C.; Thompson, S. J.; Maitlis, P.M. *J. Chem. Soc., Dalton Trans.* 1977, 1654.

<sup>155</sup> Netherton, M. R.; Fu, G. C. *Org. Lett.* 2001, 3, 4295.

Chapters 3 and 4) were set up without regard for exclusion of ambient air or moisture, and when stated were run under an atmosphere of oxygen. Room temperature in the laboratory was  $21 \pm 2^\circ\text{C}$ , reactions heated above this temperature were done so in an oil bath heated externally by a Heidolph MR Hei-Standard heating/stirring mantel equipped with a Heidolph EKT HeiCON temperature control, unless otherwise stated. Microwave reactions were performed in a CEM Discover Microwave (specific conditions described below). All reactions were stirred by a magnetic stir bar, unless otherwise stated. Analysis of crude reaction mixtures was done on an Agilent 6890 Network GC System with an Agilent 5973 Network Mass Selective Detector or by thin-layer chromatography (TLC) on Merck TLC plates (silica gel 60Å F<sub>254</sub>) and visualized by UV or KMnO<sub>4</sub> stain. Reactions were purified by flash chromatography on Silicycle Ultra Pure silica gel (60 Å), unless otherwise stated. NMR spectra were recorded in CDCl<sub>3</sub>, DMSO-*d*<sub>6</sub>, or acetone-*d*<sub>6</sub> solutions on a Bruker AVANCE 400 MHz spectrometer at ambient temperature and chemical shifts are reported relative to tetramethylsilane (TMS). The following notation is used: br – broad, s – singlet, d – doublet, t – triplet, q – quartet, m – multiplet, dd – doublet of doublets, ddd – doublet of doublet of doublets. Fourier-transform infrared (FTIR) spectra were obtained as thin films on sodium chloride plates. High resolution mass spectra were obtained with a Kratos Concept IIIH mass spectrometer. Melting points were recorded using a Gallenkamp Melting Point apparatus and are reported uncorrected. All <sup>1</sup>H, <sup>13</sup>C, and 2-D (where applicable) NMR spectra of compounds completely characterized in this thesis are provided as electronic supporting information (attached CD). All other compounds that have been previously synthesized or are commercially available have been appropriately referenced or the CAS number provided and their NMR spectra are not presented here.

## 5.2. Quinoline and Isoquinoline *N*-Oxides

### 5.2.1. Oxidation Methods and Characterization of Oxidation Products.

**Oxidation Procedure A:** Preferred method for preparation using an adapted methyltrioxorhenium oxidation protocol first reported by Sharpless and co-workers. Easily scalable with limited by products.

The azine is dissolved in reagent grade  $\text{CH}_2\text{Cl}_2$  (2.5M). This mixture is added  $\text{MeReO}_3$  (1-4mol%) which usually results in a significant color change to deep yellow. This solution is then capped with a rubber septa which is pierced with a small needle as a vent and placed in an ice bath. To the cold solution is added dropwise a 50w% aqueous solution of  $\text{H}_2\text{O}_2$  (2 equiv.). Once all peroxide has been added, the reaction is allowed to warm to room temperature where it is stirred for 12-24h. After consumption of starting material, a small amount of  $\text{MnO}_2$  (5-10mg) is added to destroy unreacted peroxyde. After stirring this solution of 1-2 hours (until bubbling stops) the mixture is poured into an extraction funnel where the phases are seperated. The aqueous phase is washed with two volumes of  $\text{CH}_2\text{Cl}_2$  and the organic are combined, dried with  $\text{MgSO}_4$ , filtered and concentrated under reduced pressure. The *N*-oxides were then purified *via* silica gel column chromatography using the individually specified solvent system as the eluent to afford the corresponding *N*-oxide.

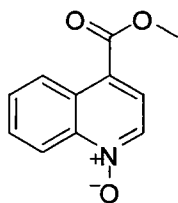
**Oxidation Procedure B:** Produces large amounts of waste *m*-chlorobenzoic acid, not recommended for large scale. Compatible with diazines.

Azine (1 eq.) and *m*-chloroperoxybenzoic acid (1.2 eq.) are dissolved in reagent grade dichloroethane (0.5M). The reaction is allowed to stir at room temperature overnight from which precipitates a white solid (*m*-chlorobenzoic acid). The solvent is then evaporated under reduced pressure and the crude reaction mixture is purified by column chromatography on silica gel using the individually specified solvent system as the eluent to afford the corresponding *N*-oxide.

**Oxidation Procedure C:** Caution, this reaction is in water. Azines with limited solubility in water showed diminished reactivity in these systems. Also, azine *N*-oxides which were highly water soluble were difficult to isolate.

Azine (1 eq.) is dissolved in acetone (2.5M) in a three neck round bottom flask and phosphate buffer is added (0.25M). One neck is fitted with an addition funnel carrying oxone (2.4 eq.) in distilled water (0.3M). A second neck is fitted with a solution of 2M NaOH. Both solutions are added dropwise simultaneously at room temperature and the pH of the reaction is monitored and kept between 7-8. Typically reactions are complete within 3 hours. The mixture is extracted twice with  $\text{CH}_2\text{Cl}_2$  and once with  $\text{CHCl}_3$ . The organic layer

is then dried over MgSO<sub>4</sub>, filtered and evaporated under reduced pressure to afford the pyridine *N*-oxide, often in analytically pure form.



The above compound was prepared according oxidation procedure B and was isolated in 68% yield.

**<sup>1</sup>H NMR (400 MHz, CDCl<sub>3</sub>, 293 K):** δ 9.06 (d, *J* = 8.0 Hz, 1H), 8.75 (d, *J* = 8.3 Hz, 1 H), 8.51 (d, *J* = 6.5 Hz, 1H), 8.00 (d, *J* = 6.5 Hz, 1H), 7.81 – 7.72 (m, 2H), 4.02 (s, 3H).

**<sup>13</sup>C NMR (100 MHz, CDCl<sub>3</sub>, 293 K):** δ 165.1, 142.3, 134.4, 130.4, 130.2, 128.4, 126.8, 124.4, 122.9, 119.8, 52.6.

**FTIR:** 3080, 1716, 1556, 1514, 783, 771 cm<sup>-1</sup>.

**HRMS (EI):** calculated for C<sub>11</sub>H<sub>9</sub>NO<sub>3</sub> (M<sup>+</sup>) 203.0582; found for C<sub>11</sub>H<sub>9</sub>NO<sub>3</sub> (M<sup>+</sup>) 203.0575.

**Melting point (acetone/hexanes):** 152 – 153°C.

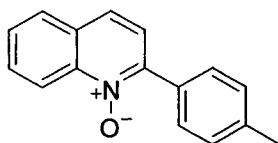
**R<sub>f</sub> (10% acetone in dichloromethane):** 0.24.

## 5.2.2. Methods and Characterization for 2-Arylquinoline *N*-Oxide Products

### Representative procedure for the direct arylation of quinoline *N*-oxide:

A 0.3 M solution of 4-bromotoluene was prepared in dry toluene and degassed with argon. Palladium (II) acetate (0.0033 g, 0.015 mmol, 5 mol %), di-*tert*-butylmethylphosphonium tetrafluoroborate (0.0037 g, 0.015 mmol, 5 mol %), K<sub>2</sub>CO<sub>3</sub> (0.083 g, 0.599 mmol, 2 eq), and quinoline *N*-oxide (0.131 g, 0.9093 mmol, 3 eq) were weighed out in air into a round bottom flask and fitted with a reflux condenser capped with a septa. This system was evacuated and refilled with argon to sufficiently purge the system of oxygen (~ 5 times). The aryl halide solution (1.0 mL, 0.3 mmol) was transferred *via* syringe to the round bottom flask, and the reaction was heated to 110°C for 16 hours under an atmosphere of argon. The cooled reaction mixture was filtered over celite and washed with acetone and dichloromethane. The solvent was removed under vacuum and the resulting residue subjected to column chromatography on silica gel.

**Table 2.1, entry 7:**



The above procedure was followed and the residue was subjected to column chromatography on silica gel (7 x 3 cm) with 15% acetone in dichloromethane as the solvent to afford the title compound in 96% yield.

**<sup>1</sup>H NMR (400 MHz, CDCl<sub>3</sub>, 293 K):** δ 8.86 (d, J = 9.0 Hz, 1H), 7.90 (d, J = 8.2 Hz, 2 H), 7.85 (d, J = 8.2 Hz, 1H), 7.77 (dd, J = 7.8 = 7.8 Hz, 1H), 7.73 (d, J = 9.0 Hz, 1H), 7.62 (dd, J = 7.8 = 7.8 Hz, 1H), 7.50 (d, J = 8.6 Hz, 1H), 7.33 (d, J = 8.2 Hz, 2H), 2.43 (s, 3H).

**<sup>13</sup>C NMR (75 MHz, CDCl<sub>3</sub>, 293 K):** δ 145.1, 142.3, 139.7, 136.6, 130.5, 129.5, 129.4, 129.0, 128.2, 127.9, 125.2, 123.3, 120.3, 21.5.

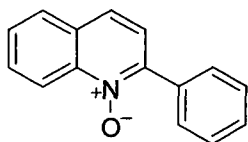
**FTIR:** 3059, 1608, 1556, 1499, 806, 734 cm<sup>-1</sup>.

**HRMS (EI):** calculated for C<sub>16</sub>H<sub>13</sub>NO (M<sup>+</sup>) 235.0997; found for C<sub>16</sub>H<sub>13</sub>NO (M<sup>+</sup>) 235.1001.

**Melting point (acetone/DCM):** 127 – 128°C.

**R<sub>f</sub> (15% acetone in dichloromethane):** 0.31.

**Table 2.2, entry 1:**



The above procedure was followed and the residue was subjected to column chromatography on silica gel (7 x 3 cm) with 10% acetone in dichloromethane as the solvent to afford the title compound in 89% yield.

**<sup>1</sup>H NMR (300 MHz, CDCl<sub>3</sub>, 293 K):** δ 8.86 (d, J = 8.7 Hz, 1H), 7.97 (d, J = 8.1 Hz, 2 H), 7.85 (d, J = 8.1 Hz, 1H), 7.80 – 7.71 (m, 2H), 7.62 (dd, J = J = 7.4 Hz, 1H), 7.54 – 7.42 (m, 4H).

**<sup>13</sup>C NMR (75 MHz, CDCl<sub>3</sub>, 293 K):** δ 144.9, 142.2, 133.5, 130.5, 129.6, 129.5, 129.5, 128.4, 128.3, 128.0, 125.2, 123.3, 120.2.

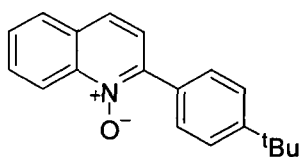
**FTIR:** 3054, 1560, 1491, 764 cm<sup>-1</sup>.

**HRMS (EI):** calculated for C<sub>15</sub>H<sub>11</sub>NO (M<sup>+</sup>) 221.0841; found for C<sub>15</sub>H<sub>11</sub>NO (M<sup>+</sup>) 221.0852.

**Melting point (acetone/hexanes):** 148.5 – 149.7°C.

**R<sub>f</sub> (10% acetone in dichloromethane):** 0.19.

**Table 2.2, entry 2:**



The above procedure was followed and the residue was subjected to column chromatography on silica gel (7 x 3 cm) with 15% acetone in dichloromethane as the solvent to afford the title compound in 94% yield.

**<sup>1</sup>H NMR (400 MHz, CDCl<sub>3</sub>, 293 K):** δ 8.87 (d, J = 8.6 Hz, 1H), 7.95 (d, J = 8.6 Hz, 2 H), 7.87 (d, J = 8.2 Hz, 1H), 7.78 (dd, J = 8.2 = 8.2 Hz, 1H), 7.74 (d, J = 8.6 Hz, 1H), 7.63 (dd, J = 7.8 = 7.8 Hz, 1H), 7.58 – 7.50 (m, 3H, overlapping signals), 1.38 (s, 9H).

**<sup>13</sup>C NMR (100 MHz, CDCl<sub>3</sub>, 293 K):** δ 152.8, 147.1, 145.0, 144.7, 142.3, 130.5, 129.3, 128.3, 127.9, 125.3, 125.2, 123.3, 120.3, 34.9, 31.2.

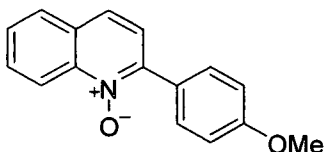
**FTIR:** 2965, 1597, 1563, 1499, 806, 738 cm<sup>-1</sup>.

**HRMS (EI):** calculated for C<sub>19</sub>H<sub>19</sub>NO (M<sup>+</sup>) 277.1467; found for C<sub>19</sub>H<sub>19</sub>NO (M<sup>+</sup>) 277.1440.

**Melting point (acetone/DCM):** 159.6 – 162.9°C.

**R<sub>f</sub> (15% acetone in dichloromethane):** 0.46.

**Table 2.2, entry 3**



The above procedure was followed and the residue was subjected to column chromatography on silica gel (7 x 3 cm) with 15% acetone in dichloromethane as the solvent to afford the title compound in 87% yield.

**<sup>1</sup>H NMR (400 MHz, CDCl<sub>3</sub>, 293 K):** δ 8.85 (d, J = 8.9 Hz, 1H), 8.03 (d, J = 8.7 Hz, 2 H), 7.84 (d, J = 8.4 Hz, 1H), 7.77 (ddd, J = 8.5, J = 7.0, J = 1.6 Hz, 1H), 7.71 (d, J = 9.1 Hz, 1H), 7.61 (ddd, J = 7.9, J = unresolved, J = 1.0 Hz, 1H), 7.51 (d, J = 8.7 Hz, 1H), 7.04 (d, J = 8.5 Hz, 2H), 3.88 (s, 3H).

**<sup>13</sup>C NMR (100 MHz, CDCl<sub>3</sub>, 293 K):** δ 160.5, 144.7, 142.3, 131.2, 130.5, 129.3, 128.1, 127.9, 125.7, 125.2, 123.1, 120.2, 113.7, 55.4.

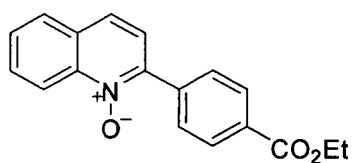
**FTIR:** 3064, 1605, 1560, 1501, 806, 732 cm<sup>-1</sup>.

**HRMS (EI):** calculated for C<sub>16</sub>H<sub>13</sub>NO<sub>2</sub> (M<sup>+</sup>) 251.0946; found for C<sub>16</sub>H<sub>13</sub>NO<sub>2</sub> (M<sup>+</sup>) 251.0922.

**Melting point (acetone/DCM):** 124.9 – 126.0°C.

**R<sub>f</sub> (15% acetone in dichloromethane):** 0.31.

**Table 2.2, entry 4:**



The above procedure was followed and the residue was subjected to column chromatography on silica gel (7 x 3 cm) with 10% acetone in dichloromethane as the solvent to afford the title compound in 61% yield.

**<sup>1</sup>H NMR (300 MHz, CDCl<sub>3</sub>, 293 K):** δ 8.85 (d, J = 8.7 Hz, 1H), 8.20 (d, J = 8.1 Hz, 2 H), 8.07 (d, J = 8.7 Hz, 2H), 7.90 (d, J = 8.1 Hz, 1H), 7.85 – 7.70 (m, 2H), 7.68 (dd, J = J = 6.8 Hz, 1H), 7.5 (d, J = 8.7 Hz, 1H), 4.43 (q, J = 7.4 Hz, 2H), 1.43 (t, J = 7.4 Hz, 3H).

**<sup>13</sup>C NMR (75 MHz, CDCl<sub>3</sub>, 293 K):** δ 166.1, 144.0, 142.3, 137.7, 131.1, 130.8, 129.8, 129.6, 129.5, 128.8, 128.1, 125.4, 123.1, 120.3, 61.2, 14.4.

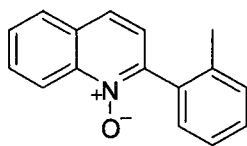
**FTIR:** 3074, 1710, 1612, 1558, 1501, 818, 734 cm<sup>-1</sup>.

**HRMS (EI):** calculated for C<sub>18</sub>H<sub>15</sub>NO<sub>3</sub> (M<sup>+</sup>) 293.1052; found for C<sub>18</sub>H<sub>15</sub>NO<sub>3</sub> (M<sup>+</sup>) 293.1032.

**Melting point (acetone/DCM):** 204 – 205°C.

**R<sub>f</sub> (10% acetone in dichloromethane):** 0.56.

**Table 2.2, entry 5:**



The above procedure was followed with the addition of Ag<sub>2</sub>CO<sub>3</sub> (0.5 eq) and the residue was subjected to column chromatography on silica gel (7 x 3 cm) with 10% acetone in dichloromethane as the solvent to afford the title compound in 70% yield.

**<sup>1</sup>H NMR (300 MHz, CDCl<sub>3</sub>, 293 K):** δ 8.85 (d, J = 8.7 Hz, 1H), 7.90 (d, J = 8.1 Hz, 1 H), 7.82 – 7.71 (m, 2H), 7.66 (dd, J = J = 8.1 Hz, 1H), 7.43 – 7.29 (m, 5H), 2.27 (s, 3H).

**<sup>13</sup>C NMR (75 MHz, CDCl<sub>3</sub>, 293 K):** δ 146.7, 142.0, 137.7, 133.9, 130.4, 130.1, 129.9, 129.3, 129.1, 128.4, 128.0, 125.9, 124.6, 123.8, 120.3, 19.7.

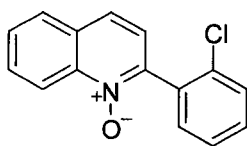
**FTIR:** 3064, 1603, 1561, 1514, 812, 735 cm<sup>-1</sup>.

**HRMS (EI):** calculated for C<sub>16</sub>H<sub>13</sub>NO (M<sup>+</sup>) 235.0997; found for C<sub>16</sub>H<sub>13</sub>NO (M<sup>+</sup>) 235.0990.

**Melting point (acetone/DCM):** 103 – 104°C.

**R<sub>f</sub> (10% acetone in dichloromethane):** 0.31.

**Table 2.2, entry 6**



The above procedure was followed with the addition of  $\text{Ag}_2\text{CO}_3$  (0.5 eq) and the residue was subjected to column chromatography on silica gel (7 x 3 cm) with 10% acetone in dichloromethane as the solvent to afford the title compound in 70% yield.

**$^1\text{H}$  NMR (300 MHz,  $\text{CDCl}_3$ , 293 K):**  $\delta$  8.84 (d,  $J = 8.7$  Hz, 1H), 7.90 (d,  $J = 8.1$  Hz, 1H), 7.82 – 7.74 (m, 2H), 7.67 (dd,  $J = J = 8.1$  Hz, 1H), 7.59 – 7.49 (m, 2H), 7.46 – 7.36 (m, 3H).

**$^{13}\text{C}$  NMR (75 MHz,  $\text{CDCl}_3$ , 293 K):**  $\delta$  143.9, 142.0, 133.8, 133.2, 131.0, 130.6, 130.5, 130.1, 129.8, 128.8, 128.1, 126.3, 124.6, 123.6, 120.3.

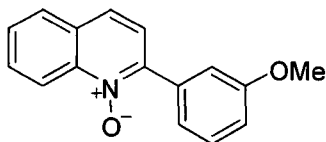
**FTIR:** 3058, 1561, 811, 739  $\text{cm}^{-1}$ .

**HRMS (EI):** calculated for  $\text{C}_{15}\text{H}_{10}\text{NOCl}$  ( $\text{M}^+$ ) 255.0451; found for  $\text{C}_{15}\text{H}_{10}\text{NOCl}$  ( $\text{M}^+$ ) 255.0465.

**Melting point (acetone/DCM):** 106 – 107°C.

**$R_f$  (10% acetone in dichloromethane):** 0.28.

**Table 2.2, entry 7:**



The above procedure was followed and the residue was subjected to column chromatography on silica gel (7 x 3 cm) with 15% acetone in dichloromethane as the solvent to afford the title compound in 87% yield.

**$^1\text{H}$  NMR (400 MHz,  $\text{CDCl}_3$ , 293 K):**  $\delta$  8.86 (d,  $J = 8.6$  Hz, 1H), 7.86 (dd,  $J = 8.2, 1.2$  Hz, 1H), 7.78 (ddd,  $J = 8.2, 6.7, 1.2$  Hz, 1H), 7.74 (d,  $J = 8.6$  Hz, 1H), 7.64 (ddd,  $J = 7.8, 6.7, 0.8$  Hz, 1H), 7.63 – 7.61 (m, 1H, overlapping signals), 7.50 (d,  $J = 9.0$ , 1H), 7.47 (ddd,  $J = 7.4, 1.2, 1.2$ , 1H), 7.43 (dd,  $J = 7.8 = 7.8$  Hz, 1H), 7.02 (ddd,  $J = 7.8, 2.7, 1.2$  Hz, 1H), 3.88 (s, 3H).

**$^{13}\text{C}$  NMR (100 MHz,  $\text{CDCl}_3$ , 293 K):**  $\delta$  159.4, 144.9, 142.3, 134.8, 130.6, 129.6, 129.4, 128.5, 128.0, 125.2, 123.4, 122.0, 120.3, 115.8, 114.7, 55.5.

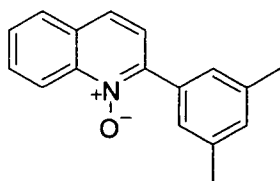
**FTIR:** 3061, 1596, 1580, 1486, 1341, 1042, 804, 770  $\text{cm}^{-1}$ .

**HRMS (EI):** calculated for  $\text{C}_{16}\text{H}_{13}\text{NO}_2$  ( $\text{M}^+$ ) 251.0946; found for  $\text{C}_{16}\text{H}_{13}\text{NO}_2$  ( $\text{M}^+$ ) 251.0959.

**Melting point (acetone/DCM):** 111.8 – 112.6°C.

**$R_f$  (15% acetone in dichloromethane):** 0.25.

**Table 2.2, entry 8:**



The above procedure was followed and the residue was subjected to column chromatography on silica gel (7 x 3 cm) with 15% acetone in dichloromethane as the solvent to afford the title compound in 92% yield.

**<sup>1</sup>H NMR (400 MHz, CDCl<sub>3</sub>, 293 K):** δ 8.86 (d, J = 8.6 Hz, 1H), 7.86 (d, J = 7.8 Hz, 1H), 7.78 (dd, J = 7.8 = 7.8 Hz, 1H), 7.73 (d, J = 8.6 Hz, 1H), 7.63 (dd, J = 7.4 = 7.4 Hz, 1H), 7.56 (s, 2H), 7.48 (d, J = 8.6 Hz, 1H), 7.11 (s, 1H), 2.40 (s, 6H).

**<sup>13</sup>C NMR (75 MHz, CDCl<sub>3</sub>, 293 K):** δ 145.5, 142.3, 137.9, 133.4, 131.2, 130.5, 129.5, 128.3, 127.9, 127.2, 125.1, 123.5, 120.3, 21.4.

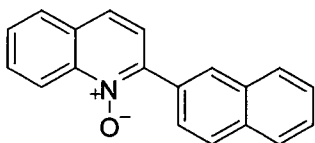
**FTIR:** 3060, 1599, 1561, 1509, 810, 732 cm<sup>-1</sup>.

**HRMS (EI):** calculated for C<sub>16</sub>H<sub>13</sub>NO (M<sup>+</sup>) 249.1154; found for C<sub>16</sub>H<sub>13</sub>NO (M<sup>+</sup>) 249.1170.

**Melting point (acetone/DCM):** 94 – 95°C.

**R<sub>f</sub> (15% acetone in dichloromethane):** 0.34.

**Table 2.2, entry 9**



The above procedure was followed and the residue was subjected to column chromatography on silica gel (7 x 3 cm) with 10% acetone in dichloromethane as the solvent to afford the title compound in 73% yield.

**<sup>1</sup>H NMR (300 MHz, CDCl<sub>3</sub>, 293 K):** δ 8.89 (d, J = 8.7 Hz, 1H), 8.46 (s, 1H), 8.10 (dd, J = 8.7, J = 1.9 Hz, 1H), 8.00 – 7.85 (m, 4H), 7.83 – 7.74 (m, 2H), 7.68 – 7.48 (m, 4H).

**<sup>13</sup>C NMR (75 MHz, CDCl<sub>3</sub>, 293 K):** δ 145.0, 142.3, 133.6, 133.0, 131.0, 130.6, 129.6, 129.6, 128.6, 128.5, 128.0, 127.7, 127.1, 126.4, 126.3, 125.3, 123.5, 120.2. There is one overlapping carbon signal as 1 peak is missing even with prolonged scans.

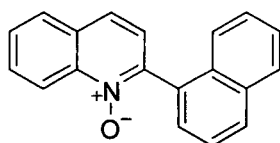
**FTIR:** 3122, 1560, 1496, 803, 730 cm<sup>-1</sup>.

**HRMS (EI):** calculated for C<sub>19</sub>H<sub>13</sub>NO (M<sup>+</sup>) 271.0997; found for C<sub>19</sub>H<sub>13</sub>NO (M<sup>+</sup>) 271.1008.

**Melting point (acetone/DCM):** 209 – 210°C.

**R<sub>f</sub> (10% acetone in dichloromethane):** 0.24.

**Table 2.2, entry 10:**



The above procedure was followed with the addition of  $\text{Ag}_2\text{CO}_3$  (0.5 eq) and the residue was subjected to column chromatography on silica gel (7 x 3 cm) with 10% acetone in dichloromethane as the solvent to afford the title compound in 83% yield.

**$^1\text{H}$  NMR (300 MHz,  $\text{CDCl}_3$ , 293 K):**  $\delta$  8.88 (d,  $J = 9.3$  Hz, 1H), 8.02 – 7.91 (m, 3H), 7.85 – 7.77 (m, 2H), 7.69 (ddd,  $J = 8.1$ ,  $J = 6.8$ ,  $J = 1.2$  Hz, 1H), 7.60 (d,  $J = 5.6$  Hz, 2H), 7.55 – 7.41 (m, 4H).

**$^{13}\text{C}$  NMR (75 MHz,  $\text{CDCl}_3$ , 293 K):**  $\delta$  145.6, 142.1, 133.4, 132.1, 130.7, 130.5, 130.1, 129.9, 128.6, 128.6, 128.1, 127.7, 126.9, 126.2, 125.4, 125.4, 124.7, 124.5, 120.4.

**FTIR:** 3057, 1592, 1561, 1503, 890, 774, 731  $\text{cm}^{-1}$ .

**HRMS (EI):** calculated for  $\text{C}_{19}\text{H}_{13}\text{NO}$  ( $\text{M}^+$ ) 271.0997; found for  $\text{C}_{19}\text{H}_{13}\text{NO}$  ( $\text{M}^+$ ) 271.0991.

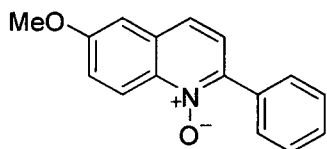
**Melting point (acetone/hexanes):** 168 – 169°C.

**$R_f$  (10% acetone in dichloromethane):** 0.25.

#### **Representative Procedure for the direct arylation of 6-methoxyquinoline N-oxides:**

This was analogous to the general procedure for the direct arylation of unsubstituted quinoline N-oxides, however dioxane was used as the reaction solvent instead of toluene.

**Table 2.2, entry 11:**



The above procedure was followed and the residue was subjected to column chromatography on silica gel (7 x 3 cm) with 10% acetone in dichloromethane as the solvent to afford the title compound in 72% yield.

**$^1\text{H}$  NMR (300 MHz,  $\text{CDCl}_3$ , 293 K):**  $\delta$  8.76 (d,  $J = 9.3$  Hz, 1H), 7.95 (d,  $J = 7.4$  Hz, 2H), 7.64 (d,  $J = 8.7$  Hz, 1H), 7.55 – 7.43 (m, 4H), 7.40 (dd,  $J = 9.9$  Hz,  $J = 2.5$  Hz, 1H), 7.11 (d,  $J = 2.5$  Hz, 1H), 3.96 (s, 3H).

**$^{13}\text{C}$  NMR (75 MHz,  $\text{CDCl}_3$ , 293 K):**  $\delta$  159.2, 143.2, 137.8, 133.5, 131.0, 129.5, 129.2, 128.2, 124.3, 123.8, 122.6, 122.0, 105.8, 55.7.

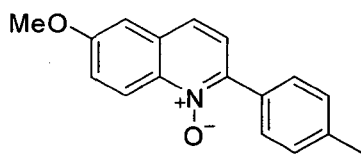
**FTIR:** 3058, 1616, 1567, 1489, 850, 764  $\text{cm}^{-1}$ .

**HRMS (EI):** calculated for  $\text{C}_{16}\text{H}_{13}\text{NO}_2$  ( $\text{M}^+$ ) 251.0946; found for  $\text{C}_{16}\text{H}_{13}\text{NO}_2$  ( $\text{M}^+$ ) 251.0972.

**Melting point (acetone/DCM):** 176 – 177°C.

**$R_f$  (10% acetone in dichloromethane):** 0.20.

**Table 2.2, entry 12:**



The above procedure was followed and the residue was subjected to column chromatography on silica gel (7 x 3 cm) with 10% acetone in dichloromethane as the solvent to afford the title compound in 85% yield.

**<sup>1</sup>H NMR (300 MHz, CDCl<sub>3</sub>, 293 K):** δ 8.76 (d, J = 9.9 Hz, 1H), 7.87 (d, J = 8.1 Hz, 2 H), 7.62 (d, J = 8.7 Hz, 1H), 7.45 (d, J = 8.7 Hz, 1H), 7.39 (dd, J = 9.9 Hz, J = 3.1 Hz, 1H), 7.32 (d, J = 8.1 Hz, 2H), 7.10 (d, J = 2.5 Hz, 1H), 3.95 (s, 3H), 2.43 (s, 3H).

**<sup>13</sup>C NMR (75 MHz, CDCl<sub>3</sub>, 293 K):** δ 159.1, 143.4, 139.4, 137.9, 130.8, 130.6, 129.4, 129.0, 124.3, 123.8, 122.4, 122.0, 105.9, 55.7, 21.5.

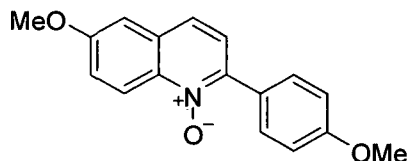
**FTIR:** 3030, 1615, 1575, 1498, 801, 723 cm<sup>-1</sup>.

**HRMS (EI):** calculated for C<sub>17</sub>H<sub>15</sub>NO<sub>2</sub> (M<sup>+</sup>) 265.1103; found for C<sub>17</sub>H<sub>15</sub>NO<sub>2</sub> (M<sup>+</sup>) 265.1094.

**Melting point (acetone/DCM):** 173 – 174°C.

**R<sub>f</sub> (10% acetone in dichloromethane):** 0.25.

**Table 2.2, entry 13:**



The above procedure was followed and the residue was subjected to column chromatography on silica gel (7 x 3 cm) with 10% acetone in dichloromethane as the solvent to afford the title compound in 77% yield.

**<sup>1</sup>H NMR (300 MHz, CDCl<sub>3</sub>, 293 K):** δ 8.76 (d, J = 9.3 Hz, 1H), 7.98 (d, J = 8.7 Hz, 2H), 7.62 (d, J = 8.7 Hz, 1H), 7.46 (d, J = 8.7 Hz, 1H), 7.39 (dd, J = 9.3 Hz, J = 2.5 Hz, 1H), 7.10 (d, J = 2.5 Hz, 1H), 7.03 (d, J = 9.3 Hz, 2H), 3.95 (s, 3H), 3.88 (s, 3H).

**<sup>13</sup>C NMR (75 MHz, CDCl<sub>3</sub>, 293 K):** δ 160.3, 159.1, 143.0, 137.9, 131.1, 130.6, 125.8, 124.3, 123.6, 122.4, 121.9, 113.6, 105.9, 55.7, 55.4.

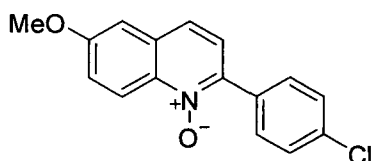
**FTIR:** 2962, 1618, 1604, 1564, 1495, 834, 722 cm<sup>-1</sup>.

**HRMS (EI):** calculated for C<sub>17</sub>H<sub>15</sub>NO<sub>3</sub> (M<sup>+</sup>) 281.1052; found for C<sub>17</sub>H<sub>15</sub>NO<sub>3</sub> (M<sup>+</sup>) 281.1070.

**Melting point (acetone/DCM):** 193 – 194°C.

**R<sub>f</sub> (10% acetone in dichloromethane):** 0.18.

**Table 2.2, entry 14:**



Column chromatography was performed on silica gel (7 x 3 cm) with 5% acetone in dichloromethane as the solvent to afford the title compound in 55% yield.

**<sup>1</sup>H NMR (300 MHz, CDCl<sub>3</sub>, 293 K):** δ 8.74 (d, J = 9.6 Hz, 1H), 7.93 (d, J = 8.8 Hz, 2H), 7.64 (d, J = 8.5 Hz, 1H), 7.48 (d, J = 8.8 Hz, 2H), 7.43 (d, J = 8.8 Hz, 1H), 7.40 (dd, J = 9.5 Hz, J = 2.6 Hz, 1H), 7.11 (d, J = 2.6 Hz, 1H), 3.96 (s, 3H).

**<sup>13</sup>C NMR (75 MHz, CDCl<sub>3</sub>, 293 K):** δ 159.4, 142.1, 137.9, 135.3, 131.9, 131.1, 131.0, 128.5, 124.4, 123.4, 122.7, 122.0, 105.9, 55.7.

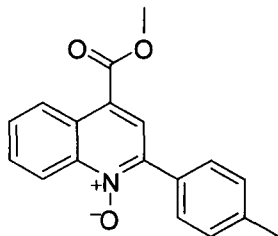
**FTIR:** 2999, 1620, 1574, 1567, 1487, 828 cm<sup>-1</sup>.

**HRMS (EI):** calculated for C<sub>16</sub>H<sub>12</sub>NO<sub>2</sub>Cl (M<sup>+</sup>) 285.0557; found for C<sub>16</sub>H<sub>12</sub>NO<sub>2</sub>Cl (M<sup>+</sup>) 285.0537.

**Melting point (acetone/DCM):** 186 – 187°C.

**R<sub>f</sub> (5% acetone in dichloromethane):** 0.38.

**Table 2.2, entry 15:**



The general procedure for the arylation of quinoline *N*-oxides was followed and the residue was subjected to column chromatography on silica gel (7 x 3 cm) with 10% acetone in dichloromethane as the solvent to afford the title compound in 91% yield.

**<sup>1</sup>H NMR (400 MHz, CDCl<sub>3</sub>, 293 K):** δ 9.01 (dd, J = 8.5 Hz, J = 0.9 Hz, 1H), 8.85 (d, J = 8.6 Hz, 0.9 Hz, 1H), 8.22 (s, 1H), 7.88 (d, J = 8.2, 2H), 7.78 (ddd, J = J = 8.4 Hz, J = 1.4 Hz, 1H), 7.70 (ddd, J = J = 8.4 Hz, J = 1.4 Hz, 1H), 7.33 (d, J = 7.9 Hz, 2H), 4.00 (s, 3H), 2.43 (s, 3H).

**<sup>13</sup>C NMR (100 MHz, CDCl<sub>3</sub>, 293 K):** δ 165.4, 144.1, 143.1, 140.1, 130.4, 129.8, 129.5, 129.4, 129.1, 127.1, 126.7, 126.6, 122.2, 120.3, 52.6, 21.5.

**FTIR:** 2951, 1719, 1556, 1502, 1437, 786, 740 cm<sup>-1</sup>.

**HRMS (EI):** calculated for C<sub>18</sub>H<sub>15</sub>NO<sub>3</sub> (M<sup>+</sup>) 293.1052; found for C<sub>18</sub>H<sub>15</sub>NO<sub>3</sub> (M<sup>+</sup>) 293.1067.

**Melting point (acetone/DCM):** 136 – 137°C.

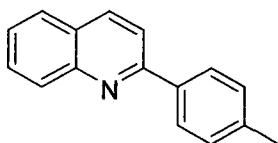
**R<sub>f</sub> (2% acetone in dichloromethane):** 0.22.

### 5.2.3. Reduction Methods and Characterization of 2-Arylquinoline Products.

#### General Procedure

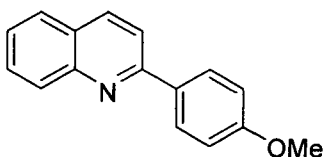
The *N*-oxide (1 eq) and 10% Pd/C (10 mol% Pd) were weighed into a thick-walled test tube and sealed with a rubber septa and purged with argon. Methanol (0.14 M in isoquinoline *N*-oxide) was added and ammonium formate (14 eq) was then added to the the black reaction mixture which was stirred at room temperature. The reaction was monitored by thin layer chromatography until it was observed that the *N*-oxide had been completely consumed. The reaction was then filtered over celite and washed with DCM, the solvent was removed and the residue subjected to flash chromatography with an appropriate solvent system.

#### Table 2.3, entry 1:



The general procedure was followed and column chromatography was performed on silica gel with dichloromethane as the solvent to afford the title compound in 94% yield. NMR data is consistent with that previously reported in the literature.<sup>156</sup>

#### Table 2.3, Entry 2:

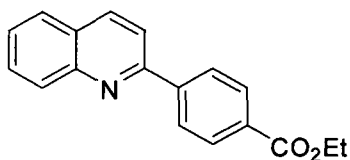


Procedure A was followed and column chromatography was performed on silica gel with dichloromethane as the solvent to afford the title compound in 93% yield. NMR data is consistent with that previously reported in the literature.<sup>157</sup>

<sup>156</sup> Egi, M.; Liebeskind, L. S. *Org. Lett.*, **2003**, *5*, 801.

<sup>157</sup> Sangu, K.; Fuchibe, K.; Akiyama, T. *Org. Lett.*, **2004**, *6*, 353.

**Table 2.3, Entry 3:**



Procedure A was followed and column chromatography was performed on silica gel with dichloromethane as the solvent to afford the title compound in 80% yield.

**<sup>1</sup>H NMR (400 MHz, CDCl<sub>3</sub>, 293 K):** δ 8.26 – 8.24 (m, 3H), 8.21 – 8.18 (m, 3H), 7.91 (d, J = 8.6 Hz, 1H), 7.85 (dd, J = 8.1 Hz, J = 1.2 Hz, 1H), 7.75 (ddd, J = J = 8.4 Hz, J = 1.5 Hz, 1H), 7.56 (ddd, J = J = 8.0 Hz, J = 1.2 Hz, 1H), 4.42 (q, J = 7.1 Hz, 2H), 1.44 (t, J = 7.2 Hz, 3H).

**<sup>13</sup>C NMR (100 MHz, CDCl<sub>3</sub>, 293 K):** δ 166.5, 156.1, 148.3, 143.7, 137.0, 131.0, 130.1, 129.9, 129.9, 127.5, 127.5, 127.4, 126.8, 119.0, 61.1, 14.4.

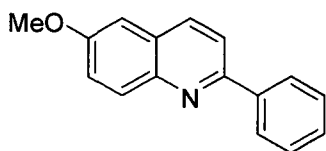
**FTIR:** 2923, 1706, 1270, 822, 773 cm<sup>-1</sup>.

**HRMS (EI):** calculated for C<sub>12</sub>H<sub>11</sub>NO<sub>2</sub> (M<sup>+</sup>) 277.1103; found for C<sub>12</sub>H<sub>11</sub>NO<sub>2</sub> (M<sup>+</sup>) 277.1074.

**Melting point (acetone/DCM):** 86 – 87°C.

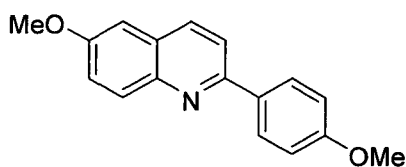
**R<sub>f</sub> (25% Et<sub>2</sub>O in Pet. Ether):** 0.31.

**Table 2.3, Entry 4:**



Procedure A was followed and column chromatography was performed on silica gel with dichloromethane as the solvent to afford the title compound in 93% yield. NMR data is consistent with that previously reported in the literature.<sup>56</sup>

**Table 2.3, Entry 5:**



Procedure A was followed and column chromatography was performed on silica gel with dichloromethane as the solvent to afford the title compound in 79% yield.

**<sup>1</sup>H NMR (400 MHz, CDCl<sub>3</sub>, 293 K):** δ 8.09 (d, J = 8.8 Hz, 2H), 8.07 (d, J = 8.6 Hz, 1H), 8.03 (d, J = 9.2 Hz, 1H), 7.78 (d, 8.62 Hz, 1H), 7.36 (dd, J = 9.2 Hz, J = 2.8 Hz, 1H), 7.07 (d, J = 2.7 Hz, 1H), 7.03 (d, 8.8 Hz, 2H), 3.94 (s, 3H), 3.88 (s, 3H).

**<sup>13</sup>C NMR (100 MHz, CDCl<sub>3</sub>, 293 K):** δ 160.5, 157.4, 154.7, 144.3, 135.4, 132.4, 131.0, 128.6, 127.8, 122.1, 118.8, 114.2, 105.1, 55.5, 55.4.

**FTIR:** 2931, 1254, 1026, 831 cm<sup>-1</sup>.

**HRMS (EI):** calculated for C<sub>17</sub>H<sub>15</sub>NO<sub>2</sub> (M<sup>+</sup>) 265.1103; found for C<sub>17</sub>H<sub>15</sub>NO<sub>2</sub> (M<sup>+</sup>) 265.1086.

**Melting point (acetone/DCM):** 164 – 166°C.

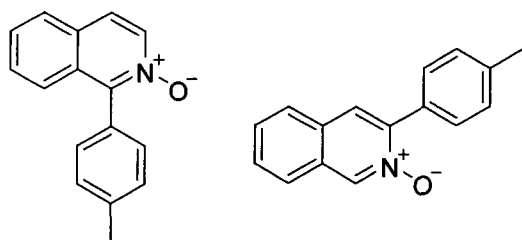
**R<sub>f</sub> (dichloromethane):** 0.28.

## 5.2.4. Methods and Characterization of 1-Arylisoquinoline Products.

### General Procedure for direct arylation of Isoquinoline N-Oxides:

A 0.3 M solution of aryl halide was prepared in dry toluene and degassed with argon. Palladium (II) acetate (0.0033 g, 0.015 mmol, 5 mol %), di-*tert*-butylmethylphosphonium tetrafluoroborate (0.030 mmol, 10 mol %), K<sub>2</sub>CO<sub>3</sub> (0.599 mmol, 2 eq), and quinoline N-oxide (0.9093 mmol, 3 eq) were weighed out in air into a round bottom flask and fitted with a reflux condenser capped with a septa. This system was evacuated and refilled with argon to sufficiently purge the system of oxygen (~ 5 times). The aryl halide solution (1.0 mL, 0.3 mmol) was transferred *via* syringe to the round bottom flask, and the reaction was heated to 110°C for 12 hours under an atmosphere of argon. The cooled reaction mixture was filtered over celite and washed with acetone and dichloromethane. The solvent was removed under vacuum and the resulting residue subjected to column chromatography on silica gel.

**Table 2.5, entry 1 – 3 (N-oxide):**



The above procedure was followed and column chromatography was performed on silica gel with MeOH:acetone:DCM (2:20:78) as the solvent to afford the product as a mixture of isomers (**2.5a** : **2.5b** 13.5:1 by <sup>1</sup>H NMR spectroscopy) in 98% yield.

### Isomer 2.5a:

**<sup>1</sup>H NMR (400 MHz, CDCl<sub>3</sub>, 293 K):** δ 8.28 (d, J = 7.2 Hz, 1H), 7.79 (d, J = 8.0 Hz, 1H), 7.65 (d, J = 7.2 Hz, 1H), 7.54 (m, 1H), 7.50 – 7.37 (m, 6H), 2.47 (s, 3H).

**<sup>13</sup>C NMR (100 MHz, CDCl<sub>3</sub>, 293 K):** δ 146.3, 139.4, 137.4, 130.0, 129.7, 129.5, 129.1, 128.9, 128.2, 127.9, 126.8, 125.8, 123.1, 21.5.

**FTIR:** 3056, 1620, 1551, 1493, 817, 745 cm<sup>-1</sup>.

**HRMS (EI):** calculated for C<sub>16</sub>H<sub>13</sub>NO (M<sup>+</sup>) 235.0997; found for C<sub>16</sub>H<sub>13</sub>NO (M<sup>+</sup>) 235.0979.

**Melting point (acetone/DCM):** 166 – 167°C.

**R<sub>f</sub> (MeOH:acetone:DCM (2:20:78)):** 0.16.

**Isomer 2.5b:**

**<sup>1</sup>H NMR (400 MHz, CDCl<sub>3</sub>, 293 K):** δ 8.90 (s, 1H), 7.80 – 7.75 (m, 2H), 7.74 – 7.68 (m, 3H), 7.61 – 7.52 (m, 2H), 7.31 (d, J = 7.9 Hz, 2H), 2.43 (s, 3H).

**<sup>13</sup>C NMR (100 MHz, CDCl<sub>3</sub>, 293 K):** δ 147.3, 139.5, 137.0, 130.0, 129.6, 129.2, 128.9, 128.9, 128.7, 126.6, 124.5, 124.4, 21.4. There is one overlapping carbon signal as 1 peak is missing even with prolonged scans.

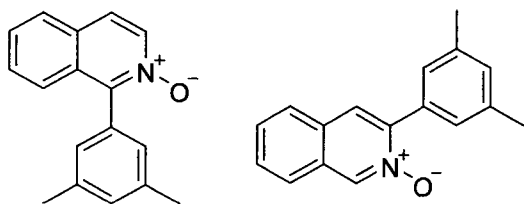
**FTIR:** 3029, 1635, 1560, 1487, 811, 746 cm<sup>-1</sup>.

**HRMS (EI):** calculated for C<sub>16</sub>H<sub>13</sub>NO (M<sup>+</sup>) 235.0997; found for C<sub>16</sub>H<sub>13</sub>NO (M<sup>+</sup>) 235.0995.

**Melting point (acetone/DCM):** 150 – 152°C.

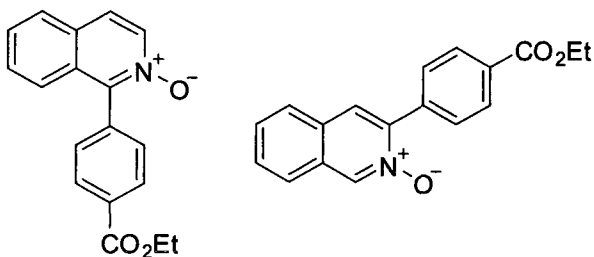
**R<sub>f</sub> (MeOH:acetone:DCM (2:20:78)):** 0.22.

**Table 2.5, entry 4 (N-oxide):**



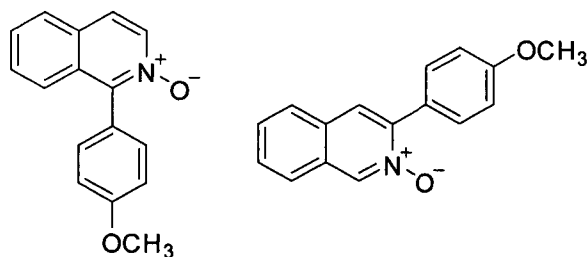
The above procedure was followed and column chromatography was performed on silica gel with MeOH:acetone:DCM (2:20:78) as the solvent to afford the product as a mixture of isomers (**2.5a** : **2.5b** 12.4:1 by <sup>1</sup>H NMR spectroscopy) in 92% yield. Structural proof based on reduction, see below.

**Table 2.5, entry 5 (N-oxide):**



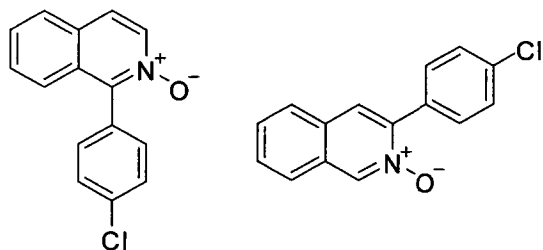
The above procedure was followed and column chromatography was performed on silica gel with MeOH:acetone:DCM (2:20:78) as the solvent to afford the product as a mixture of isomers (**2.5a** : **2.5b** 15.8:1 by <sup>1</sup>H NMR spectroscopy) in 95% yield. Structural proof based on reduction, see below.

**Table 2.5, entry 6 (*N*-oxide):**



The above procedure was followed and column chromatography was performed on silica gel with MeOH:acetone:DCM (2:20:78) as the solvent to afford the product as a mixture of isomers (**2.5a** : **2.5b** 13.5:1 by  $^1\text{H}$  NMR spectroscopy) in 96% yield. Structural proof based on reduction, see below.

**Table 2.5, entry 7 (*N*-oxide):**



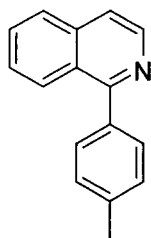
The above procedure was followed and column chromatography was performed on silica gel with MeOH:acetone:DCM (2:20:78) as the solvent to afford the product as a mixture of isomers (**2.5a** : **2.5b** 14.1:1 by  $^1\text{H}$  NMR spectroscopy) in 63% yield. Structural proof based on reduction, see below.

**General procedure for the reduction of 1-aryl- and 3-arylisquinoline *N*-oxides<sup>158</sup>:**

The regioisomeric mixture of 1- and 3-arylisquinoline *N*-oxides (1 eq) and 10% Pd/C (10 mol% Pd) were weighed into a thick-walled test tube and sealed with a rubber septa and purged with argon. Methanol (0.14 M in isoquinoline *N*-oxide) was added and ammonium formate (14 eq) was then added to the the black reaction mixture which was heated to 40°C. The reaction was monitored by thin layer chromatography until it was observed that the *N*-oxide had been completely consumed. The reaction was then filtered over celite and washed with DCM, the solvent was removed and the residue subjected to flash chromatography with an appropriate solvent system.

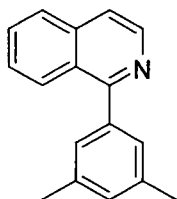
<sup>158</sup> Balicki, R. *Synthesis*, **1989**, 8, 645

**Table 2.5, entry 1 (isoquinoline):**



The above procedure was followed and column chromatography was performed on silica gel with acetone:DCM (2:98) as the solvent to afford the title compound in 80% yield. NMR data is consistent with that previously reported in the literature.<sup>159</sup>

**Table 2.5, entry 4 (isoquinoline):**



The above procedure was followed and column chromatography was performed on silica gel with acetone:DCM (1:99) as the solvent to afford the title compound in 73% yield.

**<sup>1</sup>H NMR (400 MHz, CDCl<sub>3</sub>, 293 K):** δ 8.59 (d, J = 5.7 Hz, 1H), 8.12 (dd, J = 8.5 Hz, J = 0.8 Hz, 1H), 7.85 (d, J = 8.2 Hz, 1H), 7.66 (ddd, J = J = 8.1 Hz, J = 1.2 Hz, 1H), 7.61 (d, J = 5.6 Hz, 1H), 7.52 (ddd, J = J = 8.3 Hz, J = 1.3 Hz, 1H), 7.30 (s, 2H), 7.12 (s, 1H), 2.41 (s, 6H).

**<sup>13</sup>C NMR (100 MHz, CDCl<sub>3</sub>, 293 K):** δ 161.1, 142.2, 139.5, 137.8, 136.8, 130.2, 129.9, 127.8, 127.7, 127.0, 126.9, 126.8, 119.7, 21.4.

**FTIR:** 2916, 1390, 825, 707 cm<sup>-1</sup>.

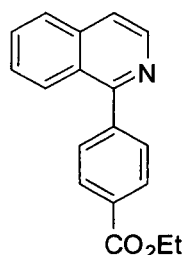
**HRMS (EI):** calculated for C<sub>17</sub>H<sub>15</sub>N (M<sup>+</sup>) 233.1205; found for C<sub>17</sub>H<sub>15</sub>N (M<sup>+</sup>) 233.1196.

**Melting point (acetone/DCM):** 89 – 91°C.

**R<sub>f</sub> (acetone:DCM (1:99)):** 0.21.

<sup>159</sup> Fang, K.-H.; Wu, L.-L.; Huang, Y.-T.; Yang, C.-H.; Sun, I.-W. *Inorganica Chimica Acta*, **2006**, 359, 441.

**Table 2.5, entry 5 (isoquinoline):**



The above procedure was followed and column chromatography was performed on silica gel with acetone:DCM (2:98) as the solvent to afford the title compound in 83% yield.

**<sup>1</sup>H NMR (400 MHz, CDCl<sub>3</sub>, 293 K):** δ 8.63 (d, J = 5.7 Hz, 1H), 8.22 (d, J = 8.6 Hz, 2H), 8.03 (d, J = 8.5 Hz, 1H), 7.90 (d, J = 8.2 Hz, 1H), 7.78 (d, J = 8.5 Hz, 2H), 7.72 – 7.67 (m, 2H), 7.55 (ddd, J = J = 8.3 Hz, J = 1.3 Hz, 1H), 4.44 (q, J = 7.2 Hz, 2H), 1.44 (t, J = 7.2 Hz, 3H).

**<sup>13</sup>C NMR (100 MHz, CDCl<sub>3</sub>, 293 K):** δ 166.4, 159.6, 143.9, 142.3, 136.8, 130.5, 130.2, 130.0, 129.6, 127.5, 127.1, 127.1, 126.6, 120.4, 61.1, 14.4.

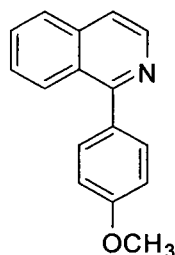
**FTIR:** 2981, 1715, 1273, 1102, 827, 772, 707 cm<sup>-1</sup>.

**HRMS (EI):** calculated for C<sub>12</sub>H<sub>11</sub>NO<sub>2</sub> (M<sup>+</sup>) 277.1103; found for C<sub>12</sub>H<sub>11</sub>NO<sub>2</sub> (M<sup>+</sup>) 277.1098.

**Melting point (acetone/DCM):** 68 – 70°C.

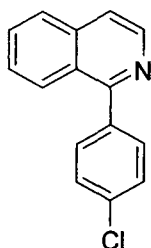
**R<sub>f</sub> (acetone:DCM (2:98)):** 0.21.

**Table 2.5, entry 6 (isoquinoline):**



The above procedure was followed and column chromatography was performed on silica gel with acetone:DCM (1:99) as the solvent to afford the title compound in 83% yield. NMR data is consistent with that previously reported in the literature.<sup>159</sup>

**Table 2.5, entry 7 (isoquinoline):**



The following alternate procedure was used.<sup>160</sup> The regioisomeric mixture of 1- and 3-arylisquinoline *N*-oxides (1 eq) was dissolved in THF:NH<sub>4</sub>Cl(sat) (1:1 v/v) (0.03 M in isoquinoline *N*-oxide). Zinc dust (5 eq) was added to this solution and it was stirred at room temp. for 1 hour. The reaction was filtered over celite, extracted with ether and the organic layer dried over MgSO<sub>4</sub>. The residue was subjected to column chromatography on silica gel with DCM:Pet. Ether (60:40) as the solvent to afford the title compound in 85% yield.

**<sup>1</sup>H NMR (400 MHz, CDCl<sub>3</sub>, 293 K):** δ 8.60 (d, *J* = 5.7 Hz, 1H), 8.05 (dd, *J* = 8.5 Hz, *J* = 0.9 Hz, 1H), 7.89 (d, *J* = 8.2 Hz, 1H), 7.70 (ddd, *J* = *J* = 8.1 Hz, *J* = 1.2 Hz, 1H), 7.67 – 7.63 (m, 3H), 7.57 – 7.50 (m, 3H).

**<sup>13</sup>C NMR (100 MHz, CDCl<sub>3</sub>, 293 K):** δ 159.4, 142.2, 138.0, 136.9, 134.8, 131.3, 130.1, 128.6, 127.4, 127.1, 127.1, 126.6, 120.2.

**FTIR:** 3051, 1488, 1028, 818 cm<sup>-1</sup>.

**HRMS (EI):** calculated for C<sub>15</sub>H<sub>10</sub>NCl (M<sup>+</sup>) 239.0502; found for C<sub>15</sub>H<sub>10</sub>NCl (M<sup>+</sup>) 239.0478.

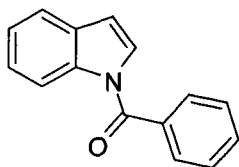
**Melting point (acetone/DCM):** 73 – 75°C.

**R<sub>f</sub> (DCM: Pet. Ether (60:40)):** 0.10.

## 5.3. Oxidative Arylation of Indoles

### 5.3.1. Intramolecular Oxidative Ring Closure of *N*-Benzoylindole.

#### Compound 3.13



The above compound was prepared according to literature procedure<sup>15e</sup> and its <sup>1</sup>H NMR spectral data was consistent with that previously reported.<sup>77a</sup>

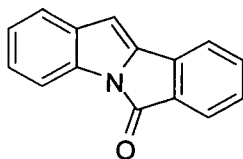
**<sup>1</sup>H NMR (400 MHz, CDCl<sub>3</sub>, 293 K):** δ 8.41 (dd, *J* = 8.1 Hz, *J* = 0.8 Hz, 1H), 7.74 – 7.72 (m, 2H), 7.61 – 7.57 (m, 2H), 7.53 – 7.49 (m, 2H), 7.38 (ddd, *J* = *J* = 7.3 Hz, *J* = 1.2 Hz, 1H), 7.32 (dd, *J* = 7.7 Hz, *J* = 1.1 Hz, 1H), 7.29 (d, *J* = 3.7 Hz, 1H), 6.61 (d, *J* = 3.8 Hz, 1H).

<sup>160</sup> Aoyagi, Y.; Abe, T.; Ohta, A. *Synthesis*, 1997, 8, 891

## Representative procedure for the intramolecular oxidative coupling of *N*-benzoylindoles

Pd(TFA)<sub>2</sub> (0.0081 g, 0.024 mmol, 10 mol%), 3-nitropyridine (0.0033 g, 0.027 mmol, 10 mol%) and CsOPiv (0.0261 g, 0.111 mmol, 0.47 mol%) were weighed into a Schlenk flask containing a stir bar open to air. The flask was partially sealed and evacuated and re-filled with oxygen (this cycle was done 5 times). A stock solution of *N*-benzoylindole (0.1 M) in *t*-AmOH : PivOH (4 : 1) was prepared (gentle heating is necessary to completely solubilize all of the *N*-benzoylindole). The stock solution (2.3 mL, 0.237 mmol, 1 eq of *N*-benzoylindole) was added to the Schlenk flask via syringe under a flow of O<sub>2</sub>. The flask was then completely sealed and stirred at 100°C for 2 days. After cooling to room temperature the reaction was filtered over celite washing with DCM. The organic layer was washed twice with a saturated solution of Na<sub>2</sub>CO<sub>3</sub> and the combined aqueous layers were washed once with an additional amount of DCM. The combined organic layers were dried over MgSO<sub>4</sub>, filtered and the solvent removed under reduced pressure. Purification by flash chromatography on silica gel with 45% DCM in hexanes afforded the desired product in 74% yield.

### Compound 3.14



This compound was prepared by the above procedure and its <sup>1</sup>H NMR spectral data was consistent with that previously reported.<sup>15e</sup>

**<sup>1</sup>H NMR (400 MHz, CDCl<sub>3</sub>, 293 K):** δ 7.88 (d, *J* = 8.0 Hz, 1H), 7.74 (d, *J* = 7.5 Hz, 1H), 7.50 – 7.48 (m, 2H), 7.43 (d, 7.8 Hz, 1H), 7.34 – 7.25 (m, 2H), 7.14 (ddd, *J* = *J* = 7.7 Hz, *J* = 0.9 Hz, 1H), 6.59 (s, 1H).

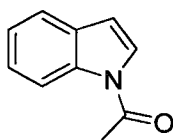
### 5.3.2. Acetylation of Indoles and Characterization Data.

#### General procedure for the acetylation of indoles

Indole (1.0194 g, 8.70 mmol, 1 eq.) and DMAP (0.2030 g, 1.66 mmol, 0.19 eq) were weighed into a flask. A reflux condenser (fitted with a rubber septum) was placed on the

flask and the system was purged with argon. DCE (20 mL, 0.44 M) was added to the flask via syringe followed by triethylamine (1.8 mL, 12.9 mmol, 1.5 eq), and acetic anhydride (1.6 mL, 16.9 mmol, 1.9 eq). The reaction was heated at 80°C for 24 hours. Upon cooling to room temperature the reaction was diluted with EtOAc (50 mL) and washed with a saturated solution of ammonium chloride (40 mL), and the aqueous layer was further extracted with EtOAc (3 x 20 mL). The combined organic layers were dried over MgSO<sub>4</sub> and the solvent evaporated. The residue was purified by flash chromatography on silica gel with ethyl acetate/hexanes as the solvent.

### Compound 3.15a

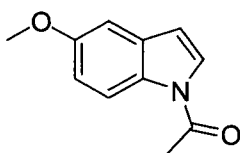


The above compound was prepared according to the general procedure and was subjected to column chromatography on silica gel with 15% ethyl acetate in hexanes as the eluent to afford the product in 86% yield (1.1911 g, 7.48 mmol). NMR spectra was consistent with that previously reported.<sup>161</sup>

**<sup>1</sup>H NMR (400 MHz, CDCl<sub>3</sub>, 293 K):** δ 8.43 (d, J = 8.1 Hz, 1H), 7.55 (d, J = 7.7 Hz, 1H), 7.38 – 7.31 (m, 2H), 7.26 (ddd, J = J = 7.6 Hz, J = 1.0 Hz, 1H), 6.61 (d, J = 3.8 Hz, 1H), 2.59 (s, 3H).

**<sup>13</sup>C NMR (100 MHz, CDCl<sub>3</sub>, 293 K):** δ 168.6 (C), 135.5 (C), 130.4 (C), 125.2 (CH), 125.0 (CH), 123.6 (CH), 120.8 (CH), 116.5 (CH), 109.1 (CH), 23.9 (CH<sub>3</sub>).

### Compound 3.15b



The above compound was prepared according to the general procedure and was subjected to column chromatography on silica gel with 15% ethyl acetate in hexanes as the eluent to afford the product in 83% yield (0.4304 g, 2.27 mmol). NMR spectra was consistent with that previously reported.<sup>162</sup>

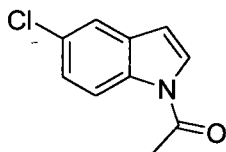
**<sup>1</sup>H NMR (400 MHz, CDCl<sub>3</sub>, 293 K):** δ 8.32 (d, J = 8.5 Hz, 1H), 7.38 (d, J = 3.2 Hz, 1H), 7.02 (d, J = 2.5 Hz, 1H), 6.95 (dd, J = 9.0 Hz, J = 2.5 Hz, 1H), 6.56 (d, J = 3.7 Hz, 1H), 3.85 (s, 3H), 2.60 (s, 3H).

<sup>161</sup> Aldrich. Reg. # 576-15-8.

<sup>162</sup> Kametani, T.; Ohsawa, M.; Ihara, M. *J. Chem. Soc.* **1981**, *1*, 290.

**<sup>13</sup>C NMR (100 MHz, CDCl<sub>3</sub>, 293 K):** δ 168.3 (C), 156.5 (C), 131.4 (C), 130.3 (C), 125.9 (CH), 117.3 (CH), 113.5 (CH), 109.0 (CH), 103.6 (CH), 55.6 (CH<sub>3</sub>), 23.7 (CH<sub>3</sub>).

### Compound 3.15c



The above compound was prepared according to the general procedure and was subjected to column chromatography on silica gel with 15% ethyl acetate in hexanes as the eluent to afford the product in 97% yield (0.3722 g, 1.92 mmol).

**<sup>1</sup>H NMR (400 MHz, CDCl<sub>3</sub>, 293 K):** δ 8.36 (d, J = 8.8 Hz, 1H), 7.51 (d, J = 1.9 Hz, 1H), 7.42 (d, J = 3.8 Hz, 1H), 7.29 (dd, J = 8.8 Hz, J = 2.0 Hz, 1H), 6.57 (d, J = 3.7 Hz, 1H), 2.62 (s, 3H).

**<sup>13</sup>C NMR (100 MHz, CDCl<sub>3</sub>, 293 K):** δ 168.5 (C), 133.9 (C), 131.6 (C), 129.2 (C), 126.4 (CH), 125.2 (CH), 120.4 (CH), 117.6 (CH), 108.4 (CH), 23.8 (CH<sub>3</sub>).

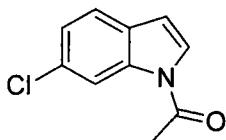
**FTIR:** 3148, 1702, 720 cm<sup>-1</sup>.

**HRMS (EI):** calculated for C<sub>10</sub>H<sub>8</sub>NOCl (M<sup>+</sup>) 193.0294; found for C<sub>10</sub>H<sub>8</sub>NOCl (M<sup>+</sup>) 193.0310.

**Melting point (ethyl acetate/hexanes):** 101 – 102°C.

**R<sub>f</sub> (15% ethyl acetate in hexanes):** 0.25.

### Compound 3.15d



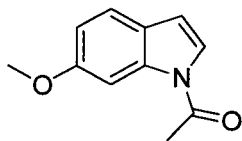
The above compound was prepared according to the general procedure and was subjected to column chromatography on silica gel with 15% ethyl acetate in hexanes as the eluent to afford the product in 95% yield (0.4876 g, 2.52 mmol). NMR spectra was consistent with that previously reported.<sup>163</sup>

**<sup>1</sup>H NMR (400 MHz, CDCl<sub>3</sub>, 293 K):** δ 8.49 (s, 1H), 7.45 (d, J = 8.3 Hz, 1H), 7.39 (d, J = 3.7 Hz, 1H), 7.24 (dd, J = 8.3 Hz, J = 1.9 Hz, 1H), 6.60 (d, J = 3.8 Hz, 1H), 2.62 (s, 3H).

**<sup>13</sup>C NMR (100 MHz, CDCl<sub>3</sub>, 293 K):** δ 168.5 (C), 135.8 (C), 131.1 (C), 128.8 (C), 125.8 (CH), 124.3 (CH), 121.5 (CH), 116.8 (CH), 108.8 (CH), 23.9 (CH<sub>3</sub>).

<sup>163</sup> Kasahara, A.; Izumi, T.; Murakami, S.; Miyamoto, K.; Hino, T. *J. Het. Chem.* **1989**, *26*, 1405.

### Compound 3.15e

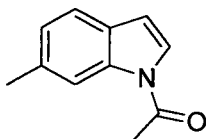


The above compound was prepared according to the general procedure and was subjected to column chromatography on silica gel with 15% ethyl acetate in hexanes as the eluent to afford the product in 82% yield (0.4223 g, 2.23 mmol). NMR spectra was consistent with that previously reported.<sup>163</sup>

**<sup>1</sup>H NMR (400 MHz, CDCl<sub>3</sub>, 293 K):**  $\delta$  8.06 (s, 1H), 7.41 (d, J = 8.5 Hz, 1H), 7.27 (d, J = 3.7 Hz, 1H), 6.91 (dd, J = 8.5 Hz, J = 2.4 Hz, 1H), 6.55 (d, J = 3.7 Hz, 1H), 3.87 (s, 3H), 2.60 (s, 3H).

**<sup>13</sup>C NMR (100 MHz, CDCl<sub>3</sub>, 293 K):**  $\delta$  168.9 (C), 158.4 (C), 136.6 (C), 124.0 (C), 123.9 (CH), 121.1 (CH), 113.0 (CH), 109.1 (CH), 100.7 (CH), 55.7 (CH<sub>3</sub>), 24.0 (CH<sub>3</sub>).

### Compound 3.15f

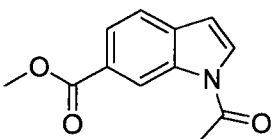


The above compound was prepared according to the general procedure and was subjected to column chromatography on silica gel with 10% ethyl acetate in hexanes as the eluent to afford the product in 89% yield (0.5874 g, 3.39 mmol). NMR spectra was consistent with that previously reported.<sup>163</sup>

**<sup>1</sup>H NMR (400 MHz, CDCl<sub>3</sub>, 293 K):**  $\delta$  8.28 (s, 1H), 7.43 (d, J = 7.9 Hz, 1H), 7.32 (d, J = 3.7 Hz, 1H), 7.10 (d, J = 7.9 Hz, 1H), 6.58 (d, J = 3.8 Hz, 1H), 2.61 (s, 3H), 2.49 (s, 3H).

**<sup>13</sup>C NMR (100 MHz, CDCl<sub>3</sub>, 293 K):**  $\delta$  168.7 (C), 135.9 (C), 135.2 (C), 128.1 (C), 125.1 (CH), 124.6 (CH), 120.3 (CH), 116.8 (CH), 109.1 (CH), 24.0 (CH<sub>3</sub>), 21.9 (CH<sub>3</sub>).

### Compound 3.15g



The above compound was prepared according to the general procedure and was subjected to column chromatography on silica gel with 30% ethyl acetate in hexanes as the eluent to afford the product in 99% yield (0.4871 g, 2.24 mmol). NMR spectra was consistent with that previously reported.<sup>163</sup>

**<sup>1</sup>H NMR (400 MHz, CDCl<sub>3</sub>, 293 K):** δ 9.10 (s, 1H), 7.98 (dd, J = 8.2 Hz, J = 1.6 Hz, 1H), 7.60 (d, J = 8.2 Hz, 1H), 7.58 (d, J = 3.7 Hz, 1H), 6.68 (d, J = 3.7 Hz, 1H), 3.95 (s, 3H), 2.67 (s, 3H).

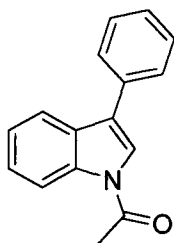
**<sup>13</sup>C NMR (100 MHz, CDCl<sub>3</sub>, 293 K):** δ 168.4 (C), 167.6 (C), 135.0 (C), 134.1 (C), 128.1 (CH), 126.9 (C), 124.9 (CH), 120.6 (CH), 118.2 (CH), 108.9 (CH), 52.1 (CH<sub>3</sub>), 24.0 (CH<sub>3</sub>).

### 5.3.3. Oxidative C3-Arylation of *N*-Acetylindoles and Characterization Data.

#### General procedure for the C-3 arylation of indoles (First Generation Conditions):

All coupling reactions were performed on a 0.6 mmol (indole substrate) scale at 0.3 M unless otherwise stated. A stock solution of *N*-acetylindole (0.1069 g, 0.6715 mmol, 0.295 M) was prepared in benzene:PivOH (2.2 mL; 4:1 v/v). Pd(TFA)<sub>2</sub> (0.0197 g, 0.059 mmol, 10 mol %), 3-nitropyridine (0.0074 g, 0.059 mmol, 10 mol %), Cu(OAc)<sub>2</sub> (0.3314 g, 1.82 mmol, 3 eq), and CsOPiv (0.0588 g, 0.25 mmol, 0.40 eq) were weighed into a microwave tube. 2.0 mL of the *N*-acetylindole (0.589 mmol, 1 eq) stock solution was added to the tube and it was sealed. The tube was placed in a CEM Discover Microwave (conditions: power: 300 W; temp.: 140°C; max. pressure: 250 psi; time: 5 hours). The crude reaction mixture was analyzed by GC-MS and showed 88% yield for the C3 arylation product in a ~10:1 ratio for C3:C2 arylation. The crude reaction mixture was then filtered over celite and washed with EtOAc. The solvent was removed and the residue was partitioned between EtOAc (50 mL) and a saturated aqueous solution of ammonium chloride (50 mL) and stirred at room temperature for ~30 min.. The layers were separated and the small emulsion that formed was removed to a separate flask. The organic layer was washed with a further 50 mL of ammonium chloride, followed by 50 mL of brine. The combined aqueous fractions were back extracted with EtOAc (3 x 50 mL). 50 mL of EtOAc was added to the removed emulsion and sonicated to break-up the emulsion; this was washed with 50 mL of brine. This was repeated a second time on any remaining emulsion. The combined organic layers were dried over MgSO<sub>4</sub>. The solvent was removed and the resulting residue was flashed over a short pad of silica gel (5 x 3 cm) with 30% EtOAc in hexanes (a second flash on a longer pad of silica with the solvent systems described below is necessary to separate the indole regioisomers and to completely remove all of the pivalic acid).

### Compound 3.37a



The above compound was prepared according to the general procedure and was subjected to column chromatography on silica gel with 15% ethyl acetate in hexanes as the eluent to afford the product in 87% yield (0.1210 g, 0.514 mmol).

**<sup>1</sup>H NMR (400 MHz, CDCl<sub>3</sub>, 293 K):** δ 8.52 (d, J = 8.1 Hz, 1H), 7.80 (d, J = 7.9 Hz, 1H), 7.63 (dd, J = 8.2, J = 1.4 Hz, 2H), 7.52 – 7.45 (m, 3H), 7.44 – 7.31 (m, 3H), 2.68 (s, 3H).

**<sup>13</sup>C NMR (100 MHz, CDCl<sub>3</sub>, 293 K):** δ 168.6 (C), 136.3 (C), 133.4 (C), 129.0 (C), 128.9 (CH), 128.0 (CH), 127.6 (CH), 125.5 (CH), 124.0 (C), 123.9 (CH), 122.0 (CH), 119.9 (CH), 116.8 (CH), 24.1 (CH<sub>3</sub>).

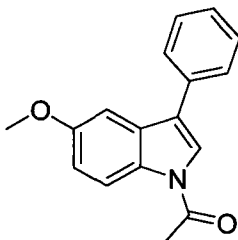
**FTIR:** 3116, 1697, 768, 751, 698 cm<sup>-1</sup>.

**HRMS (EI):** calculated for C<sub>16</sub>H<sub>13</sub>NO (M<sup>+</sup>) 235.0997; found for C<sub>16</sub>H<sub>13</sub>NO (M<sup>+</sup>) 235.0995.

**Melting point (ethyl acetate/hexanes):** 138 – 139°C.

**R<sub>f</sub> (10% ethyl acetate in hexanes):** 0.22.

### Compound 3.37b



The above compound was prepared according to the general procedure and was subjected to column chromatography on silica gel with 15% ethyl acetate in hexanes as the eluent to afford the product in 84% yield (0.1332 g, 0.502 mmol).

**<sup>1</sup>H NMR (400 MHz, CDCl<sub>3</sub>, 293 K):** δ 8.41 (d, J = 8.5 Hz, 1H), 7.61 (d, J = 7.3 Hz, 2H), 7.51 – 7.46 (m, 3H), 7.39 (t, J = 7.2, 1H), 7.23 (d, J = 2.5, 1H), 7.01 (dd, J = 9.0 Hz, J = 2.5 Hz, 1H), 3.85 (s, 3H), 2.64 (s, 3H).

**<sup>13</sup>C NMR (100 MHz, CDCl<sub>3</sub>, 293 K):** δ 168.2 (C), 156.8 (C), 133.4 (C), 131.0 (C), 130.0 (C), 129.0 (CH), 127.9 (CH), 127.5 (CH), 123.8 (C), 122.7 (CH), 117.6 (CH), 113.7 (CH), 102.8 (CH), 55.7 (CH<sub>3</sub>), 24.1 (CH<sub>3</sub>).

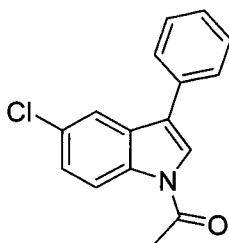
**FTIR:** 3009, 1699, 762, 698 cm<sup>-1</sup>.

**HRMS (EI):** calculated for C<sub>17</sub>H<sub>15</sub>NO<sub>2</sub> (M<sup>+</sup>) 265.1103; found for C<sub>17</sub>H<sub>15</sub>NO<sub>2</sub> (M<sup>+</sup>) 265.1098.

**Melting point (ethyl acetate/hexanes):** 131.7 – 132.5°C.

**R<sub>f</sub> (15% ethyl acetate in hexanes):** 0.25.

### Compound 3.37c



Under the general procedure described above a significant amount (~ 10%) of dehalogenated product and trace amounts of dehalogenated starting material were observed. The above compound was prepared according to an alternative procedure described below. A stock solution of *N*-acetyl-5-chloroindole (0.0720 g, 0.372 mmol, 0.31 M) was prepared in benzene:PivOH (1.2 mL, 4:1 v/v). Pd(TFA)<sub>2</sub> (0.0106 g, 0.03 mmol, 10 mol %), 3-nitropyridine (0.0040 g, 0.03 mmol, 10 mol %), Cu(OAc)<sub>2</sub> (0.1695 g, 0.933 mmol, 3 eq), and CsOPiv (0.0322 g, 0.13 mmol, 0.40 eq) were weighed into a Schlenk tube. 1.0 mL (0.31 mmol, 1 eq.) of the stock solution was transferred to the Schlenk tube via syringe and the tube was sealed and heated to 110°C for 48 hours. The work-up described in the general procedure was carried out and the product was isolated in 63% yield (0.0532 g, 0.195 mmol).

**<sup>1</sup>H NMR (400 MHz, CDCl<sub>3</sub>, 293 K):** δ 8.44 (d, *J* = 8.8 Hz, 1H), 7.74 (d, *J* = 2.0 Hz, 1H), 7.58 (d, *J* = 8.4 Hz, 2H), 7.51 – 7.46 (m, 3H), 7.40 (t, *J* = 7.3, 1H), 7.34 (dd, *J* = 8.9 Hz, *J* = 2.0 Hz, 1H), 2.67 (s, 3H).

**<sup>13</sup>C NMR (100 MHz, CDCl<sub>3</sub>, 293 K):** δ 168.4 (C), 134.6 (C), 132.6 (C), 130.3 (C), 129.7 (C), 129.1 (CH), 127.9 (CH), 127.8 (CH), 125.7 (CH), 123.4 (C), 123.1 (CH), 119.6 (CH), 117.9 (CH), 23.9 (CH<sub>3</sub>).

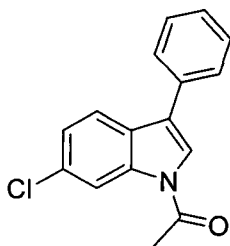
**FTIR:** 3115, 1708, 925, 801, 762 cm<sup>-1</sup>.

**HRMS (EI):** calculated for C<sub>16</sub>H<sub>12</sub>NOCl (M<sup>+</sup>) 269.0607; found for C<sub>16</sub>H<sub>12</sub>NOCl (M<sup>+</sup>) 269.0607.

**Melting point (ethyl acetate/hexanes):** 138 – 139°C.

**R<sub>f</sub> (15% ethyl acetate in hexanes):** 0.29.

### Compound 3.37d



The above compound was prepared according to the procedure described for **1c** (however on 0.6 mmol scale) and was subjected to column chromatography on silica gel with toluene:ethyl acetate:hexanes (1:1:8) as the eluent to afford the product in 61% yield (0.0988 g, 0.366 mmol).

**<sup>1</sup>H NMR (400 MHz, CDCl<sub>3</sub>, 293 K):** δ 8.57 (s, 1H), 7.68 (d, J = 8.4 Hz, 1H), 7.59 (d, J = 7.0 Hz, 2H), 7.50 – 7.46 (m, 3H), 7.39 (t, J = 7.3 Hz, 1H), 7.30 (dd, J = 8.4 Hz, J = 1.9 Hz, 1H), 2.66 (s, 3H).

**<sup>13</sup>C NMR (100 MHz, CDCl<sub>3</sub>, 293 K):** δ 168.5 (C), 136.5 (C), 132.8 (C), 131.5 (C), 129.0 (CH), 127.9 (CH), 127.8 (CH), 127.5 (C), 124.5 (CH), 123.8 (C), 122.4 (CH), 120.6 (CH), 117.1 (CH), 23.9 (CH<sub>3</sub>).

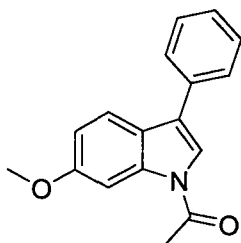
**FTIR:** 3114, 1705, 962, 820, 696 cm<sup>-1</sup>.

**HRMS (EI):** calculated for C<sub>16</sub>H<sub>12</sub>NOCl (M<sup>+</sup>) 269.0607; found for C<sub>16</sub>H<sub>12</sub>NOCl (M<sup>+</sup>) 269.0601.

**Melting point (toluene/ethyl acetate/hexanes):** 132 – 133°C.

**R<sub>f</sub> (toluene:ethyl acetate:hexanes (1:1:8)):** 0.19.

### Compound 3.37e



The above compound was prepared according to the general procedure and was subjected to column chromatography on silica gel with 15% ethyl acetate in hexanes as the eluent to afford the product in 74% yield (0.1183 g, 0.446 mmol) as an oil.

**<sup>1</sup>H NMR (400 MHz, CDCl<sub>3</sub>, 293 K):** δ 8.13 (s, 1H), 7.68 – 7.61 (m, 3H), 7.47 (dd, J = J = 7.5 Hz, 2H), 7.40 – 7.35 (m, 2H), 6.96 (dd, J = 8.7 Hz, J = 2.5 Hz, 1H), 3.90 (s, 3H), 2.66 (s, 3H).

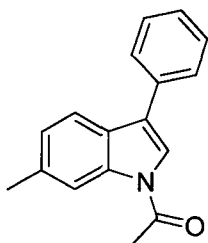
**<sup>13</sup>C NMR (100 MHz, CDCl<sub>3</sub>, 293 K):** δ 168.8 (C), 158.6 (C), 137.4 (C), 133.5 (C), 128.9 (CH), 127.8 (CH), 127.5 (CH), 124.0 (C), 122.7 (C), 120.6 (CH), 120.3 (CH), 113.2 (CH), 100.9 (CH), 55.7 (CH<sub>3</sub>), 24.1 (CH<sub>3</sub>).

**FTIR:** 2939, 1705, 963, 700, 657 cm<sup>-1</sup>.

**HRMS (EI):** calculated for C<sub>17</sub>H<sub>15</sub>NO<sub>2</sub> (M<sup>+</sup>) 265.1103; found for C<sub>17</sub>H<sub>15</sub>NO<sub>2</sub> (M<sup>+</sup>) 265.1084.

**R<sub>f</sub> (15% ethyl acetate in hexanes):** 0.27.

### Compound 3.37f



The above compound was prepared according to the general procedure and was subjected to column chromatography on silica gel with 10% ethyl acetate in hexanes as the eluent to afford the product in 81% yield (0.1234 g, 0.495 mmol).

**<sup>1</sup>H NMR (400 MHz, CDCl<sub>3</sub>, 293 K):** δ 8.36 (s, 1H), 7.68 (d, J = 8.0 Hz, 1H), 7.63 (d, J = 7.1 Hz 2H), 7.49 – 7.43 (m, 3H), 7.37 (t, J = 7.4, 1H), 7.16 (dd, J = 8.1 Hz, J = 0.8 Hz, 1H), 2.66 (s, 3H), 2.51 (s, 3H).

**<sup>13</sup>C NMR (100 MHz, CDCl<sub>3</sub>, 293 K):** δ 168.6 (C), 136.7 (C), 135.7 (C), 133.5 (C), 128.9 (CH), 127.9 (CH), 127.5 (CH), 126.7 (C), 125.4 (CH), 124.0 (C), 121.4 (CH), 119.5 (CH), 117.1 (CH), 24.1 (CH<sub>3</sub>) 21.9 (CH<sub>3</sub>).

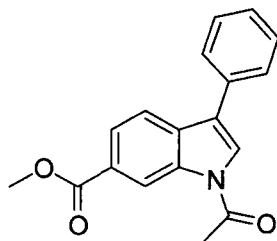
**FTIR:** 3031, 1705, 963, 699 cm<sup>-1</sup>.

**HRMS (EI):** calculated for C<sub>17</sub>H<sub>15</sub>NO (M<sup>+</sup>) 249.1154; found for C<sub>17</sub>H<sub>15</sub>NO (M<sup>+</sup>) 249.1156.

**Melting point (ethyl acetate/hexanes):** 110 – 111°C.

**R<sub>f</sub> (10% ethyl acetate in hexanes):** 0.17.

### Compound 3.37g



The above compound was prepared according to the general procedure (20 mol% Pd(TFA)<sub>2</sub> and 3-nitropyridine; time: 10 hours) and was subjected to column chromatography on silica gel with toluene:ethyl acetate:hexanes (1:2:7) as the eluent to afford the product in 54% yield (0.0950 g, 0.324 mmol).

**<sup>1</sup>H NMR (400 MHz, CDCl<sub>3</sub>, 293 K):** δ 9.13 (s, 1H), 8.03 (dd, J = 8.3 Hz, J = 1.5 Hz, 1H), 7.83 (d, J = 8.3 Hz, 1H), 7.66 (s, 1H), 7.62 (d, J = 7.0 Hz, 2H), 7.50 (dd, J = J = 7.3 Hz, 2H), 7.41 (t, J = 7.3 Hz, 1H), 3.96 (s, 3H), 2.72 (s, 3H).

**<sup>13</sup>C NMR (100 MHz, CDCl<sub>3</sub>, 293 K):** δ 168.3 (C), 167.4 (C), 135.7 (C), 132.7 (C), 132.6 (C), 129.1 (CH), 128.0 (CH), 127.9 (CH), 127.2 (C), 125.2 (CH), 124.8 (CH), 123.8 (C), 119.6 (CH), 118.5 (CH) 52.2 (CH<sub>3</sub>), 24.1 (CH<sub>3</sub>).

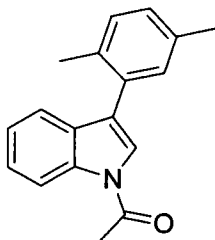
**FTIR:** 3139, 1714, 773, 741 cm<sup>-1</sup>.

**HRMS (EI):** calculated for C<sub>18</sub>H<sub>15</sub>NO<sub>3</sub> (M<sup>+</sup>) 293.1052; found for C<sub>18</sub>H<sub>15</sub>NO<sub>3</sub> (M<sup>+</sup>) 293.1054.

**Melting point (toluene/ethyl acetate/hexanes):** 161 – 163°C.

**R<sub>f</sub> (toluene:ethyl acetate:hexanes (1:2:7)):** 0.28.

### Compound 3.37h



The above compound was prepared according to the general procedure (20 mol% Pd(TFA)<sub>2</sub> and 3-nitropyridine; time: 10 hours) and was purified by preparative thin-layer chromatography on silica gel with 15% ethyl acetate in hexanes as the eluent to afford the product in 45% yield (0.0672 g, 0.26 mmol).

**<sup>1</sup>H NMR (400 MHz, CDCl<sub>3</sub>, 293 K):** δ 8.50 (d, J = 7.9 Hz, 1H), 7.41 – 7.35 (m, 3H), 7.27 (ddd, J = J = 7.9 Hz, J = 1.0 Hz, 1H), 7.23 (d, J = 7.6 Hz, 1H), 7.17 – 7.12 (m, 2H), 2.66 (s, 3H), 2.36 (s, 3H), 2.24 (s, 3H).

**<sup>13</sup>C NMR (100 MHz, CDCl<sub>3</sub>, 293 K):** δ 168.6 (C), 135.6 (C), 135.3 (C), 133.8 (C), 132.2 (C), 131.2 (CH), 130.4 (CH, two overlapping signals), 128.7 (CH), 125.3 (CH), 123.8 (CH), 123.7 (CH), 122.9 (CH), 120.3 (CH), 116.7 (CH), 24.1 (CH<sub>3</sub>), 20.9 (CH<sub>3</sub>), 20.0 (CH<sub>3</sub>).

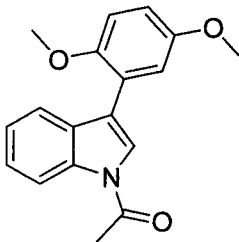
**FTIR:** 3019, 1709, 750 cm<sup>-1</sup>.

**HRMS (EI):** calculated for C<sub>18</sub>H<sub>17</sub>NO (M<sup>+</sup>) 263.1310; found for C<sub>18</sub>H<sub>17</sub>NO (M<sup>+</sup>) 263.1322.

**Melting point (ethyl acetate/hexanes):** 82 – 84°C.

**R<sub>f</sub> (15% ethyl acetate in hexanes):** 0.4.

### Compound 3.37i



The 1,4-dimethoxybenzene coupling partner was a solid and therefore an alternate procedure was used. *N*-Acetylindole (0.0968 g, 0.608 mmol), 1,4-dimethoxybenzene (1.6832 g, 12.2 mmol, 20 eq.) and pivalic acid (0.3576 g, 3.51 mmol, 5.8 eq.) were weighed into a microwave tube. Pd(TFA)<sub>2</sub> (0.0411 g, 0.123 mmol, 20 mol%), 3-nitropyridine (0.0150 g, 0.121 mmol, 20 mol%), CsOPiv (0.0548 g, 0.234 mmol, 40 mol%), and Cu(OAc)<sub>2</sub> (0.3320 g, 1.83 mmol, 3 eq.) were weighed onto a single weighing paper. The *N*-acetylindole/1,4-dimethoxybenzene/pivalic acid mixture was heated with a heat gun until all the solids had melted into a clear light yellow solution and then the Pd(TFA)<sub>2</sub>, 3-nitropyridine, CsOPiv, and Cu(OAc)<sub>2</sub> were added in one portion and the tube was sealed. It was heated in a CEM Discover Microwave (conditions: power: 300 W; temp.: 140°C; max. pressure: 250 psi; time: 10 hours and was subjected to the work-up described in the general procedure and purified

by column chromatography on silica gel with 20% ethyl acetate in hexanes as the eluent to afford the product in 52% yield (0.0921 g, 0.312 mmol).

**<sup>1</sup>H NMR (400 MHz, (CD<sub>3</sub>)<sub>2</sub>SO, 293 K):** δ 8.39 (d, J = 8.2 Hz, 1H), 7.94 (s, 1H), 7.50 (d, J = J = 7.6 Hz, 1H), 7.35 (dd, J = J = 7.7 Hz, 1H), 7.28 (dd, J = J = 7.6 Hz, 1H), 7.10 (d, J = 8.9 Hz, 1H), 7.05 (d, J = 3.0 Hz, 1H), 6.97 (dd, J = 9.0 Hz, J = 3.1 Hz, 1H), 3.77 (s, 3H), 3.73 (s, 3H), 2.69 (s, 3H).

**<sup>13</sup>C NMR (100 MHz, (CD<sub>3</sub>)<sub>2</sub>SO, 293 K):** δ 169.4 (C), 153.0 (C), 150.9 (C), 134.9 (C), 129.3 (C), 125.4 (CH), 124.5 (CH), 123.3 (CH), 122.3 (C), 120.5 (CH), 118.8 (C), 116.3 (CH), 115.8 (CH), 113.4 (CH), 112.6 (CH), 55.7 (CH<sub>3</sub>), 55.4 (CH<sub>3</sub>), 23.8 (CH<sub>3</sub>).

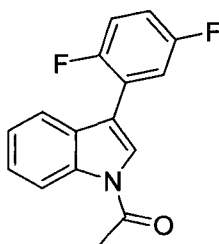
**FTIR:** 2934, 1707, 750 cm<sup>-1</sup>.

**HRMS (EI):** calculated for C<sub>18</sub>H<sub>17</sub>NO<sub>3</sub> (M<sup>+</sup>) 295.1208; found for C<sub>18</sub>H<sub>17</sub>NO<sub>3</sub> (M<sup>+</sup>) 295.1198.

**Melting point (ethyl acetate/hexanes):** 102 – 104°C.

**R<sub>f</sub> (20% ethyl acetate in hexanes):** 0.21.

### Compound 3.37j



The above compound was prepared according to the general procedure (20 mol% Pd(TFA)<sub>2</sub> and 3-nitropyridine; time: 10 hours) and was purified by preparative thin-layer chromatography on silica gel with 30% ethyl acetate in hexanes as the eluent to afford the product in 42% yield (0.0681 g, 0.251 mmol).

**<sup>1</sup>H NMR (400 MHz, CDCl<sub>3</sub>, 293 K):** δ 8.53 (d, J = 8.2 Hz, 1H), 7.71 – 7.66 (m, 2H), 7.42 (dd, J = J = 8.3 Hz, 1H), 7.39 – 7.32 (m, 2H), 7.20 – 7.14 (m, 1H), 7.06 – 7.00 (m, 1H), 2.69 (s, 3H).

**<sup>13</sup>C NMR (100 MHz, CDCl<sub>3</sub>, 293 K):** δ 168.6 (C), 158.7 (dd, J<sub>FC</sub> = 242.5 Hz, J<sub>FC</sub> = 2.2 Hz, C), 156.0 (dd, J<sub>FC</sub> = 243.6 Hz, J<sub>FC</sub> = 2.2 Hz, C), 135.8 (C), 128.7 (C), 125.7 (CH), 124.8 (d, J<sub>FC</sub> = 5.9 Hz, CH), 124.1 (CH), 122.4 (dd, J<sub>FC</sub> = 17.2 Hz, J<sub>FC</sub> = 8.8 Hz, C), 119.7 (d, J<sub>FC</sub> = 1.8 Hz, CH), 117.2 (dd, J<sub>FC</sub> = 25.7 Hz, J<sub>FC</sub> = 8.8 Hz, CH), 116.8 (CH), 116.8 (dd, J<sub>FC</sub> = 24.6 Hz, J<sub>FC</sub> = 4.0 Hz, CH), 115.9 (C), 115.2 (dd, J<sub>FC</sub> = 24.2 Hz, J<sub>FC</sub> = 8.4 Hz, CH), 24.1 (CH<sub>3</sub>).

**FTIR:** 3075, 1720, 747 cm<sup>-1</sup>.

**HRMS (EI):** calculated for C<sub>16</sub>H<sub>11</sub>NOF<sub>2</sub> (M<sup>+</sup>) 271.0809; found for C<sub>16</sub>H<sub>11</sub>NOF<sub>2</sub> (M<sup>+</sup>) 271.0825.

**Melting point (ethyl acetate/hexanes):** 133 – 134°C.

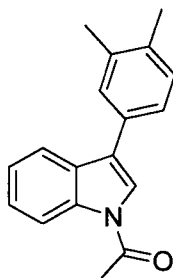
**R<sub>f</sub> (15% ethyl acetate in hexanes):** 0.3.

### General procedure for the C-3 arylation of indoles (Second Generation Conditions):

All coupling reactions were performed on a 0.60 mmol (indole substrate) scale at 0.30 M unless otherwise stated. Pd(acac)<sub>2</sub> (0.0176 g, 0.06 mmol, 10 mol %), *N*-acetylindole (0.0950

g, 0.60 mmol, 1 eq), Cu(OAc)<sub>2</sub> (0.3340 g, 1.8 mmol, 3 eq), and PivOH (0.3717 g, 3.6 mmol, 6 eq) were weighed into a 4 mL glass vial. 1.6 mL of *o*-xylene was added and the vial was sealed with a Teflon-lined cap. The vial was placed into one of the wells of an aluminum block and heated to 110°C for ~ 16 hours. The crude reaction mixture was filtered over celite and washed with ethyl acetate. The solvent was removed and the remaining *o*-xylene was removed under reduced pressure. The residue was redissolved in ethyl acetate and extracted with an aqueous solution of ammonium chloride (2 x 30 mL), the aqueous extracts were re-extracted with ethyl acetate. The solvent was removed and the residue was purified by flash chromatography with hexanes (50 mL), hexanes:EtOAc (98:2; 200 mL), hexanes:EtOAc (95:5; 200 mL) and hexanes (90:10; 100 mL)

### Compound 3.37k



The title compound was prepared according to the above procedure to afford the title compound in 61% yield.

**<sup>1</sup>H NMR (400 MHz, CDCl<sub>3</sub>, 293 K):** δ 8.51 (d, J = 8.1 Hz, 1H), 7.80 (d, J = 7.5 Hz, 1H), 7.46 (s, 1H), 7.41 – 7.37 (m, 3H), 7.33 (ddd, J = J = 7.9 Hz, J = 1.2 Hz 1H), 7.24 (d, J = 7.6 Hz, 1H), 2.67 (s, 3H), 2.35 (s, 3H), 2.33 (s, 3H).

**<sup>13</sup>C NMR (100 MHz, CDCl<sub>3</sub>, 293 K):** δ 168.5 (C), 137.2 (C), 136.3 (C), 136.1 (C), 130.8 (C), 130.2 (CH), 129.2 (C), 129.1 (CH), 125.4 (C), 125.4 (CH), 124.1 (C), 123.8 (CH), 121.6 (CH), 120.0 (CH), 116.8 (CH), 24.1 (CH<sub>3</sub>), 19.9 (CH<sub>3</sub>), 19.6 (CH<sub>3</sub>).

**FTIR:** 2921, 1705, 1448, 747 cm<sup>-1</sup>.

**HRMS (EI):** calculated for C<sub>18</sub>H<sub>17</sub>NO (M<sup>+</sup>) 263.1310; found for C<sub>18</sub>H<sub>17</sub>NO (M<sup>+</sup>) 263.1315.

**Melting point** (hexane/ethyl acetate) 123 – 125°C.

**R<sub>f</sub>** (10% ethyl acetate in hexanes): 0.22.

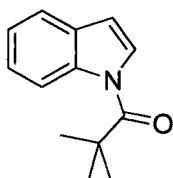
### 5.3.4. Pivaloylation of Indoles and Characterization Data.

#### General procedure for the pivaloylation of indoles :

Indole (2.0345 g, 17.4 mmol, 1 eq.) and DMAP (0.2097 g, 1.72 mmol, 0.1 eq.) were weighed into a round bottom flask. The flask was purged with argon and dry DCM (30 mL) was

added to yield a clear, colorless solution. Triethylamine (3.6 mL, 25.8 mmol, 1.48 eq.) was added and the flask was submerged into an ice-water bath and cooled to 0°C. Pivaloyl chloride (2.5 mL, 20.3 mmol, 1.17 eq.) was added to the flask slowly (over a period of 1 min.) via syringe and the reaction was allowed to stir at 0°C for ~ 10 min. The reaction was allowed to warm to room temperature and stirred overnight. The following morning the progress of the reaction was checked by tlc. The DCM was removed by rotary evaporation and the residue was partitioned between diethyl ether (50 mL) and a saturated solution of ammonium chloride (50 mL). The layers were separated and the etherial layer was washed with brine (25 mL). The combined aqueous layers were back extracted with a further 50 mL of diethyl ether and the combined organic fractions were dried with MgSO<sub>4</sub> and evaporated to dryness. Purification was performed under the specific conditions described below.

### Compound 3.15h



The title compound was prepared according to the above procedure and was subjected to column chromatography on silica gel with 5% diethyl ether in hexanes as the solvent to afford the title compound in 94% yield.

**<sup>1</sup>H NMR (400 MHz, CDCl<sub>3</sub>, 293 K):** δ 8.52 (dd, J = 8.4 Hz, J = 0.7 Hz, 1H), 7.72 (d, J = 3.8 Hz, 1H), 7.55 (d, J = 8.1 Hz, 1H), 7.34 (ddd, J = J = 8.3 Hz, J = 1.2 Hz, 1H), 7.26 (ddd, J = J = 8.3 Hz, J = 1.1 Hz, 1H), 6.61 (d, J = 3.8 Hz, 1H), 1.51 (s, 9H).

**<sup>13</sup>C NMR (100 MHz, CDCl<sub>3</sub>, 293 K):** δ 177.1 (C), 136.7 (C), 129.4 (C), 125.6 (CH), 125.1 (CH), 123.5 (CH), 120.5 (CH), 117.3 (CH), 108.2 (CH), 41.2 (C), 28.7 (CH<sub>3</sub>).

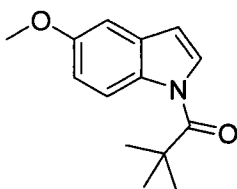
**FTIR:** 2980, 1692, 1448, 907 cm<sup>-1</sup>.

**HRMS (EI):** calculated for C<sub>13</sub>H<sub>15</sub>NO (M<sup>+</sup>) 201.1154; found for C<sub>13</sub>H<sub>15</sub>NO (M<sup>+</sup>) 201.1137.

**Melting point** (diethyl ether/hexanes) 68 - 70°C.

**R<sub>f</sub>** (5% diethyl ether in hexanes): 0.4.

### Compound 3.15i



The title compound was prepared according to the above procedure and was subjected to column chromatography on silica gel with 5% diethyl ether in hexanes to 10% diethyl ether in hexanes as the solvent to afford the title compound in 93% yield.

**<sup>1</sup>H NMR (400 MHz, CDCl<sub>3</sub>, 293 K):** δ 8.41 (d, J = 9.1 Hz, 1H), 7.70 (d, J = 3.8 Hz, 1H), 7.01 (d, J = 2.5 Hz, 1H), 6.95 (dd, J = 9.1 Hz, J = 2.6 Hz, 1H), 6.54 (d, J = 3.8 Hz, 1H), 3.85 (s, 3H), 1.51 (s, 9H).

**<sup>13</sup>C NMR (100 MHz, CDCl<sub>3</sub>, 293 K):** δ 176.7 (C), 156.4 (C), 131.5 (C), 130.3 (C), 126.3 (CH), 118.1 (CH), 113.4 (CH), 108.1 (CH), 103.3 (CH), 55.6 (CH<sub>3</sub>), 41.1 (C), 28.8 (CH<sub>3</sub>).

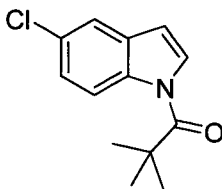
**FTIR:** 2981, 1689, 1473, 905 cm<sup>-1</sup>.

**HRMS (EI):** calculated for C<sub>14</sub>H<sub>17</sub>NO<sub>2</sub> (M<sup>+</sup>) 231.1259; found for C<sub>14</sub>H<sub>17</sub>NO<sub>2</sub> (M<sup>+</sup>) 231.1263.

**Melting point** (diethyl ether/hexanes) 99 - 100°C.

**R<sub>f</sub>** (10% diethyl ether in hexanes): 0.24.

### Compound 3.15j



The title compound was prepared according to the above procedure and was subjected to column chromatography on silica gel with 5% diethyl ether in hexanes as the solvent to afford the title compound in 76% yield.

**<sup>1</sup>H NMR (400 MHz, CDCl<sub>3</sub>, 293 K):** δ 8.44 (d, J = 8.9 Hz, 1H), 7.76 (d, J = 3.8 Hz, 1H), 7.52 (d, J = 2.2 Hz, 1H), 7.29 (dd, J = 8.9 Hz, J = 2.2 Hz, 1H), 6.56 (d, J = 3.8 Hz, 1H), 1.52 (s, 9H).

**<sup>13</sup>C NMR (100 MHz, CDCl<sub>3</sub>, 293 K):** δ 177.0 (C), 135.1 (C), 130.6 (C), 129.0 (C), 126.8 (CH), 125.2 (CH), 120.1 (CH), 118.3 (CH), 107.5 (CH), 41.3 (C), 28.7 (CH<sub>3</sub>).

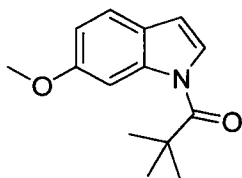
**FTIR:** 2973, 1690, 1493, 905 cm<sup>-1</sup>.

**HRMS (EI):** calculated for C<sub>13</sub>H<sub>14</sub>NOCl (M<sup>+</sup>) 235.0764; found for C<sub>13</sub>H<sub>14</sub>NOCl (M<sup>+</sup>) 235.0757.

**Melting point** (diethyl ether/hexanes) 106 - 107°C.

**R<sub>f</sub>** (5% diethyl ether in hexanes): 0.28.

### Compound 3.15k



The title compound was prepared according to the above procedure and was subjected to column chromatography on silica gel with 10% diethyl ether in hexanes as the solvent to afford the title compound in 78% yield.

**<sup>1</sup>H NMR (400 MHz, CDCl<sub>3</sub>, 293 K):** δ 8.16 (d, J = 2.4 Hz, 1H), 7.62 (d, J = 3.8 Hz, 1H), 7.41 (d, J = 8.5 Hz, 1H), 6.91 (dd, J = 8.5 Hz, J = 2.5 Hz, 1H), 6.54 (d, J = 3.8 Hz, 1H), 3.88 (s, 3H), 1.51 (s, 9H).

**<sup>13</sup>C NMR (100 MHz, CDCl<sub>3</sub>, 293 K):** δ 177.4 (C), 158.4 (C), 137.7 (C), 124.4 (CH), 123.1 (C), 120.8 (CH), 113.2 (CH), 108.2 (CH), 101.2 (CH), 55.6 (CH<sub>3</sub>), 41.3 (C), 28.7 (CH<sub>3</sub>).

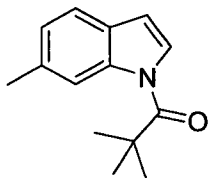
**FTIR:** 2980, 1692, 1310, 903. 804 cm<sup>-1</sup>.

**HRMS (EI):** calculated for C<sub>14</sub>H<sub>17</sub>NO<sub>2</sub> (M<sup>+</sup>) 231.1259; found for C<sub>14</sub>H<sub>17</sub>NO<sub>2</sub> (M<sup>+</sup>) 231.1249.

**Melting point** (diethyl ether/hexanes) 110 - 112°C.

**R<sub>f</sub>** (10% diethyl ether in hexanes): 0.39.

### Compound 3.15l



The title compound was prepared according to the above procedure and was subjected to column chromatography on silica gel with 2% diethyl ether in hexanes as the solvent to afford the title compound in 72% yield.

**<sup>1</sup>H NMR (400 MHz, CDCl<sub>3</sub>, 293 K):** δ 8.38 (d, J = 0.7 Hz, 1H), 7.65 (d, J = 3.8 Hz, 1H), 7.42 (d, J = 7.9 Hz, 1H), 7.09 (dd, J = 7.9 Hz, J = 0.9 Hz, 1H), 6.56 (d, J = 3.8 Hz, 1H), 2.48 (s, 3H), 1.50 (s, 9H).

**<sup>13</sup>C NMR (100 MHz, CDCl<sub>3</sub>, 293 K):** δ 177.2 (C), 137.1 (C), 135.2 (C), 127.1 (C), 125.1 (CH), 124.9 (CH), 120.0 (CH), 117.6 (CH), 108.2 (CH), 41.2 (C), 28.7 (CH<sub>3</sub>), 22.0 (CH<sub>3</sub>).

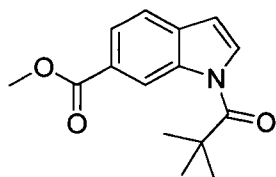
**FTIR:** 2980, 1692, 1310, 903, 804 cm<sup>-1</sup>.

**HRMS (EI):** calculated for C<sub>14</sub>H<sub>17</sub>NO<sub>1</sub> (M<sup>+</sup>) 215.1310; found for C<sub>14</sub>H<sub>17</sub>NO<sub>1</sub> (M<sup>+</sup>) 215.1312.

**Melting point** (diethyl ether/hexanes) 63 - 65°C.

**R<sub>f</sub>** (2% diethyl ether in hexanes): 0.27.

### Compound 3.15m



The title compound was prepared according to the above procedure and was subjected to column chromatography on silica gel with 10% diethyl ether in hexanes as the solvent to afford the title compound in 87% yield.

**<sup>1</sup>H NMR (400 MHz, CDCl<sub>3</sub>, 293 K):** δ 9.21 (s, 1H), 7.98 (dd, J = 8.2 Hz, J = 1.5 Hz, 1H), 7.88 (d, J = 3.8 Hz, 1H), 7.59 (d, J = 8.2 Hz, 1H), 6.65 (d, J = 3.8 Hz, 1H), 3.94 (s, 3H), 1.53 (s, 9H).

**<sup>13</sup>C NMR (100 MHz, CDCl<sub>3</sub>, 293 K):** δ 177.0 (C), 167.7 (C), 136.2 (C), 133.0 (C), 128.4 (CH), 126.8 (C), 124.9 (CH), 120.2 (CH), 119.1 (CH), 108.0 (CH), 52.0 (CH<sub>3</sub>), 41.4 (C), 28.6 (CH<sub>3</sub>).

**FTIR:** 2983, 1717, 904, 780 cm<sup>-1</sup>.

**HRMS (EI):** calculated for C<sub>15</sub>H<sub>17</sub>NO<sub>3</sub> (M<sup>+</sup>) 259.1208; found for C<sub>15</sub>H<sub>17</sub>NO<sub>3</sub> (M<sup>+</sup>) 259.1208.

**Melting point** (diethyl ether/hexanes) 93 - 94°C.

**R<sub>f</sub>** (10% diethyl ether in hexanes): 0.19.

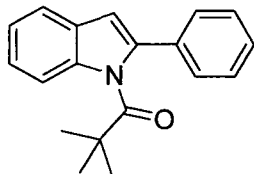
### 5.3.5. Oxidative C2-Arylation of *N*-Pivaloylindoles.

#### General procedure for the C2 arylation of *N*-pivaloylindoles (Third Generation Conditions)

All coupling reactions were performed on a 0.45 mmol (indole substrate) scale at 0.15 M unless otherwise stated. Pd(TFA)<sub>2</sub> (0.0079 g, 0.0237 mmol, 5 mol %), *N*-pivaloylindole (0.0923 g, 0.45 mmol, 1 eq), AgOAc (0.2291 g, 1.37 mmol, 3 eq), and PivOH (0.2788 g, 2.73 mmol, 6 eq) were weighed into a 4 mL glass vial. 2.7 mL of benzene was added and the vial was sealed with a Teflon lined closed cap. The vial was placed into one of the wells of an aluminum block and heated to 110°C for ~ 3 hours. The crude reaction mixture was analyzed by GC-MS and showed > 99% consumption of *N*-pivaloylindole and a C2:C3:diarylated product distribution of 25:1:0.7. The crude reaction mixture was filtered over celite (washing with Et<sub>2</sub>O). The solvent was removed and the residue was dissolved in Et<sub>2</sub>O (30 mL) and washed with a saturated solution of Na<sub>2</sub>CO<sub>3</sub> (3 x 20 mL). The aqueous layers were back extracted with Et<sub>2</sub>O (3 x 20 mL) and the combined organic layers were

dried over MgSO<sub>4</sub> and concentrated. The crude reactions were purified by Chromatotron on 2 – 4 mm silica plates (Et<sub>2</sub>O/hexanes) (see below for individual compounds).

### Compound 3.16a



The title compound was prepared according to the general procedure for C2 arylation and was purified by Chromatotron (loaded with DCM) with hexanes (50 mL) then hexanes/Et<sub>2</sub>O (99:1; 200 mL) as the solvent to afford the title compound as an oil in 84% yield.

**<sup>1</sup>H NMR (400 MHz, CDCl<sub>3</sub>, 293 K):** δ 7.62 (d, J = 7.3 Hz, 1H), 7.53 (d, J = 7.0 Hz, 2H), 7.43 (dd, J = J = 7.0 Hz, 2H), 7.38 – 7.33 (m, 2H), 7.24 (ddd, J = J = 7.2 Hz, J = 1.4 Hz, 1H), 7.18 (ddd, J = J = 7.1 Hz, J = 1.2 Hz, 1H), 6.68 (s, 1H), 0.96 (s, 9H).

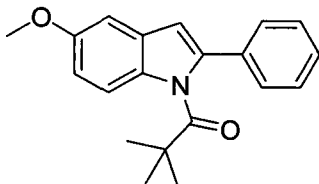
**<sup>13</sup>C NMR (100 MHz, CDCl<sub>3</sub>, 293 K):** δ 187.4 (C), 139.4 (C), 137.2 (C), 133.9 (C), 129.1 (CH), 128.4 (C), 128.3 (CH), 127.8 (CH), 123.4 (CH), 121.5 (CH), 120.6 (CH), 111.2 (CH), 104.7 (CH) 45.2 (C), 27.9 (CH<sub>3</sub>).

**FTIR:** 2969, 1717, 935, 763, 742 cm<sup>-1</sup>.

**HRMS (EI):** calculated for C<sub>19</sub>H<sub>19</sub>NO (M<sup>+</sup>) 277.1467; found for C<sub>19</sub>H<sub>19</sub>NO (M<sup>+</sup>) 277.1470.

**R<sub>f</sub>** (5% diethyl ether in hexanes): 0.3.

### Compound 3.16b



The title compound was prepared according to the general procedure for C2 arylation and was purified by Chromatotron (loaded with DCM) with hexanes (50 mL) then hexanes/Et<sub>2</sub>O (99:1; 200 mL) as the solvent to afford the title compound in 90% yield.

**<sup>1</sup>H NMR (400 MHz, CDCl<sub>3</sub>, 293 K):** δ 7.51 (d, J = 7.0 Hz, 2H), 7.43 (dd, J = J = 7.2 Hz, 2H), 7.36 (dd, J = J = 7.3 Hz, 1H), 7.26 (d, J = 8.9 Hz, 1H), 7.06 (d, J = 2.4 Hz, 1H), 6.89 (dd, J = 8.9 Hz, J = 2.5 Hz, 1H), 6.61 (s, 1H), 3.86 (s, 3H), 0.95 (s, 9H).

**<sup>13</sup>C NMR (100 MHz, CDCl<sub>3</sub>, 293 K):** δ 187.3 (C), 155.3 (C), 140.1 (C), 134.1 (C), 132.4 (CH), 129.1 (C), 128.9 (C), 128.3 (CH), 127.7 (CH), 113.3 (CH), 112.1 (CH), 104.6 (CH), 102.3 (CH), 55.8 (CH<sub>3</sub>), 45.2 (C), 28.0 (CH<sub>3</sub>).

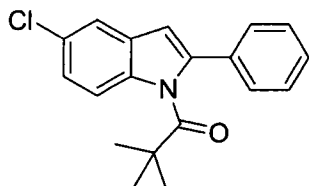
**FTIR:** 2968, 1713, 935, 762, 698 cm<sup>-1</sup>.

**HRMS (EI):** calculated for C<sub>20</sub>H<sub>21</sub>NO<sub>2</sub> (M<sup>+</sup>) 307.1572; found for C<sub>20</sub>H<sub>21</sub>NO<sub>2</sub> (M<sup>+</sup>) 307.1576.

**Melting point** (diethyl ether/hexanes) 75 - 76°C.

$R_f$  (10% diethyl ether in hexanes): 0.41.

### Compound 3.16c



The title compound was prepared according to the general procedure for C2 arylation and was purified by Chromatotron (loaded with DCM) with hexanes (50 mL) then hexanes/Et<sub>2</sub>O (99:1; 200 mL) as the solvent to afford the title compound in 86% yield.

**<sup>1</sup>H NMR (400 MHz, CDCl<sub>3</sub>, 293 K):**  $\delta$  7.58 (d,  $J = 1.8$  Hz, 1H), 7.51 (dd,  $J = 8.2$  Hz,  $J = 1.6$  Hz, 2H), 7.44 (dd,  $J = J = 8.3$  Hz, 2H), 7.38 (t,  $J = 7.3$  Hz, 1H), 7.26 (d,  $J = 8.8$  Hz, 1H), 7.19 (dd,  $J = 8.8$  Hz,  $J = 2.0$  Hz, 1H), 6.61 (s, 1H), 0.94 (s, 9H).

**<sup>13</sup>C NMR (100 MHz, CDCl<sub>3</sub>, 293 K):**  $\delta$  187.0 (C), 140.7 (C), 135.5 (C), 133.4 (C), 129.4 (C), 129.2 (CH), 128.7 (CH), 127.8 (CH), 127.1 (C), 123.6 (CH), 120.0 (CH), 112.2 (CH), 103.9 (CH), 45.2 (C), 27.9 (CH<sub>3</sub>).

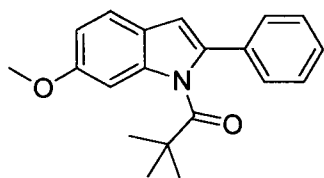
**FTIR:** 2971, 1720, 917, 762, 695 cm<sup>-1</sup>.

**HRMS (EI):** calculated for C<sub>19</sub>H<sub>18</sub>NOCl (M<sup>+</sup>) 311.1077; found for C<sub>19</sub>H<sub>18</sub>NOCl (M<sup>+</sup>) 311.1066.

**Melting point** (diethyl ether/hexanes) 83 - 85°C.

$R_f$  (1% diethyl ether in hexanes): 0.3.

### Compound 3.16d



The title compound was prepared according to the general procedure for C2 arylation and was purified by Chromatotron (loaded with DCM) with hexanes (50 mL), hexanes/Et<sub>2</sub>O (99:1; 200 mL), and hexanes/Et<sub>2</sub>O (98/2; 200 mL) as the solvent to afford the title compound in 76% yield.

**<sup>1</sup>H NMR (400 MHz, CDCl<sub>3</sub>, 293 K):**  $\delta$  7.50 - 7.47 (m, 3H), 7.42 (dd,  $J = J = 7.6$  Hz, 2H), 7.33 (t,  $J = 7.3$  Hz, 1H), 6.87 - 6.83 (m, 2H), 6.61 (s, 1H), 3.84 (s, 3H), 0.97 (s, 9H).

**<sup>13</sup>C NMR (100 MHz, CDCl<sub>3</sub>, 293 K):**  $\delta$  187.5 (C), 157.5 (C), 138.4 (C), 138.1 (C), 134.2 (C), 129.1 (CH), 127.9 (CH), 127.5 (CH), 122.6 (C), 121.2 (CH), 111.5 (CH), 104.8 (CH), 94.8 (CH), 55.7 (CH<sub>3</sub>), 45.3 (C), 28.0 (CH<sub>3</sub>).

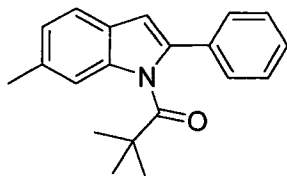
**FTIR:** 2969, 1717, 932, 757 cm<sup>-1</sup>.

**HRMS (EI):** calculated for C<sub>20</sub>H<sub>21</sub>NO<sub>2</sub> (M<sup>+</sup>) 307.1572; found for C<sub>20</sub>H<sub>21</sub>NO<sub>2</sub> (M<sup>+</sup>) 307.1566.

**Melting point** (diethyl ether/hexanes) 111 - 113°C.

$R_f$  (5% diethyl ether in hexanes): 0.25.

### Compound 3.16e



The title compound was prepared according to the general procedure for  $C2$  arylation and was purified by Chromatotron (loaded with DCM) with hexanes (50 mL) and hexanes/Et<sub>2</sub>O (99:1; 200 mL) as the solvent to afford the title compound in 88% yield.

**<sup>1</sup>H NMR (400 MHz, CDCl<sub>3</sub>, 293 K):**  $\delta$  7.52 – 7.48 (m, 3H), 7.42 (dd,  $J = J = 7.5$  Hz, 2H), 7.35 (t,  $J = 7.3$  Hz, 1H), 7.16 (s, 1H), 7.02 (d,  $J = 8.0$  Hz, 1H), 6.63 (s, 1H), 2.46 (s, 3H), 0.96 (s, 9H).

**<sup>13</sup>C NMR (100 MHz, CDCl<sub>3</sub>, 293 K):**  $\delta$  187.5 (C), 138.8 (C), 137.6 (C), 134.2 (C), 133.5 (C), 129.1 (CH), 128.1 (CH), 127.7 (CH), 126.2 (C), 123.3 (CH), 120.2 (CH), 111.1 (CH), 104.7 (CH), 45.1 (C), 28.0 (CH<sub>3</sub>), 21.9 (CH<sub>3</sub>).

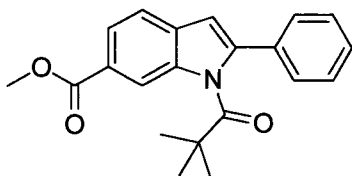
**FTIR:** 2971, 1721, 931, 815, 757 cm<sup>-1</sup>.

**HRMS (EI):** calculated for C<sub>20</sub>H<sub>21</sub>NO (M<sup>+</sup>) 291.1623; found for C<sub>20</sub>H<sub>21</sub>NO (M<sup>+</sup>) 291.1622.

**Melting point** (diethyl ether/hexanes) 82 - 83°C.

$R_f$  (1% diethyl ether in hexanes): 0.26.

### Compound 3.16f



The title compound was prepared according to the general procedure for  $C2$  arylation and was purified by Chromatotron (loaded with DCM) with hexanes (50 mL) and hexanes/Et<sub>2</sub>O (95:5) (300 mL) as the solvent to afford the title compound in 86% yield.

**<sup>1</sup>H NMR (400 MHz, CDCl<sub>3</sub>, 293 K):**  $\delta$  8.06 (s, 1H), 7.89 (dd,  $J = 8.3$  Hz,  $J = 1.4$  Hz, 1H), 7.64 (d,  $J = 8.3$  Hz, 1H), 7.56 – 7.53 (m, 2H), 7.48 – 7.38 (m, 3H), 6.72 (s, 1H), 3.93 (s, 3H), 0.97 (s, 9H).

**<sup>13</sup>C NMR (100 MHz, CDCl<sub>3</sub>, 293 K):**  $\delta$  186.8 (C), 167.6 (C), 142.5 (C), 136.5 (C), 133.3 (C), 131.9 (C), 129.2 (CH), 128.9 (CH), 128.0 (CH), 125.0 (C), 122.6 (CH), 120.2 (CH), 113.3 (CH), 104.4 (CH), 52.0 (CH<sub>3</sub>), 45.3 (C), 27.9 (CH<sub>3</sub>).

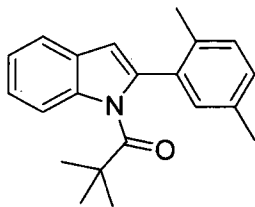
**FTIR:** 2973, 1720, 933, 766 cm<sup>-1</sup>.

**HRMS (EI):** calculated for C<sub>21</sub>H<sub>21</sub>NO<sub>3</sub> (M<sup>+</sup>) 335.1521; found for C<sub>21</sub>H<sub>21</sub>NO<sub>3</sub> (M<sup>+</sup>) 335.1508.

**Melting point** (diethyl ether/hexanes) 128 - 129°C.

$R_f$  (5% diethyl ether in hexanes): 0.12.

### Compound 3.16g



The title compound was prepared according to the following procedure. Pd(TFA)<sub>2</sub> (0.0154 g, 0.045 mmol, 10 mol %), *N*-pivaloylindole (0.0922 g, 0.45 mmol, 1 eq), AgOAc (0.2373 g, 1.42 mmol, 3 eq), and PivOH (0.2850 g, 2.79 mmol, 6 eq) were weighed into a 15 mL sealed tube. 5.5 mL of *p*-xylene was added and the tube was sealed. The sealed tube was placed into an oil bath and heated to 110°C for ~ 16 hours. The crude reaction mixture was filtered over celite and washed with diethyl ether. The solvent was removed and the remaining *p*-xylene was removed on a Kugelrohr and the residue was purified by Chromatotron (loaded with DCM) with hexanes (50 mL) and hexanes:Et<sub>2</sub>O (99:1, 200 mL) to afford the title compound as an oil in 58% yield.

**<sup>1</sup>H NMR (400 MHz, CDCl<sub>3</sub>, 293 K):** δ 7.61 (d, *J* = 8.2 Hz, 1H), 7.39 (d, *J* = 8.2 Hz, 1H), 7.25 (ddd, *J* = *J* = 7.6 Hz, *J* = 1.3 Hz, 1H), 7.21 – 7.17 (m, 2H), 7.12 – 7.07 (m, 2H), 6.58 (s, 1H), 2.43 (s, 3H), 2.31 (s, 3H), 0.94 (s, 9H).

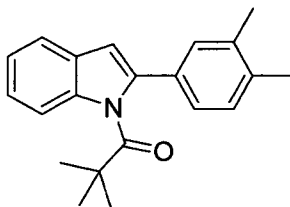
**<sup>13</sup>C NMR (100 MHz, CDCl<sub>3</sub>, 293 K):** δ 186.7 (C), 137.5 (C), 136.6 (C), 135.5 (C), 133.4 (C), 132.8 (C), 131.1 (CH) (two overlapping peaks), 129.1 (CH), 128.3 (C), 123.3 (CH), 121.5 (CH), 120.4 (CH), 111.5 (CH), 106.7 (CH), 44.4 (C), 27.7 (CH<sub>3</sub>), 20.8 (CH<sub>3</sub>), 20.1 (CH<sub>3</sub>).

**FTIR:** 2969, 1715, 1449, 901, 810, 740 cm<sup>-1</sup>.

**HRMS (EI):** calculated for C<sub>21</sub>H<sub>23</sub>NO (M<sup>+</sup>) 305.1780; found for C<sub>21</sub>H<sub>23</sub>NO (M<sup>+</sup>) 305.1761.

**R<sub>f</sub>** (2% diethyl ether in hexanes): 0.29.

### Compound 3.16h



The title compound was prepared according to the general procedure for C2 arylation though was heated at 110°C for ~ 16 hours and was purified by Chromatotron (loaded with DCM) with hexanes (250 mL) to afford the title compound as an oily solid in 76% yield.

**<sup>1</sup>H NMR (400 MHz, CDCl<sub>3</sub>, 293 K):** δ 7.59 (d, *J* = 7.8 Hz, 1H), 7.35 (d, *J* = 8.2 Hz, 1H), 7.30 (d, *J* = 1.4 Hz, 1H), 7.26 – 7.15 (m, 4H), 6.63 (s, 1H), 2.30 (s, 6H), 0.98 (s, 9H).

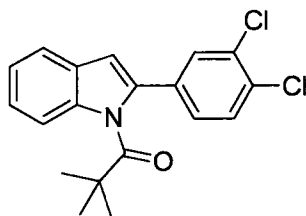
**<sup>13</sup>C NMR (100 MHz, CDCl<sub>3</sub>, 293 K):** δ 187.5 (C), 139.7 (C), 137.4 (C), 137.1 (C), 136.9 (C), 131.5 (C), 130.3 (CH), 128.8 (CH), 128.5 (C), 125.2 (CH), 123.1 (CH), 121.4 (CH), 120.4 (CH), 111.2 (CH), 104.0 (CH), 45.2 (C), 28.0 (CH<sub>3</sub>), 19.8 (CH<sub>3</sub>), 19.6 (CH<sub>3</sub>).

**FTIR:** 2969, 1718, 957, 904, 744  $\text{cm}^{-1}$ .

**HRMS (EI):** calculated for  $\text{C}_{21}\text{H}_{23}\text{NO}$  ( $\text{M}^+$ ) 305.1780; found for  $\text{C}_{21}\text{H}_{23}\text{NO}$  ( $\text{M}^+$ ) 305.1781.

**R<sub>f</sub>** (1% diethyl ether in hexanes): 0.16.

### Compound 3.16i



The title compound was prepared according to the general procedure for C2 arylation though was heated at 110°C for ~ 16 hours and was purified by Chromatotron (loaded with DCM) with hexanes (50 mL) and hexanes/Et<sub>2</sub>O (99:1, 200 mL) to afford the title compound in 55% yield.

**<sup>1</sup>H NMR (400 MHz, CDCl<sub>3</sub>, 293 K):**  $\delta$  7.64 – 7.61 (m, 2H), 7.51 (d,  $J = 8.3$  Hz, 1H), 7.36 – 7.33 (m, 2H), 7.28 (ddd,  $J = J = 8.2$  Hz,  $J = 1.3$ , 1H), 7.20 (ddd,  $J = J = 7.9$  Hz,  $J = 1.2$  Hz, 1H), 6.71 (s, 1H), 1.02 (s, 9H).

**<sup>13</sup>C NMR (100 MHz, CDCl<sub>3</sub>, 293 K):**  $\delta$  186.8 (C), 137.4 (C), 136.7 (C), 133.9 (C), 133.4 (C), 132.4 (C), 131.1 (CH), 129.1 (CH), 128.1 (C), 126.7 (CH), 124.1 (CH), 121.9 (CH), 120.9 (CH), 111.4 (CH), 105.9 (CH), 45.2 (C), 28.0 (CH<sub>3</sub>).

**FTIR:** 2972, 1719, 1445, 950, 740  $\text{cm}^{-1}$ .

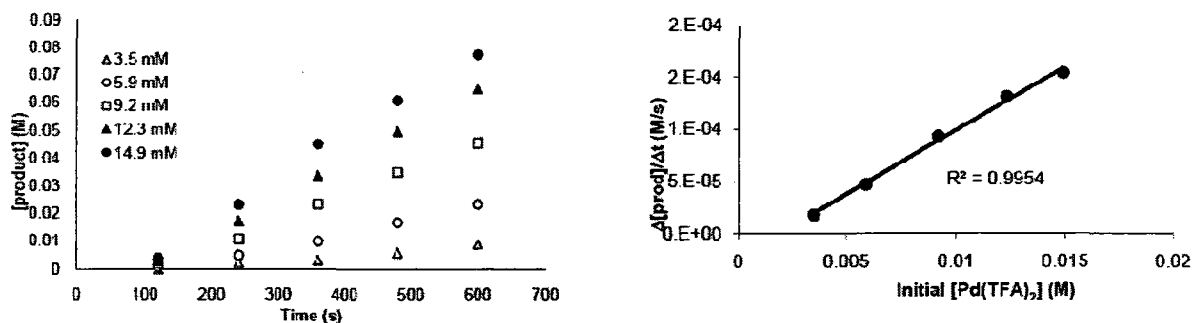
**HRMS (EI):** calculated for  $\text{C}_{19}\text{H}_{17}\text{NOCl}_2$  ( $\text{M}^+$ ) 345.0687; found for  $\text{C}_{19}\text{H}_{17}\text{NOCl}_2$  ( $\text{M}^+$ ) 345.0696.

**Melting point** (diethyl ether/hexanes) 132 - 134°C.

**R<sub>f</sub>** (1% diethyl ether in hexanes): 0.28.

### 5.3.6. Preparation of Materials for Mechanistic Investigation and Kinetic Experiments

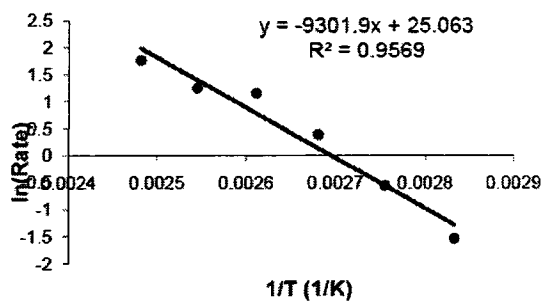
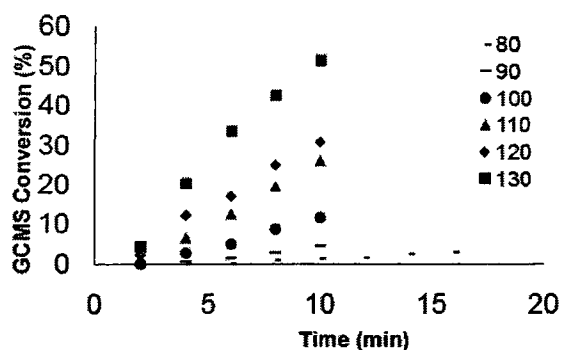
**Order of reagents:** The order of reagents was determined by setting up the experiment as described previously (C3-arylation: second generation conditions; C2-arylation: third generation conditions) and placing the vial into a pre-heated block. Aliquots were removed at specified time intervals (C3-arylation: every 5 minutes; C2-arylation: every 2 minutes) by microsyringe (~ 10 – 20  $\mu\text{L}$ ) and analyzed by GCMS. This procedure was done for at least 4 different concentrations of each reagent. Below are sample plots for the variation of initial rate with catalyst ( $\text{Pd}(\text{TFA})_2$ ) concentration (3.5 – 14.9 mM) in the C2 oxidative arylation (left) and the determination of the dependence of reaction rate on catalyst concentration (right).



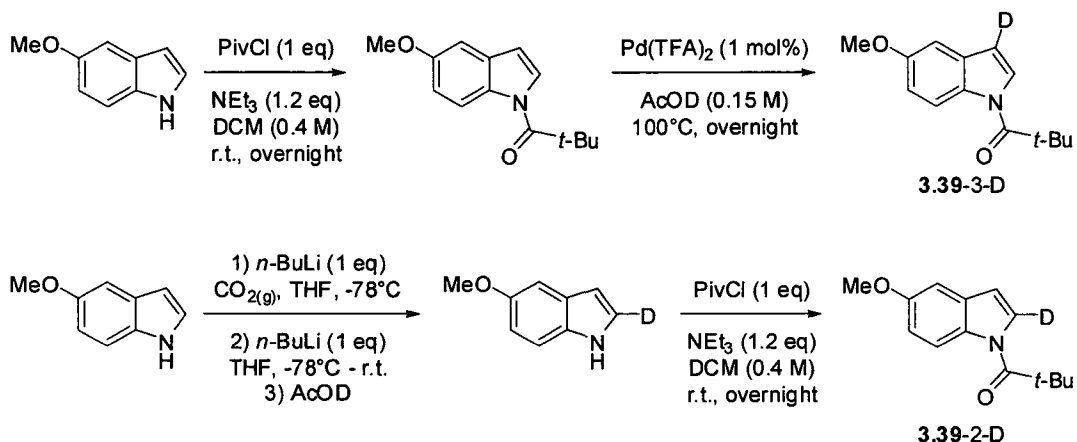
**Deuterium kinetic isotope effect (at benzene):** The DKIE was determined by setting up the experiment as described previously (C3-arylation: second generation conditions; C2-arylation: third generation conditions) using benzene and benzene-*d*<sub>6</sub> in separate reaction vials and placing the vials into a pre-heated block. Aliquots were removed at specified time intervals (C3-arylation: every 5 minutes; C2-arylation: every 2 minutes) for the first hour and then at larger time intervals for the remainder of the reaction and analyzed by GCMS. The rate of the reaction in benzene and the rate in benzene-*d*<sub>6</sub> were compared to obtain the DKIE.

**Competition experiments (at benzene):** The competition experiments were done by setting up the experiment as described previously (C3-arylation: second generation conditions; C2-arylation: third generation conditions) using an equimolar mixture of the arenes under study and placing the vial into a pre-heated block. After ~ 10 minutes (< 10% conversion) an aliquot was removed and analyzed by GCMS to provide the ratio of products.

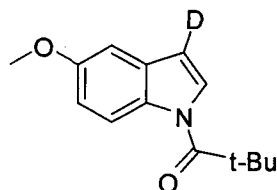
**Arrhenius plot:** The  $E_a$  was determined by setting up the experiment as described previously (C2-arylation: third generation conditions) and placing the vials into a pre-heated block. This was done for six different temperatures. Aliquots were removed at specified time intervals (C2-arylation: every 2 minutes) by microsyringe (~ 10 – 20  $\mu$ L) and analyzed by GCMS. The conversion vs time was plotted (left below) to determine the initial rate. The natural logarithm of the initial rate was plotted against the inverse of the absolute temperature (right below) and the  $E_a$  determined from the slope of the linear plot.



### Preparation of deuterium labeled indole substrates:



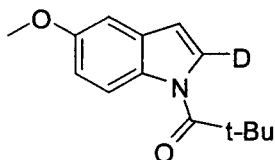
### Compound 3.39-3-D



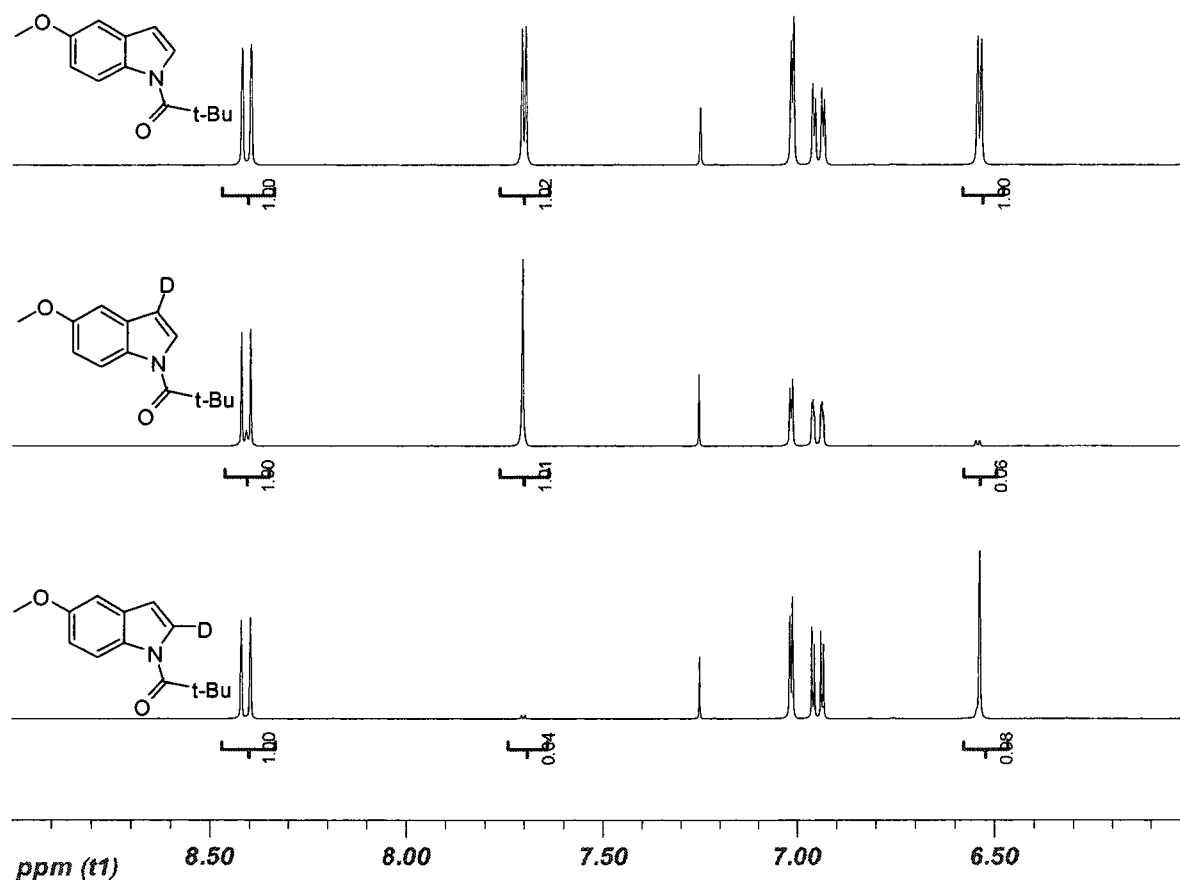
**3.15i** (0.1519 g, 0.62 mmol, 1 eq), Pd(TFA)<sub>2</sub> (0.0042 g, 0.012 mmol, 2 mol%), and AcOD (2 mL) were added to a glass tube, sealed with a rubber septa (and electrical tape) and heated to 110°C for 12 hours. The solvent was removed and the residue flashed over silica gel (with 5% diethyl ether in hexanes) to afford the title compound in 88% isolated yield (0.1344 g).

The product was found to have 94% deuterium incorporation at the C3 position (see below) by  $^1\text{H}$  NMR analysis.

### Compound 3.39-2-D



5-Methoxyindole (0.5064 g, 3.45 mmol, 1 eq.) was added to a flame-dried round-bottom flask. The flask was then sealed with a rubber septa and purged with argon. Freshly distilled THF (10 mL) was added to the flask and it was cooled to  $-78^\circ\text{C}$ . *n*-BuLi (2.0 mL, 2.5 M, 1.5 eq) was added to the flask *via* syringe at  $-78^\circ\text{C}$  and the reaction allowed to stir at this temperature for 1 hour.  $\text{CO}_2(\text{g})$  was bubbled through the reaction for 20 minutes and the reaction stirred for an additional 10 minutes. The reaction was then allowed to warm to  $0^\circ\text{C}$  and the THF removed *in vacuo*. The resulting white powder was re-dissolved in THF (10 mL) and cooled to  $-78^\circ\text{C}$ . *t*-BuLi (3.0 mL, 1.7 M,  $\sim 1.5$  eq) was added *via* syringe and the reaction was allowed to stir for 1.5 hours at  $-78^\circ\text{C}$ .  $\text{D}_2\text{O}$  (10 mL) was added and the reaction allowed to warm to room temperature and stirred overnight. The crude product was obtained by separation of the layers and extraction with DCM. The crude product was subject to the standard pivaloylation conditions (*vide infra*) and isolated in 75% yield.  $^1\text{H}$  NMR analysis revealed that the product had 96% deuterium incorporation at the C2-position (see below).



**Deuterium kinetic isotope effect at indole (via competition experiments):** The DKIE was determined by competition experiments by setting up the reaction as described previously (C2-arylation: third generation conditions) using an equimolar mixture of the two indoles under study and placing the vial into a pre-heated block. After ~ 10 minutes (< 10% conversion) an aliquot was removed and analyzed by GCMS to provide the ratio of products and the DKIE.

**Deuterium erosion experiments:** The deuterium erosion experiments were determined by setting up the experiment as described previously (C2-arylation: third generation conditions) using the appropriately deuterium labeled indole and placing the vials into a pre-heated block. Aliquots were removed at specified time intervals (C3-arylation: every 5 minutes; C2-arylation: every 2 minutes) for the first hour and then at larger time intervals for the remainder of the reaction and analyzed by GCMS. The deuterium incorporation was

determined by comparing the relative intensity of the M and M+1 peak in the mass spectra generated from the GCMS trace.

**Hammett correlation (at indole):** The Hammett correlation was obtained by setting up the experiment as described previously (C3-arylation: second generation conditions; C2-arylation: third generation conditions) using an equimolar mixture of the 6-substituted *N*-acetyl or *N*-pivaloylindole and the unsubstituted *N*-acetyl or *N*-pivaloylindole and placing the vial into a pre-heated block. After ~ 10 minutes (< 10% conversion) an aliquot was removed and analyzed by GCMS to provide the ratio of products. The natural logarithm of the ratio of products was plotted against the  $\sigma_{para}$ -values and the slope provided the  $\rho$ -value.

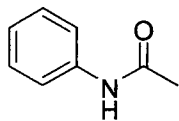
## 5.4. Oxidative Annulation of Acetanilide and Enamides with Internal Alkynes

### 5.4.1. Preparation and Characterization of Acetanilides.

#### **Representative procedure for the preparation of acetanilides:**

Aniline (10.1 mL, 109.7 mmol, 1 eq) was added to a round-bottom flask via syringe and fitted with a rubber septum. The flask was purged with argon and dry DCM (300 mL, 0.4 M) was added. Acetic anhydride (12.5 mL, 132.2 mmol, 1.2 eq) was added and the reaction was stirred at room temperature and monitored by TLC. Upon completion (generally a couple of hours, but as short as 20 minutes) the reaction mixture was washed with a saturated solution of sodium carbonate, the organic layers dried with MgSO<sub>4</sub> and the solvent removed under reduced pressure. The product was obtained in quantitative yield (14.8 g). In most cases analytically pure acetanilides can be obtained after extraction with sodium carbonate however if necessary purification by flash chromatography with ethyl acetate/pet. ether was used (see below for specific conditions).

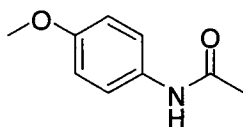
### Compound 4.1a



The above procedure was followed to afford the product in quantitative yield. This compound can also be purchased from commercial sources (CAS: 103-84-4).

**<sup>1</sup>H NMR (400 MHz, CDCl<sub>3</sub>, 293 K):** δ 7.50 (d, *J* = 7.8 Hz, 2H), 7.32 (t, *J* = 7.9 Hz, 2H), 7.10 (t, *J* = 7.4 Hz, 1H), 2.17 (s, 3H). The signal for the exchangeable NH does not appear in the spectrum.

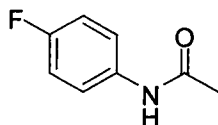
### Compound 4.1b



The above procedure was followed to afford the product in 84% yield. This compound can also be purchased from commercial sources (CAS: 51-66-1).

**<sup>1</sup>H NMR (400 MHz, CDCl<sub>3</sub>, 293 K):** δ 7.44 (brs, 1H), 7.38 (d, *J* = 8.8 Hz, 2H), 6.84 (d, *J* = 9.2 Hz, 2H), 3.78 (s, 3H), 2.14 (s, 3H).

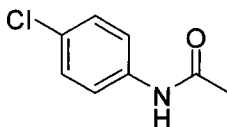
### Compound 4.1c



The above procedure was followed to afford the product in 83% yield. This compound can also be purchased from commercial sources (CAS: 351-83-7).

**<sup>1</sup>H NMR (400 MHz, CDCl<sub>3</sub>, 293 K):** δ 7.45 (dd, *J* = 9.2 Hz, *J* = 5.2 Hz, 2H), 7.30 (brs, 1H), 7.01 (brt, *J* = 8.8 Hz, 2H), 2.17 (s, 3H).

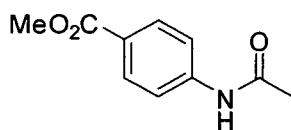
### Compound 4.1d



The above procedure was followed to afford the product in 51% yield. This compound can also be purchased from commercial sources (CAS: 539-03-7).

**<sup>1</sup>H NMR (400 MHz, CDCl<sub>3</sub>, 293 K):** δ 7.46 (d, *J* = 8.8 Hz, 2H), 7.28 (d, *J* = 8.4 Hz, 2H), 2.17 (s, 3H). The signal for the exchangeable NH does not appear in the spectrum.

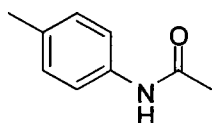
### Compound 4.1e



The above procedure was followed to afford the product in 83% yield. Spectral data was consistent with that previously reported.<sup>164</sup>

**<sup>1</sup>H NMR (400 MHz, CDCl<sub>3</sub>, 293 K):**  $\delta$  8.00 (d,  $J$  = 8.8 Hz, 2H), 7.59 (d,  $J$  = 8.6 Hz, 2H), 7.40 (brs, 1H), 3.90 (s, 3H), 2.11 (s, 3H).

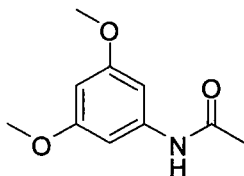
### Compound 4.1f



The above procedure was followed to afford the product in 97% yield. This compound can also be purchased from commercial sources (CAS: 103-89-9).

**<sup>1</sup>H NMR (400 MHz, CDCl<sub>3</sub>, 293 K):**  $\delta$  7.63 (br. s, 1H), 7.37 (d,  $J$  = 8.4 Hz, 2H), 7.11 (d,  $J$  = 8.2 Hz, 2H), 2.30 (s, 3H), 2.13 (s, 3H).

### Compound 4.1g



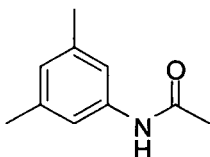
The above procedure was followed to afford the product in 73% yield. Spectral data was consistent with that previously reported.<sup>165</sup>

**<sup>1</sup>H NMR (400 MHz, CDCl<sub>3</sub>, 293 K):**  $\delta$  7.23 (brs, 1H), 6.75 (d,  $J$  = 2.0 Hz, 2H), 6.23 (t,  $J$  = 1.6 Hz, 1H), 3.77 (s, 6H), 2.16 (s, 3H).

<sup>164</sup> Ikawa, T.; Barder, T. E.; Biscoe, M. R.; Buchwald, S. L. *J. Am. Chem. Soc.* **2007**, *43*, 13001

<sup>165</sup> Hadjeri, M.; Mariotte, A.-M.; Boumendjel, A. *J. Chem. Res. (S)*, **2002**, *9*, 463

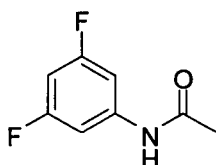
### Compound 4.1h



The above procedure was followed to afford the product in 95% yield. This compound can also be purchased from commercial sources (CAS: 2050-45-5).

**<sup>1</sup>H NMR (400 MHz, CDCl<sub>3</sub>, 293 K):**  $\delta$  7.23 (br s, 1H), 7.12 (s, 2H), 6.75 (s, 1H), 2.28 (s, 6H), 2.15 (s, 3H).

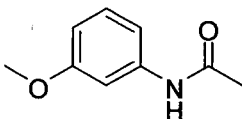
### Compound 4.1i



The above procedure was followed to afford the product in 70% yield. This compound can also be purchased from commercial sources (CAS: 404-01-3).

**<sup>1</sup>H NMR (300 MHz, CDCl<sub>3</sub>, 293 K):**  $\delta$  7.65 (br s, 1H), 7.14 – 7.11 (m, 2H), 6.59 – 6.52 (m, 1H), 2.19 (s, 3H).

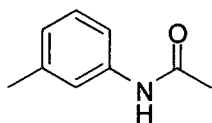
### Compound 4.1j



The above procedure was followed to afford the product in 75% yield. This compound can also be purchased from commercial sources (CAS: 588-16-9).

**<sup>1</sup>H NMR (400 MHz, CDCl<sub>3</sub>, 293 K):**  $\delta$  7.65 (br. s, 1H), 7.27 (t,  $J$  = 2.0 Hz, 1H), 7.19 (t,  $J$  = 8.0 Hz, 1H), 6.98 (br. d,  $J$  = 8.0 Hz, 1H), 6.65 (br. d,  $J$  = 8.0 Hz, 1H), 3.77 (s, 3H), 2.15 (s, 3H).

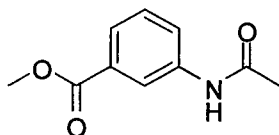
### Compound 4.1k



A previously reported procedure was followed to afford the product in quantitative yield. This compound can also be purchased from commercial sources (CAS: 537-92-8).

**<sup>1</sup>H NMR (400MHz, CDCl<sub>3</sub>, 293K):** δ 7.35 (1H, br s), 7.27-7.18 (3H, m), 6.92 (1H, d, *J*=7.4Hz), 2.34 (3H, s), 2.17 (3H, s).

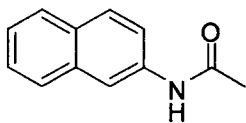
#### Compound 4.1l



The above procedure was followed to afford the product in 64% yield. This compound can also be purchased from commercial sources (CAS: 52189-36-3).

**<sup>1</sup>H NMR (300 MHz, CDCl<sub>3</sub>, 293 K):** δ 8.03 (s, 1H), 7.91 (d, *J* = 8.1 Hz, 1H), 7.80 – 7.76 (m, 2H), 7.38 (dd, *J* = *J* = 7.9 Hz, 1H), 3.90 (s, 3H), 2.20 (s, 3H).

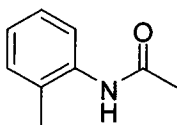
#### Compound 4.1m



The above procedure was followed to afford the product in 77% yield. This compound can also be purchased from commercial source (CAS: 581-97-5).

**<sup>1</sup>H NMR (300 MHz, CDCl<sub>3</sub>, 293 K):** δ 8.17 (s, 1H), 7.92 (br., s, 1H), 7.76 – 7.67 (m, 3H), 7.48 – 7.32 (m, 3H), 2.19 (s, 3H).

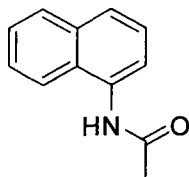
#### Compound 4.1n



The above procedure was followed and column chromatography was performed on silica gel with ethyl acetate/pet. ether (70:30) as the solvent to afford the product in 73% yield. This compound can also be purchased from commercial source (CAS: 120-66-1).

**<sup>1</sup>H NMR (400 MHz, CDCl<sub>3</sub>, 293 K):** δ 7.75 (d, *J* = 8.0 Hz, 1H), 7.22 – 7.17 (m, 2H), 7.08 (t, *J* = 7.6 Hz, 1H), 7.01 (brs, 1H), 2.26 (s, 3H), 2.20 (s, 3H).

### Compound 4.1o

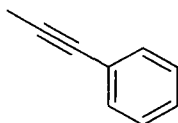


The above procedure was followed to afford the product in 50% yield. This compound can also be purchase for commercial source (CAS: 575-36-0).

**<sup>1</sup>H NMR (300 MHz, DMSO-*d*<sub>6</sub>, 293 K):** δ 9.93 (br. s, 1H), 8.12 – 8.07 (m, 1H), 7.96 – 7.89 (m, 1H), 7.74 (d, *J* = 8.2 Hz, 1H), 7.70 (d, *J* = 7.3 Hz, 1H), 7.58 – 7.46 (m, 3H), 2.19 (s, 3H).

### 5.4.2. Preparation and Characterization of Internal Alkynes.

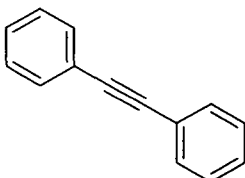
#### Compound 4.2a



To a flame-dried round-bottom flask under argon was added phenylacetylene (5 mL, 46 mmol, 1 eq) followed by THF (300 mL, 0.15 M). The flask was placed in an ice-water/salt bath and allowed to cool. *n*-Butyllithium (40 mL, 2.5 M in hexanes, 100 mmol, 2 eq) was added slowly and the reaction was allowed to stir for ~ 1 hour. Iodomethane (6 mL, 96.2 mmol, 2.1 eq) was added at -20C and the reaction was allowed to stir at room temperature for ~ 1 hour. The reaction was quenched with a saturated solution of ammonium chloride and extracted with dichloromethane. The organics were dried over MgSO<sub>4</sub> and the solvent removed under pressure. The residue was purified by Kugelrohr distillation to afford the product in quantitative yield. This compound can also be purchased from commercial sources (CAS: 673-32-5).

**<sup>1</sup>H NMR (400 MHz, CDCl<sub>3</sub>, 293 K):** δ 7.41 – 7.36 (m, 2H), 7.30 – 7.23 (m, 3H), 2.05 (s, 3H).

#### Compound 4.2b

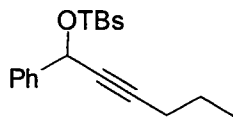


Pd(PPh<sub>3</sub>)<sub>2</sub>Cl<sub>2</sub> (0.3429g, 0.49 mmol, 2 mol%) and CuI (0.0925g, 0.49 mmol, 2 mol%) were weighed out to a round bottom flask equipped with a magnetic stir bar and fitted with a rubber septa. The flask was purged with argon and THF (120 mL, 0.2 M) followed by

triethylamine (6 mL) were added via syringe. Iodobenzene (2.9 mL, 26 mmol, 1.1 eq) followed by phenylacetylene (2.7 mL, 25 mmol, 1 eq) were added to the stirring mixture and the reaction was stirred overnight at room temperature. The volatiles were evaporated under reduced pressure and the residue was extracted with ethyl acetate/ether/brine. The organics were dried over MgSO<sub>4</sub> and the solvent removed under reduced pressure. The residue was purified by flash column chromatography on silica gel with ether : pet. ether as the solvent to afford the title compound in 71% yield. This compound can also be purchased from commercial sources (CAS: 501-65-5).

<sup>1</sup>H NMR (400 MHz, CDCl<sub>3</sub>, 293 K): δ 7.56 – 7.51 (m, 4H), 7.36 – 7.31 (m, 6H).

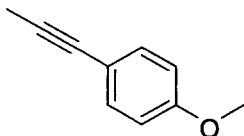
#### Compound 4.2c



The above compound was prepared according to literature procedure and displayed identical spectral data to that previously reported.<sup>131</sup>

<sup>1</sup>H NMR (400MHz, CDCl<sub>3</sub>, 293K): δ 7.52 – 7.47 (m, 2H), 7.37 – 7.30 (m, 2H), 7.29 – 7.23 (m, 1H), 5.52 – 5.48 (m, 1H), 2.23 – 2.18 (m, 2H), 1.50 – 1.49 (m, 2H), 0.98 (t, *J* = 7.3 Hz, 3H), 0.94 (s, 9H), 0.17 (s, 3H), 0.15 (s, 3H).

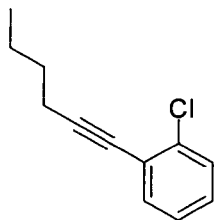
#### Compound 4.2d



The above compound was prepared in quantitative yield and spectral data was consistent with that previously reported.<sup>166</sup>

<sup>1</sup>H NMR (400MHz, CDCl<sub>3</sub>, 293K): δ 7.32 (2H, br d, *J*=8.8Hz) 6.81 (2H, br d, *J*=8.9Hz), 3.80 (1H, s), 2.03 (3H, s).

#### Compound 4.2e

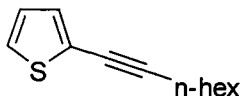


The above compound was prepared in quantitative yield and spectral data was consistent with that previously reported.<sup>167</sup>

<sup>166</sup> Zhang, W.; Kraft, S.; Moore, J. S. *J. Am. Chem. Soc.* **2004**, 126, 329.

**<sup>1</sup>H NMR (400MHz, CDCl<sub>3</sub>, 293K, TMS):** δ 7.45-7.42 (1H, m), 7.38-7.36 (1H, m), 7.21-7.15 (2H, m), 2.48 (2H, t, *J*=7.0Hz), 1.66-1.59 (2H, m), 1.56-1.47 (2H, m), 0.96 (3H, t, *J*=7.3Hz).

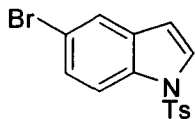
### Compound 4.2f



A mixture of 2-bromothiophene (126 uL, 1.3 mmol, 1 eq), 1-octyne (148 uL, 1.6 mmol, 1.2 eq), pyrrolidine (217 uL, 2.6 mmol, 2 eq), PdCl<sub>2</sub> (4.6 mg, 0.03 mmol, 2 mol%), PPh<sub>3</sub> (13.6 mg, 0.05 mmol, 4 mol%), and degassed water (2.6 mL, 0.5 M) under argon in a dried test tube was heated at 120 °C for 2 hours. It was then cooled and extracted with diethyl ether (3 x 5 mL). The organic layers were combined, washed with brine and dried with MgSO<sub>4</sub>. After evaporation under reduced pressure, the residue was purified by flash chromatography (15 cm x 3 cm) with hexanes to afford a light yellow oil in 26% yield. Spectral data was consistent with previously reported data.<sup>168</sup>

**<sup>1</sup>H NMR (300 MHz, CDCl<sub>3</sub>, 293 K):** δ 7.16 (dd, *J* = 5.1 Hz, 1.2 Hz, 1H), 7.11 (dd, *J* = 3.6 Hz, 0.9 Hz, 1H), 6.93 (dd, *J* = 5.4 Hz, 3.6 Hz, 1H), 2.42 (t, *J* = 7.2 Hz, 2H), 1.64 – 1.26 (m, 8H), 0.90 (t, *J* = 6.9 Hz, 3H).

### *N*-Tosyl-5-bromoindole:



NaH (60% suspension in paraffin) (210 mg, 5.3 mmol, 1.05 eq) was added to a stirred solution of 5-bromoindole (980 mg, 5 mmol, 1 eq) in anhydrous THF (10 mL, 0.5 M) at 0 °C over a 5 minute period. After stirring at room temperature for 1 h, tosyl chloride (1.0 g, 5.3 mmol, 1.05 eq) was added slowly. The reaction mixture was stirred for an additional 1 hour at room temperature and then poured into 50 mL of 5% aq. NaHCO<sub>3</sub> and extracted with ether (3 x 30 mL). The combined organic layers were washed with brine, dried with MgSO<sub>4</sub> and concentrated. Two recrystallizations from ethanol afforded the desired compound in 59% yield. Spectral data was consistent with previously reported data.<sup>169</sup>

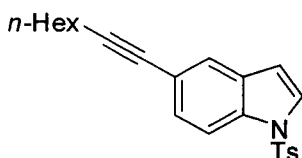
**<sup>1</sup>H NMR (400 MHz, CDCl<sub>3</sub>, 293 K):** δ 7.86 (d, *J* = 8.8 Hz, 1H), 7.74 (d, *J* = 8.4 Hz, 2H), 7.66 (d, *J* = 1.8 Hz, 1H), 7.56 (d, *J* = 3.7 Hz, 1H), 7.40 (dd, *J* = 8.8 Hz, 1.9 Hz, 1H), 7.23 (d, *J* = 8.1 Hz, 2H), 6.59 (d, *J* = 3.6 Hz, 1H), 2.35 (s, 3H).

<sup>167</sup> Bytsckov, I.; Siebeneicher, H.; Doye, S. *Eur. J. Org. Chem.* **2003**, 68, 2888.

<sup>168</sup> Guan, J. T.; Weng, T. Q.; Yu, G.-A.; Liu, S. H. *Tetrahedron Lett.* **2007**, 48, 7129.

<sup>169</sup> Fresneda, P. M.; Molina, P.; Bleda, J. A. *Tetrahedron* **2001**, 57, 2355.

## Compound 4.2g



A mixture of 1-octyne (80  $\mu$ L, 0.8 mmol, 1.2 eq), *N*-Tosyl-5-bromoindole (245 mg, 0.7 mmol, 1 eq) and Pd(PPh<sub>3</sub>)<sub>4</sub> (40 mg, 0.04 mmol, 5 mol%) in pyrrolidine (1.8 mL, 0.4 M) under argon in a dried test tube were stirred at 50 °C overnight. The pyrrolidine was evaporated and the residue purified by column chromatography (10 cm x 3 cm) with 10% ether/hexanes to give 73% of the desired product.

**<sup>1</sup>H NMR (400 MHz, CDCl<sub>3</sub>, 293 K):**  $\delta$  7.89 (d,  $J$  = 8.6 Hz, 1H), 7.73 (d,  $J$  = 8.4 Hz, 2H), 7.56 (d,  $J$  = 1.0 Hz, 1H), 7.54 (d,  $J$  = 3.7 Hz, 1H), 7.33 (dd,  $J$  = 8.6 Hz, 1.5 Hz, 1H), 7.21 (d,  $J$  = 8.0 Hz, 2H), 6.59 (dd,  $J$  = 3.7 Hz, 0.7 Hz, 1H), 2.39 (t,  $J$  = 7.1 Hz, 2H), 2.33 (s, 3H), 1.63 – 1.56 (m, 2H), 1.48 – 1.41 (m, 2H), 1.34 – 1.30 (m, 4H), 0.90 (t,  $J$  = 7.2 Hz, 3H).

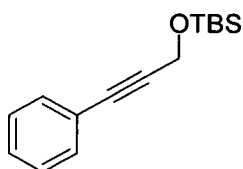
**<sup>13</sup>C NMR (100 MHz, CDCl<sub>3</sub>, 293 K):**  $\delta$  145.1 (C), 135.2 (C), 133.9 (C), 130.7 (C), 129.9 (CH), 128.1 (CH), 127.1 (CH), 127.8 (CH), 124.6 (CH), 119.2 (C), 113.4 (CH), 108.9 (CH), 89.6 (C), 80.5 (C), 31.4 (CH<sub>2</sub>), 28.8 (CH<sub>2</sub>), 28.6 (CH<sub>2</sub>), 22.6 (CH<sub>3</sub>), 21.6 (CH<sub>2</sub>), 19.4 (CH<sub>2</sub>), 14.1 (CH<sub>3</sub>).

**FTIR:** 2930, 1457, 1375, 1175, 670 cm<sup>-1</sup>.

**HRMS (EI):** calculated for C<sub>23</sub>H<sub>25</sub>NO<sub>2</sub>S (M<sup>+</sup>) 379.1606; found for C<sub>23</sub>H<sub>25</sub>NO<sub>2</sub>S (M<sup>+</sup>) 379.1616.

**R<sub>f</sub> (Ether/Hexanes (20:80)):** 0.48.

## Compound 4.2h



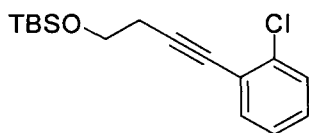
A previously reported procedure was followed<sup>170</sup> to afford the product in 89% yield. Slight modifications brought to the procedure are as follows: 3-phenyl-2-propyn-1-ol (0.500g, 3.78mmol, 1.0eq) as the starting alcohol and imidazole (2.0eq.) were used. The crude product was isolated as an oil using column chromatography on silica gel using 2.5% ether in pet. ether. This compound has been previously described in the literature.<sup>171</sup>

**<sup>1</sup>H NMR (400MHz, CDCl<sub>3</sub>, 293 K):**  $\delta$  7.41-7.44 (2H, m), 7.28-7.31 (3H, m), 4.54 (2H, s), 0.94 (9H, s), 0.17 (6H, s).

<sup>170</sup> Ilardi, E. A.; Stivala, C. E.; Zakarian, A. *Org. Lett.* **2008**, *10*, 1727.

<sup>171</sup> Oh, C. H.; Reddy, V. R. *Synlett* **2004**, 2091.

### Compound 4.2i



Literature procedure<sup>172</sup> was followed to afford the product in 94% yield as a colourless oil. However, 2 equivalents of imidazole were used. Crude product was purified by chromatography on silica gel (0-2% Et<sub>2</sub>O/Pet. Ether).

**<sup>1</sup>H NMR (400MHz, CDCl<sub>3</sub>, 293K, TMS):** δ 7.44-7.42 (1H, m), 7.38-7.36 (1H, m), 7.22-7.15 (2H, m), 3.85 (2H, t, *J*=7.1Hz), 2.69 (2H, t, *J*=7.1Hz), 0.92 (9H, br s), 0.10 (6H, br s);

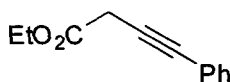
**<sup>13</sup>C NMR (400MHz, CDCl<sub>3</sub>, 293K, TMS):** δ 135.8 (C), 133.4 (CH), 129.1 (CH), 128.1 (CH), 126.3 (CH), 123.6 (C), 92.8 (C), 78.4 (C), 61.8 (CH<sub>2</sub>), 25.9 (CH<sub>3</sub>), 24.0 (CH<sub>2</sub>), 18.3 (C), -5.3 (CH<sub>3</sub>);

**IR (ν<sub>max</sub>, cm<sup>-1</sup>):** 2933, 2855, 1474, 1108, 834, 749;

**HRMS:** calculated for C<sub>16</sub>H<sub>23</sub>ClOSi (M-*t*Bu) 237.0502; Found: 237.0520;

**R<sub>f</sub>:** 0.561 on silica gel (5% Et<sub>2</sub>O:Pet.Ether)

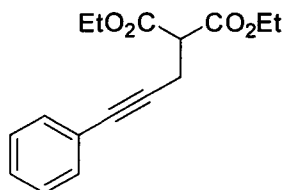
### Compound 4.2j



This compound was prepared by literature methods and displayed identical spectral data to that previously reported.<sup>146d</sup>

**<sup>1</sup>H NMR (400MHz, CDCl<sub>3</sub>, 293 K):** δ 7.46 – 7.43 (m, 2H), 7.30 – 7.28 (m, 3H), 4.22 (q, *J* = 7.1 Hz, 2H), 3.50 (s, 2H), 1.31 (t, *J* = 7.1 Hz, 3H).

### Compound 4.2k



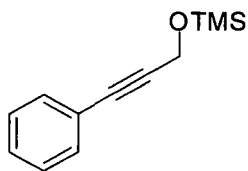
Prepared according to literature procedure; use of this compound has been described previously in the literature.<sup>173</sup>

**<sup>1</sup>H NMR (400MHz, CDCl<sub>3</sub>, 293 K):** δ 7.38 – 7.35 (m, 2H), 7.28 – 7.26 (m, 3H), 4.25 (q, *J* = 7.1 Hz, 4H), 3.65 (t, *J* = 7.8 Hz, 1H), 3.01 (d, *J* = 7.8 Hz, 2H), 1.29 (t, *J* = 7.1 Hz, 6H).

<sup>172</sup> Ilardi, E. A.; Stivala, C. E.; Zakarian, A. *Org. Lett.* **2008**, 10, 1727.

<sup>173</sup> Sturla, S. J.; Buchwald, S. L. *J. Org. Chem.* **2002**, 67, 3398.

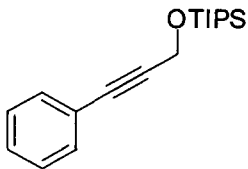
### Compound 4.2l



A previously reported procedure<sup>170</sup> was followed to afford the product in 31% yield. Slight modifications brought to the procedure are as follows: 3-phenyl-2-propyn-1-ol (0.300g, 2.27mmol, 1.0eq.) as the starting alcohol, imidazole (2.0eq.) and trimethylsilyl chloride (1.5eq.) were used. The crude product was isolated as an oil using column chromatography on silica gel using 10% ethyl acetate in pet. ether.

**<sup>1</sup>H NMR (400MHz, CDCl<sub>3</sub>, 293 K):** δ 7.42-7.44 (2H, m), 7.28-7.31 (3H, m), 4.51 (2H, s), 0.22 (9H, s).

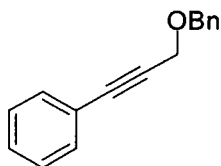
### Compound 4.2m



A previously reported procedure<sup>170</sup> was followed to afford the product in 70% yield. Slight modifications brought to the procedure are as follows: 3-phenyl-2-propyn-1-ol (0.300g, 2.27mmol, 1.0eq.) as the starting alcohol, imidazole (2.0eq.) and triisopropylsilyl chloride (1.5eq.) were used. The crude product was isolated as an oil using column chromatography on silica gel using 5% ether in pet. ether.

**<sup>1</sup>H NMR (300MHz, CDCl<sub>3</sub>, 293 K):** δ 7.41-7.43 (2H, m), 7.28, 7.31 (3H, m), 4.61 (2H, s), 1.10-1.22 (21H, m).

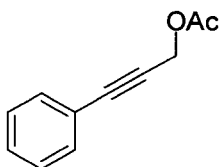
### Compound 4.2n



A previously reported procedure<sup>174</sup> was followed to afford the product in 59% yield. Slight modifications brought to the procedure are as follows: NaH (0.057g, 2.38mmol) was purged under argon for 10 minutes in a round bottom flask, to which dry THF (2.27ml) was subsequently added and cooled to 0°C. Benzyl bromide (0.504g, 2.95mmol) was added and stirred for 5 minutes, followed by the addition of 3-phenyl-2-propyn-1-ol (0.300g, 2.27mmol). The reaction mixture was stirred for 2 hours, gradually warming to room temperature. The crude product was isolated as an oil using column chromatography on silica gel using 5% ether in pet. ether.

<sup>1</sup>H NMR (400MHz, CDCl<sub>3</sub>, 293 K): δ 7.26-7.46 (10H, m), 4.64 (2H, s), 4.36 (2H, s).

### Compound 4.2o



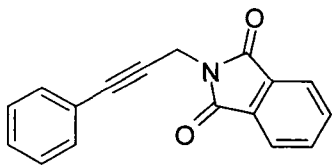
3-phenyl-2-propyn-1-ol (0.300g, 2.27mmol, 1 eq.) was added to dry DCM (12.0ml, 0.2M) in a round bottom flask equipped with a magnetic teflon stir bar, placed under argon atmosphere. Acetic anhydride (0.536g, 4.54mmol, 2 eq.) was subsequently added, followed by triethyl amine (0.345g, 3.41mmol, 1.5 eq.). The mixture was stirred for approximately 1 hours, until completion. The compound was purified via silica gel column chromatography using 5% ethyl acetate in pet. ether and isolated as an oil in 62% yield. Spectral data was consistent with that previously reported.<sup>175</sup>

<sup>1</sup>H NMR (400MHz, CDCl<sub>3</sub>, 293 K): δ 7.43-7.46 (2H, m), 7.26-7.31 (3H, m), 4.89 (2H, s), 2.09 (3H, s).

<sup>174</sup> Kadnikov, D. V.; Larock, R. C. *J. Org. Chem.* **2003**, *68*, 9423.

<sup>175</sup> Okuro, K.; Furuune, M.; Enna, M.; Miura, M.; Nomura, M. *J. Org. Chem.* **1993**, *58*, 4716.

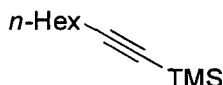
### Compound 4.2p



The above compound was prepared by heating (100°C) 1-phenyl-propargylbromide (0.3408 g, 1.75 mmol, 1 eq) and the potassium salt of phthalimide (0.3585 g, 1.94 mmol, 1.1 eq) in DMF (6 mL) for ~ 16 hours. This compound is also commercially available (CAS #: 4656-94-4).

**<sup>1</sup>H NMR (400MHz, CDCl<sub>3</sub>, 293 K):** δ 7.89 (m, 2H), 7.74 (m, 2H), 7.41 (m, 2H), 7.27 (m, 3H), 4.68 (s, 2H).

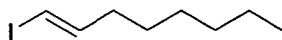
### Compound 4.7



A literature procedure was followed and spectral data was consistent with that previously reported.<sup>176</sup>

**<sup>1</sup>H NMR (400MHz, CDCl<sub>3</sub>, 293 K):** δ 2.21 (t, *J* = 7.1 Hz, 2H), 1.55 – 1.48 (m, 2H), 1.41 – 1.26 (m, 6H), 0.89 (t, *J* = 6.8 Hz, 3H), 0.15 (s, 9H).

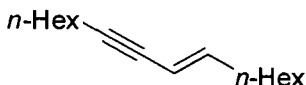
### *E*-1-iodooctene



The above compound was prepared from the following literature procedure and spectral data was consistent with that previously reported.<sup>177</sup>

**<sup>1</sup>H NMR (400MHz, CDCl<sub>3</sub>, 293 K):** δ 6.55 – 6.48 (m, 1H), 5.96 (d, *J* = 14.3 Hz, 1H), 2.08 – 2.02 (m, 2H), 1.40 – 1.23 (m, 8H), 0.88 (t, *J* = 6.7 Hz, 3H).

### Compound 4.11



The above compound was prepared *via* literature procedure and spectral data was consistent with that previously reported.<sup>178</sup>

<sup>176</sup> Blug, M.; Piechaczyk, O.; Fustier, M.; Mézailles, N.; Le Floch, P. *J. Org. Chem.* **2008**, *73*, 3258.

<sup>177</sup> Ren, H.; Krasovskiy, A.; Knochel, P. *Org. Lett.* **2004**, *6*, 4215.

<sup>178</sup> Li, J.-H.; Li, J.-L.; Wang, D.-P.; Pi, S.-F.; Xie, Y.-X.; Zhang, M.-B.; Hu, X.-C. *J. Org. Chem.* **2007**, *72*, 2053.

<sup>1</sup>H NMR (400MHz, CDCl<sub>3</sub>, 293 K): δ 6.08 – 6.01 (m, 1H), 5.48 – 5.42 (m, 1H), 2.30 – 2.26 (m, 2H), 2.10 – 2.04 (m, 2H), 1.55 – 1.25 (m, 16H), 0.92 – 0.86 (m, 6H).

### 5.4.3. Oxidative Annulation of Acetanilides and Characterization Data.

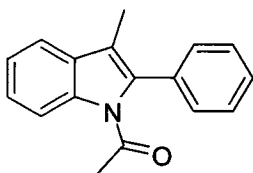
#### Representative procedure for the preparation of indoles (First generation conditions):

To a 1 dram screw-cap vial was added AgSbF<sub>6</sub> (0.0200 g, 0.06 mmol, 10 mol%) in the glove-box. The vial was sealed and removed from the glove-box. [Cp\*RhCl<sub>2</sub>]<sub>2</sub> (0.0092 g, 0.015 mmol, 2.5 mol%), Cu(OAc)<sub>2</sub>·H<sub>2</sub>O (0.252 g, 1.26 mmol, 2.1 eq) and acetanilide (0.6 mmol, 1 eq) are weighed into the vial open to air (if a solid, the alkyne is added at this point). *t*-AmOH (3 mL, 0.2 M) and alkyne (0.66 mmol, 1.1 eq) if a liquid are added via syringe and the reaction is sealed and placed in a pre-heated (120°C) block. The reaction is stirred for 1 hour (unless otherwise stated) and then cooled to room temperature and checked by TLC or GCMS. The reaction is filtered over Celite washing with ether into a 50 mL round-bottom flask and silica is added. The solvent is removed and the compound purified by flash column chromatography on silica gel (10 cm x 3 cm) with ether/pet. ether as the solvent (see below for specific eluent composition).

#### Representative procedure for the preparation of indoles (Second generation conditions):

The acetanilide (0.3 mmol, 1 eq.), [Cp\*Rh(MeCN)<sub>3</sub>][SbF<sub>6</sub>]<sub>2</sub> (0.0125 g, 0.015 mmol, 5 mol%), and Cu(OAc)<sub>2</sub>·H<sub>2</sub>O (0.0120 g, 0.06 mmol, 20 mol%) were weighed out to air and placed in a 15.0 × 1.5 cm Pyrex® tube with a stir bar (if the alkyne was a solid it was weighed out at this point as well (0.33 mmol, 1.1 eq)). *t*-AmOH (1.5 mL, 0.2 M) was added to the tube via syringe followed by the alkyne (if a liquid) (0.33 mmol, 1.1 eq.). A rubber septum was placed on the tube and it was sealed with electrical tape. Molecular oxygen was briefly purged through the solution (< 30 seconds) *via* a 16 cm needle (18 gauge) and a balloon of oxygen. The tube was then placed in a pre-heated (60°C) oil bath for 12 – 24 hours and left under a positive pressure of oxygen. After TLC analysis the reaction is filtered over celite washing with ether or dichloromethane into a 50 mL round-bottom flask. The solvent is removed and the compound purified by flash column chromatography on silica gel (10 cm x 3 cm) with ether/pet. ether as the solvent (typically 5 – 20% ether in pet. ether).

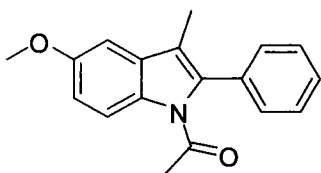
### Compound 4.3a



Prepared under first generation conditions (0.6 mmol scale) and isolated in 79% yield. Prepared under second generation conditions (0.3 mmol scale) and isolated in 90% yield. Spectral data was consistent with that previously reported.<sup>179</sup>

**<sup>1</sup>H NMR (400 MHz, CDCl<sub>3</sub>, 293 K):**  $\delta$  8.42 (d,  $J$  = 8.0 Hz, 1H), 7.55 – 7.30 (m, 8H), 2.14 (s, 3H), 1.96 (s, 3H).

### Compound 4.3b



Prepared under first generation conditions (0.6 mmol scale) and isolated in 82% yield. Prepared under second generation conditions (0.3 mmol scale) and isolated in 76% yield.

**<sup>1</sup>H NMR (400 MHz, CDCl<sub>3</sub>, 293 K):**  $\delta$  8.35 (d,  $J$  = 9.6 Hz, 1H), 7.51 – 7.41 (m, 3H), 7.38 (dd,  $J$  = 8.1 Hz,  $J$  = 1.7 Hz, 2H), 6.97 (dd,  $J$  = 8.6,  $J$  = 2.6 Hz, 1H), 6.96 (s, 1H), 3.89 (s, 3H), 2.10 (s, 3H), 1.93 (s, 3H).

**<sup>13</sup>C NMR (100 MHz, CDCl<sub>3</sub>, 293 K):**  $\delta$  170.0 (C), 156.5 (C), 135.6 (C), 133.7 (C), 131.6 (C), 131.2 (C), 130.3 (CH), 128.7 (CH), 128.5 (CH), 118.0 (C), 117.4 (CH), 113.3 (CH), 101.6 (CH), 55.8 (CH<sub>3</sub>), 27.5 (CH<sub>3</sub>), 9.3 (CH<sub>3</sub>).

**FTIR:** 2834, 1652, 1371, 1229, 947 cm<sup>-1</sup>.

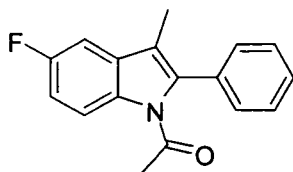
**HRMS (EI):** calculated for C<sub>18</sub>H<sub>17</sub>NO<sub>2</sub> (M<sup>+</sup>) 279.1259; found for C<sub>18</sub>H<sub>17</sub>NO<sub>2</sub> (M<sup>+</sup>) 279.1251.

**Melting point (Ether/Pet. Ether):** 92 – 93°C.

**R<sub>f</sub> (Ether/Pet. Ether (10:90)):** 0.19.

<sup>179</sup> Larock, R. C.; Yum, E. K.; Refvik, M. D. *J. Org. Chem.* **1998**, *63*, 7652

### Compound 4.3c



Prepared under first generation conditions (0.6 mmol scale) and isolated in 47% yield.  
Prepared under second generation conditions (0.3 mmol scale) and isolated in 74% yield.

**<sup>1</sup>H NMR (400 MHz, CDCl<sub>3</sub>, 293 K):** δ 8.39 (dd, *J* = 9.1 Hz, *J* = 4.7 Hz, 1H), 7.53 – 7.43 (m, 3H), 7.38 (dd, *J* = 8.1 Hz, *J* = 1.8 Hz, 2H), 7.16 (dd, *J* = 8.6 Hz, *J* = 2.6 Hz, 1H), 7.08 (dd, *J* = 9.1 Hz, *J* = 2.6 Hz, 1H), 2.09 (s, 3H), 1.94 (s, 3H).

**<sup>13</sup>C NMR (100 MHz, CDCl<sub>3</sub>, 293 K):** δ 170.8 (C), 159.7 (d, *J* = 240.3, C), 136.5 (C), 133.3 (C), 133.1 (C), 131.4 (d, *J* = 9.3 Hz, C), 130.2 (CH), 128.8 (CH), 128.7 (CH), 117.8 (d, *J* = 4.0 Hz, C), 117.6 (d, *J* = 8.8 Hz, CH), 112.7 (d, *J* = 24.4 Hz, CH), 104.2 (d, *J* = 23.5 Hz, CH), 27.5 (CH<sub>3</sub>), 9.3 (CH<sub>3</sub>).

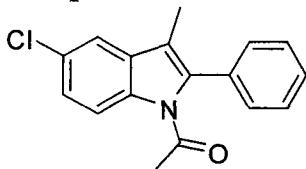
**FTIR:** 1645, 1452, 1308, 1210 cm<sup>-1</sup>.

**HRMS (EI):** calculated for C<sub>17</sub>H<sub>14</sub>FNO (M<sup>+</sup>) 267.1059; found for C<sub>17</sub>H<sub>14</sub>FNO (M<sup>+</sup>) 267.1072.

**Melting point (Ether/Pet. Ether):** 126 – 128°C.

**R<sub>f</sub> (Ether/Pet. Ether (5:95)):** 0.21.

### Compound 4.3d



Prepared under first generation conditions (0.6 mmol scale) and isolated in 62% yield.  
Prepared under second generation conditions (0.3 mmol scale) and isolated in 78% yield.

**<sup>1</sup>H NMR (400 MHz, CDCl<sub>3</sub>, 293 K):** δ 8.35 (d, *J* = 8.8 Hz, 1H), 7.52 – 7.30 (m, 7H), 2.10 (s, 3H), 1.94 (s, 3H).

**<sup>13</sup>C NMR (100 MHz, CDCl<sub>3</sub>, 293 K):** δ 170.9 (C), 136.2 (C), 135.1 (C), 133.1 (C), 131.6 (C), 130.2 (CH), 129.0 (C), 128.8 (CH), 125.3 (CH), 118.3 (CH), 117.5 (CH), 117.4 (C), 27.6 (CH<sub>3</sub>), 9.2 (CH<sub>3</sub>). There is one overlapping carbon signal as 1 peak is missing even after prolonged scans.

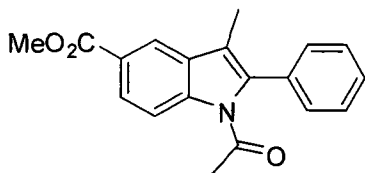
**FTIR:** 2923, 1700, 1450, 1306, 706 cm<sup>-1</sup>.

**HRMS (EI):** calculated for C<sub>17</sub>H<sub>14</sub>ClNO (M<sup>+</sup>) 283.0764; found for C<sub>17</sub>H<sub>14</sub>ClNO (M<sup>+</sup>) 283.0748.

**Melting point (Ether/Pet, Ether):** 65-66°C.

**R<sub>f</sub> (Ether/Pet. Ether (5:95)):** 0.28.

### Compound 4.3e



Prepared under first generation conditions (0.6 mmol scale) and isolated in 69% yield.

**<sup>1</sup>H NMR (400 MHz, CDCl<sub>3</sub>, 293 K):** δ 8.42 (d, *J* = 8.8 Hz, 1H), 8.26 (d, *J* = 2.4 Hz, 1H), 8.06 (dd, *J* = 8.8 Hz, *J* = 1.7 Hz, 1H), 7.54 – 7.39 (m, 5H), 3.96 (s, 3H), 2.18 (s, 3H), 1.97 (s, 3H).

**<sup>13</sup>C NMR (100 MHz, CDCl<sub>3</sub>, 293 K):** δ 171.2 (C), 167.5 (C), 139.4 (C), 136.1 (C), 133.0 (C), 130.2 (CH), 130.1 (C), 128.9 (CH), 128.8 (CH), 126.6 (CH), 125.3 (C), 120.9 (CH), 118.4 (C), 115.9 (CH), 52.1 (CH<sub>3</sub>), 27.7 (CH<sub>3</sub>), 9.2 (CH<sub>3</sub>).

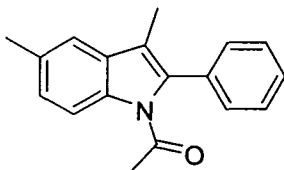
**FTIR:** 2850, 1711, 1303, 1250 cm<sup>-1</sup>.

**HRMS (EI):** calculated for C<sub>19</sub>H<sub>17</sub>NO<sub>3</sub> (M<sup>+</sup>) 307.1208; found for C<sub>19</sub>H<sub>17</sub>NO<sub>3</sub> (M<sup>+</sup>) 307.1240.

**Melting point (Ether/Pet. Ether):** 112 - 114°C.

**R<sub>f</sub> (Ether/Pet. Ether (10:90)):** 0.21.

### Compound 4.3f



Prepared under second generation conditions (0.3 mmol scale) and isolated as a yellow oil in 89% yield.

**<sup>1</sup>H NMR (400 MHz, CDCl<sub>3</sub>, 293 K):** δ 8.30 (d, *J* = 8.5 Hz, 1H), 7.50 – 7.36 (m, 5H), 7.31 (d, *J* = 1.7 Hz, 1H), 7.19 (dd, *J* = 8.5 Hz, *J* = 1.8 Hz, 1H), 2.48 (s, 3H), 2.11 (s, 3H), 1.94 (s, 3H).

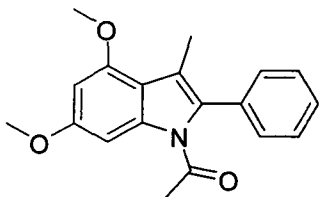
**<sup>13</sup>C NMR (100 MHz, CDCl<sub>3</sub>, 293 K):** δ 170.9 (C), 135.0 (C), 135.0 (C), 133.7 (C), 133.0 (C), 130.5 (C), 130.3 (CH), 128.7 (CH), 128.4 (CH), 126.6 (CH), 118.6 (CH), 118.0 (C), 116.1 (CH), 27.6 (CH<sub>3</sub>), 21.4 (CH<sub>3</sub>), 9.3 (CH<sub>3</sub>).

**FTIR:** 2917, 1698, 1302, 808, 773 cm<sup>-1</sup>.

**HRMS (EI):** calculated for C<sub>18</sub>H<sub>17</sub>NO (M<sup>+</sup>) 263.1310; found for C<sub>18</sub>H<sub>17</sub>NO (M<sup>+</sup>) 263.1333.

**R<sub>f</sub> (Ether/Pet. Ether (10:90)):** 0.26.

### Compound 4.3g



Prepared under first generation conditions (0.6 mmol scale) and isolated in 70% yield.  
Prepared under second generation conditions (0.3 mmol scale) and isolated in 69% yield.

**<sup>1</sup>H NMR (400 MHz, CDCl<sub>3</sub>, 293 K):**  $\delta$  7.65 (d,  $J = 2.0$  Hz, 1H), 7.46 (dd,  $J = J = 7.4$  Hz, 2H), 7.39 (tt,  $J = 7.3$  Hz,  $J = 1.5$  Hz, 1H), 7.34 (dd,  $J = 8.3$  Hz,  $J = 1.6$  Hz, 2H), 6.38 (d,  $J = 2.0$  Hz, 1H), 3.89 (s, 3H), 3.88 (s, 3H), 2.25 (s, 3H), 1.91 (s, 3H).

**<sup>13</sup>C NMR (100 MHz, CDCl<sub>3</sub>, 293 K):**  $\delta$  171.7 (C), 159.5 (C), 154.7 (C), 138.7 (C), 133.9 (C), 132.0 (C), 130.5 (CH), 128.6 (CH), 128.0 (CH), 118.4 (C), 113.7 (C), 95.3 (CH), 92.3 (CH), 55.8 (CH<sub>3</sub>), 55.4 (CH<sub>3</sub>), 27.9 (CH<sub>3</sub>), 11.7 (CH<sub>3</sub>).

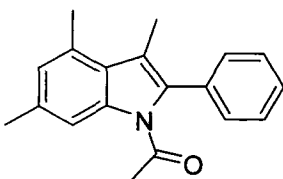
**FTIR:** 1647, 1421, 1285, 1043 cm<sup>-1</sup>.

**HRMS (EI):** calculated for C<sub>19</sub>H<sub>19</sub>NO<sub>3</sub> (M<sup>+</sup>) 309.1365; found for C<sub>19</sub>H<sub>19</sub>NO<sub>3</sub> (M<sup>+</sup>) 309.1374.

**Melting point (Ether/Pet. Ether):** 103 – 104°C.

**R<sub>f</sub> (Ether/Pet. Ether (15:85)):** 0.37.

### Compound 4.3h



The general procedure was carried out on 0.6 mmol of 3-methylacetanilide and 0.66 mmol of 1-phenylpropyne. Chromatography on silica gel (4-5% Et<sub>2</sub>O/Pet. ether) afforded the product in 7% yield as an off-white solid.

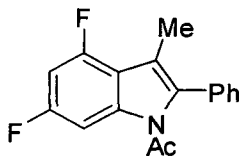
**<sup>1</sup>H NMR (400MHz, CDCl<sub>3</sub>, 293K, TMS):**  $\delta$  8.13 (1H, br s), 7.50-7.40 (3H, m), 7.37-7.35 (2H, m), 6.88 (1H, br s), 2.67 (3H, s), 2.45 (3H, s), 2.28 (3H, m), 1.89 (3H, m).

**<sup>13</sup>C NMR (400MHz, CDCl<sub>3</sub>, 293K, TMS):**  $\delta$  171.2 (C), 137.6 (C), 135.1(C), 134.2 (C), 133.9 (C), 130.5 (CH), 130.4 (C), 128.7 (CH), 128.3 (CH), 126.9 (CH), 126.1 (C), 118.7 (C), 114.1 (CH), 27.8 (CH<sub>3</sub>), 21.7 (CH<sub>3</sub>), 20.2 (CH<sub>3</sub>), 12.5 (CH<sub>3</sub>).

**HRMS:** calculated for C<sub>19</sub>H<sub>19</sub>NO (M<sup>+</sup>) 277.1467; Found: 277.1477

**R<sub>f</sub>:** 0.194 on silica gel (5% Et<sub>2</sub>O:Pet.Ether)

### Compound 4.3i



Prepared under the second generation conditions, purified by flash column chromatography with ether:pet. ether (5 : 95) as the solvent, and isolated in 74% yield.

**<sup>1</sup>H NMR (400MHz, CDCl<sub>3</sub>, 293K, TMS):** δ 8.01 (1H, ddd,  $J_{FH}=0.7\text{Hz}$ ,  $J=2.2\text{Hz}$ ,  $J_{FH}=10.3\text{Hz}$ ), 7.53-7.44 (3H, m), 7.38-7.36 (2H, m), 6.77 (1H, ddd,  $J=2.2\text{Hz}$ ,  $J_{FH}=9.5\text{Hz}$ ,  $J_{FH}=10.5\text{Hz}$ ), 2.23 (3H, d,  $J=1.3\text{Hz}$ ), 1.92 (3H, s)

**<sup>13</sup>C NMR (400MHz, CDCl<sub>3</sub>, 293K, TMS):** δ 171.1 (C), 160.9 (C, dd,  $J=11.8\text{Hz}$ ,  $J=241.8\text{Hz}$ ), 156.0 (C, dd,  $J=14.7\text{Hz}$ ,  $J=249.5\text{Hz}$ ), 138.1 (C, dd,  $J=11.9\text{Hz}$ ,  $J=15.1\text{Hz}$ ), 135.0-134.9 (C, m), 132.7 (CH), 130.4 (CH), 128.9 (C), 115.9-115.8 (C, m), 115.0 (C, dd,  $J=2.2\text{Hz}$ ,  $J=18.3\text{Hz}$ ), 100.0 (CH, dd,  $J=4.5\text{Hz}$ ,  $J=28.9\text{Hz}$ ), 99.0 (CH, dd,  $J=23.5\text{Hz}$ ,  $J=28.1\text{Hz}$ ), 27.5 (CH<sub>3</sub>), 10.9 (CH<sub>3</sub>, d,  $J=3.1\text{Hz}$ ). One carbon is not visible due to overlapping peaks.

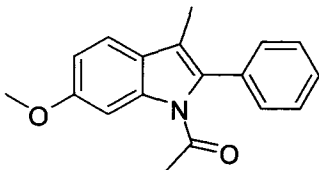
**IR (ν<sub>max</sub>, cm<sup>-1</sup>):** 3087, 2930, 1694, 1435, 1283, 837, 724

**HRMS:** calculated for C<sub>17</sub>H<sub>13</sub>F<sub>2</sub>NO (M<sup>+</sup>) 285.0965; Found: 285.0961;

**R<sub>f</sub>:** 0.270 on silica gel (5% Et<sub>2</sub>O:hexanes)

**Melting point:** 121-124°C

### Compound 4.3j



Prepared under first generation conditions (0.6 mmol scale) and isolated in 73% yield.  
Prepared under second generation conditions (0.3 mmol scale) and isolated in 67% yield.

**<sup>1</sup>H NMR (400 MHz, CDCl<sub>3</sub>, 293 K):** δ 8.05 (d,  $J=2.3\text{ Hz}$ , 1H), 7.50 – 7.35 (m, 6H), 6.96 (dd,  $J=8.5\text{ Hz}$ ,  $J=2.4\text{ Hz}$ , 1H), 3.90 (s, 3H), 2.12 (s, 3H), 1.94 (s, 3H).

**<sup>13</sup>C NMR (100 MHz, CDCl<sub>3</sub>, 293 K):** δ 171.4 (C), 158.7 (C), 137.8 (C), 133.8 (C), 133.6 (C), 130.2 (CH), 128.7 (CH), 128.2 (CH), 124.2 (C), 119.0 (CH), 118.2 (C), 112.6 (CH), 100.6 (CH), 55.8 (CH<sub>3</sub>), 27.7 (CH<sub>3</sub>), 9.3 (CH<sub>3</sub>).

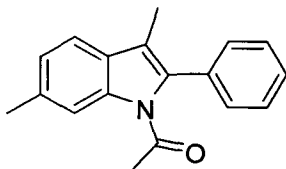
**FTIR:** 2936, 1695, 1484, 1320, 776 cm<sup>-1</sup>.

**HRMS (EI):** calculated for C<sub>18</sub>H<sub>17</sub>NO<sub>2</sub> (M<sup>+</sup>) 279.1259; found for C<sub>18</sub>H<sub>17</sub>NO<sub>2</sub> (M<sup>+</sup>) 279.1254.

**Melting point (Ether/Pet. Ether):** 76 – 78°C.

**R<sub>f</sub> (Ether/Pet. Ether (10:90)):** 0.21.

### Compound 4.3k



Prepared under the second generation conditions, purified by flash column chromatography with ether:pet. ether (4 : 96 to 5 : 95) as the solvent, and isolated in 78% yield.

**<sup>1</sup>H NMR (400MHz, (CD<sub>3</sub>)<sub>2</sub>CO, 293K):** δ 8.21-8.20 (1H, m), 7.58-7.54 (2H, m), 7.51-7.47 (3H, m), 7.45 (1H, d, *J*=7.9Hz), 7.15 (1H, ddd, *J*=0.6Hz, *J*=1.5Hz, *J*=7.9Hz), 2.48 (3H, s), 2.10 (3H, s), 1.92 (3H, s)

**<sup>13</sup>C NMR (400MHz, (CD<sub>3</sub>)<sub>2</sub>CO, 293K):** δ 172.2 (C), 139.1 (C), 136.6 (C), 136.5 (C), 135.7 (C), 132.2 (CH), 130.6 (CH), 130.3 (CH), 130.0 (C), 126.3 (CH), 120.1 (CH), 119.1 (C), 118.1 (CH), 28.7 (CH<sub>3</sub>), 23.1 (CH<sub>3</sub>), 10.3 (CH<sub>3</sub>)

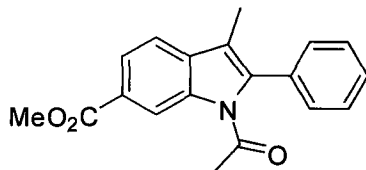
**IR (ν<sub>max</sub>, cm<sup>-1</sup>):** 3058, 2921, 1701, 1424, 1315, 1026, 699;

**HRMS:** calculated for C<sub>18</sub>H<sub>17</sub>NO (M<sup>+</sup>) 263.1310; Found: 263.1312;

**R<sub>f</sub>:** 0.148 on silica gel (4% Et<sub>2</sub>O:hexanes)

**Melting point:** 78-81°C

### Compound 4.3l



Prepared under the second generation conditions, purified by flash column chromatography with ether:pet. ether (10 : 90) as the solvent, and isolated in 22% yield.

**<sup>1</sup>H NMR (400MHz, CDCl<sub>3</sub>, 293K, TMS):** δ 9.08 (1H, dd, *J*=0.6Hz, *J*=1.4Hz), 8.03 (1H, dd, *J*=1.5Hz, *J*=8.2Hz), 7.57-7.49 (4H, m), 7.42-7.39 (2H, m), 3.96 (3H, s), 2.16 (3H, s), 1.98 (3H, s)

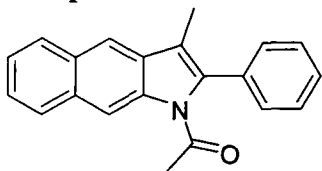
**<sup>13</sup>C NMR (400MHz, CDCl<sub>3</sub>, 293K, TMS):** δ 170.8 (C), 167.7 (C), 137.9 (C), 136.1 (C), 133.8 (C), 133.0 (C), 130.1 (CH), 128.9 (CH), 128.8 (CH), 126.9 (C), 124.8 (CH), 118.3 (CH), 117.9 (CH), 117.8 (C), 52.1 (CH<sub>3</sub>), 27.6 (CH<sub>3</sub>), 9.2 (CH<sub>3</sub>).

**HRMS:** calculated for C<sub>19</sub>H<sub>17</sub>NO<sub>3</sub> (M<sup>+</sup>) 307.1208; Found: 307.1223;

**R<sub>f</sub>:** 0.250 on silica gel (30% Et<sub>2</sub>O:hexanes)

**Melting point:** 124-127°C

### Compound 4.3m



Prepared under first generation conditions (0.6 mmol scale) and isolated in 62% yield.

**<sup>1</sup>H NMR (400 MHz, CDCl<sub>3</sub>, 293 K):** δ 8.96 (s, 1H), 8.03 – 7.99 (m, 1H), 7.97 – 7.92 (m, 1H), 7.92 (s, 1H), 7.54 – 7.41 (m, 7H), 2.21 (s, 3H), 1.97 (s, 3H).

**<sup>13</sup>C NMR (100 MHz, CDCl<sub>3</sub>, 293 K):** δ 170.7 (C), 137.6 (C), 136.4 (C), 133.5 (C), 132.4 (C), 131.2 (C), 130.7 (C), 130.1 (CH), 128.9 (CH), 128.8 (CH), 128.7 (CH), 127.8 (CH), 124.8 (CH), 124.6 (CH), 118.4 (C), 116.3 (CH), 113.8 (CH), 27.6 (CH<sub>3</sub>), 9.5 (CH<sub>3</sub>).

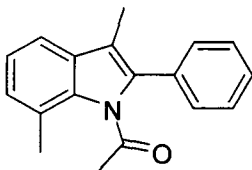
**FTIR:** 3056, 1689, 1318, 871, 746 cm<sup>-1</sup>.

**HRMS (EI):** calculated for C<sub>21</sub>H<sub>17</sub>NO (M<sup>+</sup>) 299.1310; found for C<sub>21</sub>H<sub>17</sub>NO (M<sup>+</sup>) 299.1325.

**Melting point (Ether/Pet. Ether):** 121 – 123°C.

**R<sub>f</sub> (Ether/Pet. Ether (10:90)):** 0.21.

### Compound 4.3n



Prepared under first generation conditions (0.6 mmol scale) and isolated in 66% yield.

Prepared under second generation conditions (0.3 mmol scale) and isolated in 72% yield.

**<sup>1</sup>H NMR (400 MHz, CDCl<sub>3</sub>, 293 K):** δ 7.49 – 7.38 (m, 6H), 7.22 (dd, *J* = 8.2 Hz, *J* = 6.8 Hz, 1H), 7.14 (d, *J* = 7.0 Hz, 1H), 2.41 (s, 3H), 2.13 (s, 3H), 1.99 (s, 3H).

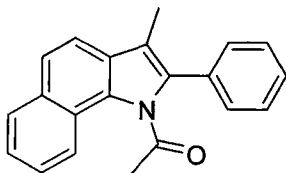
**<sup>13</sup>C NMR (100 MHz, CDCl<sub>3</sub>, 293 K):** δ 172.1 (C), 135.8 (C), 135.1 (C), 133.2 (C), 131.4 (C), 130.3 (CH), 128.6 (CH), 128.5 (CH), 127.6 (CH), 125.2 (C), 123.0 (CH), 116.5 (CH), 116.2 (C), 28.2 (CH<sub>3</sub>), 21.6 (CH<sub>3</sub>), 9.2 (CH<sub>3</sub>).

**FTIR:** 2926, 1714, 1303, 1198, 703 cm<sup>-1</sup>.

**HRMS (EI):** calculated for C<sub>18</sub>H<sub>17</sub>NO (M<sup>+</sup>) 263.1310; found for C<sub>18</sub>H<sub>17</sub>NO (M<sup>+</sup>) 263.1312.

**R<sub>f</sub> (Ether/Pet. Ether (10:90)):** 0.29.

### Compound 4.3o



Prepared under first generation conditions (0.6 mmol scale) and isolated in 72% yield.

**<sup>1</sup>H NMR (400 MHz, CDCl<sub>3</sub>, 293 K):** δ 8.16 (d, *J* = 9.1 Hz, 1H), 7.93 (d, *J* = 6.6 Hz, 1H), 7.72 (d, *J* = 8.5 Hz, 1H), 7.64 (d, *J* = 8.5 Hz, 1H), 7.52 – 7.41 (m, 7H), 2.25 (s, 3H), 2.19 (s, 3H).

**<sup>13</sup>C NMR (100 MHz, CDCl<sub>3</sub>, 293 K):** δ 175.2 (C), 135.2 (C), 132.8 (C), 132.3 (C), 130.7 (C), 130.5 (CH), 130.1 (C), 129.2 (CH), 128.6 (CH), 128.4 (CH), 128.0 (C), 125.6 (CH), 124.6 (CH), 124.3 (CH), 123.1 (C), 122.8 (CH), 118.1 (CH), 29.0 (CH<sub>3</sub>), 9.3 (CH<sub>3</sub>).

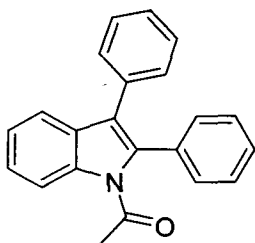
**FTIR:** 2919, 1721, 1376, 1298, 808 cm<sup>-1</sup>.

**HRMS (EI):** calculated for C<sub>21</sub>H<sub>17</sub>NO (M<sup>+</sup>) 299.1310; found for C<sub>21</sub>H<sub>17</sub>NO (M<sup>+</sup>) 299.1322.

**Melting point (Ether/Pet. Ether):** 86-88°C.

**R<sub>f</sub> (Ether/Pet. Ether (10:90)):** 0.35.

### Compound 4.3p



Prepared under first generation conditions (0.6 mmol scale) and isolated in 81% yield.

Prepared under second generation conditions (0.3 mmol scale) and isolated in 90% yield.

**<sup>1</sup>H NMR (400 MHz, CDCl<sub>3</sub>, 293 K):** δ 8.46 (d, *J* = 8.5 Hz, 1H), 7.56 (d, *J* = 8.2 Hz, 1H), 7.44 – 7.19 (m, 12H), 2.00 (s, 3H).

**<sup>13</sup>C NMR (100 MHz, CDCl<sub>3</sub>, 293 K):** δ 171.6 (C), 136.8 (C), 135.0 (C), 133.1 (C), 133.0 (C), 130.8 (CH), 130.4 (CH), 129.3 (C), 128.6 (CH), 128.6 (CH), 128.2 (CH), 126.9 (CH), 125.5 (CH), 123.8 (CH), 123.4 (C), 119.6 (CH), 116.2 (CH), 27.9 (CH<sub>3</sub>).

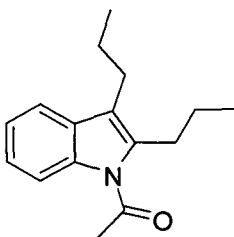
**FTIR:** 1650, 1443, 1313, 929 cm<sup>-1</sup>.

**HRMS (EI):** calculated for C<sub>22</sub>H<sub>17</sub>NO (M<sup>+</sup>) 311.1310; found for C<sub>22</sub>H<sub>17</sub>NO (M<sup>+</sup>) 311.1330.

**Melting point (Ether/Pet. Ether):** 123 – 124°C.

**R<sub>f</sub> (Ether/Pet. Ether (5:95)):** 0.21.

### Compound 4.3q



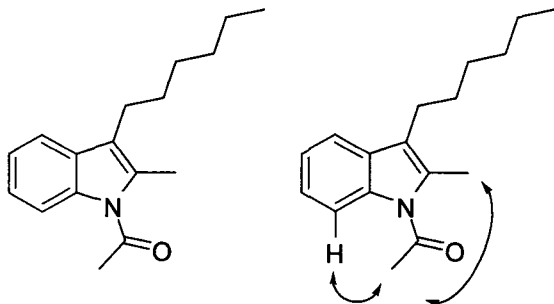
Prepared under first generation conditions (0.6 mmol scale) and isolated in 68% yield.

Prepared under second generation conditions (0.3 mmol scale) and isolated in 67% yield.

Spectral data was consistent with previously reported data.<sup>3</sup>

**<sup>1</sup>H NMR (400 MHz, CDCl<sub>3</sub>, 293 K):** δ 7.77 – 7.73 (m, 1H), 7.51 – 7.46 (m, 1H), 7.27 – 7.21 (m, 2H), 2.97 (t, *J* = 7.7 Hz, 2H), 2.76 (s, 3H) 2.63 (t, *J* = 7.6 Hz, 2H), 1.68 – 1.56 (m, 4H), 1.03 – 0.96 (m, 6H).

**Compound 4.3r (major isomer):**



The above procedure was followed and column chromatography was performed on silica gel with ether/pet. ether (5:95) as the solvent to afford the product in 50% yield.

**<sup>1</sup>H NMR (400 MHz, CDCl<sub>3</sub>, 293 K):** δ 7.78 – 7.74 (m, 1H), 7.47 – 7.43 (m, 1H), 7.27 – 7.22 (m, 2H), 3.00 (t, *J* = 7.6 Hz, 2H), 2.76 (s, 3H), 2.20 (s, 3H), 1.62 – 1.54 (m, 2H), 1.38 – 1.28 (m, 6H), 0.90 – 0.86 (m, 3H).

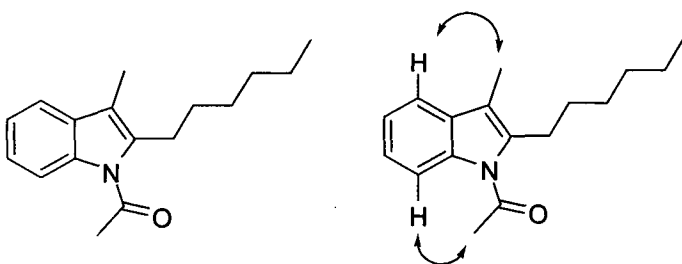
**<sup>13</sup>C NMR (100 MHz, CDCl<sub>3</sub>, 293 K):** δ 170.0 (C), 138.3 (C), 135.5 (C), 131.5 (C), 123.5 (CH), 122.7 (CH), 118.5 (CH), 115.3 (C), 114.5 (CH), 31.7 (CH<sub>2</sub>), 29.9 (CH<sub>2</sub>), 29.3 (CH<sub>2</sub>), 27.7 (CH<sub>3</sub>), 27.1 (CH<sub>2</sub>), 22.7 (CH<sub>2</sub>), 14.1 (CH<sub>3</sub>), 8.7(CH<sub>3</sub>).

**FTIR:** 2926, 1644, 1317, 750 cm<sup>-1</sup>.

**HRMS (EI):** calculated for C<sub>17</sub>H<sub>23</sub>NO (M<sup>+</sup>) 257.1780; found for C<sub>17</sub>H<sub>23</sub>NO (M<sup>+</sup>) 257.1788.

**R<sub>f</sub> (Ether/Pet. Ether (5:95)):** 0.49.

**Compound 4.3r (minor isomer):**



The above procedure was followed and column chromatography was performed on silica gel with ether/pet. ether (5:95) as the solvent to afford the product in 28% yield.

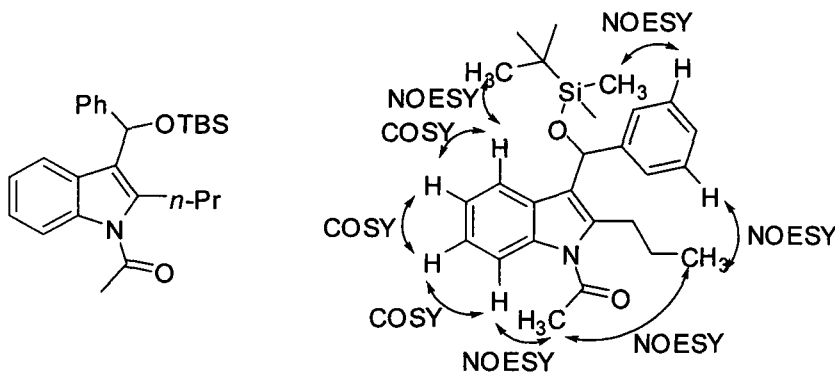
**<sup>1</sup>H NMR (400 MHz, CDCl<sub>3</sub>, 293 K):** δ 7.97 – 7.94 (m, 1H), 7.47 – 7.45 (m, 1H), 7.27 – 7.21 (m, 2H), 2.72 (s, 3H), 2.64 (t, *J* = 7.6 Hz, 2H), 2.55 (s, 3H), 1.61 – 1.54 (m, 2H), 1.38 – 1.28 (m, 6H), 0.90 – 0.86 (m, 3H).

**<sup>13</sup>C NMR (100 MHz, CDCl<sub>3</sub>, 293 K):** δ 170.3 (C), 135.8 (C), 132.6 (C), 130.7 (C), 123.6 (CH), 122.8 (CH), 120.4 (C), 118.3 (CH), 115.0 (CH), 31.8 (CH<sub>2</sub>), 30.0 (CH<sub>2</sub>), 29.3 (CH<sub>2</sub>), 27.6 (CH<sub>3</sub>), 23.9 (CH<sub>2</sub>), 22.7 (CH<sub>2</sub>), 14.4 (CH<sub>3</sub>), 14.1 (CH<sub>3</sub>).

**FTIR:** 2929, 1700, 1311, 746 cm<sup>-1</sup>.

**HRMS (EI):** calculated for  $C_{17}H_{23}NO$  ( $M^+$ ) 257.1780; found for  $C_{17}H_{23}NO$  ( $M^+$ ) 257.1877.  
**R<sub>f</sub> (Ether/Pet. Ether (5:95)):** 0.31.

**Compound 4.3s (major isomer)**



Second generation conditions were followed (0.3 mmol of acetanilide) and the residue was purified via silica gel chromatography using 5% Et<sub>2</sub>O, 5% benzene in pet. ether. The product was isolated as an oil in 47% yield (0.0593 g, 0.141 mmol).

**<sup>1</sup>H NMR (400MHz, CDCl<sub>3</sub>, 293 K):**  $\delta$  7.65 – 7.68 (2H, m), 7.42 – 7.44 (2H, m), 7.09 – 7.29 (5H, m), 6.15 (1H, s), 3.11 – 3.19 (1H, m), 2.96 – 3.04 (1H, m), 2.77 (3H, s), 1.50 – 1.64 (2H, m), 0.99 (3H, t,  $J = 7.3$ Hz), 0.92 (9H, s), 0.11 (3H, s), -0.17 (3H, s).

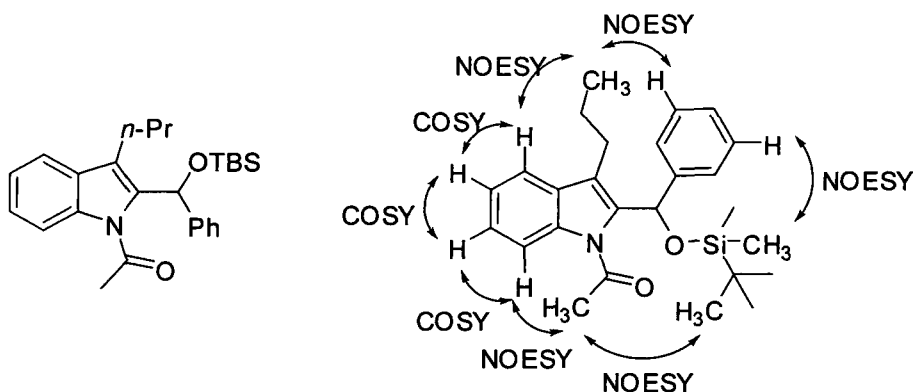
**<sup>13</sup>C NMR (400 MHz, CDCl<sub>3</sub>, 293 K):** 170.4 (C), 144.2 (C), 138.6 (C), 135.7 (C), 129.0 (C), 128.3 (CH), 128.0 (CH), 126.7 (CH), 126.3 (CH), 125.7 (CH), 123.4 (CH), 122.5 (CH), 122.2 (C), 121.4 (CH), 114.0 (CH), 69.1 (CH), 29.4 (CH<sub>2</sub>), 27.8 (CH<sub>3</sub>), 25.9 (CH<sub>3</sub>), 23.6 (CH<sub>2</sub>), 18.3 (C), 14.5 (CH<sub>3</sub>), -4.8 (CH<sub>3</sub>), -5.0 (CH<sub>3</sub>).

**FTIR:** 1708, 1462, 1062, 776, 744  $cm^{-1}$ .

**HRMS (EI):** calculated for  $C_{26}H_{35}NO_2Si$  ( $M^+$ ) 421.2437; found for  $C_{26}H_{35}NO_2Si$  ( $M^+$ ) 421.2448.

**R<sub>f</sub> (ether/benzene/pet. ether (1:1:18)):** 0.26

### Compound 4.3s (minor isomer)



Second generation conditions were followed (0.3 mmol of acetanilide) and the residue was purified via silica gel chromatography using 5% Et<sub>2</sub>O, 5% benzene in pet. ether. The product was isolated as an oil in 10% yield (0.0123 g, 0.029 mmol).

**<sup>1</sup>H NMR (400 MHz, CDCl<sub>3</sub>, 293 K):** δ 7.99 (1H, br d, *J* = 8.1 Hz), 7.55 (1H, br d, *J* = 7.5 Hz), 7.38 – 7.40 (2H, m), 7.21 – 7.40 (5H, m), 6.71 (1H, s), 2.77 – 2.85 (1H, m), 2.63 – 2.70 (1H, m), 2.50 (3H, s), 1.55 – 1.64 (1H, m), 1.42 – 1.52 (1H, m), 0.94 (3H, s), 0.94 (9H, s), 0.15 (3H, s), -0.14 (3H, s).

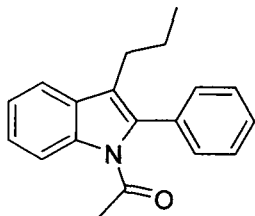
**<sup>13</sup>C NMR (400 MHz, CDCl<sub>3</sub>, 293 K):** δ 171.8 (C), 143.4 (C), 136.4 (C), 136.2 (C), 129.8 (C), 128.2 (CH), 128.2 (CH), 126.9 (CH), 126.0 (CH), 125.5 (CH), 124.7 (CH), 123.3 (C), 122.7 (CH), 119.2 (CH), 115.4 (CH), 68.5 (CH), 65.0 (C), 27.9 (CH<sub>3</sub>), 27.0 (CH<sub>2</sub>), 26.0 (CH<sub>3</sub>), 25.9 (CH<sub>3</sub>), 23.3 (CH<sub>2</sub>), 18.3 (CH<sub>3</sub>), 14.6 (CH<sub>3</sub>), -4.9 (CH<sub>3</sub>), -5.2 (CH<sub>3</sub>).

**FTIR:** 1702, 1457, 1062, 774, 741 cm<sup>-1</sup>.

**HRMS (EI):** calculated for C<sub>26</sub>H<sub>35</sub>NO<sub>2</sub>Si (M<sup>+</sup>) 421.2437; found for C<sub>26</sub>H<sub>35</sub>NO<sub>2</sub>Si (M<sup>+</sup>) 421.2421.

**R<sub>f</sub> (ether/pet. ether (1:1:18)):** 0.33

### Compound 4.3t



The above procedure was followed and column chromatography was performed on silica gel with ether/pet. ether (5:95) as the solvent to afford the product in 84% yield.

**<sup>1</sup>H NMR (400 MHz, CDCl<sub>3</sub>, 293 K):** δ 8.44 (br. d, *J* = 8.0 Hz, 1H), 7.56 (br. d, *J* = 7.2 Hz, 1H), 7.50 – 7.28 (m, 7H), 2.51 (t, *J* = 7.6 Hz, 2H), 1.93 (s, 3H), 1.66 – 1.56 (m, 2H), 0.86 (t, *J* = 7.4 Hz, 3H).

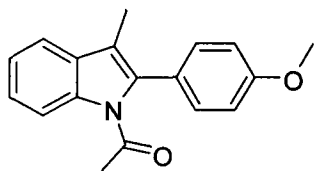
**<sup>13</sup>C NMR (100 MHz, CDCl<sub>3</sub>, 293 K):** δ 171.1 (C), 136.9 (C), 134.9 (C), 133.7 (C), 130.4 (CH), 129.6 (C), 128.7 (CH), 128.6 (CH), 125.2 (CH), 123.4 (CH), 122.8 (C), 118.9 (CH), 116.5 (CH), 27.7 (CH<sub>2</sub>), 26.4 (CH<sub>3</sub>), 23.4 (CH<sub>3</sub>), 14.2 (CH<sub>2</sub>).

**FTIR:** 2959, 1698, 1453, 1306, 749  $\text{cm}^{-1}$ .

**HRMS (EI):** calculated for  $\text{C}_{19}\text{H}_{19}\text{NO}$  ( $\text{M}^+$ ) 277.1467; found for  $\text{C}_{19}\text{H}_{19}\text{NO}$  ( $\text{M}^+$ ) 277.1452.

**R<sub>f</sub> (Ether/Pet. Ether (5:95)):** 0.27.

### Compound 4.3u



The general procedure was carried out on 0.6 mmol of acetanilide. Chromatography on silica gel (5-7%  $\text{Et}_2\text{O}$ /Pet. ether) afforded the product in 70% yield as an off-white solid.

**$^1\text{H}$  NMR (400MHz,  $\text{CDCl}_3$ , 293K, TMS):**  $\delta$  8.42 (1H, d,  $J=8.1\text{Hz}$ ), 7.52-7.50 (1H, m), 7.37-7.29 (4H, m), 7.03-7.01 (2H, m), 3.89 (3H, s), 2.13 (3H, m), 1.97 (3H, m)

**$^{13}\text{C}$  NMR (400MHz,  $\text{CDCl}_3$ , 293K, TMS):**  $\delta$  171.1 (C), 159.7 (C), 136.7 (C), 134.8 (C), 131.5 (CH), 130.3 (C), 125.7 (C), 125.1 (CH), 123.4 (CH), 118.4 (CH), 117.8 (C), 116.3 (CH), 114.2 (CH), 55.3 ( $\text{CH}_3$ ), 27.7 ( $\text{CH}_3$ ), 9.3 ( $\text{CH}_3$ )

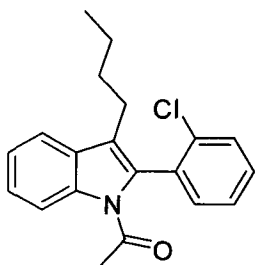
**IR ( $\nu_{\text{max}}$ ,  $\text{cm}^{-1}$ ):** 2940, 2836, 1696, 1453, 1308, 1030, 750

**HRMS:** calculated for  $\text{C}_{18}\text{H}_{17}\text{NO}_2$  ( $\text{M}^+$ ) 279.1259; Found: 279.1255

**R<sub>f</sub>:** 0.098 on silica gel (5%  $\text{Et}_2\text{O}$ :Pet.Ether)

**Melting point:** 92-95°C

### Compound 4.3v



The general procedure was carried out on 0.48 mmol of acetanilide. Chromatography on silica gel (5%  $\text{Et}_2\text{O}$ /Pet. ether) afforded the product in 73% yield as a yellow oil.

**$^1\text{H}$  NMR (400MHz,  $\text{CDCl}_3$ , 293K, TMS):**  $\delta$  8.46 (1H, br d,  $J=8.3\text{Hz}$ ), 7.59 (1H, ddd,  $J=0.7\text{Hz}$ ,  $J=1.3\text{Hz}$ ,  $J=7.7\text{Hz}$ ), 7.55-7.52 (1H, m), 7.45-7.37 (4H, m), 7.34-7.30 (1H, m), 2.54-2.38 (2H, m), 2.03 (3H, s), 1.60-1.43 (2H, m), 1.29-1.20 (2H, m), 0.80 (3H, t,  $J=7.3\text{Hz}$ );

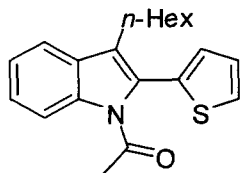
**$^{13}\text{C}$  NMR (400MHz,  $\text{CDCl}_3$ , 293K, TMS):**  $\delta$  170.1 (C), 136.8 (C), 135.5 (C), 133.1 (C), 132.6 (CH), 131.6 (C), 130.4 (CH), 129.9 (CH), 129.6 (C), 127.0 (CH), 125.4 (CH), 123.7 (C), 123.3 (CH), 119.1 (CH), 116.8 (CH), 31.7 ( $\text{CH}_2$ ), 26.3 ( $\text{CH}_3$ ), 24.0 ( $\text{CH}_2$ ), 22.6 ( $\text{CH}_2$ ), 13.8 ( $\text{CH}_3$ );

**IR ( $\nu_{\text{max}}$ ,  $\text{cm}^{-1}$ ):** 3054, 2956, 1701, 1370, 1309, 1041, 750

**HRMS:** calculated for  $\text{C}_{20}\text{H}_{20}\text{ClNO}$  ( $\text{M}^+$ ) 325.1233; Found: 325.1215

R<sub>f</sub>: 0.180 on silica gel (5% Et<sub>2</sub>O:Pet.Ether)

### Compound 4.3w



The above procedure was followed and column chromatography was performed on silica gel with ether/pet. ether (5:95) as the solvent to afford the product in 71% yield.

**<sup>1</sup>H NMR (400 MHz, CDCl<sub>3</sub>, 293 K):** δ 8.44 (dt, *J* = 8.4 Hz, 1H), 7.56 (br. d, *J* = 8.0 Hz, 1H), 7.51 (dd, *J* = 5.2 Hz, 1.2 Hz, 1H), 7.38 (ddd, *J* = 8.5 Hz, 7.2 Hz, 1.4 Hz, 1H), 7.30 (ddd, *J* = 7.7 Hz, 7.6 Hz, 1.1 Hz, 1H), 7.15 (dd, *J* = 5.2 Hz, 3.5 Hz, 1H), 7.11 (dd, *J* = 3.5 Hz, 1.2 Hz, 1H), 2.48 (t, *J* = 8.0 Hz, 2H), 2.10 (s, 3H), 1.63 – 1.56 (m, 3H), 1.32 – 1.19 (m, 5H), 0.85 (t, *J* = 6.9 Hz, 3H).

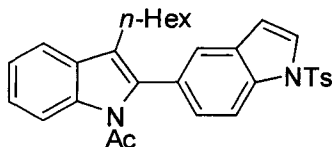
**<sup>13</sup>C NMR (100 MHz, CDCl<sub>3</sub>, 293 K):** δ 171.0 (C), 137.2 (C), 133.7 (C), 130.1 (CH), 129.2 (C), 128.2 (CH), 127.4 (CH), 126.8 (C), 126.0 (C), 125.7 (CH), 123.4 (CH), 119.0 (CH), 116.6 (CH), 31.6 (CH<sub>2</sub>), 30.3 (CH<sub>2</sub>), 29.4 (CH<sub>2</sub>), 26.4 (CH<sub>3</sub>), 24.6 (CH<sub>2</sub>), 22.6 (CH<sub>2</sub>), 14.1 (CH<sub>3</sub>).

**FTIR:** 2954, 1698, 1454, 1305, 750 cm<sup>-1</sup>.

**HRMS (EI):** calculated for C<sub>20</sub>H<sub>23</sub>NOS (M<sup>+</sup>) 325.1500; found for C<sub>20</sub>H<sub>23</sub>NOS (M<sup>+</sup>) 325.1512.

**R<sub>f</sub> (Ether/Pet. Ether (5:95)):** 0.29.

### Compound 4.3x



The above procedure was followed and column chromatography was performed on silica gel with ether/pet. ether (20:80) as the solvent to afford the product in 81% yield.

**<sup>1</sup>H NMR (400 MHz, CDCl<sub>3</sub>, 293 K):** δ 8.42 (d, *J* = 8.0 Hz, 1H), 8.01 (d, *J* = 8.1 Hz, 1H), 7.83 (d, *J* = 8.4 Hz, 2H), 7.65 (d, *J* = 3.7 Hz, 1H), 7.56 (br. s, 1H), 7.54 (br. s, 1H), 7.38 – 7.27 (m, 5H), 6.70 (dd, *J* = 3.7 Hz, 0.7 Hz, 1H), 2.49 (t, *J* = 7.6 Hz, 2H), 2.38 (s, 3H), 1.81 (s, 3H), 1.58 – 1.51 (m, 3H), 1.26 – 1.11 (m, 5H), 0.77 (t, *J* = 7.0 Hz, 3H).

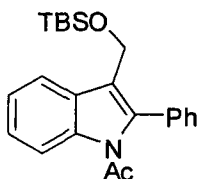
**<sup>13</sup>C NMR (100 MHz, CDCl<sub>3</sub>, 293 K):** δ 171.1 (C), 145.3 (C), 136.9 (C), 135.3 (C), 134.7 (C), 134.6 (C), 130.9 (C), 130.0 (CH), 129.6 (C), 128.7 (C), 127.5 (CH), 126.9 (CH), 126.8 (CH), 125.2 (CH), 123.4 (CH), 123.2 (C), 123.1 (CH), 118.9 (CH), 116.5 (CH), 113.7 (CH), 108.9 (CH), 31.4 (CH<sub>2</sub>), 30.1 (CH<sub>2</sub>), 29.2 (CH<sub>2</sub>), 27.7 (CH<sub>3</sub>), 24.2 (CH<sub>2</sub>), 22.5 (CH<sub>2</sub>), 21.6 (CH<sub>3</sub>), 14.0 (CH<sub>3</sub>).

**FTIR:** 2927, 2856, 1696, 1448, 1372, 1307 cm<sup>-1</sup>.

**HRMS (EI):** calculated for  $C_{31}H_{32}N_2O_3S$  ( $M^+$ ) 512.2134; found for  $C_{31}H_{32}N_2O_3S$  ( $M^+$ ) 512.2128.

**R<sub>f</sub> (Ether/Hexanes (20:80)):** 0.23.

### Compound 4.3y



Prepared under the second generation conditions, purified by flash column chromatography with ether:pet. ether (10 : 90) as the solvent, and isolated in 67% yield.

**<sup>1</sup>H NMR (400MHz, CDCl<sub>3</sub>, 293 K):** δ 8.39 (1H, br d,  $J = 8.1\text{Hz}$ ), 7.73 (1H, br d,  $J = 7.3\text{Hz}$ ), 7.51 – 7.43 (5H, m), 7.37 (1H, ddd,  $J = 7.3\text{Hz}$ ,  $J = 1.4\text{Hz}$ ), 7.32 (1H, ddd,  $J = 7.3\text{Hz}$ ,  $J = 1.2\text{Hz}$ ), 4.62 (2H, s), 1.97 (3H, s), 0.87 (9H, s), -0.02 (6H, s).

**<sup>13</sup>C NMR (400 MHz, CDCl<sub>3</sub>, 293 K):** δ 171.3 (C), 137.0 (C), 136.1 (C), 132.7 (C), 130.3 (CH), 129.0 (C), 128.9 (CH), 128.6 (CH), 125.4 (CH), 123.6 (CH), 121.4 (C), 119.6 (CH), 116.1 (CH), 56.6 (CH<sub>2</sub>), 27.8 (CH<sub>3</sub>), 25.9 (CH<sub>3</sub>), 18.3 (C), -5.3 (CH<sub>3</sub>).

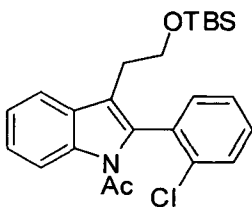
**FTIR:** 1750, 1452, 1303, 1085, 837  $\text{cm}^{-1}$ .

**HRMS (EI):** calculated for  $C_{23}H_{29}NO_2Si$  ( $M^+$ ) 379.1968; found for  $C_{23}H_{29}NO_2Si$  ( $M^+$ ) 379.1962.

**R<sub>f</sub> (ether/pet. ether (1:9)):** 0.43

**Melting point:** 58°C

### Compound 4.3z



The second generation conditions were used to afford the product in 82% yield as a yellow oil.

**<sup>1</sup>H NMR (400MHz, CDCl<sub>3</sub>, 293K, TMS):** δ 8.45 (1H, d,  $J=8.3\text{Hz}$ ), 7.64-6.62 (1H, m), 7.55-7.53 (1H, m), 7.47-7.37 (4H, m), 7.34-7.30 (1H, m), 3.77-3.66 (2H, m), 2.78-2.66 (2H, m), 2.04 (3H, s), 0.82 (9H, s), -0.06 (3H, s), -0.07 (3H, s).

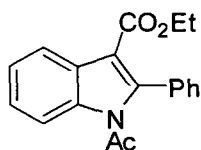
**<sup>13</sup>C NMR (400MHz, CDCl<sub>3</sub>, 293K, TMS):** δ 170.0 (C), 136.6 (C), 135.4 (C), 132.8 (C), 132.7 (C), 132.6 (CH), 130.6 (CH), 130.0 (CH), 129.6 (C), 127.2 (CH), 125.5 (CH), 123.4 (CH), 119.8 (C), 119.2 (CH), 116.8 (CH), 62.5 (CH<sub>2</sub>), 28.3 (CH<sub>2</sub>), 26.2 (CH<sub>3</sub>), 25.9 (CH<sub>3</sub>), 18.3 (C), -5.4 (CH<sub>3</sub>);

**IR (ν<sub>max</sub>,  $\text{cm}^{-1}$ ):** 2954, 2856, 1701, 1309, 1096, 750;

**HRMS:** calculated for  $C_{24}H_{30}ClNO_2Si$  ( $M^+$ ) 427.1734; Found: 427.1745;

**R<sub>f</sub>:** 0.118 on silica gel (5% Et<sub>2</sub>O:Pet.Ether)

### Compound 4.3aa



Prepared under the second generation conditions, purified by flash column chromatography with ether:pet. ether (5 : 95) as the solvent, and isolated in 57% yield.

**<sup>1</sup>H NMR (400 MHz, CDCl<sub>3</sub>, 293 K):** δ 8.33 – 8.31 (m, 1H), 8.23 – 8.20 (m 1H), 7.52 – 7.46 (m, 5H), 7.42 – 7.39 (m, 2H), 4.20 (q, J = 7.1 Hz, 2H), 1.91 (s, 3H), 1.16 (t, J = 7.1 Hz, 3H).

**<sup>13</sup>C NMR (100 MHz, CDCl<sub>3</sub>, 293 K):** δ □ 171.8 (C), 164.2 (C), 143.6 (C), 136.3 (C), 132.7 (C), 130.4 (CH), 129.5 (CH), 128.3 (CH), 126.9 (C), 125.7 (CH), 124.5 (CH), 121.7 (CH), 115.6 (CH), 112.5 (C), 60.2 (CH<sub>2</sub>), 27.7 (CH<sub>3</sub>), 14.0 (CH<sub>3</sub>).

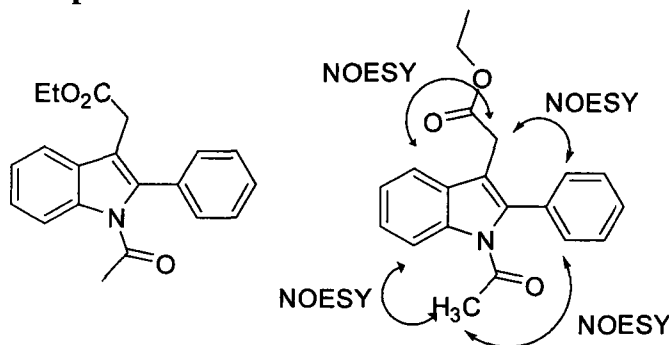
**FTIR:** 2984, 1707, 1177, 755, 701 cm<sup>-1</sup>.

**HRMS (EI):** calculated for C<sub>19</sub>H<sub>17</sub>NO<sub>3</sub> (M<sup>+</sup>) 307.1208; found for C<sub>19</sub>H<sub>17</sub>NO<sub>3</sub> (M<sup>+</sup>) 307.1215.

**Melting point (ether/pet. ether):** 100 – 102.

**R<sub>f</sub> (ether/pet. ether (10:90)):** 0.11.

### Compound 4.3ab



Prepared under the second generation conditions, purified by flash column chromatography with ether:pet. ether (5 : 95) as the solvent, and isolated in 85% yield.

**<sup>1</sup>H NMR (400 MHz, CDCl<sub>3</sub>, 293 K):** δ 8.42 (d, J = 8.3 Hz, 1H), 7.58 (d, J = 8.4 Hz, 1H), 7.52 – 7.46 (m, 5H), 7.39 (ddd, J = J = 8.6 Hz, J = 1.4 Hz, 1H), 7.32 (ddd, J = J = 8.7 Hz, J = 1.2 Hz, 1H), 4.14 (q, J = 7.1 Hz, 2H), 3.52 (s, 2H), 1.97 (s, 3H), 1.24 (t, J = 7.1 Hz, 3H).

**<sup>13</sup>C NMR (100 MHz, CDCl<sub>3</sub>, 293 K):** δ □ 171.1 (C), 136.9 (C), 136.8 (C), 132.6 (CH), 130.4 (C), 129.1 (CH), 129.1 (C), 128.8 (CH), 125.5 (CH), 123.7 (CH), 118.9 (CH), 116.4 (CH), 115.3 (C), 61.0 (CH<sub>2</sub>), 31.0 (CH<sub>2</sub>), 27.7 (CH<sub>3</sub>), 14.2 (CH<sub>3</sub>). Note: one signal missing due to overlapping peaks.

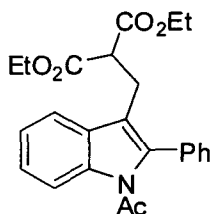
**FTIR:** 2985, 1737, 1702, 1302, 745, 702 cm<sup>-1</sup>.

**HRMS (EI):** calculated for C<sub>20</sub>H<sub>19</sub>NO<sub>3</sub> (M<sup>+</sup>) 321.1365; found for C<sub>20</sub>H<sub>19</sub>NO<sub>3</sub> (M<sup>+</sup>) 321.1353.

**Melting point (ether/pet. ether):** 76 – 78.

**R<sub>f</sub> (ethyl acetate/pet. ether (40:60)):** 0.74.

### Compound 4.3ac



Prepared under the second generation conditions, purified by flash column chromatography with ether:pet. ether (10:90 to 20:80) as the solvent, and isolated in 83% yield.

**<sup>1</sup>H NMR (400 MHz, CDCl<sub>3</sub>, 293 K):** δ 8.41 (d, J = 8.1 Hz, 1H), 7.58 (d, J = 8.4 Hz, 1H), 7.53 – 7.47 (m, 3H), 7.43 – 7.40 (m, 2H), 7.36 (ddd, J = J = 8.5 Hz, J = 1.4 Hz, 1H), 7.30 (ddd, J = J = 8.7 Hz, J = 1.2 Hz, 1H), 4.02 (q, J = 7.1 Hz, 4H), 3.52 (t, J = 7.8 Hz, 1H), 3.24 (d, J = 7.7 Hz, 2H), 1.92 (s, 3H), 1.10 (t, J = 7.1 Hz, 6H).

**<sup>13</sup>C NMR (100 MHz, CDCl<sub>3</sub>, 293 K):** δ 171.1 (C), 168.8 (C), 136.7 (C), 136.3 (C), 132.9 (C), 130.4 (CH), 129.0 (CH), 128.9 (CH), 125.4 (CH), 123.6 (CH), 118.8 (CH), 118.1 (C), 116.4 (CH).

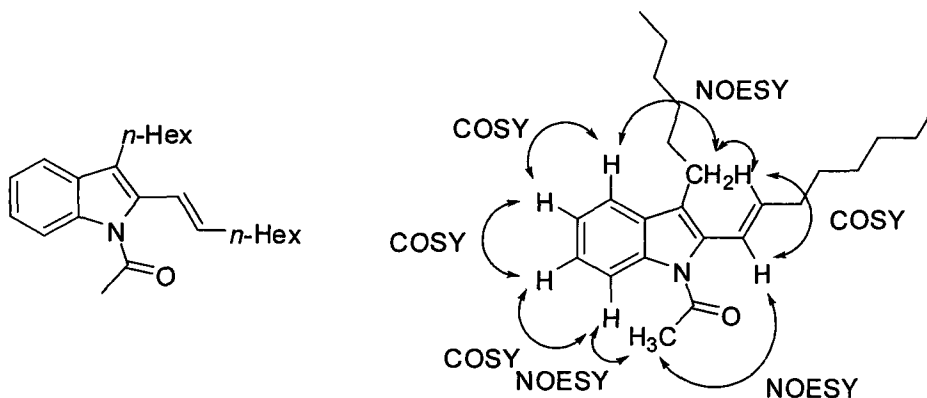
**FTIR:** 2983, 1734, 1702, 1301, 751, 700, 652 cm<sup>-1</sup>.

**HRMS (EI):** calculated for C<sub>24</sub>H<sub>25</sub>NO<sub>5</sub> (M<sup>+</sup>) 407.1733; found for C<sub>24</sub>H<sub>25</sub>NO<sub>5</sub> (M<sup>+</sup>) 407.1722.

**Melting point (ether/pet. ether):** 87 – 88.

**R<sub>f</sub> (ether/pet. ether (20:80)):** 0.25.

### Compound 4.12



First generation conditions were followed (0.367 mmol of acetanilide) and the residue was purified via silica gel chromatography using 5% Et<sub>2</sub>O in pet. ether. The product was isolated in 11% (0.0149 g, 0.042 mmol).

**<sup>1</sup>H NMR (400 MHz, CDCl<sub>3</sub>, 293 K):** δ 8.28 (d, J = 7.5 Hz, 1H), 7.49 (d, J = 7.2 Hz, 1H), 7.31 – 7.23 (m, 2H), 6.38 (d, J = 15.9 Hz, 1H), 5.90 (dt, J = 15.9 Hz, J = 7.0 Hz, 1H), 2.69 – 2.65 (m, 2H), 2.61 (s, 3H), 2.33 – 2.27 (m, 2H), 1.66 – 1.23 (m, 16H), 0.94 – 0.85 (m, 6H).

**<sup>13</sup>C NMR (100 MHz, CDCl<sub>3</sub>, 293 K):** δ 170.7 (C), 137.0 (CH), 136.3 (C), 133.6 (C), 130.3 (C), 124.8 (CH), 123.1 (CH), 122.3 (C), 121.4 (CH), 118.7 (CH), 116.1 (CH), 33.3 (CH<sub>2</sub>),

31.7 (CH<sub>2</sub>), 31.7 (CH<sub>2</sub>), 30.7 (CH<sub>2</sub>), 29.6 (CH<sub>2</sub>), 29.2 (CH<sub>2</sub>), 29.0 (CH<sub>2</sub>), 27.7 (CH<sub>3</sub>), 24.8 (CH<sub>2</sub>), 22.7 (CH<sub>2</sub>), 22.7 (CH<sub>2</sub>), 14.1 (CH<sub>3</sub>), 14.0 (CH<sub>3</sub>).

FTIR: 2927, 1700, 1314, 748 cm<sup>-1</sup>.

HRMS (EI): calculated for C<sub>24</sub>H<sub>35</sub>NO (M<sup>+</sup>) 353.2719; found for C<sub>24</sub>H<sub>35</sub>NO (M<sup>+</sup>) 353.2738.

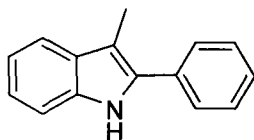
R<sub>f</sub> (ether/pet. ether (5:95)): 0.15.

#### 5.4.4. Deacetylation of *N*-Acetylindoles.

##### Representative Procedure for the deacetylation of *N*-Acetylindoles:

To a 4 dram vial containing a magnetic stir bar was weighed out 1-Acetyl-3-methyl-2-phenylindole (**4.3a**) (0.1004 g, 0.4 mmol, 1 eq). Methanol (2 mL) and dichloromethane (1 mL) (total concentration: 0.13 M) were added and **4.3a** dissolved. Potassium hydroxide (0.1278 g, 2 mmol, 5 eq) was added to the stirring reaction mixture and it was monitored by TLC analysis until deemed complete. After 1 hour (or specified time) of stirring at room temperature the reaction was diluted with dichloromethane and washed with a saturated solution of ammonium chloride. The organics were dried over MgSO<sub>4</sub> and the solvent removed under reduced pressure. The residue was loaded onto silica and flashed over silica with Ether/Pet. Ether.

##### Compound 4.6a

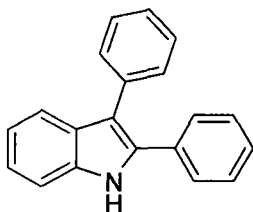


The above procedure was followed to afford the product in 90% yield. This compound can be purchased from commercial sources (CAS: 10257-92-8) and spectral data was consistent with that previously reported.<sup>180</sup>

<sup>1</sup>H NMR (400 MHz, CDCl<sub>3</sub>, 293 K): δ 7.97 (br. s, 1H), 6.61 – 6.54 (m, 3H), 7.48 – 7.44 (m, 2H), 7.36 – 7.32 (m, 2H), 7.20 (ddd, *J* = *J* = 7.1 Hz, *J* = 1.6 Hz, 1H), 7.14 (ddd, *J* = *J* = 7.4 Hz, *J* = 1.2 Hz, 1H), 2.45 (s, 3H).

<sup>180</sup> Jones, C.P.; Anderson, K.W.; Buchwald, S.L. *J. Org. Chem.* **2007**, *72*, 7968

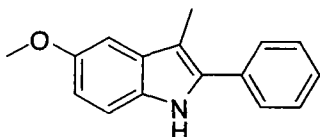
### Compound 4.6b



The above procedure was followed to afford the product in 97% yield. This compound can be purchased from commercial sources (CAS: 3469-20-3) and spectral data was consistent with that previously reported.<sup>181</sup>

**<sup>1</sup>H NMR (400 MHz, CDCl<sub>3</sub>, 293 K):**  $\delta$  8.14 (br. s, 1H), 7.68 (d,  $J = 7.6$  Hz, 1H), 7.44 – 7.33 (m, 7H), 7.31 – 7.19 (m, 5H), 7.15 (t,  $J = 8.0$  Hz, 1H).

### Compound 4.6c

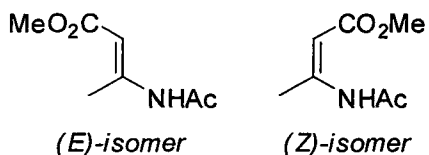


The above procedure was followed with stirring for 15 minutes to afford the product in 98% yield. Spectral data was consistent with that previously reported.<sup>182</sup>

**<sup>1</sup>H NMR (400 MHz, CDCl<sub>3</sub>, 293 K):**  $\delta$  7.90 (br. s, 1H), 7.56 – 7.53 (m, 2H), 7.48 – 7.42 (m, 2H), 7.33 (tt,  $J = 7.4$  Hz,  $J = 1.3$  Hz, 1H), 7.23 (d,  $J = 8.7$  Hz, 1H), 7.03 (d,  $J = 2.5$  Hz, 1H), 6.86 (dd,  $J = 8.7$  Hz,  $J = 2.5$  Hz, 1H), 3.88 (s, 3H), 2.42 (s, 3H).

## 5.4.5. Preparation and Characterization of Enamides.

### Compound 4.13



Prepared according to literature procedure. Spectral data was consistent with that previously reported.<sup>183</sup>

**(Z)-isomer:**

**<sup>1</sup>H NMR (400 MHz, CDCl<sub>3</sub>, 293 K):**  $\delta$  11.10 (br s, 1H), 4.91 (s, 1H), 3.70 (s, 3H), 2.39 (s, 3H), 2.15 (s, 3H).

**(E)-isomer:**

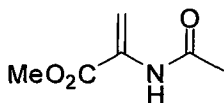
<sup>181</sup> Banerjee, S.; Barnea, E.; Odom, A.L. *Organometallics*. **2008**, *27*, 1005

<sup>182</sup> Swenton, J.S.; Shih, C.; Chen, C.-P.; Chou, C.-T. *J. Org. Chem.* **1990**, *55*, 2019

<sup>183</sup> Peña, D.; Minnaard, A. J.; de Vries, J. G.; Feringa, B.L. *J. Am. Chem. Soc.* **2002**, *124*, 14552.

$^1\text{H NMR}$  (400 MHz,  $\text{CDCl}_3$ , 293 K):  $\delta$  6.99 (br s, 1H), 6.77 (s, 1H), 3.68 (s, 3H), 2.35 (s, 3H), 2.12 (s, 3H).

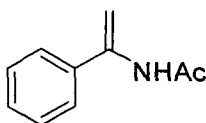
#### Compound 4.15a



Prepared according to literature procedure. Spectral data was consistent with that previously reported.<sup>184</sup>

$^1\text{H NMR}$  (400 MHz,  $\text{CDCl}_3$ , 293 K):  $\delta$  7.75 (br s, 1H), 6.60 (s, 1H), 5.88 (s, 1H), 3.85 (s, 3H), 2.13 (s, 3H).

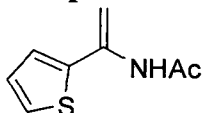
#### Compound 4.15b



Prepared according to literature procedure. Spectral data was consistent with that previously reported.<sup>185</sup>

$^1\text{H NMR}$  (300 MHz,  $\text{CDCl}_3$ , 293 K):  $\delta$  7.43 – 7.35 (m, 5H), 6.87 (br. s, 1H), 5.87 (s, 1H), 5.09 (s, 1H), 2.12 (s, 3H).

#### Compound 4.15c



Prepared according to literature procedure. Spectra data consistent with that previously reported.<sup>186</sup>

$^1\text{H NMR}$  (400 MHz,  $\text{CDCl}_3$ , 293 K):  $\delta$  7.22 – 6.97 (m, 4H), 5.73 (s, 1H), 5.22 (s, 1H), 2.10 (s, 3H).

### 5.4.6. Oxidative Annulations of Enamides and Characterization Data.

#### General Procedure A:

The enamide (0.3 mmol, 1 eq.),  $[\text{Cp}^*\text{Rh}(\text{MeCN})_3][\text{SbF}_6]_2$  (0.0125 g, 0.015 mmol, 5 mol%), and  $\text{Cu}(\text{OAc})_2\cdot\text{H}_2\text{O}$  (0.0120 g, 0.06 mmol, 20 mol%) were weighed out to air and placed in a

<sup>184</sup> Cresty, F.; Collot, V.; Stiebing, S.; Rault, S. *Synthesis* **2006**, 3506.

<sup>185</sup> Enthaler, S.; Hagemann, B.; Junge, K.; Erre, G.; Beller, M. *Eur. J. Org. Chem.* **2006**, 2912.

<sup>186</sup> Van der Burg, M.; Haak, R. M.; Minnaard, A. J.; De Vries, A. H. M.; De Vries, J. G.; Feringa, B. L. *Adv. Synth. Catal.* **2002**, *344*, 1003

15.0 × 1.5 cm glass tube with a stir bar (if the alkyne was a solid it was weighed out at this point as well (0.33 mmol, 1.1 eq)). *t*-AmOH (1.5 mL, 0.2 M) was added to the tube via syringe followed by the alkyne (if a liquid) (0.33 mmol, 1.1 eq.). A rubber septum was placed on the tube and it was sealed with electrical tape. Molecular oxygen was briefly purged through the solution (~ 30 seconds) via a 16 cm needle (18 gauge) and a balloon of oxygen. The tube was then placed in a pre-heated (60°C) oil bath overnight and left under a positive pressure of oxygen.

#### General Procedure B:

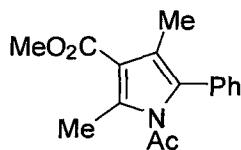
As above, however, the reaction was stirred for only 4 hours at 60°C.

#### General Procedure C:

As above, however the reaction solvent was acetone and the reaction was stirred for 18 hours at room temperature (21°C).

In all cases the reaction mixture was filtered over celite, washing with dichloromethane, and the volatiles removed under reduced pressure. The residue is purified via silica gel flash chromatography using the solvent systems described below.

#### Compound 4.14



The general procedure A was followed (0.3 mmol of enamide) and the residue was purified via silica gel chromatography using 10% Et<sub>2</sub>O in pet. ether. The product was isolated in 6% (0.0050 g, 0.018 mmol).

**<sup>1</sup>H NMR (400 MHz, CDCl<sub>3</sub>, 293 K):** δ 7.44 – 7.36 (m, 3H), 7.28 – 7.26 (m 2H), 3.85 (s, 3H), 2.67 (s, 3H), 2.13 (s, 3H), 1.91 (s, 3H).

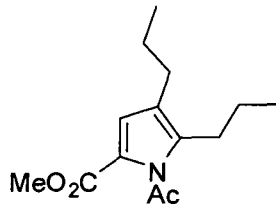
**<sup>13</sup>C NMR (100 MHz, CDCl<sub>3</sub>, 293 K):** δ 173.2 (C), 166.3 (C), 138.0 (C), 133.0 (C), 129.9 (CH), 129.4 (C), 128.8 (CH), 128.0 (CH), 121.3 (C), 114.9 (C), 51.0 (CH<sub>3</sub>), 28.4 (CH<sub>3</sub>), 13.5 (CH<sub>3</sub>), 11.6 (CH<sub>3</sub>).

**FTIR:** 2955, 1729, 1705, 1238, 767, 705 cm<sup>-1</sup>.

**HRMS (EI):** calculated for C<sub>16</sub>H<sub>17</sub>NO<sub>3</sub> (M<sup>+</sup>) 271.1208; found for C<sub>16</sub>H<sub>17</sub>NO<sub>3</sub> (M<sup>+</sup>) 271.1211.

**R<sub>f</sub> (ether/pet. ether (10:90)):** 0.30.

### Compound 4.16b



The general procedure A was followed (0.3 mmol of enamide) and the residue was purified via silica gel chromatography using 10% Et<sub>2</sub>O in pet. ether. The product was isolated in 83% (0.0621 g, 0.25 mmol).

**<sup>1</sup>H NMR (400 MHz, CDCl<sub>3</sub>, 293 K):** δ 6.84 (s, 1H), 3.81 (s, 3H), 2.59 (t, J = 7.7 Hz, 2H), 2.52 (s, 3H), 2.33 (t, J = 7.4 Hz, 2H), 1.61 – 1.49 (m, 4H), 0.96 – 0.90 (m, 6H).

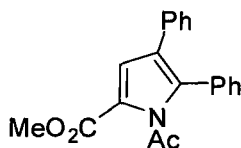
**<sup>13</sup>C NMR (100 MHz, CDCl<sub>3</sub>, 293 K):** δ 174.1 (C), 161.1 (C), 138.5 (C), 123.4 (C), 121.6 (C), 121.5 (CH), 51.6 (CH<sub>3</sub>), 28.6 (CH<sub>3</sub>), 27.5 (CH<sub>2</sub>), 27.1 (CH<sub>2</sub>), 23.6 (CH<sub>2</sub>, two overlapping signals), 14.0 (CH<sub>3</sub>), 14.0 (CH<sub>3</sub>).

**FTIR:** 2961, 1741, 1701, 763 cm<sup>-1</sup>.

**HRMS (EI):** calculated for C<sub>14</sub>H<sub>21</sub>NO<sub>3</sub> (M<sup>+</sup>) 251.1521; found for C<sub>14</sub>H<sub>21</sub>NO<sub>3</sub> (M<sup>+</sup>) 251.1507.

**R<sub>f</sub> (ether/pet. ether (10:90)):** 0.26.

### Compound 4.16c



The general procedure A was followed (0.3 mmol of enamide) and the residue was purified via silica gel chromatography using 10% Et<sub>2</sub>O in pet. ether. The product was isolated in 89% (0.0867 g, 0.27 mmol).

**<sup>1</sup>H NMR (400 MHz, CDCl<sub>3</sub>, 293 K):** δ 7.39 – 7.28 (m, 5H), 7.22 – 7.12 (m, 6H), 3.88 (s, 3H), 2.31 (s, 3H).

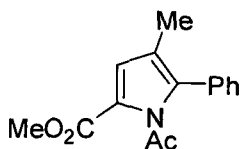
**<sup>13</sup>C NMR (100 MHz, CDCl<sub>3</sub>, 293 K):** δ 173.9 (C), 161.1 (C), 134.6 (C), 134.0 (C), 130.7 (CH), 128.9 (CH), 128.6 (CH), 128.3 (CH), 128.1 (CH), 126.5 (CH), 124.9 (C), 123.0 (C), 118.4 (CH), 51.9 (CH<sub>3</sub>), 28.9 (CH<sub>3</sub>).

**FTIR:** 2957, 1762, 1704, 756, 695 cm<sup>-1</sup>.

**HRMS (EI):** calculated for C<sub>20</sub>H<sub>17</sub>NO<sub>3</sub> (M<sup>+</sup>) 319.1208; found for C<sub>20</sub>H<sub>17</sub>NO<sub>3</sub> (M<sup>+</sup>) 319.1211.

**R<sub>f</sub> (ether/pet. ether (10:90)):** 0.26.

### Compound 4.16a



The general procedure A was followed (0.3 mmol of enamide) and the residue was purified via silica gel chromatography using 10% Et<sub>2</sub>O in pet. ether. The product was isolated in 85% (0.0658 g, 0.26 mmol). When general procedure C was followed an isolated yield of 81% (0.0623 g, 0.24 mmol) was obtained.

**<sup>1</sup>H NMR (400 MHz, CDCl<sub>3</sub>, 293 K):** δ 7.44 – 7.38 (m, 3H), 7.30 – 7.28 (m, 2H), 6.86 (s, 1H), 3.84 (s, 3H), 2.27 (s, 3H), 1.99 (s, 3H).

**<sup>13</sup>C NMR (100 MHz, CDCl<sub>3</sub>, 293 K):** δ 173.6 (C), 161.2 (C), 135.7 (C), 131.1 (C), 129.9 (CH), 128.5 (CH), 128.5 (CH), 122.7 (C), 120.5 (CH), 119.7 (C), 51.8 (CH<sub>3</sub>), 28.5 (CH<sub>3</sub>), 11.2 (CH<sub>3</sub>).

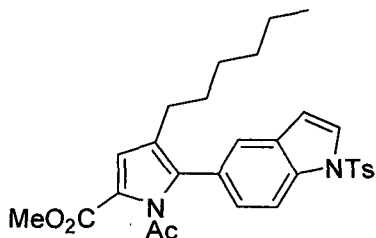
**FTIR:** 2955, 1747, 1694, 772, 702 cm<sup>-1</sup>.

**HRMS (EI):** calculated for C<sub>15</sub>H<sub>15</sub>NO<sub>3</sub> (M<sup>+</sup>) 257.1052; found for C<sub>15</sub>H<sub>15</sub>NO<sub>3</sub> (M<sup>+</sup>) 257.1042.

**Melting point (ether/pet. ether):** 103 – 104°C.

**R<sub>f</sub> (ether/pet. ether (10:90)):** 0.26.

### Compound 4.16d



The general procedure C was followed (0.171 mmol of enamide) and the residue was purified via silica gel chromatography using 20% EtOAc in pet. ether. The product was isolated in 70% (0.0622 g, 0.119 mmol).

**<sup>1</sup>H NMR (400 MHz, CDCl<sub>3</sub>, 293 K):** δ 8.02 (d, *J* = 8.6 Hz, 1H), 7.82 (d, *J* = 8.4 Hz, 2H), 7.61 (d, *J* = 3.7 Hz, 1H), 7.45 (d, *J* = 1.2 Hz, 1H), 7.27 (s, *J* = 8.1 Hz, 2H), 7.21 (dd, *J* = 8.6 Hz, *J* = 1.6 Hz, 1H), 6.89 (s, 1H), 6.66 (d, *J* = 4.1 Hz, 1H), 3.84 (s, 3H), 2.37 (s, 3H), 2.26 (t, *J* = 7.5 Hz, 2H), 2.20 (s, 3H), 1.48 – 1.41 (m, 2H), 1.26 – 1.10 (m, 6H), 0.80 (t, *J* = 6.8 Hz, 3H).

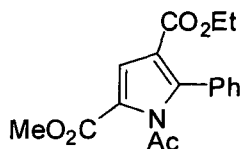
**<sup>13</sup>C NMR (100 MHz, CDCl<sub>3</sub>, 293 K):** δ 173.7 (C), 161.3 (C), 145.2 (C), 135.5 (C), 135.3 (C), 134.5 (C), 130.6 (C), 130.0 (CH), 127.1 (CH), 126.9 (CH), 126.6 (CH), 126.1 (C), 125.3 (C), 123.2 (CH), 122.7 (C), 119.3 (CH), 113.4 (CH), 108.8 (CH), 51.8 (CH<sub>3</sub>), 31.5 (CH<sub>2</sub>), 30.5 (CH<sub>2</sub>), 28.8 (CH<sub>2</sub>), 28.6 (CH<sub>3</sub>), 25.3 (CH<sub>2</sub>), 22.5 (CH<sub>2</sub>), 21.6 (CH<sub>3</sub>), 14.0 (CH<sub>3</sub>).

**FTIR:** 2933, 1752, 1701, 670, 586, 540 cm<sup>-1</sup>.

**HRMS (EI):** calculated for C<sub>29</sub>H<sub>32</sub>N<sub>2</sub>O<sub>5</sub>S (M<sup>+</sup>) 520.2032; found for C<sub>29</sub>H<sub>32</sub>N<sub>2</sub>O<sub>5</sub>S (M<sup>+</sup>) 520.2064.

$R_f$  (EtOAc/pet. ether (20:80)): 0.28.

#### Compound 4.16e



The general procedure C was followed (0.3 mmol of enamide) and the residue was purified via silica gel chromatography using 30% Et<sub>2</sub>O in pet. ether. The product was isolated in 82% (0.0776 g, 0.246 mmol).

**<sup>1</sup>H NMR (400 MHz, CDCl<sub>3</sub>, 293 K):**  $\delta$  7.47 – 7.37 (m, 6H), 4.13 (q,  $J$  = 7.1 Hz, 2H), 3.87 (s, 3H), 2.25 (s, 3H), 1.14 (t,  $J$  = 7.1 Hz, 3H).

**<sup>13</sup>C NMR (100 MHz, CDCl<sub>3</sub>, 293 K):**  $\delta$  173.1 (C), 163.3 (C), 160.8 (C), 140.9 (C), 130.3 (CH), 129.7 (C), 129.5 (CH), 128.1 (CH), 122.9 (C), 119.2 (CH), 115.4 (C), 60.1 (CH<sub>2</sub>), 52.1 (CH<sub>3</sub>), 28.8 (CH<sub>3</sub>), 14.0 (CH<sub>3</sub>).

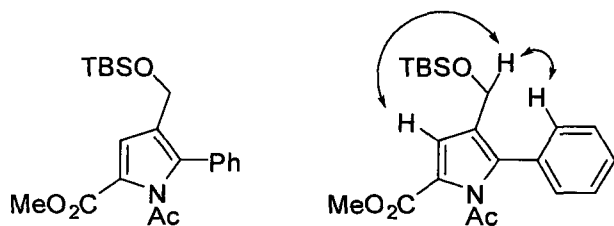
**FTIR:** 2987, 1772, 1710, 1223, 760, 702 cm<sup>-1</sup>.

**HRMS (EI):** calculated for C<sub>17</sub>H<sub>17</sub>NO<sub>5</sub> (M<sup>+</sup>) 315.1107; found for C<sub>17</sub>H<sub>17</sub>NO<sub>5</sub> (M<sup>+</sup>) 315.1097.

**Melting point (ether/pet. ether):** 91 – 93°C.

$R_f$  (ether/pet. ether (30:70)): 0.24.

#### Compound 4.16f



The general procedure C was followed (0.3 mmol of enamide) and the residue was purified via silica gel chromatography using 10% Et<sub>2</sub>O in pet. ether. The product was isolated in 81% (0.0964 g, 0.249 mmol).

**<sup>1</sup>H NMR (400 MHz, CDCl<sub>3</sub>, 293 K):**  $\delta$  7.43 – 7.40 (m, 3H), 7.36 – 7.34 (m, 2H), 7.04 (s, 1H), 4.40 (s, 2H), 3.85 (s, 3H), 2.28 (s, 3H), 0.88 (s, 9H), 0.01 (s, 6H).

**<sup>13</sup>C NMR (100 MHz, CDCl<sub>3</sub>, 293 K):**  $\delta$  173.7 (C), 161.2 (C), 135.8 (C), 130.3 (C), 130.0 (CH), 128.8 (CH), 128.4 (CH), 124.2 (C), 123.1 (C), 119.2 (CH), 57.5 (CH<sub>2</sub>), 51.8 (CH<sub>3</sub>), 28.7 (CH<sub>3</sub>), 25.9 (CH<sub>3</sub>), 18.4 (C), -5.3 (CH<sub>3</sub>).

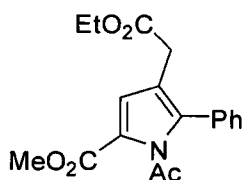
**FTIR:** 2954, 1761, 1709, 837, 775, 701 cm<sup>-1</sup>.

**HRMS (EI):** calculated for C<sub>21</sub>H<sub>29</sub>NO<sub>4</sub>Si (M<sup>+</sup>) 387.1866; found for C<sub>21</sub>H<sub>29</sub>NO<sub>4</sub>Si (M<sup>+</sup>) 387.1853.

**Melting point (ether/pet. ether):** 78 – 80°C.

$R_f$  (ether/pet. ether (10:90)): 0.24.

### Compound 4.16g



The general procedure **B** was followed (0.3 mmol of enamide) and the residue was purified via silica gel chromatography using 10% Et<sub>2</sub>O in pet. ether. The product was isolated in 79% (0.0780 g, 0.237 mmol).

**<sup>1</sup>H NMR (400 MHz, CDCl<sub>3</sub>, 293 K):** δ 7.44 – 7.41 (m, 3H), 7.34 – 7.31 (m, 2H), 7.01 (s, 1H), 4.13 (q, J = 7.1 Hz, 2H), 3.85 (s, 3H), 3.33 (s, 2H), 2.28 (s, 3H), 1.24 (t, J = 7.1 Hz, 3H).

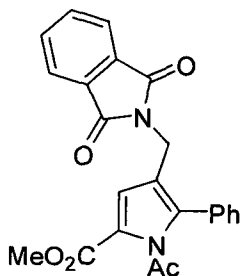
**<sup>13</sup>C NMR (100 MHz, CDCl<sub>3</sub>, 293 K):** δ 173.4 (C), 171.5 (C), 161.1 (C), 136.6 (C), 130.1 (CH), 130.1 (C), 129.0 (CH), 128.6 (CH), 123.1 (C), 119.7 (CH), 116.7 (C), 60.9 (CH<sub>2</sub>), 51.8 (CH<sub>3</sub>), 31.7 (CH<sub>2</sub>), 28.6 (CH<sub>3</sub>), 14.2 (CH<sub>3</sub>).

**FTIR:** 2988, 1735, 1706, 1234, 757, 699 cm<sup>-1</sup>.

**HRMS (EI):** calculated for C<sub>18</sub>H<sub>19</sub>NO<sub>5</sub> (M<sup>+</sup>) 329.1263; found for C<sub>18</sub>H<sub>19</sub>NO<sub>5</sub> (M<sup>+</sup>) 329.1235.

**R<sub>f</sub> (ether/pet. ether (30:70)):** 0.27.

### Compound 4.16h



The general procedure **C** was followed (0.3 mmol of enamide) and the residue was purified via silica gel chromatography using 30% EtOAc in pet. ether. The product was isolated in 77% (0.0928 g, 0.231 mmol).

**<sup>1</sup>H NMR (400 MHz, CDCl<sub>3</sub>, 293 K):** δ 7.82 (dd, J = 5.6 Hz, J = 3.1 Hz, 2H), 7.71 (dd, J = 5.5 Hz, J = 3.0 Hz, 2H), 7.01 (s, 1H), 4.62 (s, 2H), 3.80 (s, 3H), 2.25 (s, 3H).

**<sup>13</sup>C NMR (100 MHz, CDCl<sub>3</sub>, 293 K):** δ 173.2 (C), 167.9 (C), 161.0 (C), 136.2 (C), 134.0 (CH), 132.1 (C), 130.4 (CH), 129.7 (C), 129.2 (CH), 128.6 (CH), 123.4 (C), 123.3 (CH), 119.2 (C), 118.7 (CH) 51.9 (CH<sub>3</sub>), 33.5 (CH<sub>2</sub>), 28.5 (CH<sub>3</sub>).

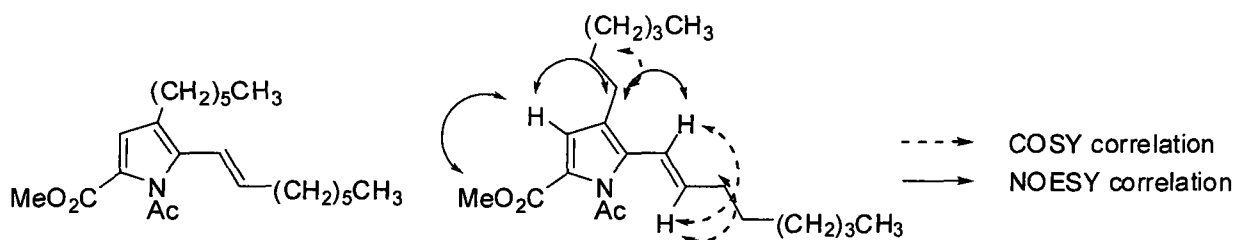
**FTIR:** 2958, 1769, 1718, 1393, 1220, 726, 715 cm<sup>-1</sup>.

**HRMS (EI):** calculated for C<sub>23</sub>H<sub>18</sub>N<sub>2</sub>O<sub>5</sub> (M<sup>+</sup>) 402.1216; found for C<sub>23</sub>H<sub>18</sub>N<sub>2</sub>O<sub>5</sub> (M<sup>+</sup>) 402.1199.

**Melting point (ether/pet. ether):** 139 – 140°C.

**R<sub>f</sub> (EtOAc/pet. ether (30:70)):** 0.26.

### Compound 4.16i



The general procedure **C** was followed (0.3 mmol of enamide) and the residue was purified via silica gel chromatography using 2.5 – 5% Et<sub>2</sub>O in pet. ether. The product was isolated in 58% (0.0621 g, 0.172 mmol) yield. When general procedure **B** was followed the product was isolated in 60% yield.

**<sup>1</sup>H NMR (400 MHz, CDCl<sub>3</sub>, 293 K):** δ 6.83 (s, 1H), 6.27 (d, J = 16.1 Hz, 1H), 5.91 (dt, J = 16.1 Hz, J = 7.0 Hz, 1H), 3.82 (s, 3H), 2.52 (s, 3H), 2.44 (t, J = 7.6 Hz, 2H), 2.20 (td (appears as q), J = J = 7.0 Hz, 2H), 1.59 – 1.52 (m, 2H), 1.48 – 1.41 (m, 2H), 1.38 – 1.25 (m, 12H), 0.91 – 0.87 (m, 6H).

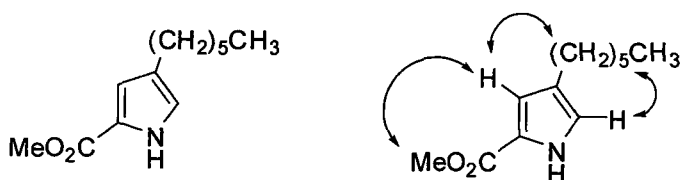
**<sup>13</sup>C NMR (100 MHz, CDCl<sub>3</sub>, 293 K):** δ 174.4 (C), 161.2 (C), 137.6 (CH), 133.9 (C), 124.6 (C), 121.5 (C), 120.9 (CH), 118.3 (CH), 51.7 (CH<sub>3</sub>), 33.6 (CH<sub>2</sub>), 31.7 (CH<sub>2</sub>), 31.7 (CH<sub>2</sub>), 30.2 (CH<sub>2</sub>), 29.2 (CH<sub>2</sub>), 28.8 (CH<sub>2</sub>), 28.7 (CH<sub>3</sub>), 26.4 (CH<sub>2</sub>), 22.6 (CH<sub>2</sub>), 14.1 (CH<sub>3</sub>). Three aliphatic carbon signals missing due to overlapping peaks.

**FTIR:** 2927, 1747, 1706, 1243, 761 cm<sup>-1</sup>.

**HRMS (EI):** calculated for C<sub>22</sub>H<sub>35</sub>NO<sub>3</sub> (M<sup>+</sup>) 361.2617; found for C<sub>22</sub>H<sub>35</sub>NO<sub>3</sub> (M<sup>+</sup>) 361.2626.

**R<sub>f</sub> (ether/pet. ether (10:90)):** 0.26.

### Compound 4.16j



The general procedure **C** was followed (0.3 mmol of enamide) employing 1-trimethylsilyl-1-octyne as the alkyne coupling partner. The solvent was removed and the reaction mixture filtered over a plug of silica (2 x 2.5 cm, 1 x w) washing with diethyl ether. Ether was removed under reduced pressure and the residue was dissolved in THF (1.5 mL, 0.2 M) and cooled to 0°C. TBAF (1 M in THF, 360 μL, 1.2 eq) was added and the reaction was stirred at room temp. The residue was purified via silica gel chromatography using 10% EtOAc in pet. ether. The product was isolated in 55% (0.0621 g, 0.172 mmol) yield over two steps.

**<sup>1</sup>H NMR (400 MHz, (CD<sub>3</sub>)<sub>2</sub>CO, 293 K):** δ 10.62 (br. s, 1H), 6.85 (s, 1H), 6.67 (s, 1H), 3.75 (s, 3H), 2.45 (t, J = 7.5 Hz, 2H), 1.60 – 1.52 (m, 2H), 1.37 – 1.26 (m, 6H), 0.88 (t, J = 6.6 Hz, 3H).

**$^{13}\text{C}$  NMR (100 MHz,  $(\text{CD}_3)_2\text{CO}$ , 293 K):**  $\delta$  162.8 (C), 127.7 (C), 123.9 (CH), 116.5 (CH), 52.1 ( $\text{CH}_3$ ), 33.4 ( $\text{CH}_2$ ), 32.9 ( $\text{CH}_2$ ), 30.7 ( $\text{CH}_2$ ), 28.3 ( $\text{CH}_2$ ), 24.3 ( $\text{CH}_2$ ), 15.3 ( $\text{CH}_3$ ).

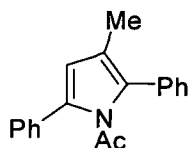
**FTIR:** 2924, 1700, 1216, 771  $\text{cm}^{-1}$ .

**HRMS (EI):** calculated for  $\text{C}_{12}\text{H}_{19}\text{NO}_2$  ( $\text{M}^+$ ) 209.1416; found for  $\text{C}_{12}\text{H}_{19}\text{NO}_2$  ( $\text{M}^+$ ) 209.1418.

**Melting point ( $(\text{CD}_3)_2\text{CO}$ ):** 66 – 68°C.

**$R_f$  (ether/pet. ether (10:90)):** 0.20.

### Compound 4.16k



The general procedure A was followed (using a 2 : 1 ratio of enamide to alkene; 0.3 mmol of alkyne) and the residue was purified via silica gel chromatography using 5%  $\text{Et}_2\text{O}$  in pet. ether to 10%  $\text{Et}_2\text{O}$  in pet. ether. The product was isolated in 71%.

**$^1\text{H}$  NMR (400 MHz,  $\text{CDCl}_3$ , 293 K):**  $\delta$  7.44 – 7.30 (m, 10H), 6.19 (s, 1H), 2.01 (s, 3H), 1.99 (s, 3H).

**$^{13}\text{C}$  NMR (100 MHz,  $\text{CDCl}_3$ , 293 K):**  $\delta$  172.2 (C), 134.6 (C), 133.9 (C), 133.3 (C), 131.6 (C), 130.1 (CH), 128.6 (CH), 128.3 (CH), 128.2 (CH), 127.5 (CH), 127.3 (CH), 121.0 (C), 115.5 (CH), 28.3 ( $\text{CH}_3$ ), 11.4 ( $\text{CH}_3$ ).

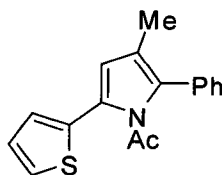
**FTIR:** 2923, 1729, 1294, 755, 699  $\text{cm}^{-1}$ .

**HRMS (EI):** calculated for  $\text{C}_{19}\text{H}_{17}\text{NO}$  ( $\text{M}^+$ ) 275.1310; found for  $\text{C}_{19}\text{H}_{17}\text{NO}$  ( $\text{M}^+$ ) 275.1322.

**Melting point (ether/pet. ether):** 82 – 86°C.

**$R_f$  (ether/pet. ether (10:90)):** 0.28.

### Compound 4.16l



The general procedure A was followed (using a 2 : 1 ratio of enamide to alkene; 0.3 mmol of alkyne) and the residue was purified via silica gel chromatography using 2 – 5%  $\text{Et}_2\text{O}$  in pet. ether. The product was isolated in 26%.

**$^1\text{H}$  NMR (400 MHz,  $\text{CDCl}_3$ , 293 K):**  $\delta$  7.44 – 7.30 (m, 6H), 7.12 (dd,  $J = 3.6$  Hz,  $J = 1.1$  Hz, 1H), 7.03 (dd,  $J = 5.1$  Hz,  $J = 3.6$  Hz, 1H), 6.29 (s, 1H), 2.02 (s, 3H), 2.00 (s, 3H).

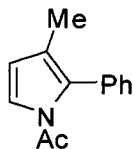
**$^{13}\text{C}$  NMR (100 MHz,  $\text{CDCl}_3$ , 293 K):**  $\delta$  172.2 (C), 134.5 (C), 133.2 (C), 131.8 (C), 129.7 (CH), 128.4 (CH), 127.7 (CH), 127.6 (CH), 127.0 (CH), 126.9 (C), 125.9 (CH), 121.1 (C), 116.8 (CH), 28.0 ( $\text{CH}_3$ ), 11.4 ( $\text{CH}_3$ ).

**FTIR:** 2924, 1730, 1292, 700  $\text{cm}^{-1}$ .

**HRMS (EI):** calculated for  $C_{17}H_{15}NOS$  ( $M^+$ ) 281.0874; found for  $C_{17}H_{15}NOS$  ( $M^+$ ) 281.0868.

**$R_f$  (ether/pet. ether (10:90)):** 0.42.

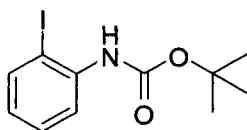
#### Compound 4.16m



The general procedure C was followed (using a 2 : 1 ratio of enamide to alkene; 0.3 mmol of alkyne) and the residue was purified *via* silica gel chromatography. The product was isolated in 32% and exhibited spectral data consistent with that previously reported.<sup>187</sup>

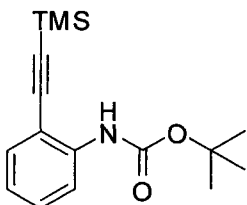
**$^1H$  NMR (400 MHz,  $CDCl_3$ , 293 K):**  $\delta$  7.42 – 7.26 (m, 6H), 6.18 (d,  $J$  = 3.4 Hz, 1H), 2.18 (s, 3H), 1.92 (s, 3H).

#### 5.4.7. Synthesis and Characterization of Intermediates *en route* to Paullone.



A literature procedure was followed to prepare the above compound.<sup>146a</sup> The desired compound may be purified via flash column chromatography on silica gel using  $Et_2O$  : Pet. ether (5 : 95) ( $R_f$  = 0.79 in  $Et_2O$  : Pet. ether (20 : 80)) and isolated in 99% yield. Alternatively, it may be used crude after extraction of the reaction mixture from  $Et_2O$  and saturated ammonium chloride. This compound can also be purchased from commercial sources (CAS: 161117-84-6) and NMR spectral data was consistent with that previously reported.<sup>146a</sup>

**$^1H$  NMR (400MHz,  $CDCl_3$ , 293K):**  $\delta$  8.05 (d,  $J$ =8.3 Hz, 1H), 7.75 (dd,  $J$ =1.3 Hz,  $J$ =8.0Hz, 1H), 7.33-7.29 (m, 1H), 6.82 (br s, 1H), 6.77 (ddd,  $J$ =1.4 Hz,  $J$ = $J$ =7.6 Hz, 1H), 1.54 (s, 9H).

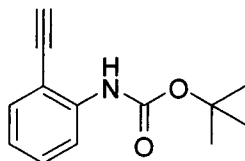


A literature procedure was followed to prepare the above compound.<sup>146b</sup> The desired compound may be purified via flash column chromatography on silica gel using  $Et_2O$  : Pet.

<sup>187</sup> Costagnolo, D.; Giorgi, G.; Spinosa, R.; Corelli, F.; Bota, M. *Eur. J. Org. Chem.* **2007**, 3676.

ether (2 : 98) ( $R_f = 0.24$  in Et<sub>2</sub>O : Pet. ether (2 : 98)) and isolated in 78% yield. Alternatively it may be used crude after extraction of the reaction mixture from Et<sub>2</sub>O and saturated ammonium chloride. The NMR spectral data obtained was consistent with that previously reported.<sup>146b</sup>

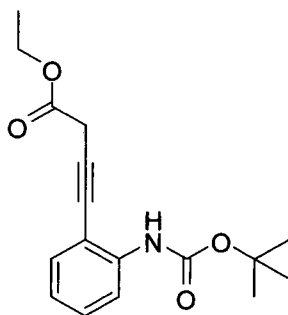
**<sup>1</sup>H NMR (300 MHz, CDCl<sub>3</sub>, 293K):**  $\delta$  8.11 (d,  $J = 8.4$  Hz, 1H), 7.38 – 7.26 (m, 3H), 6.93 (dd,  $J = J = 8.7$  Hz, 1H), 1.53 (s, 9H), 0.29 (s, 9H).



A literature procedure was followed to prepare the above compound.<sup>146c</sup> The desired compound may be purified via flash column chromatography on silica gel using Et<sub>2</sub>O : Pet. ether (4 : 96) ( $R_f = 0.35$  in Et<sub>2</sub>O : Pet. ether (4 : 96)) and isolated in 92% yield (> 95% purity by <sup>1</sup>H NMR spectroscopy). Alternatively, it may be used crude after extraction of the reaction mixture from Et<sub>2</sub>O and saturated sodium bicarbonate. The NMR spectral data obtained was consistent with that previously reported.<sup>188</sup>

**<sup>1</sup>H NMR (300 MHz, CDCl<sub>3</sub>, 293K):**  $\delta$  8.16 (d,  $J = 8.4$  Hz, 1H), 7.42 (d,  $J = 7.7$  Hz, 1H), 7.35 – 7.23 (m, 2H), 6.96 (dd,  $J = J = 8.7$  Hz, 1H), 3.48 (s, 1H), 1.54 (s, 9H).

#### Compound 4.23



A literature procedure was followed to prepare the above compound.<sup>146d</sup> The desired compound may be purified via flash column chromatography on silica gel using Et<sub>2</sub>O : Pet. ether (10 : 90) and the product obtained in 67 – 70% yield (for reactions on the scale ranging from 0.44 mmol – 2.31 mmol).

**<sup>1</sup>H NMR (400 MHz, CDCl<sub>3</sub>, 293K):**  $\delta$  8.16 (d,  $J = 8.4$  Hz, 1H), 7.53 (br. s, 1H), 7.34 (dd,  $J = 7.7$  Hz,  $J = 1.5$  Hz, 1H), 7.29 (ddd,  $J = J = 7.9$  Hz,  $J = 1.5$  Hz, 1H), 6.93 (ddd,  $J = J = 7.6$  Hz,  $J = 1.1$  Hz, 1H), 4.27 (q,  $J = 7.1$  Hz, 2H), 3.58 (s, 2H), 1.55 (s, 9H), 1.33 (t,  $J = 7.1$  Hz, 3H).

**<sup>13</sup>C NMR (100 MHz, CDCl<sub>3</sub>, 293K):**  $\delta$  168.1 (C), 152.6 (C), 140.2 (C), 131.4 (CH), 129.5 (CH), 121.8 (CH), 117.5 (CH), 110.7 (C), 88.3 (CH<sub>2</sub>), 80.7 (C), 79.5 (C), 61.9 (CH<sub>2</sub>), 28.3 (CH<sub>3</sub>), 27.0 (C), 14.2 (CH<sub>3</sub>).

<sup>188</sup> Ishizaki, M.; Zyo, M.; Kasama, Y.; Niimi, Y.; Hoshino, O.; Nishitani, K.; Hara, H. *Heterocycles* **2003**, *60*, 2259.

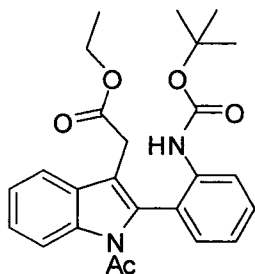
**FTIR:** 2980, 1733, 1520, 756  $\text{cm}^{-1}$ .

**HRMS (EI):** calculated for  $\text{C}_{17}\text{H}_{21}\text{NO}_4$  ( $\text{M}^+$ ) 303.1471; found for  $\text{C}_{17}\text{H}_{21}\text{NO}_4$  ( $\text{M}^+$ ) 303.1470.

**R<sub>f</sub> (ether/pet. ether (10:90)):** 0.16.

**\*NOTE:** The previously described four step sequence may be carried out without any chromatographic purification until the final step providing the alkyne in 47% overall yield.

#### Compound 4.24



The second generation conditions previously described were followed to prepare the above compound. This compound was purified via flash column chromatography on silica gel using  $\text{Et}_2\text{O}$  : Pet. ether (5 : 95 to 15 : 85) and the product obtained in 71 – 74% yield (for reactions on the scale ranging from 0.25 mmol – 0.60 mmol).

**$^1\text{H}$  NMR (400 MHz,  $\text{CDCl}_3$ , 293K):**  $\delta$  8.53 (d,  $J = 8.3$  Hz, 1H), 8.13 (d,  $J = 8.3$  Hz, 1H), 7.56 (d,  $J = 8.3$  Hz, 1H), 7.49 (ddd,  $J = J = 7.8$  Hz,  $J = 1.7$  Hz, 1H), 7.44 (ddd,  $J = J = 7.8$  Hz,  $J = 1.3$  Hz, 1H), 7.35 (ddd,  $J = J = 7.5$  Hz,  $J = 1.1$  Hz, 1H), 7.23 (dd,  $J = 7.6$  Hz,  $J = 1.5$  Hz, 1H), 7.17 (ddd,  $J = J = 7.4$  Hz,  $J = 1.1$  Hz, 1H), 6.91 (br. s, 1H), 4.13 (q,  $J = 7.1$  Hz, 2H), 3.52 (d,  $J = 16.0$  Hz, 1H), 3.41 (d,  $J = 16.0$  Hz, 1H), 1.94 (s, 3H), 1.45 (s, 9H), 1.21 (t,  $J = 7.1$  Hz, 3H).

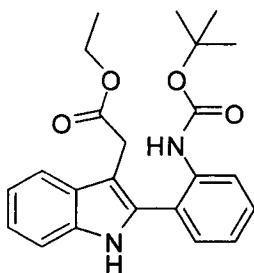
**$^{13}\text{C}$  NMR (100 MHz,  $\text{CDCl}_3$ , 293K):**  $\delta$  170.8 (C), 170.6 (C), 152.9 (C), 138.4 (C), 137.1 (C), 132.5 (C), 131.4 (CH), 130.8 (CH), 128.9 (C), 126.0 (CH), 123.9 (CH), 123.5 (CH), 122.2 (C), 121.4 (CH), 118.6 (CH), 117.2 (CH), 117.0 (C), 81 (CH<sub>2</sub>), 61.3 (CH<sub>2</sub>), 30.7 (C), 28.2 (CH<sub>3</sub>), 26.2 (CH<sub>3</sub>), 14.2 (CH<sub>3</sub>).

**FTIR:** 2981, 1730, 1305, 750  $\text{cm}^{-1}$ .

**HRMS (EI):** calculated for  $\text{C}_{25}\text{H}_{28}\text{N}_2\text{O}_5$  ( $\text{M}^+$ ) 436.1998; found for  $\text{C}_{25}\text{H}_{28}\text{N}_2\text{O}_5$  ( $\text{M}^+$ ) 436.2003.

**R<sub>f</sub> (ether/pet. ether (20:80)):** 0.19.

**Melting point:** 110 - 112°C



Compound **4.24** (0.0604 g, 0.138 mmol, 1 eq) was weighed into a vial equipped with a stir bar. EtOH : DCM (1 : 1, 0.7 mL, 0.2 M) was added to the vial followed by  $K_2CO_3$  (0.1924 g, 1.39 mmol, 10 eq). The reaction was stirred at room temperature overnight for 14 hours and then quenched by pouring into a saturated solution of ammonium chloride, followed by extraction with DCM (2  $\times$  30 mL). The combined organics were dried over  $MgSO_4$  and the solvent removed under reduced pressure. \*Note: the crude compound may be used in the following step without chromatographic purification. Alternatively, the residue was purified via flash chromatography on silica gel using Et<sub>2</sub>O : Pet. ether (20 : 80) as the eluent and the product obtained in 97% yield (0.0526 g, 0.133 mmol). \*Note: compound **4.24** and the product of the reaction co-elute on tlc; however, the product fluoresces as a bright pink spot under short wave UV irradiation where as compound **4.24** fluoresces as a more blue spot. Additionally, compound X reveals much faster when stained with permanganate.

**<sup>1</sup>H NMR (400 MHz, CDCl<sub>3</sub>, 293K):**  $\delta$  8.20 (br. s, 1H), 8.15 (d,  $J$  = 8.3 Hz, 1H), 7.64 (d,  $J$  = 8.4 Hz, 1H), 7.43 – 7.38 (m, 2H), 7.33 (dd,  $J$  = 7.7 Hz,  $J$  = 1.5 Hz, 1H), 7.27 (ddd,  $J$  =  $J$  = 8.2 Hz,  $J$  = 1.2 Hz, 1H), 7.19 (ddd,  $J$  =  $J$  = 8.0 Hz,  $J$  = 1.1 Hz, 1H), 7.11 (ddd,  $J$  =  $J$  = 7.5 Hz,  $J$  = 1.2 Hz, 1H), 6.91 (br. s, 1H), 4.12 (q,  $J$  = 7.1 Hz, 2H), 3.62 (s, 2H), 1.45 (s, 9H), 1.21 (t,  $J$  = 7.1 Hz, 3H).

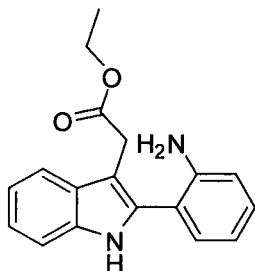
**<sup>13</sup>C NMR (100 MHz, CDCl<sub>3</sub>, 293K):**  $\delta$  171.7 (C), 153.2 (C), 137.4 (C), 136.1 (C), 132.3 (C), 131.3 (CH), 130.0 (CH), 128.2 (C), 123.0 (CH), 122.8 (CH), 121.7 (C), 120.3 (CH), 120.1 (CH), 119.2 (CH), 111.1 (CH), 108.2 (C), 80.7 (CH<sub>2</sub>), 60.9 (CH<sub>2</sub>), 30.8 (C), 28.3 (CH<sub>3</sub>), 14.2 (CH<sub>3</sub>).

**FTIR:** 2981, 1730, 1517, 746 cm<sup>-1</sup>.

**HRMS (EI):** calculated for C<sub>23</sub>H<sub>26</sub>N<sub>2</sub>O<sub>4</sub> (M<sup>+</sup>) 394.1893; found for C<sub>23</sub>H<sub>26</sub>N<sub>2</sub>O<sub>4</sub> (M<sup>+</sup>) 394.1886.

**R<sub>f</sub> (ether/pet. ether (20:80)):** 0.20.

**Melting point:** 48 - 50°C



Compound *N*-*boc* protected aniline (0.0780 g, 0.198 mmol, 1 eq.) was weighed into a vial containing a stir bar and trifluoroacetic acid (2.0 mL, 0.1 M) was added. The reaction was

stirred at room temperature for 30 min and then quenched with a saturated solution of sodium bicarbonate. This was then extracted with DCM (3 × 25 mL), dried over MgSO<sub>4</sub> and the solvent removed under reduced pressure. \*Note: the crude compound may be used in the following step without chromatographic purification. Alternatively, the residue was purified via flash chromatography on silica gel using EtOAc : Pet. ether (20 : 80) as the eluent and the product obtained in 94% yield (0.0550 g, 0.187 mmol).

**<sup>1</sup>H NMR (400 MHz, CDCl<sub>3</sub>, 293K):** δ 8.18 (br. s, 1H), 7.57 (d, *J* = 8.4 Hz, 1H), 7.26 (m, 5H), 6.79 (ddd, *J* = *J* = 7.5 Hz, *J* = 1.1 Hz, 1H), 6.73 (dd, *J* = 8.1 Hz, *J* = 0.8 Hz, 1H), 4.11 (q, *J* = 7.1 Hz, 2H), 3.92 (br. s, 1H), 3.68 (s, 2H), 1.22 (t, *J* = 7.1 Hz, 1H).

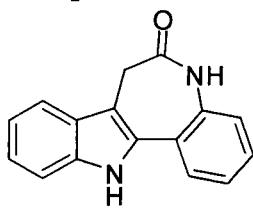
**<sup>13</sup>C NMR (100 MHz, CDCl<sub>3</sub>, 293K):** δ 172.5 (C), 145.5 (C), 135.9 (C), 133.6 (C), 131.3 (CH), 129.8 (CH), 128.3 (C), 122.3 (CH), 119.9 (CH), 118.9 (CH), 117.2 (C), 115.6 (CH), 110.9 (CH), 107.0 (C), 60.8 (CH<sub>2</sub>), 30.9 (CH<sub>2</sub>), 14.2 (CH<sub>3</sub>).

**FTIR:** 2983, 1721, 1461, 746 cm<sup>-1</sup>.

**HRMS (EI):** calculated for C<sub>18</sub>H<sub>18</sub>N<sub>2</sub>O<sub>2</sub> (M<sup>+</sup>) 294.1368; found for C<sub>18</sub>H<sub>18</sub>N<sub>2</sub>O<sub>2</sub> (M<sup>+</sup>) 294.1358.

**R<sub>f</sub> (EtOAc/pet. ether (20:80)):** 0.29.

#### Compound 4.18



The above compound was prepared by a literature procedure employing either the crude or chromatographically purified starting material and the <sup>1</sup>H NMR spectral data was consistent with that previously reported.<sup>146h</sup>

**<sup>1</sup>H NMR (400 MHz, DMSO-d<sub>6</sub>, 293K):** δ 11.56 (s, 1H), 10.10 (s, 1H), 7.75 (dd, *J* = 7.6 Hz, *J* = 1.1 Hz, 1H), 7.66 (d, *J* = 7.9 Hz, 1H), 7.44 (d, *J* = 8.1 Hz, 1H), 7.37 (ddd, *J* = *J* = 7.8 Hz, *J* = 1.5 Hz, 1H), 7.30 – 7.25 (m, 2H), 7.18 (dd, *J* = *J* = 7.0 Hz, 1H), 7.08 (dd, *J* = *J* = 7.1 Hz, 1H), 3.51 (s, 2H).

\***NOTE:** The previously described three step sequence may be carried out without any chromatographic purification until the final step providing the Paullone in 33% overall yield over the three steps.

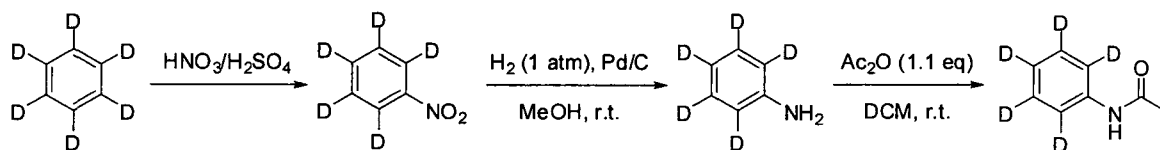
#### 5.4.8. Description of Kinetic Experiments and Mechanistic Investigation.

**Kinetic Data:** All kinetic data, including order of reagents, DKIE, Hammett correlation, and the Arrhenius plot were obtained in the following way. The acetanilide (~ 14 mg, 0.1 mmol, 1 eq), alkyne (~ 14 μL, 0.11 mmol, 1.1 eq), copper(II) acetate (~42 mg, 0.21 mmol, 2.1 eq), trimethoxybenzene (internal standard) (~ 17 mg, 0.1 mmol, 1 eq) and *t*-AmOH (0.5 mL) were added to a vial which was sealed with a plastic cap lined with a septa and heated to 60

°C for ~ 2 minutes to ensure complete dissolution of the acetanilide (note: copper(II) acetate was not completely soluble at this temperature). In a separate vial [Cp\*Rh(MeCN)<sub>3</sub>][SbF<sub>6</sub>]<sub>2</sub> (~ 0.007 g, 0.0084 mmol) was weighed out and 200 μL of acetone was added to yield a clear bright yellow solution of the catalyst (0.042 M). 140 μL of the catalyst solution (0.005 mmol, 5 mol%) was added *via* microsyringe to the reaction mixture to initiate the reaction and signify time zero (*t* = 0). Aliquots (~ 10 – 20 μL) were then removed at 20 second intervals for the first 80 seconds of the reaction. Each aliquot was diluted with ethyl acetate and extracted with a saturated solution of ammonium chloride to remove the copper. The organic layer was then analyzed by GCMS and the relative concentration of indole formed was determined from a calibration curve against the internal standard.

**Order of reagents:** This procedure was done for at least 4 different initial concentrations of each reagent. Errors were obtained for the slope of the concentration vs. time graphs using the LINEST function in Microsoft Office Excel 2007 to approximate the error in the initial rate. These errors were applied as vertical error bars in the initial rate vs. concentration graph in the determination of the dependence of reaction rate on initial concentration of each reagent.

**Preparation of deuterated acetanilide and deuterium loss experiments:**



Concentrated nitric acid and concentrated sulfuric acid (1:1 v/v) were mixed together in a round-bottom flask held in an ice-water bath. Benzene-*d*<sub>6</sub> (2.0 mL, 23 mmol, 1 eq) was added drop-wise at room temperature and the reaction was allowed to stir for an additional 15 minutes. The reaction mixture was poured into ice-water and extracted with DCM. Nitration was determined by GCMS and the product was used without further purification.

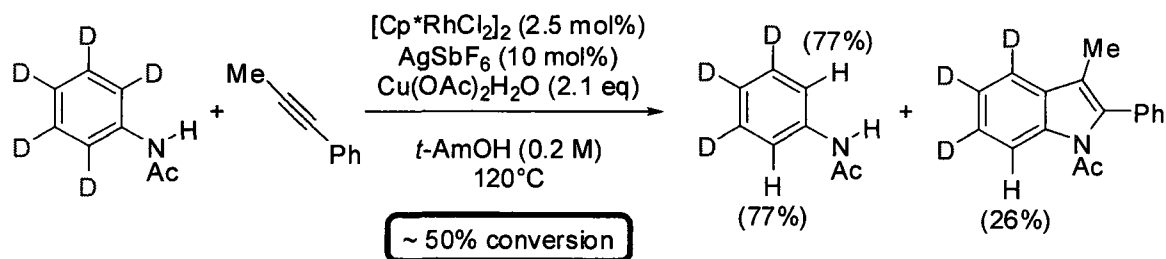
Crude nitrobenzene-*d*<sub>5</sub> was dissolved in MeOH and purged with argon. Pd/C (10 mol% Pd) was added and the reaction was purged with H<sub>2</sub> (1 atm) for 10 minutes and then held under an H<sub>2</sub> atmosphere overnight at room temperature. The reaction mixture was checked by TLC

and filtered over celite and the solvent removed under reduced pressure. The crude aniline- $d_5$  was used without further purification.

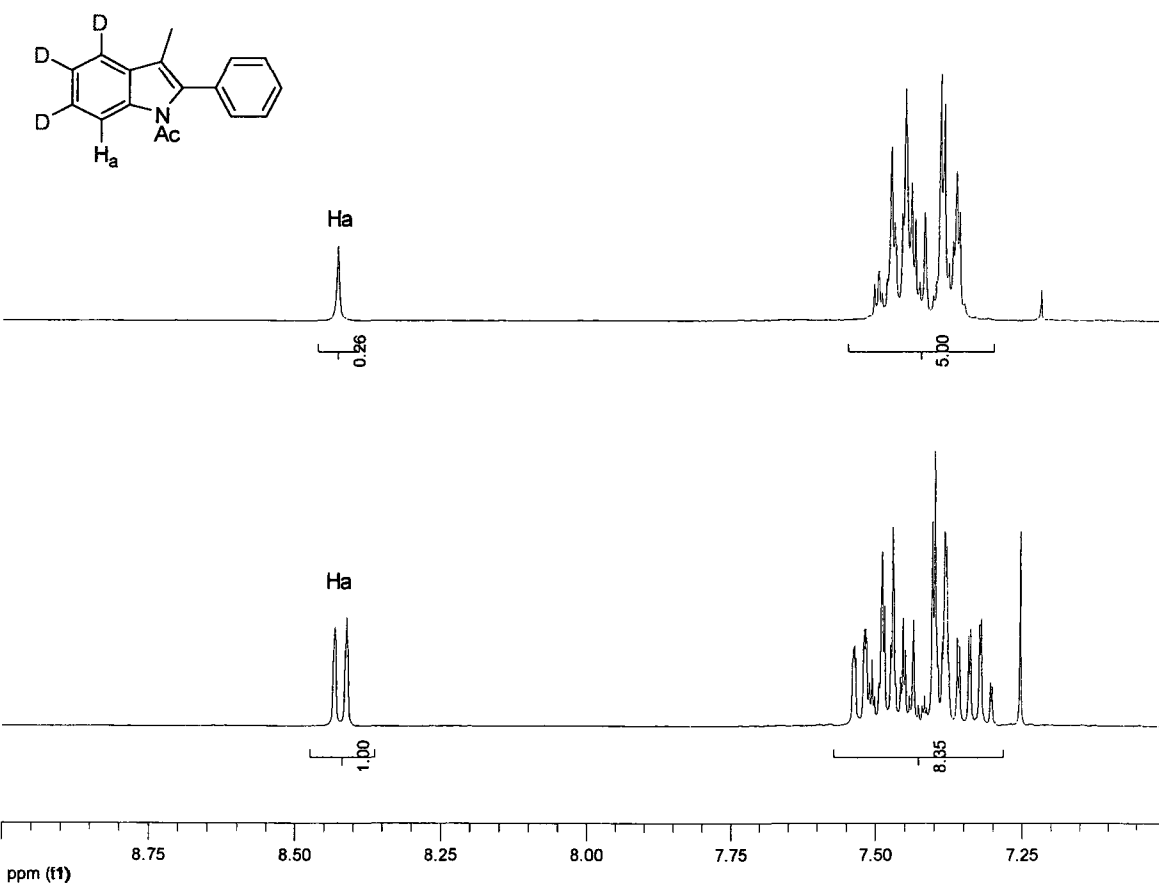
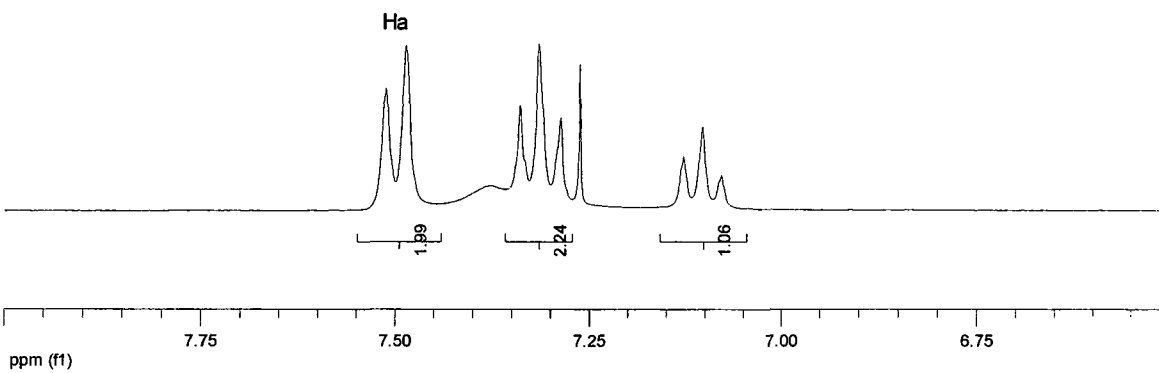
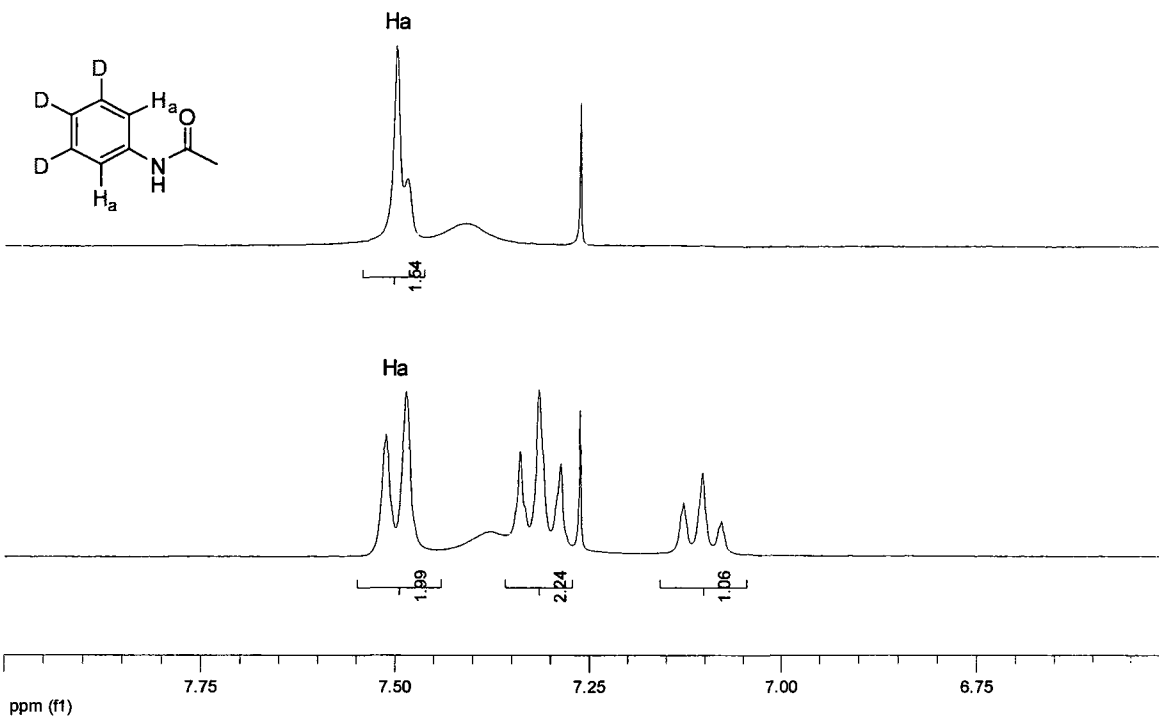
Crude aniline- $d_5$  was added to a round-bottom flask via syringe and fitted with a rubber septa. The flask was purged with argon and dry DCM was added. Acetic anhydride was added and the reaction was stirred at room temperature and monitored by TLC. Upon completion the reaction mixture was washed with a saturated solution of sodium carbonate, the organic layers dried with  $MgSO_4$  and the solvent removed under reduced pressure. The product was obtained in 48% yield (over 3 steps, based on amount of benzene- $d_6$ ) (1.5045 g). Purified by flash chromatography on silica gel with ethyl acetate : pet. ether (40 : 60). This compound can be purchased from commercial sources (CAS: 15826-91-2).

$^1H$  NMR (400 MHz,  $CDCl_3$ , 293 K):  $\delta$  7.59 (br. s, 1H), 2.16 (s, 3H).

#### Deuterium loss experiments:



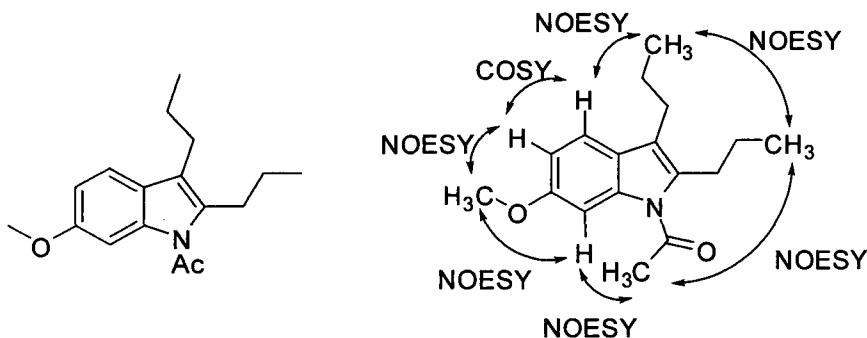
The general procedure (first generation conditions) was followed however the reaction was stopped after 2 minutes. Both product formed and remaining acetanilide were isolated by flash chromatography on silica gel (ether:pet. ether, 5:95 (product); then ethyl acetate:pet. ether, 40:60 (acetanilide) and compared with authentic samples by  $^1H$  NMR spectroscopy (300 MHz).



## Characterization of compounds used in regioselectivity studies:

### Compounds 4.25a1 and 4.25b1

Second generation conditions were followed (0.3 mmol of 3-methoxyacetanilide) and the residue was purified *via* silica gel chromatography using 10% Et<sub>2</sub>O in pet. ether.



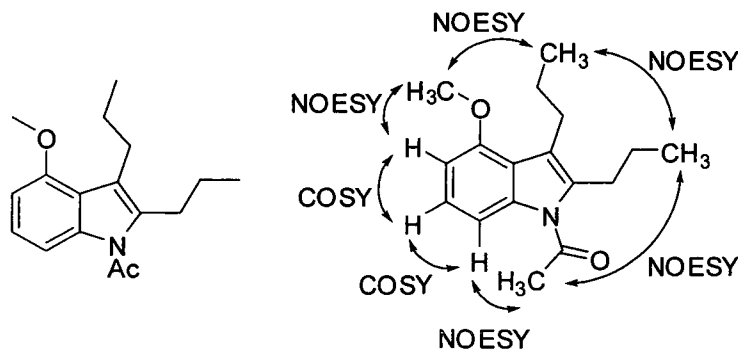
**<sup>1</sup>H NMR (400MHz, CDCl<sub>3</sub>, 293 K):** δ 7.44 (1H, d, *J* = 2.2Hz), 7.35 (1H, d, *J* = 8.5Hz), 6.87 (1H, dd, *J* = 8.5Hz, *J* = 2.2Hz), 3.86 (3H, s), 2.90 – 2.93 (2H, m), 2.72 (3H, s), 2.57 – 2.61 (2H, m), 1.54 – 1.66 (4H, m), 0.98 (3H, t, *J* = 7.4Hz), 0.97 (3H, t, *J* = 7.4Hz).

**<sup>13</sup>C NMR (400 MHz, CDCl<sub>3</sub>, 293 K):** δ 170.2 (C), 157.2 (C), 136.7 (C), 136.4 (C), 124.8 (C), 120.0 (C), 118.9 (CH), 110.2 (CH), 101.0 (CH), 55.9 (CH<sub>3</sub>), 29.0 (CH<sub>2</sub>), 27.4 (CH<sub>3</sub>), 26.2 (CH<sub>2</sub>), 23.7 (CH<sub>2</sub>), 23.4 (CH<sub>2</sub>), 14.3 (CH<sub>3</sub>), 14.1 (CH<sub>3</sub>).

**FTIR:** 1700, 1489, 1368, 1315 cm<sup>-1</sup>.

**HRMS (EI):** calculated for C<sub>17</sub>H<sub>23</sub>NO<sub>2</sub> (M<sup>+</sup>) 273.1729; found for C<sub>17</sub>H<sub>23</sub>NO<sub>2</sub> (M<sup>+</sup>) 273.1723.

**R<sub>f</sub> (ether/benzene/pet. ether (1:9)):** 0.20



**<sup>1</sup>H NMR (400MHz, CDCl<sub>3</sub>, 293 K):** δ 7.36 (1H, dd, *J* = 8.5Hz, *J* = 0.5Hz), 7.14 (1H, dd, *J* = *J* = 8.1Hz), 6.66 (1H, d, *J* = 7.9Hz), 3.91 (3H, s), 2.89 – 2.93 (2H, m), 2.72 – 2.76 (2H, m), 2.73 (3H, s), 1.53 – 1.64 (4H, m), 0.98 (3H, t, *J* = 7.4Hz), 0.98 (3H, t, *J* = 7.4Hz).

**<sup>13</sup>C NMR (400 MHz, CDCl<sub>3</sub>, 293 K):** δ 170.4 (C), 154.0 (C), 137.2 (C), 136.3 (C), 123.9 (CH), 120.3 (C), 120.0 (C), 107.5 (CH), 103.6 (CH), 55.3 (CH<sub>3</sub>), 28.4 (CH<sub>2</sub>), 27.7 (CH<sub>3</sub>), 27.5 (CH<sub>2</sub>), 24.6 (CH<sub>2</sub>), 23.8 (CH<sub>2</sub>), 14.3 (CH<sub>3</sub>), 14.1 (CH<sub>3</sub>).

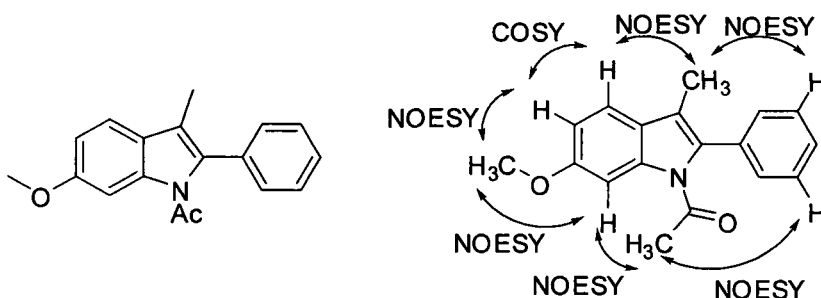
**FTIR:** 1698, 1261, 775, 733 cm<sup>-1</sup>.

**HRMS (EI):** calculated for  $C_{17}H_{33}NO_2$  ( $M^+$ ) 273.1729; found for  $C_{17}H_{23}NO_2$  ( $M^+$ ) 273.1745.

**R<sub>f</sub> (ether/benzene/pet. ether (1:9)):** 0.30

### Compounds 4.25a2 and 4.25b2

Second generation conditions were followed (0.3 mmol of 3-methoxyacetanilide) and the residue was purified *via* silica gel chromatography using 10% Et<sub>2</sub>O, 10% benzene in pet. ether.



**<sup>1</sup>H NMR (400 MHz, CDCl<sub>3</sub>, 293 K):** δ 8.05 (d,  $J = 2.3$  Hz, 1H), 7.50 – 7.35 (m, 6H), 6.96 (dd,  $J = 8.5$  Hz,  $J = 2.4$  Hz, 1H), 3.90 (s, 3H), 2.12 (s, 3H), 1.94 (s, 3H).

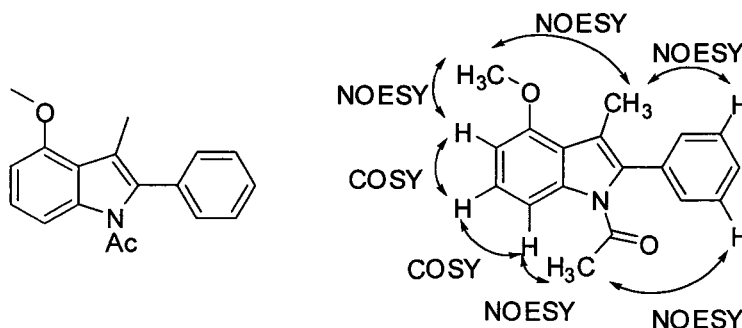
**<sup>13</sup>C NMR (100 MHz, CDCl<sub>3</sub>, 293 K):** δ 171.4 (C), 158.7 (C), 137.8 (C), 133.8 (C), 133.6 (C), 130.2 (CH), 128.7 (CH), 128.2 (CH), 124.2 (C), 119.0 (CH), 118.2 (C), 112.6 (CH), 100.6 (CH), 55.8 (CH<sub>3</sub>), 27.7 (CH<sub>3</sub>), 9.3 (CH<sub>3</sub>).

**FTIR:** 2936, 1695, 1484, 1320, 776 cm<sup>-1</sup>.

**HRMS (EI):** calculated for  $C_{18}H_{17}NO_2$  ( $M^+$ ) 279.1259; found for  $C_{18}H_{17}NO_2$  ( $M^+$ ) 279.1254.

**Melting point (Ether/Pet. Ether):** 76 – 78°C.

**R<sub>f</sub> (Ether/Pet. Ether (10:90)):** 0.21.



**<sup>1</sup>H NMR (400MHz, CDCl<sub>3</sub>, 293 K):** δ 8.02 (1H, dd,  $J = 8.4$ Hz,  $J = 0.6$ Hz), 7.35 – 7.49 (5H, m), 7.26 (1H, dd,  $J = 8.2$ Hz), 6.73 (1H, d,  $J = 8.0$ Hz), 3.92 (3H, s), 2.28 (3H, s), 1.93 (3H, s).

**<sup>13</sup>C NMR (400 MHz, CDCl<sub>3</sub>, 293 K):** δ 171.3 (C), 154.4 (C), 138.2 (C), 133.7 (C), 133.4 (C), 130.5 (CH), 128.7 (CH), 128.3 (CH), 126.0 (CH), 119.5 (C), 118.3 (C), 109.2 (CH), 104.4 (CH), 55.4 (CH<sub>3</sub>), 27.8 (CH<sub>3</sub>), 11.8 (CH<sub>3</sub>).

**FTIR:** 1698, 1432, 1307, 1261, 962, 699, 659  $\text{cm}^{-1}$ .

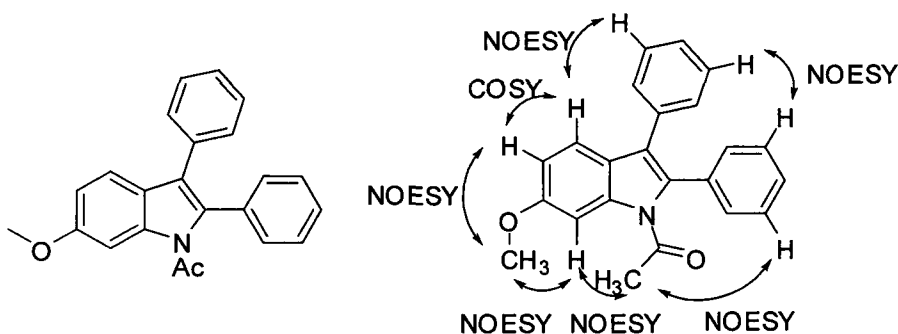
**HRMS (EI):** calculated for  $\text{C}_{18}\text{H}_{17}\text{NO}_2$  ( $\text{M}^+$ ) 279.1259; found for  $\text{C}_{18}\text{H}_{17}\text{NO}_2$  ( $\text{M}^+$ ) 279.1250.

**Rf (ether/benzene/pet. ether (1:1:8)):** 0.35

**Melting point:** 85°C

### Compounds 4.25a3 and 4.25b3

Second generation conditions were followed (0.3 mmol of 3-methoxy acetanilide) and the residue was purified via silica gel chromatography using 10%  $\text{Et}_2\text{O}$  (gradient) in pet. ether.



**<sup>1</sup>H NMR (400MHz, CDCl<sub>3</sub>, 293 K):**  $\delta$  8.08 (1H, d,  $J = 2.3\text{Hz}$ ), 7.42 (1H, d,  $J = 8.6\text{Hz}$ ), 7.19 – 7.36 (10H, m), 6.94 (1H, dd,  $J = 8.6\text{Hz}$ ,  $J = 2.4\text{Hz}$ ), 3.92 (3H, s), 1.98 (3H, s).

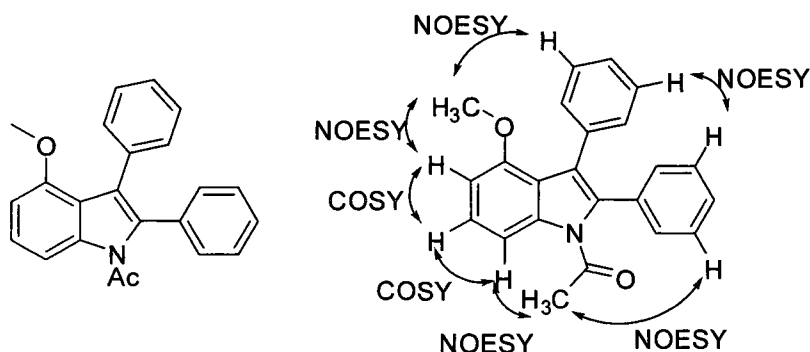
**<sup>13</sup>C NMR (400 MHz, CDCl<sub>3</sub>, 293 K):**  $\delta$  171.9 (C), 158.7 (C), 137.8 (C), 133.6 (C), 133.2 (C), 133.2 (C), 130.8 (CH), 130.0 (CH), 128.6 (CH), 128.4 (CH), 128.2 (CH), 126.9 (CH), 123.3 (C), 123.1 (C), 120.1 (CH), 113.1 (CH), 100.2 (CH), 55.8 (CH<sub>3</sub>), 28.0 (CH<sub>3</sub>).

**FTIR:** 1699, 1031, 721, 698  $\text{cm}^{-1}$ .

**HRMS (EI):** calculated for  $\text{C}_{23}\text{H}_{19}\text{NO}_2$  ( $\text{M}^+$ ) 341.1416; found for  $\text{C}_{23}\text{H}_{19}\text{NO}_2$  ( $\text{M}^+$ ) 341.1403.

**Rf (ether/benzene/pet. ether (1:9)):** 0.24

**Melting point:** 164°C



**<sup>1</sup>H NMR (400MHz, CDCl<sub>3</sub>, 293 K):**  $\delta$  8.07 (1H, dd,  $J = 8.4\text{Hz}$ ,  $J = 0.7\text{Hz}$ ), 7.23 – 7.34 (6H, m), 7.19 (5H, m), 6.73 (1H, br d,  $J = 8.0\text{Hz}$ ), 3.65 (3H, s), 1.97 (3H, s).

<sup>13</sup>C NMR (400 MHz, CDCl<sub>3</sub>, 293 K): δ 171.9 (C), 154.0 (C), 138.0 (C), 134.5 (C), 134.5 (C), 133.0 (C), 131.0 (CH), 130.8 (CH), 128.3 (CH), 128.3 (CH), 126.9 (CH), 126.3 (CH), 126.1 (CH), 123.0 (C), 118.5 (C), 108.9 (CH), 105.0 (C), 55.4 (CH<sub>3</sub>), 28.0 (CH<sub>3</sub>).

FTIR: 1702, 1103, 734, 698 cm<sup>-1</sup>

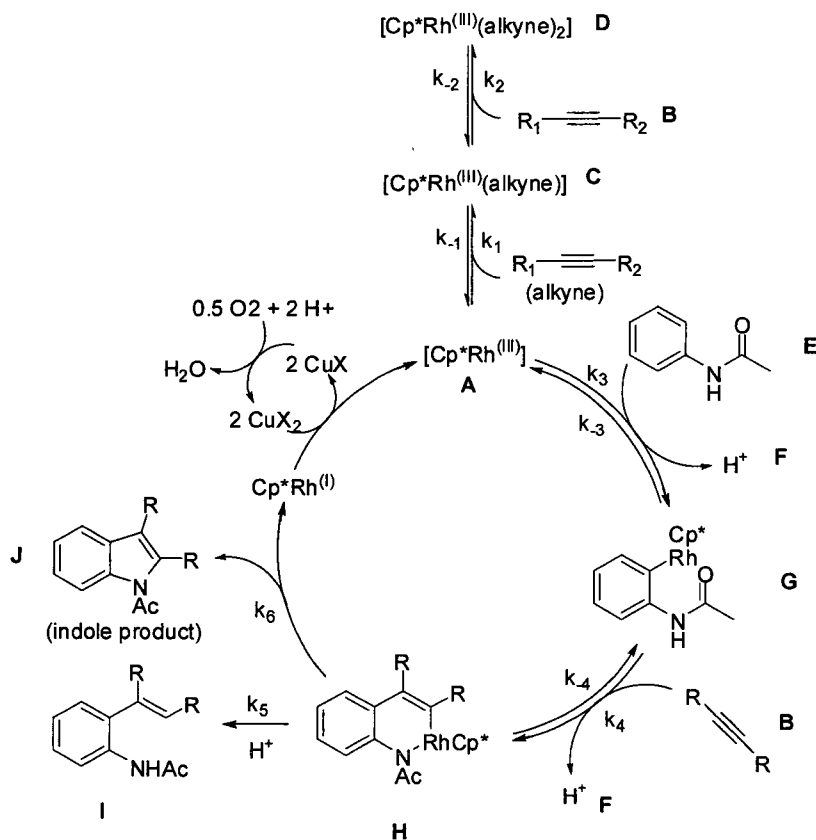
HRMS (EI): calculated for C<sub>23</sub>H<sub>19</sub>NO<sub>2</sub> (M<sup>+</sup>) 341.1416; found for C<sub>23</sub>H<sub>19</sub>NO<sub>2</sub> (M<sup>+</sup>) 341.1396.

R<sub>f</sub> (ether/pet. ether (1:9)): 0.29

Melting point: 190°C

The regioselectivity studies were set up under the standard protocol (section 5.3.3) carried out using the specified conditions in the text of this thesis (Chapter 4). Upon completion the reaction mixtures were extracted with a saturated solution of ammonium chloride to remove the residual copper and the crude mixtures were analyzed by <sup>1</sup>H NMR spectroscopy.

**Derivation of rate law:** The rate law was derived for the following catalytic cycle.



$$\text{rate} = k_6[H]$$

$$\text{also: } [Rh]_t = [A] + [C] + [D] + [G] + [H]$$

$$\text{and: } K_{eq1} = \frac{[C]}{[A][B]} \quad \therefore [C] = K_{eq1}[A][B]$$

$$K_{eq2} = \frac{[D]}{[C][B]} \quad \therefore [D] = K_{eq2}[C][B] \quad \therefore [D] = K_{eq2}K_{eq1}[A][B]^2$$

$$K_{eq3} = \frac{[G][F]}{[A][E]} \quad \therefore [G] = K_{eq3} \frac{[A][E]}{[F]}$$

$$K_{eq4} = \frac{[H][F]}{[G][B]} \quad \therefore [H] = K_{eq4} \frac{[G][B]}{[F]} \quad \therefore [H] = K_{eq4}K_{eq3} \frac{[A][E][B]}{[F]^2}$$

$$\therefore [Rh]_t = [A] + K_{eq1}[A][B] + K_{eq2}K_{eq1}[A][B]^2 + K_{eq3} \frac{[A][E]}{[F]} + K_{eq4}K_{eq3} \frac{[A][E][B]}{[F]^2}$$

$$\therefore [Rh]_t = [A] \left( 1 + K_{eq1}[B] + K_{eq2}K_{eq1}[B]^2 + K_{eq3} \frac{[E]}{[F]} + K_{eq4}K_{eq3} \frac{[E][B]}{[F]^2} \right)$$

$$\therefore [A] = \frac{[Rh]_t}{1 + K_{eq1}[B] + K_{eq2}K_{eq1}[B]^2 + K_{eq3} \frac{[E]}{[F]} + K_{eq4}K_{eq3} \frac{[E][B]}{[F]^2}}$$

$$\text{recall: rate} = k_6[H] \text{ and } [H] = K_{eq4}K_{eq3} \frac{[A][E][B]}{[F]^2}$$

$$\therefore \text{rate} = k_6K_{eq4}K_{eq3} \frac{[A][E][B]}{[F]^2}$$

$$\text{and } \therefore \text{rate} = \frac{k_6K_{eq4}K_{eq3}[Rh]_t[E][B]}{[F]^2 \left( 1 + K_{eq1}[B] + K_{eq2}K_{eq1}[B]^2 + K_{eq3} \frac{[E]}{[F]} + K_{eq4}K_{eq3} \frac{[E][B]}{[F]^2} \right)}$$

$$\therefore \text{rate}_{Rh} = a[Rh]_t + b$$

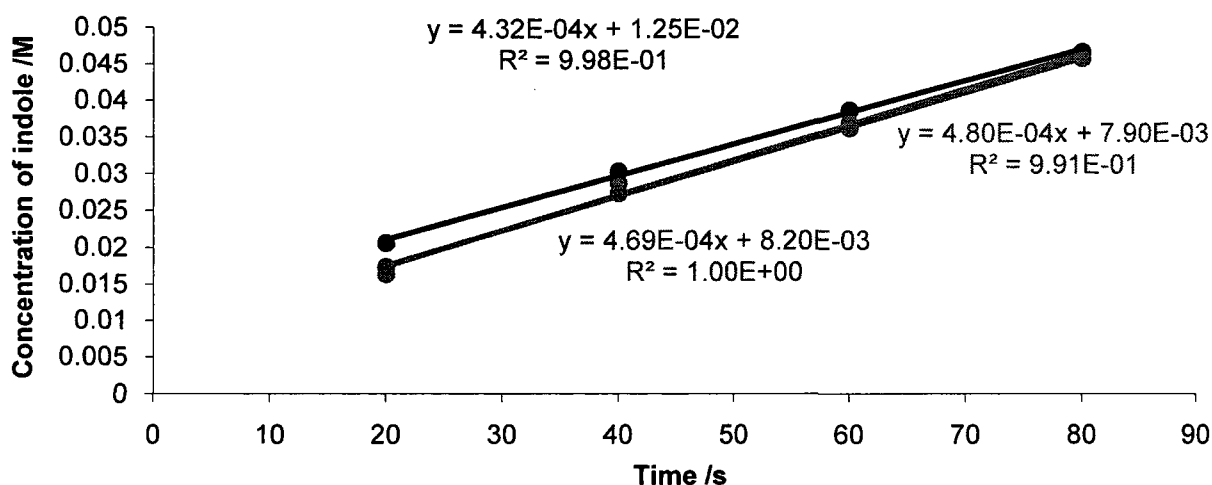
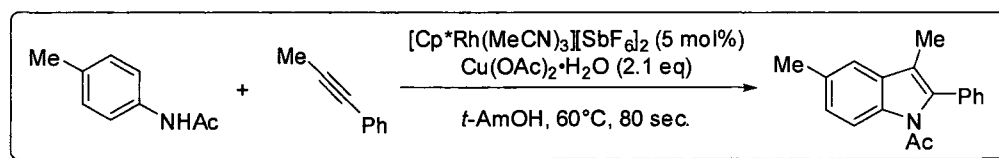
$$\therefore \text{rate}_{\text{acetanilide}} = \frac{a[\text{acetanilide}]}{b[\text{acetanilide}] + c}$$

$$\therefore \text{rate}_{\text{alkyne}} = \frac{a[\text{alkyne}]}{b[\text{alkyne}]^2 + c[\text{alkyne}] + d}$$

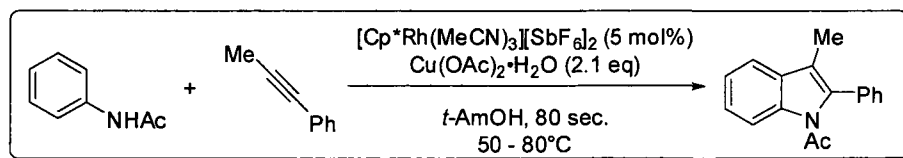
$$\therefore \text{rate}_{\text{acid}} = \frac{a}{b[\text{acid}]^2 + c[\text{acid}] + d}$$

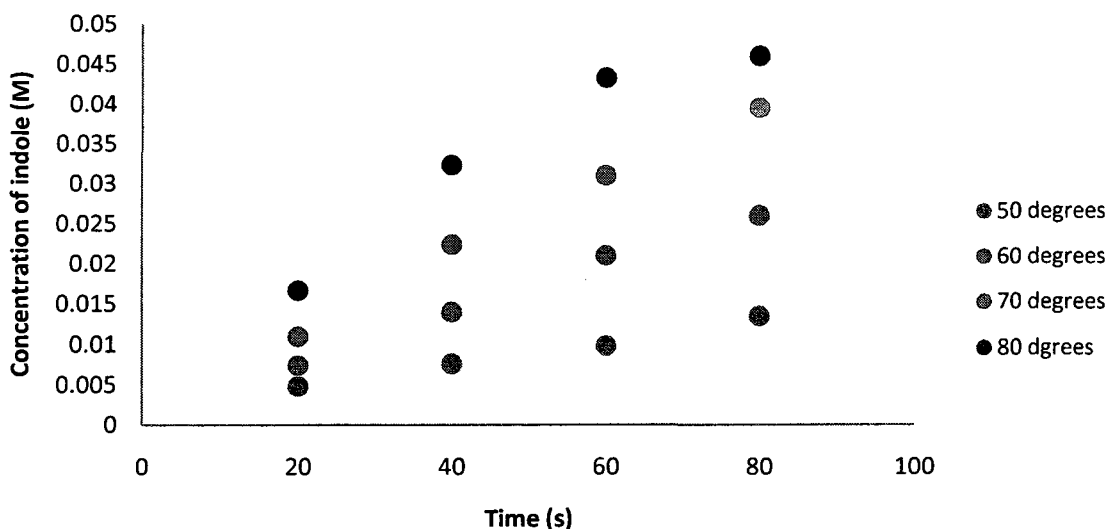
**Deuterium kinetic isotope effect:** The procedure to obtain kinetic data was repeated 3 times for acetanilide and 2 times for acetanilide-*d*<sub>5</sub>. The ratio of initial rates provides the DKIE.

**Hammett correlation:** The procedure to obtain kinetic data was repeated 3 times for each substrate and the average was taken as the initial rate. The natural logarithm of the initial rate for the substituted acetanilides over the unsubstituted acetanilide was plotted against the  $\sigma_{meta}$  values and the slope obtained was the  $\rho$ -value. A sample collection of data for 4-methylacetanilide is shown below.



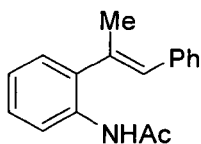
**Arrhenius plot:** The procedure to obtain kinetic data was carried out at 4 different temperatures (50 – 80°C) and the natural logarithm of the initial rate plotted against the inverse temperature (in Kelvins) and the  $E_a$  was derived from the slope of the plot (Figure 4.8).





#### 5.4.9. Procedure for the Hydroarylation of Internal Alkynes.

To a 1 dram screw-cap vial was added acetanilide (0.0430 g, 0.3 mmol, 1 eq),  $[\text{Cp}^*\text{Rh}(\text{MeCN})_3][\text{SbF}_6]_2$  (0.0063 g, 0.0076 mmol, 2.5 mol%) and PivOH (0.1551 g, 1.5 mmol, 5 eq). *t*-AmOH (1.5 mL, 0.2 M) and 1-phenyl-1-propyne (41  $\mu\text{L}$ , 0.66 mmol, 1.1 eq) are added *via* syringe and the reaction is sealed and placed in a pre-heated (70°C) block. The reaction is stirred for 16 hours and then cooled to room temperature and checked by TLC or GCMS. The reaction is filtered over Celite washing with ether into a 50 mL round-bottom flask and silica is added. The solvent is removed and the compound purified by flash column chromatography on silica gel (10 cm x 3 cm) with ether/pet. ether as the solvent (see below for specific eluent composition).



$^1\text{H}$  NMR (400 MHz, acetone- $d_6$ , 293 K):  $\delta$  8.52 (br. s, 1H), 7.94 (d,  $J = 7.6$  Hz, 1H), 7.45 – 7.38 (m, 4H), 7.30 – 7.23 (m, 3H), 7.14 (t,  $J = 7.4$  Hz, 1H), 6.48 (br. s, 1H), 2.21 (d,  $J = 1.5$  Hz, 3H), 2.07 (s, 3H).

$^{13}\text{C}$  NMR (100 MHz, acetone- $d_6$ , 293 K):  $\delta$  169.9 (C), 140.0 (C), 139.6 (CH), 138.0 (CH), 137.0 (C), 132.3 (CH), 130.9 (CH), 130.3 (CH), 130.0 (CH), 129.0 (CH), 128.5 (CH), 126.1 (C), 125.6 (C), 25.0 (CH<sub>3</sub>), 20.7 (CH<sub>3</sub>).

FTIR: 3056, 1667, 1522, 1439, 756, 699  $\text{cm}^{-1}$ .

HRMS (EI): calculated for  $\text{C}_{17}\text{H}_{17}\text{NO}$  ( $\text{M}^+$ ) 251.1310; found for  $\text{C}_{17}\text{H}_{17}\text{NO}$  ( $\text{M}^+$ ) 251.1304.

$R_f$  (ethyl acetate/pet. ether (40:60)): 0.35.

# Appendix

## Claims to Original Research

1. Development of conditions for the direct arylation of quinoline and isoquinoline *N*-oxide with a variety of arylbromides.
2. Development of conditions for the palladium(II) catalyzed oxidative cross-coupling of two unactivated arenes. In this context the regioselective C2 or C3 arylation of *N*-pivaloyl or *N*-acetylindole.
3. Mechanistic investigation into the palladium(II) catalyzed oxidative cross-coupling of unactivated arenes.
4. Development of first and second generation conditions for the rhodium(III) catalyzed oxidative annulation of acetanilides with internal alkynes to form indoles.
5. Synthesis of Paullone *via* the above described method.
6. Mechanistic evaluation of the rhodium(III) catalyzed oxidative annulation of acetanilides with internal alkynes.
7. Development of conditions for the room temperature rhodium(III) catalyzed annulation of enamides with internal alkynes.
8. Development of conditions for the rhodium(III) catalyzed hydroarylation of internal alkynes with acetanilide.

## Publications from This Work

1. *Palladium-Catalyzed Direct Arylation of Azine and Azole N-Oxides: Reaction Development, Scope, and Application in Synthesis*. Campeau, L.-C.; Stuart, D.R., Leclerc, J.-P.; Bertrand-Laperle, M.; Villemure, E.; Sun, H.-Y.; Guimond, N.; Lasserre, S.; Lecavallier, M.; Fagnou, K. *J. Am. Chem. Soc.* **2009**, *131*, 3291.
2. *Indole Synthesis via Rhodium Catalyzed Oxidative Coupling of Acetanilides and Internal Alkynes*. Stuart, D.R.; Bertrand-Laperle, M.; Burgess, K.M.N.; Fagnou, K. *J. Am. Chem. Soc.* **2008**, *130*, 16474.
3. *Intramolecular Pd(II)-Catalyzed Oxidative Biaryl Synthesis Under Air : Reaction Development and Scope*. Liegault, B.; Lee, D.; Huestis, M.P.; Stuart, D.R.; Fagnou, K. *J. Org. Chem.*, **2008**, *73*, 5022.
4. *Elements of Regiocontrol in Palladium-Catalyzed Oxidative Arene Cross-Coupling*. Stuart, D.R.; Villemure, E.; Fagnou, K. *J. Am. Chem. Soc.*, **2007**, *129*, 12072.
5. *The Catalytic Cross-Coupling of Unactivated Arenes*. Stuart, D.R.; Fagnou, K. *Science*, **2007**, *316*, 1172.
6. *Process for using N-oxide compounds in coupling reactions*. Campeau, Louis-Charles ; Leclerc, Jean-Phillippe ; Fagnou, Keith ; Stuart, David R.. U.S. Pat. Appl. Publ. (2008), 46 pp.
7. *Recent Advances in Intermolecular Direct Arylation Reactions*. Campeau, L.C.; Stuart, D.R.; Fagnou, K. *Aldrichemica Acta*, **2007**, *40*, 35.

## Presentations from This Work

1. "Rhodium-Catalyzed Oxidative Approaches to Indoles and Pyrroles" (Oral Presentation). 92<sup>nd</sup> Canadian Chemistry Conference, Hamilton, Ontario, **2009**
2. "Regiocontrol and Mechanistic Insights in Palladium Catalyzed Oxidative Cross-Coupling Reactions" (Oral Presentation). International Conference on Organometallic Chemistry (ICOMC), Rennes, France, **2008**
3. "Regiocontrol and Mechanistic Insights in Palladium Catalyzed Oxidative Cross-Coupling Reactions" (Oral Presentation). 91<sup>st</sup> Canadian Chemistry Conference, Edmonton, Alberta, **2008**
4. "Regiocontrol and Mechanistic Insights in Palladium Catalyzed Oxidative Cross-Coupling Reactions" (Poster Presentation). Synthesis Day, Ottawa, ON, **2008**  
*Awarded 2<sup>nd</sup> place in the poster competition.*
5. "Regiocontrol and Mechanistic Insights in the Catalytic Cross-Coupling of Indoles and Simple Arenes" (Oral Presentation). Quebec-Ontario Mini Symposium in Bio-organic and Organic Chemistry, Montreal, QC, **2007**
6. "The Catalytic Regioselective Cross-Coupling of Indoles and Benzene" (Poster Presentation). Quebec-Ontario Mini Symposium in Bio-organic and Organic Chemistry, London, ON, **2006**
7. "The Catalytic Direct Arylation of Quinoline and Isoquinoline N-Oxide" (Poster Presentation). Ottawa-Carleton Chemistry Institute Day, Ottawa, ON, **2006**
8. "The Catalytic Direct Arylation of Quinoline and Isoquinoline N-Oxide" (Poster Presentation). Synthesis Day, Ottawa, ON, **2006**